University of Nottingham

School of Medicine

Mental Health and Clinical Neurosciences

Autonomic and Central Nervous System Correlates of Cognitive Control Training for Attentional Disorders

Alice Emily Waitt

Thesis submitted for the degree of Doctor of Philosophy

December 2021

Abstract

Deficits in cognitive control and attentional processing are commonly observed in people with Attention-Deficit/Hyperactivity Disorder (ADHD) and Specific Learning Difficulties (SpLDs) such as Dyslexia. Poorer performance in the pro/antisaccade task have been observed in these individuals, which suggests impaired visual attention and inhibitory control mechanisms. Atypical cognitive processing is also related to a state of autonomic hypoarousal in conditions such as ADHD. In this thesis, I examined whether the computer-based gaze-control RECOGNeyes training program using the pro/antisaccade task could improve cognitive control of visual attention by targeting the visual attention network and whether such improvements correlate with increased arousal. A group of 35 volunteers with SpLDs and/or ADHD completed the pro/antisaccade task before and after two weeks of training their visual attention using RECOGNeyes. Magnetoencephalography (MEG), pupillometry and electrocardiography were recorded, while they performed the pro/antisaccade task. Our task performance measures, reaction time (RT) and accuracy, and reading indices improved after RECOGNeyes training. Our findings demonstrate for the first time that autonomic measures of sympathetic pupil dilation and parasympathetic cardiac deceleration both correlate with faster saccadic RTs together (which was stronger for antisaccade trials than prosaccade trials) and account for separate variance in RT. Additionally, distinct MEG oscillatory profiles were uncovered in different frequency bands within

regions of the visual attention network during the pro/antisaccade task. Slow-wave oscillations of delta and theta bands show anteriorising effects, suggested to mediate timing responses and bottom-up communication from the posterior to anterior network regions. Alpha-oscillations are proposed to have top-down preparatory inhibitory effects, particularly from the bilateral frontal eye field, and alpha-suppression in the right parietal eye field. Beta amplitude presents an additional "anticipatory" event-related desynchronisation (ERD) prior to target onset that is stronger on day 2 and antisaccade trials, which could relate to generalised inhibitory control mechanisms. This thesis supports the existence of complex central and autonomic processes underlying attention and arousal that are not yet fully understood and warrant further investigation. By increasing our understanding of the integrated attentional processes and inhibitory control, this could help the development of targeted treatment solutions, such as RECOGNeyes, for ADHD and SpLDs, to improve outcomes in these individuals.

Acknowledgements

The work contributing to this thesis would not have been possible to complete without the support of the people who have been there with me from start to finish.

Firstly, I would like to give a huge thank you to my partner Andrew, who has kept me motivated and provided endless encouragement throughout all the ups and downs, especially during the difficult times of the pandemic. Thanks for keeping a smile on my face and for putting up with me the whole way through. I do not know what I would have done without you, and our guinea pigs Snowball and Cinnabear to keep me going during all the long hours working at home!

I would also like to give a massive thank you to my friends and family, especially my parents Jean and Charley and my brother Tim, who have always encouraged me to follow my passion in science and have always believed in me. Your continued support and optimism mean so much to me and I would not have gotten to this point without you all.

I am grateful for the amazing group of collaborators involved in the RECOGNeyes project. I have gained so much experience from you all and thank you for making the data acquisition an educational and enjoyable process. I would particularly like to thank Jyothika Kumar and Lauren Gascoyne who were excellent teachers during the project and have provided a lot of advice and inspiration throughout the course of my PhD. Thanks to

all the other members at the Institute of Mental Health and the Sir Peter Mansfield Centre who have helped me during my time as a PhD researcher, from data acquisition to providing stimulating academic conversations.

Last, but not least, I would like to acknowledge the continual guidance, support and encouragement from my supervisors Peter and Elizabeth Liddle. You have been great academic mentors and I have appreciated learning from the extensive experiences and careers of you both. Thank you for navigating the pandemic with me from all the remote supervision meetings and keeping me going until the end!

Statement of Contributions

I hereby confirm that the work presented in this thesis is original and my own, whereby the thoughts and ideas of others are appropriately acknowledged.

The RECOGNeyes study discussed in this thesis was a team project, whereby the Chief Investigator was Dr Elizabeth Liddle, and I was one of the Lead Investigators. Project work was conducted by several post-doctoral researchers, PhD students, Masters students, and medical students. The study was funded by the Confidence in Concept grant awarded by the Medical Research Council (MRC).

I was involved in all aspects of data acquisition on the scanning days, including MEG and MRI data collection, questionnaires, eye-tracked reading assessment, etc. I did contribute to some screening and recruitment procedures, but the majority was undertaken by other post-doctoral researchers and Masters students. The experimental design, pro/antisaccade task and ethical approval were confirmed prior to my joining onto the project team. Scoring of questionnaire data and extracting reading indices in Chapter 4 was completed by other members of the team. MEG data artefact rejection in Chapter 7 was undertaken by me and two other investigators to avoid bias. However, all other data pre-processing and statistical analyses in this thesis were conducted by me.

In addition, I contributed towards a partner study involving transcranial direct current stimulation that used a very similar experimental design and nearly identical MEG scan and pro/antisaccade task to that of the RECOGNeyes study. Therefore, data collection in this project aided in my acquisition experience and deepened my understanding for the methodology in the RECOGNeyes project. I was also able to gain more experience in the experimental design, screening, and recruitment procedures from this work.

Table of Contents

List of Figures

List of Tables

List of Abbreviations

ACC	Anterior Cingulate Cortex
ACh	Acetylcholine
ADHD	Attention-Deficit/Hyperactivity Disorder
ADR	Adrenoceptor
ANOVA	Analysis of Variance
ANS	Autonomic Nervous System
Ant Ins	Anterior Insula
ASD	Autism Spectrum Disorder
BOLD	Blood-oxygen-level-dependent
BPM	Beats per minute
CNS	Central Nervous System
DA	Dopamine
DLPFC	Dorsolateral Prefrontal Cortex
DMN	Default-Mode Network
DSM	Diagnostic and Statistical Manual of Mental Disorders
ECG	Electrocardiogram

EEG	Electroencephalography
ERD	Event-Related Desynchronisation
ERS	Event-Related Synchronisation
FEF	Frontal Eye Field
fMRI	Functional Magnetic Resonance Imaging
HR	Heartrate
HRV	Heartrate Variability
IBI	Inter-beat Interval
IPS	Intraparietal Sulcus
LC	Locus Coeruleus
LIP	Lateral Intraparietal Area
MEG	Magnetoencephalography
MPH	Methylphenidate
MRI	Magnetic Resonance Imaging
NE	Norepinephrine/Noradrenaline
PEF	Parietal Eye Field
PFC	Prefrontal Cortex

PNS	Parasympathetic Nervous System
ROI	Region of Interest
RT	Reaction Time
SC	Superior Colliculus
SEF	Supplementary Eye Field
SNS	Sympathetic Nervous System
SpLDs	Specific Learning Difficulties
Std. Dev	Standard Deviation
V1	Primary Visual Cortex

Chapter 1: Introduction

1.1. Disorders affecting attention

1.1.1. Attention-Deficit/Hyperactivity Disorder

Attention-Deficit/Hyperactivity Disorder (ADHD) is a neurodevelopmental condition specifically affecting attentional functioning. Systematic reviews and meta-analyses show that the worldwide prevalence of ADHD is approximately 5 % of the population (Polanczyk et al., 2007; Willcutt, 2012). Increases in the diagnoses of ADHD have been reported over the past three decades, thought largely to reflect improved clinical and diagnostic criteria due to our increased understanding of ADHD (Polanczyk et al., 2014).

Diagnostic criteria group the behavioural symptoms of ADHD into "inattentive" and "hyperactive-impulsive" categories. The former covers problems with maintaining concentration and focus, whereas the latter covers impaired motor inhibition and impulsive and risky behaviour. Depending on whether the number of symptoms in each category reach threshold criteria, the diagnosis is further divided into three presentations as defined by *The Diagnostic and Statistical Manual of Mental Disorders* (5th ed.; *DSM–5*; American Psychiatric Association, 2013), namely: Predominantly Inattentive, Predominantly Hyperactive-Impulsive, and Combined. ADHD is classed as a neurodevelopmental disorder, because

symptoms are usually identified in childhood. Diagnostically, symptoms are required to be observed before the age of 12, be present in at least two settings (home, school, etc.), and interfere in the quality of social and academic/occupational life of the individual (American Psychiatric Association, 2013).

ADHD is more commonly diagnosed in boys than girls. However, recent studies suggest there is evidence of bias in clinician diagnosis of boys and for parents to rate 'hyperactive' symptoms and impairments as higher in boys and underrate these symptoms in girls (Mowlem et al., 2019; Ottosen et al., 2019). This may be due to a different presentation of ADHD in girls, who often have more emotional-behavioural issues than boys and may be able to socially adapt to mask symptoms and appear less impaired than boys (Mowlem et al., 2019; Ottosen et al., 2019).

Until recently, ADHD was regarded as a childhood condition that children would "grow out" of. However, our increased understanding regarding ADHD in adulthood is reflected in the *DSM-5* guidelines, that for the first time provide adult diagnostic criteria. The *DSM-5* states that children need to have 6/9 of symptoms present within a particular group, but adults only require 5 for diagnosis from either domain (American Psychiatric Association, 2013).

1.1.2. Co-occurring conditions and specific learning difficulties/disabilities

A further complication in the diagnosis and understanding the presentation of ADHD is the commonality of co-occurring diagnoses, such as anxiety, depression, oppositional defiance disorder and conduct disorder (Connor et al., 2010; Crawford et al., 2006). Additionally, the latest *DSM-5* now recognises a joint diagnosis of ADHD with Autism Spectrum Disorder (ASD) (American Psychiatric Association, 2013); prior to this, a diagnosis of ADHD was not made if the child also met criteria for ASD.

Specific learning difficulties/disabilities (SpLDs) also commonly co-occur with ADHD. SpLDs is an umbrella term to describe learning or educational deficits in a range of domains from reading to mathematics (refer to Table 1) that limit the academic potential of the individual given their general cognitive ability (Snowling, 2005). These diagnoses are not to be mistaken for general learning disabilities signified by gross cognitive impairments (Snowling, 2005). Despite previous SpLD diagnostic criteria requiring the absence of IQ deficits, there is growing support that SpLDs can occur within the whole range of intellectual abilities, adding to the complicated aetiology for these conditions (Snowling et al., 2020).

A common SpLD is Reading Disorder, also known as dyslexia. Prevalence estimates vary, but dyslexia affects approximately 7 % of the general population if a definition of 1.5 standard deviations below the mean

reading age score is used (Peterson & Pennington, 2012, 2015; Wagner et al., 2020). Dyslexia commonly co-occurs with ADHD (Eden & Vaidya, 2008; Germanò et al., 2010). ADHD and SpLDs have high rates of co-occurrence with one other (Crawford et al., 2006; Kaplan et al., 2001; Landerl & Moll, 2010; Moll et al., 2014), with estimates of up to 70 % of children with ADHD having a secondary SpLD diagnosis (Mayes et al., 2000).

The large overlap between ADHD and SpLDs suggest shared cognitive and attentional deficits. Indeed, it has been suggested that these diagnoses could be regarded as subsets of the same disorder (Friedman et al., 2003; Kaplan et al., 2001; Mayes et al., 2000). Increasing evidence indicates high familial and genetic links in ADHD, dyslexia and dyscalculia (Willcutt et al., 2010), supporting the proposal that shared neurobiological mechanisms contribute to these diagnoses. Nevertheless, the range of neurological processes contributing to ADHD and SpLDs are still not fully understood.

Table 1: Common features of specific learning disabilities/difficulties (SpLDs).

Information derived from the DSM-5 diagnostic criteria (American Psychiatric Association, 2013), Snowling (2005) and additional sources included in the table.

Diagnosis	Functional domain affected	Presentation features
Dyslexia/ Reading Disorder	Reading and language processing	• Slow reading and writing speeds • Spelling difficulties

		• Difficulties in phonological processing, word decoding and word recall • (Lyon et al., 2003; Snowling et al., 2020)
Dyspraxia/ Developmental Coordination Disorder	Movement coordination	• Motor skills deficit interfering with daily activities • Difficulty with hand-eye coordination • Trouble with balance and dexterity • (Biotteau et al., 2019)
Dyscalculia/ Mathematics Disorder	Mathematics and number processing	• Difficulties solving mathematical problems and counting • Problems understanding time and money • (Kucian & von Aster, 2015; Shalev, 2004)
Dysgraphia	Handwriting and fine motor skills	• Illegible handwriting • Issues with spelling • Incorrect usage of lower/upper case letters • Problems with organisation and spatial planning • (Biotteau et al., 2019)

1.1.3. Outcomes of attentional disorders

Whilst ADHD symptoms are often better managed and appear less noticeable/disruptive to day-to-day life by adolescence and adulthood, a smaller number of symptoms can persist that impair attentional functioning and can cause significant reductions in quality of life (Hurtig et al., 2007; Kooij et al., 2005). ADHD is associated with poorer adult outcomes in a number of areas including poorer academic and vocational

achievements, increased risk of injury to self and others, addiction and drug abuse, increased difficulty in social relationships (R. G. Klein et al., 2012; M. Shaw et al., 2012), and increased prevalence of poor physical health (Spencer et al., 2014) and mental health problems (Agnew-Blais et al., 2018). Meta-analyses also indicate that the prevalence of ADHD in prisons/incarcerated populations is five-fold higher in young offenders and ten-fold higher in adults compared to the rate of ADHD in the general population (Young et al., 2015). This includes a common prevalence of Reading difficulties in the prison population (Morken et al., 2021).

In addition, ADHD individuals are more likely to experience poorer student-teacher relationships and higher rates of school exclusions, which contribute to academic underachievement (Ewe, 2019; Parker et al., 2015). ADHD individuals are also less likely to enrol in university, which supports the view for a lasting negative impact from the diagnosis well into adulthood (Sedgwick, 2018). Those students who reach university may struggle to adjust to the very different and unstructured environment of higher education, which can also manifest in late presentations of attentional and inhibitory control difficulties for adult diagnosis of ADHD (Kwon et al., 2018). These individuals often report poorer time management, underachievement, increased worry and isolation and poorer interpersonal relationships; therefore, this can result in serious negative impacts on their quality of life if they do not have access to appropriate support and education regarding their symptoms (Kwon et al., 2018).

A deeper understanding of the specific aetiology and neurological processes underlying cognitive and attentional impairments could contribute to developing better diagnostic tools (McNorgan et al., 2020), as well as to a wider range of treatment and intervention options. More effective treatment, especially in childhood, could help to reduce some of the educational and other impacts of these disorders, and help to improve the vocational, social and health outcomes for these individuals, and benefit the community by reducing the need for public and healthcare resources.

A candidate for shared mechanisms that could be targeted for treatment are those underpinning what is sometimes referred to as "cognitive control".

1.2. Cognitive control

1.2.1. Overview

Cognitive control, executive function, and top-down control are overlapping terms encompassing goal-directed and planned behaviours. The executive functions involved in cognitive control include: inhibitory control, working memory and cognitive flexibility (Diamond, 2013). Therefore, cognitive control underlies all aspects of everyday behaviours and functions, from our social interactions, performance in education and the workplace, and organising our daily lives. Arguably, these are all

aspects of attentional control. Control of attention allows us to navigate and interpret our environments safely and productively, as well as focus on complex tasks; ultimately, control over our attention is essential for survival.

Attending to specific stimuli necessarily involves inhibiting impulses to shift our attention elsewhere: "It implies withdrawal from some things in order to deal effectively with others" (James, 1890, pp. 381- 382). Inhibitory control is essential for governing what information we need to filter out (i.e., distractor stimuli) and what physiological/neurological functions to inhibit. This enables the optimisation of our attention towards salient information for executing appropriate actions, either for the current task at hand or responding to new environmental stimuli.

As humans, we are visually dominant and take preference in visual stimuli for how we observe and interpret our environment (Colavita, 1974; Posner et al., 1976; Sinnett et al., 2007); where we are looking at is usually what our attention is focussed on at the time. Specifically, we attend to the region of the visual field that is projected onto the fovea, the part of the retina sensitive to fine detail and colour vision. Typically, we 'fixate' on regions of the visual field sequentially, shifting our gaze between fixated locations by means of rapid eye-movements known as saccades (Freedman, 2008). Each saccade brings a new region of the visual field to the fovea. Gaze-control – control over saccadic shifts in gaze-direction – are thus central to visual attention. Our reaction to salient environmental stimuli is

known as the orienting response (Sokolov, 1963). Typically, this involves a shift in gaze-direction towards the stimulus ("head-fixed saccades") and can also involve physically turning our heads or body towards the stimulus ("head-free gaze shifts") (Kardamakis & Moschovakis, 2009).

Posner (1980) summarises the orienting response as "the aligning of attention with a source of sensory input or an internal semantic structure stored in memory". The former part of this definition can be interpreted as referring to bottom-up processes of responding to stimuli, whereas the latter part is implying the involvement of top-down mechanisms for directing gaze. The work of Posner and Petersen built upon this by defining three attentional networks that constitute the attentional system in the human brain (Petersen & Posner, 2012; Posner & Petersen, 1990). These were a spatially non-specific Alerting network (see Section 2.1.2), an Orienting network involved in directing attention to a spatial location, and an Executive network involved in selective attention. Fan et al. (2005) used functional magnetic resonance imaging (fMRI) to investigate brain correlates of the alerting, orienting and executive networks. They found activation of anterior and posterior cortical regions and the thalamus for alerting, frontal eye field (FEF) and parietal cortex during orienting, and a strong activation of the anterior cingulate cortex for the executive network (Fan et al., 2005).

Orienting processes can be categorised into exogenous stimulus-driven ('bottom-up') attentional shifts and endogenous goal-directed ('top-

down') visuospatial attentional shifts (Coull et al., 2000). Exogenous and endogenous attentional processes have been attributed to ventral and dorsal frontoparietal networks, respectively (Corbetta & Shulman, 2002). The dorsal frontoparietal network primarily involves the FEF and intraparietal sulcus (IPS), corresponding to Posner's posterior orienting network (Petersen & Posner, 2012; Posner & Petersen, 1990). It is believed to be involved in top-down priming of sensory information including to the visual cortex, motor planning modulation and preparing for responses (as summarised by Corbetta et al. (2008)). Conversely, the ventral frontoparietal network primarily involves the temporoparietal junction (TPJ) and ventral frontal cortex (Petersen & Posner, 2012). A "circuit breaker" is proposed to interrupt top-down control communications between the IPS and TPJ to facilitate processing incoming visual signals for responding to behaviourally relevant stimuli (Corbetta & Shulman, 2002).

Filtering out distracting and irrelevant information involves inhibitory control processes. They enable us to prioritise salient and important stimuli, as well as avoid becoming overwhelmed with the range of multiple domains of environmental stimuli exposed to us at any given time. Deficits of inhibitory control and executive functioning are found in both ADHD and SpLDs, whether or not they are co-occurring, supporting the proposal that they share neurophysiological dysfunctions (Lonergan et al., 2019).

Currently, there is no single core deficit identified that unifies all presentations of ADHD and SpLDs. Barkley (1997) proposed that a general deficit in inhibitory control mechanisms underlies the impairments of ADHD. However, because of the heterogeneity of the different presentations and subtypes of ADHD, dual or multiple pathway models are likely to account for the range of symptomatology, for example reward system dysregulation and/or impaired inhibitory control (Sonuga-Barke, 2002). Multiple studies indicate a wide range of neurocognitive deficits in ADHD, summarised in the umbrella review by Pievsky & McGrath (2018). Nonetheless, a substantial body of evidence indicates that problems with inhibitory gaze control are common in a range of disorders, including ADHD and SpLDs (Everling & Fischer, 1998). This suggests that impaired inhibitory control over visual attention as mediated by direction of gaze may be a widespread contributor to these conditions.

1.2.2. Using the pro/antisaccade task to assess inhibitory control

A well-established task for assessing inhibitory control over gaze-direction is the pro/antisaccade task. First developed by Hallett (1978), the task requires one of two types of responses to be executed following a visual peripheral stimulus: either the participant is to make a saccadic eye movement towards the stimulus (a "prosaccade") or away from it in the opposite direction (an "antisaccade"). The latter relies heavily on inhibitory control mechanisms to inhibit the natural impulse to look towards newly

appearing visual stimuli. Therefore, additional neurological mechanisms are required to make a successful antisaccade that a) suppress the reflexive gaze action towards the stimulus, and b) to invert the visual vector to encode the action of actively making an antisaccade. These mechanisms are discussed in further detail below, and neurological processes governing saccades are described in Chapter 2, Section 2.2.

Individuals with ADHD have been found to perform the pro/antisaccade task with increased directional antisaccadic errors, increased prosaccadic express saccades (see description in Chapter 4, Section 4.3.2) and longer reaction times (RTs) (Chamorro et al., 2021; Feifel et al., 2004; Goto et al., 2010; Hakvoort Schwerdtfeger et al., 2013; C. H. Klein et al., 2003; Y. J. Lee et al., 2015; Munoz et al., 2003; Munoz & Everling, 2004; Yep et al., 2018). This has also been found in people with dyslexia (Biscaldi et al., 2000; Lukasova et al., 2016), reflecting poorer attentional and top-down inhibitory control mechanisms for both conditions.

People with Tourette Syndrome (TS) have slower prosaccadic reaction times (RT) (Jung et al., 2015), but interestingly, participants with TS and without co-occurring ADHD exhibit both greater accuracy and faster antisaccadic RTs than neurotypical controls (G. M. Jackson et al., 2007; S. C. Mueller et al., 2006; Tajik-Parvinchi & Sandor, 2013). This paradoxical finding gives rise to the theory that a compensatory strengthening of inhibitory control to manage tic suppression, as indicated by improvements

solely in antisaccade performance, may confer advantage on the pro/antisaccade task. It also corroborates the existence for additional inhibitory control mechanisms for antisaccade production compared to making prosaccades.

Additional validation for impaired inhibitory control of visual attention in ADHD includes findings showing reduced inhibitory control of voluntary eye movements (Armstrong & Munoz, 2003; Siqueiros Sanchez et al., 2020) and oculomotor dysfunction in both ADHD and SpLDs (Bilbao & Piñero, 2020). Also, a growing body of evidence has demonstrated impaired visual attention mechanisms in dyslexia as well, including a reduced ability for voluntary and involuntary saccadic control and saccadic computation (Bellocchi et al., 2013; De Luca et al., 1999), which could account for individuals with dyslexia experiencing instability of spatial positions of words or numbers on a page (Liddle et al., 2009). Since both ADHD and SpLDs exhibit impaired saccadic systems, likely to relate to poorer attentional and inhibitory control, gaze-control is a potentially useful target for training interventions to improve cognitive control in these conditions.

1.3. Therapeutic interventions for attentional issues and cognitive control training

1.3.1. Current treatment approaches

Current treatments to manage ADHD symptoms typically involve medication or behavioural therapy. Pharmacological treatments include stimulant medications targeting the dopaminergic and noradrenergic systems, such as methylphenidate and amphetamine (K. A. Brown et al., 2018; Faraone, 2018; Storebø et al., 2015; Swanson et al., 2011). An evidence-mapping review by Krinzinger et al. (2019) of long-term effects of methylphenidate (MPH) treatment indicate generally beneficial mental health outcomes. A multimodal treatment study found clear evidence for the benefits of MPH over behavioural treatments (P. S. Jensen, 1999). Although, follow-up studies suggest that effective treatment in childhood, regardless of treatment modality, is associated with better long-term outcomes (Molina et al., 2009). A systematic review of treatments for ADHD by Chan et al. (2016) found clear benefits for pharmacological treatments, but inconsistent benefits for behavioural interventions, including behaviour management, and uses of motivational, academic, organisational, and social skills training.

However, ADHD medication is associated with frequently reported side-effects (e.g., difficulty sleeping, reduced appetite), and not all individuals are responsive to medication (Storebø et al., 2015). Long-term

effects from the use of such stimulants on the developing brain are not yet fully understood, so some parents feel uncomfortable about putting their children on these types of medications (I. Berger et al., 2008). There are also concerns that the medications may become less effective with long-term use (Banaschewski et al., 2004; Storebø et al., 2018; G. J. Wang et al., 2013). Additionally, chronic use and higher dosages of stimulant medication is associated with reduced rates of growth (height and weight) throughout childhood and adolescence; this can be ameliorated with 'drug holidays' (i.e. only taking medications in termtime), but symptom management can worsen whilst off medication (Baweja et al., 2021; Troksa et al., 2019). Indeed, effects of stimulant medications typically wear off in hours, necessitating sustained release formulations to ensure that a single dose remains effective over the school day. This indicates medication is not a 'cure' for ADHD, but rather temporarily normalises brain function.

Furthermore, the misuse of stimulant medication has become an increasing problem that has gained particular attention in the USA, due to their abuse potential from their effects at high dosages (Klein-Schwartz, 2002). Stimulant medications are often used by students as a study aid to improve focus for studying at school and university (Hall et al., 2005; Hartung et al., 2013). There is also evidence for misuse in the workplace to cope with high working demands and long hours (Sales et al., 2019).

Since pharmacological treatment is not necessarily suitable for everyone, or even adequate to address the complexities of ADHD in school

(DuPaul et al., 2011; DuPaul & Stoner, 2014), alternatives and adjuncts to medication are being increasingly explored and sought after. Psychosocial treatment strategies that can be applied at home and school/work have been shown to be successful in the long-term when there is good compliance for the intervention (Antshel & Barkley, 2008; Barkley, 2002; Schultz et al., 2017; Zwi et al., 2012). There is also a growing interest in applying cognitive behavioural therapy as a treatment option for ADHD (C. M. Jensen et al., 2016).

Additionally, mindfulness is a meditative technique that has grown in popularity, which can be practiced in groups or individually and is easily accessible online or on smartphone apps. The aim of the practice is to increase awareness of the 'present moment' to help reduce stress and improve overall mental health and wellbeing. As well as a growing clinical interest in using mindfulness to reduce symptoms of chronic pain and depression (La Cour & Petersen, 2015), mindfulness has also been shown to improve executive functioning including attention (Y. Y. Tang et al., 2012). Bueno et al. (2015) found that a course of mindfulness training over 8 weeks improved sustained attention, quality of life and mood in people with ADHD.

Despite promising effects of mindfulness, long-term research is lacking, and a recent review estimates up to 25 % attrition rates are reported in mindfulness-based intervention studies (in a non-ADHD sample) (D. Zhang et al., 2021). Thus, there may be increased compliance

problems in using mindfulness and behavioural strategies in people with ADHD, who already have poorer sustained attention and focus as outlined in Section 1.1.1. Therefore, there is a need for different approaches and new types of interventions tailored for ADHD to be developed to help with symptom management.

1.3.2. Cognitive training and computer-based games

Some interesting neuromodulatory methods are now being explored, such as cognitive training designed to produce long-term changes in neural systems underpinning cognitive function. Evidence that cognitive control responds to training include neurological findings from a longitudinal study that has shown during an inhibitory control Colour-Word Stroop task, there was increased activation in cognitive control network regions bilaterally (supplementary motor cortex (SMA)/pre-SMA, anterior cingulate cortex, insula, and precentral and inferior frontal gyrus (IFG)) detected using fMRI in musically trained children compared to non-trained peers after two years (Habibi et al., 2018; Sachs et al., 2017). A continuation of this study showed that after four years, the musically trained group compared to the control group had: larger activations in the right IFG only during the Stroop task; chose larger, delayed rewards in the delayed gratification task; and significant accuracy improvements in the Flanker task compared to the beginning of the study (Hennessy et al., 2019). This suggests that involving children in extra-curricular activities such as learning to play a musical

instrument may strengthen different neural pathways that mediate different cognitive control processes in the brain.

There is now a large body of research indicating that individuals who regularly play video games excel in cognitive tasks compared to non-gamers, suggesting enhanced attentional processing has developed in these individuals (as reviewed by Bavelier & Green, 2019). This includes evidence for increased cognitive flexibility and task-switching capabilities (Glass et al., 2013; Green et al., 2012); effects that have been found even in older adults (Basak et al., 2008).

Research findings have uncovered more efficient cognitive processing abilities in "gamers" compared to non-gamers, as depicted by faster reaction times without compromising accuracy (Dye et al., 2009; Pardina-Torner et al., 2019). Additionally, gamers have been found to have better discrimination task performances than non-gamers, indicating better multisensory processing and alerting responses (Donohue et al., 2010). Improved orienting response capabilities are also evidenced by better selective visual attention and inhibition of distractor information (Hubert-Wallander et al., 2011; Wu et al., 2021). Professional or elite gamers also perform better in visuospatial tasks and selective or sustained attentional tasks compared to amateur gamers and non-gamers (Benoit et al., 2020; Boot et al., 2008). However, evidence from these observational studies do not necessarily imply that gaming activities improve attention; it may be

the case that those with enhanced attentional skills are more likely to be enthusiastic gamers.

This brings about the question of whether computer-based training could improve cognitive performance in non-gamers, particularly those with impaired aptitude in the attentional skills required for these games. Action video game training in non-gamer young adults has resulted in increased processing efficiency and enhanced performance in a wide range of visual attentional elements (Achtman et al., 2008; Green & Bavelier, 2003, 2006). Even older adults who have participated in computer game training paradigms have presented better task-switching, visuospatial processing, working and visual short-term memory capabilities (Basak et al., 2008), as well as selective visual attention (Belchior et al., 2013). This suggests that these types of cognitive training paradigms target neuroplasticity long after childhood developmental stages, when brain plasticity is greatest.

However, not all studies show significant improvements following training. For instance, no differences in cognitive abilities were observed following the longitudinal computer-based training (21.5 hours over 4-5 weeks) used by Boot et al. (2008), except for object rotation. This could be due to differences in the types of games and tasks used between the studies that may not all be suitable for eliciting cognitive control improvements. Establishing an 'exposure-response' curve (akin to a dose-response curve) would also be helpful to quantify the exposure of games for detectable cognitive improvement.

Furthermore, not all computerised training programs produce changes in cognitive function that transfer to real-life skills. Astle et al. (2015) and Barnes et al. (2016) found both improvements in working memory and enhanced intrinsic state brain connectivity and cross-frequency phase amplitude coupling measured with magnetoencephalography (MEG) in children who had undertaken the working memory training program CogMed. However, a meta-analysis of effects of CogMed training found no evidence for transfer to actual working memory dependent academic tasks, e.g., maths (Aksayli et al., 2019). One reason may be that these games may not be ideally designed for their purposes.

Habgood & Ainsworth (2011) proposed that an "intrinsic integration" of training goals with game goals may be key to effective educational games ("edutainment"). Intrinsic game rewards should be integrated with the training goal rather than the "chocolate-covered broccoli" approach. This analogy is used by Habgood & Ainsworth (2011), whereby a helpful but unappealing task (the healthy "broccoli") is made more palatable by a separate reward/activity (the non-nutritious "chocolate") that the child "earns" by success on the training game. Therefore, internal rewards from the game activity itself should make external rewards unnecessary. If the training goals are intrinsic to the game goals, no external reward is required, thus the training becomes rewarding and engaging in itself without feeling like it is an obligatory educational or training task. Using this approach, they designed a math-teaching game for children. They found

that it not only produced greater skill gains for time spent training than a traditional approach, but that children voluntarily spent additional time training (Habgood & Ainsworth, 2011).

1.3.3. Computer and video game cognitive training in ADHD and SpLDs

Curiously, no significant differences in commercial video game performance have been reported between people with ADHD diagnoses and those without, which supports parental anecdotes and preliminary experimental reports for a lack of observed ADHD symptoms in children whilst they are engaged with video games (R. Shaw et al., 2005). This, along with general findings of improved cognitive control abilities in gamers, highlights the potential for exploring the development of computer-based games as a platform to improve cognitive performance in both ADHD and SpLDs.

A large body of work by Franceschini and colleagues have researched the benefits of using action video game training in dyslexic Italian children to improve skills including visuospatial attention, reading speed (without compromising accuracy), phonological decoding and short-term memory (Bertoni et al., 2021; Franceschini et al., 2012, 2013; Franceschini & Bertoni, 2019). These findings have been further corroborated in an English-speaking sample (Franceschini et al., 2017), and also from action video game training in a French-speaking adult sample without dyslexia

who showed improved reading skills and visual attention span (Antzaka et al., 2017).

Action video games require strong gaze-control skills and are thought to encompass a wide-range of visual attention abilities that are necessary for reading (as reviewed by Franceschini et al., 2015), which could account for why these attentional and reading skill improvements were not observed in groups training on non-action video games (Bertoni et al., 2021; Franceschini et al., 2017). Despite these observed advantages, less than a quarter of the currently available technology-based reading interventions reviewed by Jamshidifarsani et al. (2019) were gamified or game-based. A more recent randomised control trial (RCT) with English-speaking dyslexic children using an action video game resource found that the groups who used eye-tracked responses or a mouse improved on reading domains for comprehension, accuracy and speed, when compared to controls who did not train (Peters et al., 2021). Therefore, this provides further support in using gamified visual attention training to benefit reading skills.

Many RCTs using computer-based training paradigms in ADHD samples have been conducted to target working memory, which have evidenced positive findings for better working memory (Holmes et al., 2010; Klingberg et al., 2002) as well as improved behavioural/parent-rated improvements in ADHD symptoms (Beck et al., 2010; Klingberg et al., 2005; Mezzacappa & Buckner, 2010). However, a meta-analysis for cognitive training in individuals with ADHD presented improvements in working

memory only rather than modulating ADHD symptoms (Cortese et al., 2015). Some RCTs have failed to uncover any signs of cognitive improvements following computer-based training programs in ADHD individuals (Bikic et al., 2015, 2018). These mixed results could be attributed to issues in the RCTs investigating computer-based training resources for ADHD, including bias in unblinded raters and inappropriate or unsuitable scales, as reported by meta-analyses and systematic reviews (Rapport et al., 2013; Strahler Rivero et al., 2015). Better blinding procedures in RCTs are also required to validate the use of computer cognitive training regimes (Sonuga-Barke et al., 2014).

Additionally, the nature of the type of game within the computer-based training is important as discussed by Craven & Groom (2015), whereby stop-signal and Go/No-go tasks may be more effective at targeting inhibitory control, which would be more likely to have a beneficial impact at ameliorating ADHD symptoms. This may account for why the majority of RCTs using working memory tasks only found improvements in this one domain, because these types of tasks have been less effective at targeting general inhibitory control mechanisms, so there has been a lack of beneficial impacts for improving a wider range of ADHD symptoms observed. Examples of more recent RCTs using tasks more relevant to inhibitory control have been more successful. Meyer et al. (2020) found inhibitory control training (using a stop-signal task) lowered resting-state theta, improved inattention (but not hyperactivity), and improved parent ratings for symptoms in ADHD children compared to the non-trained ADHD group.

1.3.4. RECOGNeyes

Elizabeth Liddle, Peter Collins and Jacob Habgood (P. Collins, 2016) developed a computer game called RECOGNeyes (remediating control of gaze: neuro-education for your eyes) designed to improve inhibitory gaze-control in ADHD and other disorders that implicate impaired inhibitory gaze control. The RECOGNeyes game is played using an eye-tracker, so that the gameplay is controlled by your direction of gaze instead of a joystick or mouse. It includes a range of oculomotor tasks, including resisting distractors, making antisaccades, cancelling or delaying attentional shifts, and exercising selective attention. Activities adjust in difficulty as skill improves. They reasoned that inhibitory gaze-control is implicated in both key domains of impairment in ADHD: control of attention and inhibitory motor control (over eye movements). The game aims to train poor fixation control, weak inhibition of premature eye movement or impulsive gaze shifts to distractors. The game developers also reasoned that gaze-control training should benefit reading, and especially target reading difficulties arising from poor saccadic control.

An RCT conducted to validate RECOGNeyes training by García-Baos et al. (2019) included children with ADHD, where the test group included playing the game using the eye-tracker and the control group used a mouse instead. The study found significant improvements in reaction time, impulsivity, and fixation gaze-control in the eye-tracker group only. Improvements in eye movement control during reading was also a key

transfer skill only observed in the eye-tracker group. In the word-recognition task, the eye-tracked group displayed improvements in longer fixation duration and reduced number of fixations, as well as faster RTs for long and short words. This indicates that using eye-tracked responses in the oculomotor tasks engages visual attention networks that enhanced overall attentional skills, which could potentially transfer to real-life skills such as reading.

Other gaze-control interventions aiming to target attentional functioning in ADHD include a gaze-control preventative measure for infants with a high risk of familial ADHD (Goodwin et al., 2016; Wass et al., 2011). There has also been a gaze-control program used in a preliminary investigation that has not been through RCTs or validation studies (Al-Shathri et al., 2013). More recently, Lee et al. (2020, 2021) developed an eye-tracked computer-based training program and found that ADHD children improved RT and accuracy for both prosaccade and antisaccade responses and improved on a battery of inhibitory control tasks (e.g. Flanker test), but no significant changes were observed in the control group that did not train. No physiological measures (e.g., neurophysiology and autonomic responses) were recorded from these studies though, which warrants these measures to be incorporated into future investigations, as supported by the authors. This, in combination with the aforementioned dyslexia interventions, shows how gaze-control training paradigms present a novel and engaging way to improve attention that could translate into real-life

skills in reading letters and numbers, the ability to follow instructions, sustained concentration and vigilance for focussing on tasks.

1.4. Thesis research scope and rationale

In summary, the current interventions for ADHD and SpLDs include pharmacological-based treatments and behavioural-based strategies. However, the heterogenous presentations of these diagnoses mean that the current treatment approaches may not be suitable for all, and compliance for behavioural and mindfulness approaches may be especially more difficult in younger children. Therefore, there is a growing interest and demand for therapeutic alternatives or adjunct interventions for ADHD and SpLDs. This includes computer-aided cognitive training (such as RECOGNeyes) to modulate effective long-term changes in cognitive control networks that could translate into positive real-life behavioural changes.

Furthermore, in the current age of computer interfaces as a prevalent medium, establishing computer and video game training programs could pave the way for similar therapeutic resources being available for a range of conditions that also exhibit attentional deficits, e.g., psychiatric, neurodegenerative, and other neurodevelopmental disorders. These computer-based technologies also have the potential to identify behavioural/physiological biomarkers for quantifying symptomology that could be incorporated into diagnostic tools. As well as educational and

clinical use, there may also be interest within the general population. Gaze-control training could be applied to improve overall attention and inhibitory control functioning in individuals without ADHD/SpLD diagnoses to optimise increasing work and educational performance demands in the modern technological world along with the ever-increasing distractors in our environment.

This thesis reports on a study designed to examine the effects of RECOGNeyes gaze-control training on neurophysiological and behavioural correlates of performance during a pro/antisaccade task in young adults with diagnoses of ADHD and/or an SpLD, and to evaluate changes in underlying inhibitory control mechanisms. Behavioural measures will include assessments of task performance as well as eye-movement efficiency during reading. Neural correlates to be investigated include phasic autonomic nervous system effects by measuring pupillometry and heartrate, as well as central nervous system electrophysiological correlates measured using magnetoencephalography (MEG).

1.5. Thesis outline

To address my thesis research scope described in Section 1.4, I first describe and review key background information in Chapter 2 regarding the autonomic nervous system and arousal and central nervous system brain regions involved in inhibitory control, including nodes of the visual

attention network. I next provide an outline of the methodological and experimental details of the RECOGNeyes study in Chapter 3. This is followed by a chapter describing the sample characteristics and baseline measures (including ADHD, general mental wellbeing and reading metrics) in Chapter 4. Behavioural and task performance measures such as reading indices, task reaction time and accuracy, as well as RECOGNeyes training compliance are also addressed in Chapter 4.

Chapters 5, 6, and 7 cover the results of the neurophysiological assessments undertaken to investigate inhibitory control mechanisms during the pro/antisaccade task, particularly in regards to anticipation and preparation for responding to a stimulus. This includes presenting the autonomic measures of pupillometry and heartrate to assess arousal, alerting and orienting responses in Chapters 5 and 6, respectively. Central nervous system neurophysiological responses in visual attention network brain regions measured via MEG are evaluated in Chapter 7. Finally, I summarise the overall implications and impact of the findings from this research in Chapter 8. This includes considering how this research provides a novel contribution of knowledge to the scientific community, and how it could aid the development of interventions to ameliorate attentional problems experienced in ADHD and SpLDs.

Chapter 2: The autonomic and central nervous system

2.1. The autonomic nervous system and arousal

2.1.1. Sympathetic and parasympathetic nervous systems

The term arousal is defined as the overall state of alertness, awareness, and wakefulness for the priming of physiological and psychological processes to enable an individual to optimally prepare for responding to internal and external environmental stimuli. Levels of arousal are mediated by interactions of both the central and peripheral nervous systems.

The autonomic nervous system (ANS), as part of the peripheral nervous system, is responsible for facilitating reflexive and involuntary autonomous bodily functions associated with different arousal states. The ANS is further divided into two branches, namely the sympathetic (SNS) and parasympathetic (PNS) nervous systems, respectively. Historically, these divisions have been functionally defined based on the bodily reactions for the SNS "fight or flight" or PNS "rest and digest" responses. Physiological mechanisms within the SNS mediate bodily changes to promote increased muscle oxygenation to prepare for action of fleeing,

fighting or fear response, which includes: raising heart rate, vasodilation, widening bronchial lung passages, sweat gland activation, pupillary dilation, reducing gut motility and closing the bladder sphincter (Bear et al., 2007). Conversely, the PNS favours energy restoration, growth and repair mechanisms as well as directing blood flow to the digestive organs, thus encompassing the following responses: increasing gut motility, stimulating salivation, bladder contraction, constricting bronchial lung passages, slowing heartrate and pupillary constriction (Bear et al., 2007). The evolutionary development of these autonomic branches were therefore vital to mediate core behaviours of feeding, predation and reproduction for survival.

Physiological differences include the mechanism of action at effector organs. PNS responses involve the cholinergic action of acetylcholine (ACh) at muscarinic receptors, whereas the SNS involves adrenergic norepinephrine/noradrenaline (NE) and adrenaline/epinephrine signalling via alpha (α) or beta (ß) adrenoceptors (ADRs). Both autonomic branches are centrally controlled by the hypothalamus but parasympathetic-mediated effects are relayed by cranial nerves that arise from the brainstem and lower portion of the spinal cord ("craniosacral"), whereas sympathetic-mediated effects are from middle spinal cord nerve connections ("thoracolumbar") to the sympathetic column that project to the effector organs (see examples in Figure 1).

Furthermore, individual organs can have multiple sympathetic and parasympathetic influences. As depicted in Figure 1, the eye has pupillary dilation and constriction effects, the extent of which is mediated by both the pupillary light reflex, cognitive control, and arousal mechanisms (Ebitz & Moore, 2017, 2019); also refer to Section 2.1.2. The eye also has the accommodation reflex for sharper focus at short distances mediated by autonomic nerves (Mathôt, 2018). PNS responses to light are thought to be mediated primarily by direct constriction pathways via the Edinger-Westphal nucleus that projects to the oculomotor nerve (III) (Mathôt, 2018). However, SNS responses are generally mediated from subcortical locus coeruleus (LC) and hypothalamic projections to sympathetic nerves that innervate the visual system (Mathôt, 2018), which is why the extent of pupil dilation is usually accepted as an index of sympathetic arousal (see further discussion in Section 2.1.2).

The heart also has a range of autonomic effects. The medulla in the brain is a key cardiac integration centre of afferent information primarily from the vagus nerve to the cortex, as well as mediating PNS and SNS cardiac responses (Shaffer et al., 2014). The heart has a unique autorhythmic pacemaker mediated primarily through the sinoatrial (SA) node, but also the atrioventricular (AV) node (see Figure 1), to elicit electrical activity in the heart (Shaffer et al., 2014). At rest, the PNS acts to slow this intrinsic myogenic rhythm to reduce the depolarisation of the nodes and cardiac muscle conduction, whereas SNS cardiac influences all contribute to amplify cardiac output for increasing oxygenated blood to be

delivered to the muscles. Therefore, multiple autonomic effector junctions mediate different aspects and work together to contribute to an overall increase or decrease in cardiac output by acting upon: rate of heartbeats, contraction force of how hard the blood is expelled from the heart, and speed of conduction between the nodes, nerves, and muscle fibres of the heart. However, the mechanisms influencing autonomic control of the heart also relate to cognitive control and arousal responses (see Section 2.1.2).

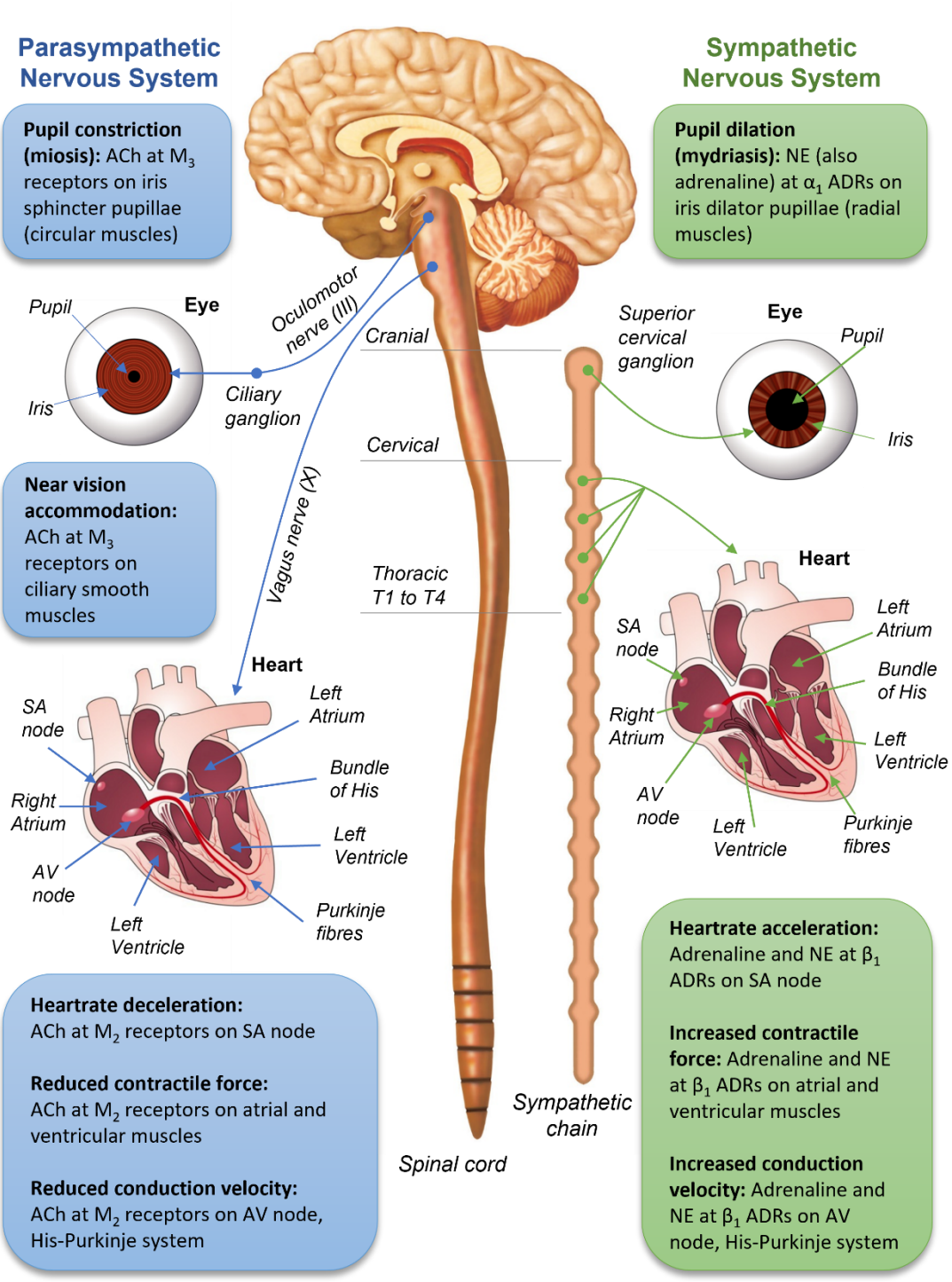

Figure 1: Projections and effects of the SNS and PNS on the heart and eyes.

This figure contains collated information to illustrate an overview of the autonomic effects on example organs, the heart and eyes (Bear et al., 2007; Brodde et al., 2001; Brodde & Michel, 1999; Mathôt, 2018; McAuliffe-Curtin & Buckley, 1989; Woldemussie et al., 1993). Abbreviations, SA node: sinoatrial node; AV node: atrioventricular node; ACh: acetylcholine; M_2 and M_3: muscarinic receptor subtypes 2 and 3; NE: norepinephrine; α_1 and β_1 ADRs: alpha and beta subtype 1 adrenoceptors. Bracketed roman numerals are the corresponding cranial nerve numbers.

2.1.2. Arousal, orienting and alerting and links to attentional processing

Increased arousal levels are important to prepare both your body and mind for anticipating or responding to a particular stimulus in the environment. The regulation of arousal is vital for many cognitive processes, such as attention, consciousness, information processing, emotion, motivation, and perception. An appreciation for the importance of a balance in arousal levels for optimal functioning is depicted by the inverted U-shaped curve of arousal and performance from Yerkes & Dodson (1908). Levels that are too low induce a fatigued or distractible state, whereas too much arousal causes an anxious, fearful, and panicked state; both of these extremes impair performance.

In the adaptive gain theory first proposed by Aston-Jones & Cohen (2005), there are two modes of arousal modulation, namely tonic and phasic. Tonic background arousal is important for 'exploratory' mode, when we are investigating new information and stimuli in the environment. In contrast, rapid phasic arousal occurs in 'exploitation' mode, when we optimise focus and sustain attention and relevant responses for a specific task. Aston-Jones & Cohen (2005) proposed that adaptive switching between the tonic and phasic modes is mediated by tonic and phasic neuronal firing from the locus coeruleus (LC), respectively. Additionally, it has since been suggested that the transition between these modes is more gradual than first

proposed, whereby these modes may lie on either end of on a "continuum" (Gilzenrat et al., 2010).

The LC is a brainstem nucleus in the pons region that is the sole source of NE (the main neurotransmitter in the SNS, described in the previous section) in the central nervous system (CNS); noradrenergic projections are found in the majority of the brain, including higher cortical regions (Berridge & Waterhouse, 2003; Waterhouse & Navarra, 2019). This wide innervation area implicates the LC in neural processes such as those governing sensory processing and arousal (Berridge & Waterhouse, 2003; Foote et al., 1983; Foote & Berridge, 2019; Samuels & Szabadi, 2008a, 2008b; Waterhouse & Navarra, 2019). These reviews include discussion of earlier animal work by Aston-Jones, Foote and colleagues who directly measured rates of LC neuronal discharge through electrodes, whereby tonic firing was greatest during novel sensory information and high-frequency phasic firing was observed during alerting stimuli. Continuing research of LC-NE activity shows its function is not only relevant for levels of wakefulness, but its role in arousal and alertness influence higher cognitive functioning like attention, perception and memory (Sara & Bouret, 2012).

The Alerting network, as mentioned previously in Chapter 1, Section 1.2.1, by the work of Posner and Petersen (Petersen & Posner, 2012; Posner & Petersen, 1990) involves arousal mechanisms that maintain optimal vigilance during tasks and for responding to new stimuli. Although the alerting and orienting responses are separate systems, they work together

in real-world scenarios to alert us *when* a stimulus appears (temporal information) and to orient us towards *where* the stimulus is (spatial information), respectively (Fan et al., 2002, 2009; Fernandez-Duque & Posner, 1997).

Differences between the alerting and orienting responses are believed to be mediated by their respective neurochemistry mechanisms. For instance, using the α_2-ADR agonist Clonidine in human subjects (which decreases axonal NE release and reduces LC firing) reduces arousal and attentional performance (Smith & Nutt, 1996), which has been specifically related to poorer alerting responses (Coull et al., 2001). Overall perceptual ability including stimulus detection and accuracy are improved with Reboxetine (NE re-uptake inhibitor that increases NE signalling) and impaired with Clonidine, but these drugs did not affect decision making bias (Gelbard-Sagiv et al., 2018). There is also evidence for Clonidine slowing down saccadic reaction times (Smith et al., 2003), thus implying that dampened NE signalling impairs the alerting responses required for fast saccadic responses.

In summary, these findings indicate a key role of NE in the alerting response. This directly complements the LC-NE model, whereby LC-NE activity influences the alerting response for maintaining vigilance and optimal arousal levels. Increases in LC-NE activity are reflected via rapid SNS noradrenergic-mediated autonomic responses, measured via increased pupil dilation (see Chapter 5) and skin conductance (electrodermal/galvanic

response) (Bast et al., 2018; Einhäuser et al., 2010; Geva et al., 2013; Gilzenrat et al., 2010; Howells et al., 2010; Jepma & Nieuwenhuis, 2011; Joshi et al., 2016; Joshi & Gold, 2020; C.-A. Wang et al., 2018; Wass et al., 2015).

Conversely, the orienting response appears to be more influenced by cholinergic neurotransmission. Injections of the muscarinic receptor antagonist Scopolamine were administered into the monkey lateral intraparietal area (a region thought to mediate visuospatial processing, see Section 2.2.4) to reduce ACh signalling, which resulted in impairing the orienting ability of shifting attention to a stimulus (Davidson & Marrocco, 2000). Human subjects that took Scopolamine demonstrated a reduced ability to filter out distractor information, which indicates an involvement of the cholinergic system in top-down visual attention processes (Laube et al., 2017). Additionally, the cholinesterase inhibitor Donepezil (resulting in increased synaptic ACh) administered to human subjects improved their ability to utilise spatial cue information, which led to better voluntary (but not involuntary) attentional performance (Rokem et al., 2010).

Where noradrenergic action is thought to mediate bottom-up cue detection (i.e., alerting), cholinergic action is more related to top-down processing (i.e., orienting) (Yu & Dayan, 2005). This role of ACh in the orienting of attention is further complicated by the proposed role of different cholinergic receptors synergistically working to modulate levels of top-down and bottom-up processing. In this way, ACh neurotransmission is suggested

to mediate the weighting given to prior expectations through muscarinic receptor action (top-down processing), whereas incoming stimuli information (bottom-up processing) is believed to be more associated with nicotinic receptor activation (Greenwood et al., 2009; Hasselmo, 2005). Research regarding these complex top-down and bottom-up dynamics is still ongoing (Lockhofen & Mulert, 2021).

During the orienting response, the heartrate decelerates (a PNS-mediated response, described in Section 2.1.1) in which activation in the vagal nerve, the principle nerve of the PNS, induces cardiac slowing. This effect has been termed "cardiac orienting" and is believed to contribute towards stimuli detection and learning mechanisms (Graham & Clifton, 1966; Graham & Jackson, 1970; J. C. Jackson et al., 1971). Porges' polyvagal theory describes a phylogenetic addition to the classical autonomous SNS and PNS survival responses in mammals that is facilitated by the myelinated vagus (in addition to the evolutionary older unmyelinated vagus), along with increased cortical pathways to the brainstem (Porges, 2001, 2007, 2011). Compared to other organs, the vast majority of nerves in the vagus (60-80 %) are afferent, meaning these fibres carry sensory information from the heart and other major organs back to the brain (Yuan & Silberstein, 2016). This communication pathway between the vagus nerve, brainstem and higher cortical regions facilitates a "vagal brake" that enables a way to self-regulate and adapt our behaviour, inhibitions, social interactions and emotional responses (Porges, 2001, 2007, 2011).

Furthering this idea, Thayer and colleagues outlined the Neurovisceral Integration Model, describing a "central autonomic network", whereby the time taken between beats, assessed via heartrate variability (HRV), is thought to reflect the integration of environmental, social, and behavioural cues from top-down and bottom-up information; hence, linking with attention and goal-directed behaviour (Thayer et al., 2009, 2012; Thayer & Lane, 2000). HRV is therefore thought to be indicative of cortical and executive functioning, mediated by complex brainstem communications via midbrain structures to higher cortical regions, which are outlined further by McCraty (2011). As summarised by Shaffer et al. (2014), greater HRV is indicative of cognitive flexibility due to the constant change required for adaptation to the environment and mediating behaviours, whereas low HRV can be found in a range of medical and psychiatric conditions (e.g., anxiety and depression). Overall, these models outline a complex mechanism that merges the CNS and ANS rather than considering cardiac control a purely ANS physiological response.

The action of vagal nerve fibres are much faster than the action of SNS fibres innervating the heart (Bigger et al., 1989; Nunan et al., 2010). This means rapid changes in HRV reflect changes in parasympathetic drive, characterised as the high-frequency band of the heart rhythm (Shaffer et al., 2014), whereas slower changes indicate changes in sympathetic drive. Additionally, animal studies have found that direct stimulation of LC neurons increases inhibitory signals to the brainstem cardiac vagal neurons, thus representing an antagonistic mechanism on the vagal brake

(X. Wang et al., 2014). Trial-wise correlations of pupil size with heartrate and skin conductance measures found that pupil size correlated positively with both, whereby skin conductance indexed SNS activity and heartrate increase indexed PNS withdrawal (C.-A. Wang et al., 2018). Hence, this supports that increases in HR ascribable to parasympathetic withdrawal align with arousal indices and reaffirms the previous discussion that pupil size is used to indicate LC-NE mediated arousal changes, including release of the vagal brake. Notably however, during anticipatory orienting to a stimulus, both pupil dilation and HR deceleration occur, indicating co-active, rather than reciprocal, SNS and PNS involvement in the orienting response (Berntson et al., 1994; Bradley et al., 2012).

To summarise, this dynamic balance of cardiac function is implicated in the orienting responses of attention, processing of sensory information, self-regulatory behaviour and implied interactions with the LC-NE arousal system (see Chapter 6).

2.1.3. Arousal and attentional disorders

Problems in regulating levels of arousal are observed in a number of medical conditions and diagnoses. For instance, in ADHD, hypoarousal is thought to contribute to cognitive difficulties for sustaining attention, executive functioning and response inhibition. Specifically, measures of autonomic functioning point to hypoarousal in ADHD, especially during mentally demanding tasks involving inhibitory control, or monotonous

tasks requiring sustained attention, as summarised in the recent review by Bellato, Arora, Hollis, et al. (2020). Also, there is evidence at rest for reduced skin conductance levels, and some findings from heartrate monitoring, that further indicate an underactive ANS in ADHD (Bellato, Arora, Hollis, et al., 2020). This also fits with neurophysiological observations of atypical resting state activations of the default-mode network (DMN) in functional magnetic resonance imaging (fMRI) data (Rubia, 2018) and increased slow wave oscillations in electroencephalography (EEG) data (Barry et al., 2003), indicating both an underactive ANS and CNS.

This contrasts with Autism Spectrum Disorder (ASD), where investigations of arousal levels at rest generally present findings of hyperarousal (Arora et al., 2021). Observations of greater phasic pupillometric arousal responses point to an overactivated LC-NE system in ASD (Blaser et al., 2014; Lynch, 2018). Also, there are differences in EEG resting-state findings, whereby reduced absolute and relative resting-state occipital alpha power has been found in ASD and ADHD, respectively (Bellato, Arora, Kochhar, et al., 2020). However, it is not as simple to define ADHD and ASD as opposite ends of a spectrum, where the former exhibits hypoarousal and the latter hyperarousal, since the diagnoses often co-occur (as recognised by the joint ASD-ADHD diagnosis in the *DSM-5*; refer to discussion in Chapter 1, Section 1.1.2). Also, the specific resting-state observations for the ADHD and ASD groups from Bellato, Arora, Kochhar, et al. (2020) described above were both observed in cases of a co-occurring diagnosis. A recent study conducted with ADHD and ASD individuals found

that measures of HRV supported hypoarousal in ADHD and hyperarousal in ASD, but interestingly regardless of the diagnosis, there were increased autistic symptoms in subjects with HRV measures showing hyperarousal (Bellato, Arora, et al., 2021). Therefore, the mechanisms mediating atypical arousal effects in these diagnoses are complex and not fully understood.

A theory for the observed inappropriate arousal levels and dysregulated cognitive behaviours exhibited in ADHD is atypical catecholaminergic (NE and dopamine (DA)) neurochemistry in the prefrontal cortex (PFC), which results in an imbalance of appropriate receptor activation. It is supported that different types of ADR activation account for simultaneous autonomic and cognitive effects from modulations in LC-NE arousal levels, i.e., α_2-ADR activation in the PFC mediates better top-down processing, but α_1- and ß-ADRs are associated with bottom-up processing (Arnsten & Pliszka, 2011; Lockhofen & Mulert, 2021; Thiele & Bellgrove, 2018).

Furthermore, dopaminergic-mediated effects on top-down modulation occur specifically at D_1 dopamine receptors (D_1Rs) in deep cortical layers, compared to D_2Rs (Arnsten & Pliszka, 2011; Lockhofen & Mulert, 2021; Thiele & Bellgrove, 2018); including top-down modulation of the visual cortex via the frontal eye field (A. Mueller et al., 2020). As depicted by Arnsten & Pliszka (2011), this relationship is akin to the Yerkes-Dodson curve, whereby a *fatigued* state is related to insufficient D_1R and α_{2A}-ADR activation (i.e., hypodopaminergic/hyponoradrenergic

signalling in ADHD), an *alert* state has moderate DA and NE levels to activate D_1Rs and α_{2A}-ADRs (i.e., phasic arousal and optimal top-down cognitive control), whereas a *stressed* state is associated with excessive DA and NE activating D_1Rs and α_1/ß-ADRs (i.e., high tonic release of catecholamines or high stimulant dosage).

Due to the involvement of DA in neurocognitive reward pathways, a *fatigued* state of low DA in ADHD is consistent with theories of dysfunctional reward and impaired motivation mechanisms in the ADHD brain. For instance, findings show that people with ADHD have greater sensitivity towards delayed rewards (Plichta et al., 2009; Tripp & Alsop, 2001). This aligns with the increased likelihood to seek smaller immediate rewards rather than wait for larger delayed rewards, as evidenced by steep temporal reward discounting observations in combined-type ADHD (Scheres et al., 2010). Hence, this indicates delay aversion behaviour when processing delay-reward trade-off decisions.

Moreover, this impaired reward response in ADHD implicates the poor processing of positive feedback in performance regulation and reduces behavioural motivation for longer-term actions and consequences. This also coincides with task behaviour performance that reflects poor error monitoring, including reduced fronto-central error positivity (Pe) amplitude and abnormal theta power modulations from EEG data (Groom, Cahill, et al., 2010). A recent systematic review and meta-analysis by Bellato, Norman, et al. (2021) revealed general findings in the literature for reduced

error-related negativity (ERN) and Pe amplitudes in ADHD, indicating poorer performance monitoring neurological mechanisms. Moreover, these observations taken together could account for compensatory maladaptive behaviours presented in these individuals to increase arousal levels, such as engaging in sensation seeking and hyperkinetic activities (Geissler et al., 2014; Sergeant, 2005), that account for some of the negative outcomes discussed in Chapter 1, Section 1.1.3.

The understanding of the neurochemistry regarding the involvement of DA and NE in the mediation of ADHD symptoms is confirmed by research investigating the actions of stimulant medications, most notably methylphenidate (MPH). MPH acts to inhibit dopamine and noradrenergic transporters, which prevents its re-uptake back into neurons, resulting in prolonging their synaptic actions at their respective receptors (Faraone, 2018). Examples of MPH effects include improving reward and motivational responses in ADHD individuals, as well as improved modulation of task-related DMN activation and electrophysiological markers of attention and response conflict (P3 and N2) (Groom et al., 2013; Groom, Scerif, et al., 2010; Liddle et al., 2011). In addition, taking MPH improves sustained attentional control in ADHD by directly acting on top-down cognitive control rather than sensory bottom-up processes (Dockree et al., 2017; Swanson et al., 2011).

This mechanism of action is also supported by low-dose microdialysis of MPH in rats increasing NE and DA signalling in the PFC rather than in

subcortical regions, which corroborates a specific cortical therapeutic action of MPH to improve top-down cognitive control (Berridge et al., 2006). Since the observed actions of MPH are facilitated via both DA and NE neurotransmitter systems, this implies a mechanism of action of MPH to 1) increase cognitive control via enhancing the action of both catecholamines, 2) modulate reward and motivation pathways via increased DA, and 3) optimise arousal levels through NE. Therefore, interventions targeting both a balance of the regulation of arousal as well as higher cognitive control mechanisms (i.e., targeting both the ANS and CNS) could contribute to improved symptom management, including attention and inhibitory control functions.

Overall, both ANS and CNS interactions contribute to observed symptomology found in ADHD, ranging from the impaired reward and motivation systems to response regulation, attention, and arousal. However, these CNS and ANS interactions are complex and yet to be fully understood, and models of arousal and executive dysfunctions are still being explored (Martella et al., 2020). They require more study and scrutiny using multi-modal methods to evaluate and characterise markers from both the ANS and CNS. Therefore, including ANS measures as indices of arousal warrants further investigation to strengthen our understanding about attentional deficits, provide new objective methods for diagnosis and how these nervous system features could be modulated to help with symptom management and improve attentional functioning.

2.2. The central nervous system and visual attention network

2.2.1. Overview of the visual attention network in the context of saccadic production

Brain regions specifically involved in the execution, processing, and planning of eye movements, including saccades, have been defined as belonging to the oculomotor network. These regions, and those encompassing a wider visual attention network, are depicted in Figure 2, based on findings from activated areas observed in functional imaging, electrophysiological and computational studies (Coe et al., 2019; Coe & Munoz, 2017; Jamadar et al., 2015; Munoz & Everling, 2004; Pierrot-Deseilligny et al., 2003; Sharma et al., 2011). The anterior insula and anterior cingulate cortex (ACC) are not directly connected to being a part of the oculomotor network, but they are nodes in the salience network that contribute to the visual attention network processing described in this chapter.

The oculomotor network first receives visual input from the retina, where signals are sent to early visual processing brain regions. This includes the primary visual cortex (V1) that receives visual information via the retino-geniculo-cortical pathway. V1 then projects to parietal and frontal cortical regions, as well as communicating back to the superior

colliculus (SC) (as illustrated in Figure 2). V1 neurons are also able to encode and predict the visual properties of a stimulus including contrast and orientation (Gawne, 2000). Research has also demonstrated the involvement of V1 in programming spatial information, particularly in regions representing the peripheral visual field (Jack et al., 2006). Additionally, V1 receives top-down modulation during attentional tasks (Martin et al., 2019), as well as predicting visual detection task performance (Ress et al., 2000). More recently, fMRI findings have implicated V1 in task-related arousal changes, whereby endogenous V1 activity corresponds to similar temporal dynamic changes in heartrate and pupil size (Roth et al., 2020).

The other main brain region that receives visual input via the retinotectal pathway is the superior colliculus (SC); a key structure involved in mediating saccadic activity (Gandhi & Katnani, 2011). The SC resides in the midbrain and contains multiple input and output pathways connected to the visual system, midbrain, brainstem, and cortical regions (as illustrated in Figure 2). Also, because of its early involvement in visual processing and executing saccades, it is now thought that express saccades are mediated by the SC, since pre-saccadic activity in monkey SC neuron recordings have been shown to predict express saccades (Marino et al., 2015); for details regarding express saccades, refer to Chapter 4, Section 4.3.2.

The SC can be further divided into superficial and intermediate layers (SCs and SCi, respectively) that communicate with one another, but are thought to perform specific roles to contribute to overall SC functionality. The SCs portion receives visual input from the retina and V1, where it is also thought to encode visual saliency (B. J. White et al., 2017). On the other hand, the SCi portion communicates with frontal, parietal and subcortical regions (Coe et al., 2019). The SCi has a retinotopic arrangement, whereby specific spatial visual input is encoded by activating specific SCi neurons, and this information is utilised to mediate saccadic eye movement signals to the extra-ocular muscles to perform correct pro- or antisaccades (D. A. Robinson, 1972). Due to this combination of roles, particularly in processing input and output signalling within the oculomotor network, the SC is believed to serve as an essential hub region for orchestrating automatic, voluntary, sensory, and inhibitory signals together for mediating saccadic activity (Coe et al., 2019).

Higher cortical regions in the oculomotor and visual attention network include the frontal eye field (FEF), dorsolateral prefrontal cortex (DLPFC) and parietal eye field (PEF)/lateral intraparietal area (LIP), these structures are believed to be part of a visual inhibitory top-down control network that closely involves the SC (Godijn & Theeuwes, 2004; Theeuwes & Godijn, 2004). In this model, an 'inhibitory tag' is sent to the FEF and DLPFC, which actively encode the visual inhibition of performing a saccade to a 'cued' location (Godijn & Theeuwes, 2004; Theeuwes & Godijn, 2004). This is achieved by sending attentional inhibitory signals to the PEF, which

holds a preocular attentional map, and inhibitory oculomotor information to the SC (Godijn & Theeuwes, 2004; Theeuwes & Godijn, 2004).

Looking at this model in the context of the inhibitory control needed for making antisaccades, visual information from seeing a target stimulus is sent from the SC and V1 to frontal regions (FEF and DLPFC), which are responsible for overriding visual input systems that automatically process saccades towards a stimulus. Frontal regions send out inhibitory visuospatial processing signals to the SC via the PEF, as well as oculomotor inhibition to the SC. These top-down control signals to the SC are also likely to prime retinotopic neurons corresponding to the peripheral field locations where the target could appear, as well as inhibiting neurons corresponding to visuospatial regions not required.

Due to the active top-down control of FEF and DLPFC, these regions should be more activated during voluntary antisaccades to mediate the suppression of the prosaccade. Also, visuospatial processing of the PEF may be more activated in antisaccades due to vector inversion of the stimulus to enable making a saccade in the opposite direction (see Section 2.2.4). The proposed involvement of the FEF and DLPFC frontal structures with top-down inhibitory control mechanisms, in comparison to the parietal cortex PEF being more implicated in vector inversion, is supported by more recent research regarding pro/antisaccadic processes (Bells et al., 2020). In addition, regions within the oculomotor network overlap with those in the dorsal and ventral orienting attention networks, in particular the roles of

the FEF and intraparietal sulcus (IPS), i.e., PEF, in endogenous top-down control (see Chapter 1, Section 1.2.1), such as for voluntary saccadic mechanisms (Mort et al., 2003); hence implicating these regions in a general visual attention network, involved in the cognitive control of antisaccades.

Furthermore, a meta-analysis by Hart et al. (2013) implicates inappropriate activation of cortical networks, including similar nodes of the frontal cortex (e.g., DLPFC) and parietal cortex, in the attentional dysfunction in ADHD. There have also been findings of reduced preparatory activation of visual attention and oculomotor network regions recorded in ADHD adults performing the antisaccade task (Hakvoort Schwerdtfeger et al., 2013). Moreover, a recent theory of developmental dyslexia has emerged, whereby protective mechanisms have evolved in reaction to early stress that limit neuroplasticity in regions required for reading and attention, including the dorsal and ventral attentional networks, as well as enhancing the DMN (Kershner, 2021). This suggests that top-down attentional networks implicated in ADHD and SpLDs may overlap with inhibitory control oculomotor regions involved in antisaccadic control.

Deeper midbrain and brainstem regions would only be detected when using magnetic resonance imaging (MRI) (i.e., regions labelled in yellow in Figure 2), but not with MEG. However, MEG enables the measurement of rapid task-related changes, and can detect these in the frontal, parietal, and visual cortical regions of the visual attention and oculomotor network (labelled in blue, green and red in Figure 2, respectively). The functions of

these cortical network regions are discussed later in more detail. Specific information regarding how regions from this network will be located for MEG analysis is included in Chapter 7, Section 7.2.1.

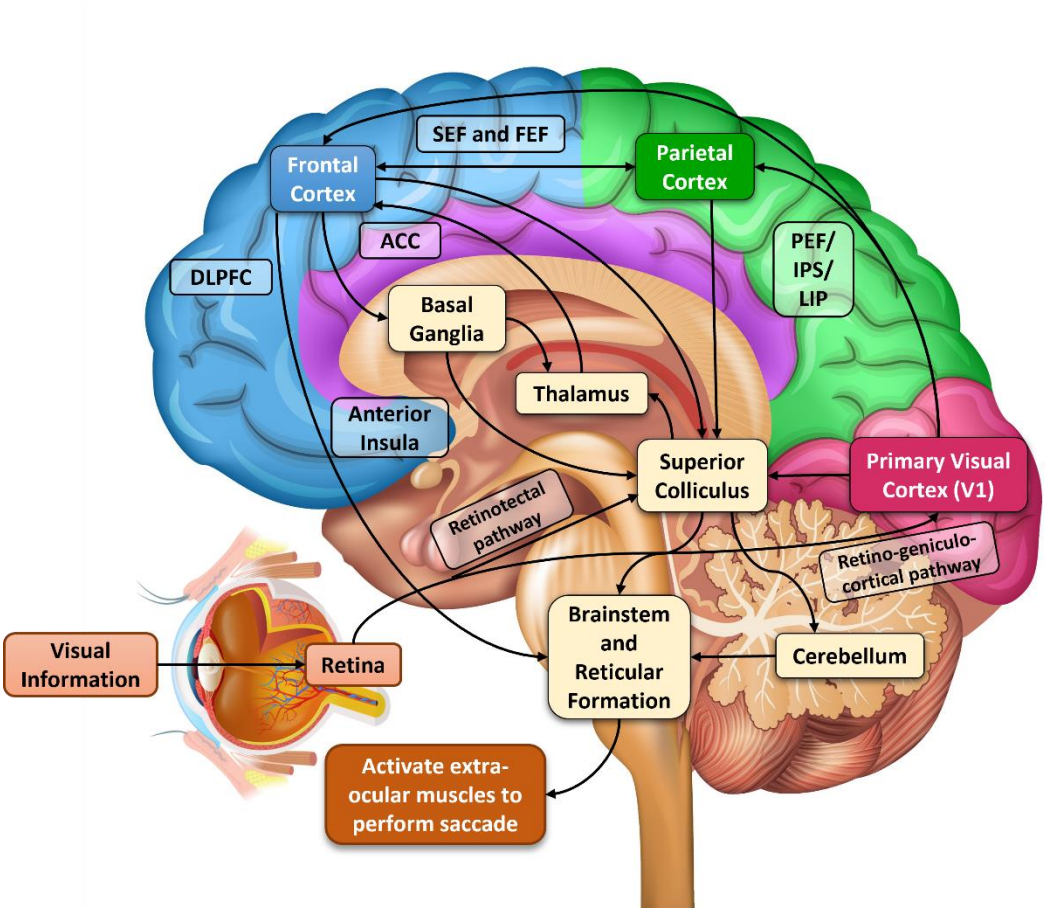

Figure 2: Diagram of anatomical regions and connections within the visual attention network.

Abbreviations, DLPFC: dorsolateral prefrontal cortex; SEF: supplementary eye fields; FEF: frontal eye fields; ACC: anterior cingulate cortex; PEF: parietal eye fields; IPS: Intraparietal sulcus; LIP: lateral intraparietal area.

2.2.2. Frontal and supplementary eye fields

The frontal eye field (FEF) was initially identified in primates by Ferrier (1874, 1875) as a bilateral region of the frontal cortex that triggers

saccadic eye movements when electrically stimulated in macaque monkeys. This finding has been replicated in multiple non-human primate species (Huerta et al., 1987). Nevertheless, the exact location of the homologous region in humans has been widely contested in neuroimaging literature (as discussed extensively in the reviews by Paus, 1996; Schall et al., 2016; Tehovnik et al., 2000; Vernet et al., 2014).

Anatomically, the FEF in non-human primate studies is believed to correspond to the equivalent human cortical location of Brodmann's area (BA) 8 or an overlap of areas 6 and 8 (Schall et al., 2017; Tehovnik et al., 2000). However, functional neuroimaging studies (i.e., using MEG, EEG, fMRI and positron emission tomography (PET)), suggest a more caudal location of FEF activation within BA 6 near the caudal part of the superior frontal sulcus at the superior precentral sulcus (sPCS) location (Vernet et al., 2014).

Moreover, functional neuroimaging methods, and non-invasive neurostimulation studies (e.g., transcranial magnetic simulation (TMS) and transcranial alternate/direct current stimulation (tACS and tDCS, respectively)) report discrepancies in not only the anatomy and location of the FEF, but also its exact function (Paus, 1996; Tehovnik et al., 2000; Vernet et al., 2014). These differences are likely to be due to variations in the imaging techniques, task type, and analysis paradigms chosen, as well as the different methods used for locating the FEF in non-invasive neurostimulation studies. Nevertheless, the general consensus is that the

FEF is located in the vicinity of the precentral sulcus at the dorsal region of the superior frontal sulcus (Vernet et al., 2014).

In terms of functionality, the FEF in both humans and non-human primates plays a key role in saccadic networks and visuospatial attention, such as facilitating top-down control of eye movements for preparing and generating voluntary saccades (Gaymard et al., 1998; Vernet et al., 2014). These functions are supported in part by findings from primate FEF neuronal recordings, which have revealed increased preparatory FEF neuronal activity prior to volitional saccades, but not for spontaneous saccades (Bruce & Goldberg, 1985). There are also measured changes in FEF neuronal activity that correspond to modulation of gaze-control (Hanes et al., 1998).

In addition, the FEF has direct projections to the SC (Everling & Munoz, 2000) and brainstem pons for mediating top-down saccadic control, as well as a bidirectional, indirect pathway via the basal ganglia to the SC that also carries signals back to the FEF (Matsumoto et al., 2018). The direct descending pathway is thought to carry top-down saccade type information (i.e. pro- or antisaccade) to prime the SC to mediate the correct saccadic response for the oculomotor muscles (Everling & Munoz, 2000). Further validation for the importance of FEF-SC communication in saccadic production includes evidence from cryogenic inactivation of the monkey FEF, which resulted in delayed saccadic onset signals to be relayed to the SC, causing longer saccadic RTs (Peel et al., 2017). More recently, FEF

recordings in a visual free-viewing task showed anticipatory dynamic neuronal responses that corresponded to integrating complex information just prior to executing the saccadic response (Mirpour & Bisley, 2021). Together, these findings indicate that the FEF plays a key role in coordinating saccadic generation and production, particularly through reciprocal communications with the SC.

Evidence from human studies regarding the function of the FEF include fMRI data showing greater FEF activity recorded during antisaccade trials than in prosaccade trials (M. R. G. Brown et al., 2007). In addition, Connolly et al. (2005) found a direct relationship between FEF activity with RT, supporting the proposed cognitive control role of the FEF in saccadic production and predicting the type of saccadic movement (prosaccade or antisaccade). Before initiating an antisaccade, lateral FEF inhibition has been observed in MEG/EEG data (McDowell et al., 2005), which supports hemispheric coordination in producing the correct saccadic response, whereby directional responses that correspond to a reflexive prosaccade are inhibited. Interestingly, continuous theta-burst stimulation used to inhibit right FEF activity resulted in reduced antisaccadic amplitude and increased number of antisaccade steps made to reach the correct final destination, but directional errors were not affected (Cameron et al., 2015). This indicates a role of the FEF more so in visuomotor programming rather than visuospatial processing (which is more likely to be related to the PEF, Section 2.2.4) for preparing an antisaccade.

An area often reported in conjunction with the FEF is the supplementary eye field (SEF). The SEF is another key region involved with saccadic eye movements, due to its association with initiating the programming of complex oculomotor sequences, including voluntary saccadic eye movements (Pierrot-Deseilligny et al., 2002; Pierrot-Deseilligny et al., 1995). Similarly to the FEF, there is not a confirmed consensus regarding the actual location of the SEF in the human brain. Although, the SEF is generally considered to be a bilateral or single region near the midline, residing dorsomedially in the frontal cortex compared to the more laterally situated FEF (as discussed in the review by Tehovnik et al. (2000)).

Earlier studies that identify the SEF region in non-human primates have detected increased pre-saccadic firing in this region and that saccadic responses can be elicited when it is electrically stimulated (Schlag & Schlag-Rey, 1987). Additionally, increased SEF neuronal activity has been recorded in monkeys during antisaccade trials compared to prosaccade trials (Schlag-Rey et al., 1997), including in preparation for making an antisaccade (Amador et al., 2004). This activity in the SEF prior to making saccadic responses indicates its role in internal decision-making as to whether to look freely towards a receptive or non-receptive field target (Coe et al., 2002). Specifically, this internal decision-making is likely to be more involved in resolving response conflict rather than error monitoring, as only the former has been found to be impaired when there are lesions affecting the SEF region in humans (Husain et al., 2003; Parton et al., 2007).

The role of the SEF within saccadic functioning is further corroborated in human neuroimaging studies, where there is greater blood-oxygen-level-dependent (BOLD) fMRI activation in the SEF during antisaccade trials rather than prosaccade trials (M. R. G. Brown et al., 2006), including in the preparatory period (M. R. G. Brown et al., 2007; Connolly et al., 2005; Ford et al., 2005). MEG/EEG response-locked data also showed increased SEF activation on antisaccade trials compared to prosaccade trials (McDowell et al., 2005). SEF activation has also been associated with saccadic gain and latency (Jamadar et al., 2015). These different studies and findings all point to a role for the SEF in the programming of voluntary antisaccades to override and inhibit reflexive prosaccades.

2.2.3. Dorsolateral prefrontal cortex

The dorsolateral prefrontal cortex (DLPFC) is another key region in the visual attention network, that has historically been equated as being in the vicinity of the middle frontal gyrus, BA 9 and 46 in the human brain (Rowe et al., 2000). The DLPFC plays a crucial role in many executive functions to mediate cognitive control in a variety of domains, from working memory (Brunoni & Vanderhasselt, 2014), language (Hertrich et al., 2021), pain (Seminowicz & Moayedi, 2017) and motor control (Yanqiu Wang et al., 2020).

Moreover, the key role of the DLPFC in the oculomotor control of saccades was discovered by early lesion studies that implicated DLPFC function. One such study conducted on epileptic patients found that frontal lobe lesions (implicating the roles of the DLPFC and FEF, due to lesions encompassing both regions) resulted in weaker inhibition of reflexive prosaccades during antisaccade trials, but the same was not observed in temporal lobe lesion patients or controls (Guitton et al., 1985). In patients with more spatially specific DLPFC lesions corresponding to BA 46, there were increased directional errors on the antisaccade task compared to lesions in the FEF, parietal cortex and supplementary motor areas (Pierrot-Deseilligny et al., 1991). A review of these earlier patient studies also support poorer prediction and short-term memory for anticipatory saccadic mechanisms in patients with damaged DLPFC regions (Pierrot-Deseilligny et al., 2002). Also, the same research group built upon these findings by showing that unilateral DLPFC lesions resulted in bilaterally increased directional errors, saccadic amplitude errors, and reduced anticipatory saccades in a predictive saccade task (Pierrot-Deseilligny et al., 2003). These observations of poorer cognitive control exhibited in DLPFC lesion patients indicate an active involvement of the DLPFC in planning, inhibiting and overriding the programming of reflexive prosaccades to elicit an antisaccade.

Non-human primate studies also revealed that like the FEF, the DLPFC contains direct neural projections to the SC, which carry signals that are indicative of pro/antisaccade task type, stimulus information and

saccade direction (Johnston & Everling, 2006). This suggests that top-down control task-related signals are mediated specifically by the DLPFC to the SC, and this modulatory mechanism could infer a wider orchestration of top-down control of the DLPFC during the antisaccade task (Johnston & Everling, 2006). Further evidence for this finding includes microstimulation of the monkey DLPFC resulting in compromised performance in the antisaccade task by increasing ipsilateral pro/antisaccade RTs and increasing directional errors for ipsilateral antisaccade trials (Wegener et al., 2008).

In regards to human neurophysiological evidence, an fMRI study found that in preparation for an antisaccade, there was no activation recorded in the DLPFC (M. R. G. Brown et al., 2007). This was interpreted as the DLPFC being more involved with higher-level priming of the saccadic network rather than direct involvement in antisaccade generation (M. R. G. Brown et al., 2007). Also, it has been found that older adults with greater DLPFC activation have less antisaccadic errors, which is a marker of better cognitive control in an aged population (Fernandez-Ruiz et al., 2018).

Similar to other regions found within the visual attention network, reported locations and functions of the DLPFC have not always been consistent, resulting in a heterogeneity of DLPFC findings reported in the body of neuroimaging studies (Cieslik et al., 2013). Cieslik et al. (2013) suggest this is possibly because the DLPFC is actually covers a wide area that should be divided into an anterior subregion that is more involved in

inhibitory control and attention, whereas the posterior subregion is linked to working memory and motor actions.

This all reveals the existence of a complex and not fully established mechanism for precisely how the DLPFC exerts its top-down effects in the oculomotor control of antisaccades. More research using different electrophysiological, neuroimaging and neurostimulation methods in humans are required to pinpoint these processes. An example of a novel approach used to investigate DLPFC function includes using continuous theta-burst stimulation, which was applied to inhibit left DLPFC activity (Cameron et al., 2015). This resulted in increased contralateral antisaccadic directional errors, but did not affect the number of saccades made or the amplitude of the saccade (unlike when the same procedure was applied to the FEF, as discussed in Section 2.2.2 (Cameron et al., 2015)).

Moreover, hyperactivity of the DLPFC has been observed for antisaccadic preparation in ADHD, which is thought to counteract the hypoactivation that is observed in other cortical regions such as the FEF, SEF and PEF (Fernandez-Ruiz et al., 2020; Hakvoort Schwerdtfeger et al., 2013). Therefore, despite the exact mechanisms behind how the DLPFC mediates these functions not being fully understood, the collation of this evidence all points to the DLPFC influencing top-down control. Furthermore, these findings outline specific differential roles within the frontal cortex of the DLPFC and FEF in top-down cognitive control processes. Whereby the DLPFC mediates high-level executive control

mechanisms for signalling to the visual attention network for performing an antisaccade, top-down FEF signalling is more likely to initiate the correct visuomotor procedures for antisaccade generation and performance.

2.2.4. Parietal eye field

The parietal eye field (PEF) is a small area of the posterior parietal cortex also known as the lateral intraparietal area (LIP) found in the intraparietal sulcus (IPS) of non-human primate brains (Andersen et al., 1992). The PEF is one of the three cortical eye fields involved in saccadic control (along with the FEF and SEF). Initial studies pointed to a role of the PEF in mediating reflexive visual exploration in comparison to the FEF, which is more involved with voluntary exploration (Pierrot-Deseilligny et al., 1995). The region of the PEF/LIP has more projections to other areas implicated in saccadic generation than the remainder of the parietal cortex, where it is also thought to function in sensorimotor integration, processing spatial information and planned saccadic eye movements (Andersen et al., 1992).

Electrode recordings from the monkey LIP have found the firing of LIP neurons to be associated with encoding the cue location in the antisaccade task, implying its early involvement in visual processing within the process of antisaccade generation (Gottlieb & Goldberg, 1999). Interestingly, in a memory antisaccade task, recordings from monkey LIP indicated specific activity during antisaccades that corresponded with

computing vector sensorimotor transformation of stimulus location into the correct direction for performing an antisaccade (M. Zhang & Barash, 2000, 2004). More recent studies recording LIP activity in monkeys during a free-viewing visual search task support that the LIP has a specific role in providing information regarding how similar stimuli are compared to the target (Sapountzis et al., 2018). Additionally, the LIP is believed to provide a stable spatial visual representation/map based on current environmental information (Mirpour & Bisley, 2021). This agrees with human posterior parietal lesions resulting in failed retention of target location information (Husain et al., 2001), thus corroborating the role of this region in the memorisation of maintaining visuospatial representations.

Upon researching a specific human brain homologue of the monkey LIP and PEF, this revealed a lack of scientific agreement in exactly where it is located and defined in humans. Pierrot-Deseilligny et al. (1995) first speculated the location of the human PEF to be situated at the IPS by the superior angular and supramarginal gyri (corresponding to BA 39 and 40). This was corroborated the following year with early fMRI studies showing activation of this region during visually guided saccades (Müri et al., 1996). Some more recent neuroimaging and computational model studies refer to a PEF location in the human brain as the equivalent of the monkey LIP (Bells et al., 2020; Coe et al., 2019; Coe & Munoz, 2017), but often the functional equivalent region in humans is referred to as the IPS, sometimes without any reference to PEF or LIP (Hwang et al., 2014, 2016).

Riddle et al. (2019) chose the superior IPS region to use as an ROI for the human LIP homologue. They reference the review by Grefkes & Fink (2005) for this decision, who state that the posterior portion of the medial IPS (rather than the lateral IPS) is the likely candidate for the human LIP, using activation peak information from the study by Koyama et al. (2004); although it is worth noting this original study does not specifically state that this is the 'medial' IPS. A TMS study that aimed to stimulate the PEF used the IPS as the reference stimulation location for the human homologue of the monkey LIP, but found considerable inter-subject variability in the observed behavioural effects (Ryan et al., 2006). Therefore, a lack of consensus regarding the correct terminology and labelling for the LIP equivalent in humans is an issue that should be addressed in future studies to avoid confusion when discussing the PEF/LIP/IPS.

Since the LIP is a region specific to non-human primate brains, and the IPS describes a whole sulcus region, the PEF appears to be the most appropriate terminology to use to describe the specific brain region corresponding to a LIP human homologue. Adopting a consistent naming and location approach would facilitate our understanding of the human PEF region to be functionally determined in neurophysiological and neurostimulation research, which would help to build our understanding for its full role within the visual attention network. See Chapter 7, Section 7.2.1 and Appendix D for details regarding specific location coordinates used in functional neurophysiology studies.

Despite discrepancies in reports of the human LIP homologue, neurophysiological studies in humans support similar findings as discussed previously in primate studies. To avoid misrepresentation, the region label used for discussing findings in human studies is the same label from the source that it was retrieved from. Observations from fMRI data include increased IPS response-related activity during antisaccade trials compared to prosaccade trials (M. R. G. Brown et al., 2007; Furlan et al., 2016). MEG and EEG data depict heightened IPS activation contralaterally to the stimulus that is proceeded by ipsilateral activity (Everling et al., 1998; Moon et al., 2007); thus indicating a 'switch' between contralateral to ipsilateral PEF on antisaccade trials to mediate vector inversion. This is backed by topographical findings confirming that parietal cortex receptive fields are lateralised to represent the contralateral visual field (Silver & Kastner, 2009). Meta-analysis of impaired brain network function in dyslexic children has revealed underactive inferior parietal cortices (Richlan et al., 2011), which could contribute to the source of visuospatial attentional dysfunction. This role is further supported by left temporo-parietal tDCS improving visuospatial working memory and motion perception in dyslexic children (Lazzaro et al., 2021).

In terms of preparatory responses, MEG studies by Hwang et al. (2014, 2016) did not find any evidence of significant IPS activation during the preparatory period of the antisaccade task. This may be because if the primary role of the IPS region is vector translation, this would occur only once the target location is revealed, meaning IPS activation may have been

recorded if the researchers had studied the response period as well (Hwang et al., 2014). However, other findings from fMRI studies have reported greater antisaccadic preparation in the IPS compared to on prosaccade trials (Furlan et al., 2016). Also, a more recent MEG study investigating pro/antisaccade temporal dynamics found contralateral PEF peak activity 10 msecs prior to making a prosaccade, and delayed ipsilateral PEF activity corresponded to slower RTs on antisaccade trials (Bells et al., 2020). This evidence supports that the timing of activation in the PEF is important, but the exact functions in anticipatory response mechanisms are currently unclear. It has been suggested from MEG and EEG recordings that lateralised alpha-band power changes may mediate the transition from the contralateral to ipsilateral hemisphere during vector inversion (Belyusar et al., 2013; Van Der Werf et al., 2008).

In summary, the current body of work for the PEF/LIP/IPS parietal cortical region within the visual attention network suggest a likely function in visuospatial processing and vector inversion for antisaccade production. This is due to the switch in activity observed in antisaccade tasks from contralateral to ipsilateral hemisphere relative to the stimulus and this fits with the inhibitory control model for antisaccade production discussed in Section 2.2.1. However, its precise role in other functions and anticipatory responses has not yet been fully defined. Additionally, there are problems with a lack of consistent terminology for labelling the region, which could hinder progress in future research investigating its specific function and location in humans.

2.2.5. Salience network

The salience network contains key nodes of the insula and anterior cingulate cortex (ACC) that have been identified from BOLD-fMRI activated regions during tasks that require cognitive functions such as attention and working memory (Menon & Uddin, 2010; Seeley, 2019; Seeley et al., 2007). The salience network plays a role in cognitive control, since there is an overlap with ACC and insula activations with cognitive control networks in neurophysiological studies (Cole & Schneider, 2007; Dosenbach et al., 2006). These regions are also involved in homeostasis regulation and autonomic processing (Beissner et al., 2013; Critchley et al., 2003, 2011; Guo et al., 2016; Namkung et al., 2017; Seeley, 2019; Sturm et al., 2018), which could also implicate these regions in arousal mechanisms.

The salience network is believed to aid sensory processing when encoding relevant information via modulating bottom-up and top-down processes. Validation for this idea is supported by findings of dysfunctional activation of this network in schizophrenia; this is known as aberrant salience, which likely contributes to positive symptoms such as distorted reality, impaired perception of sense of self, and psychosis (Kapur, 2003; Liddle et al., 2016; Palaniyappan & Liddle, 2012; T. P. White et al., 2010). Inappropriate salience processing in schizophrenia has been linked to excessive dopaminergic activation that is ameliorated through antipsychotic mediation (Kapur et al., 2005). The dopaminergic hypothesis of schizophrenia describes a complex mechanism that interacts with other

factors (genetics, environmental, prenatal factors, etc.) that all contribute to the aetiology of schizophrenia (as reviewed by Howes & Kapur, 2009). However, Heinz & Schlagenhauf (2010) summarise neuroimaging findings that support the idea for aberrant salience to also be linked to dysfunctional reward mechanisms that are attributed to hyperdopaminergic signalling. Therefore, this provides a link to ADHD, where hypodopaminergic signalling contributes to dysfunctional reward mechanisms (as discussed in Section 2.1.2); thus, this is also likely to cause inappropriate salience processing mechanisms in ADHD, but due to under- rather than over-activation of the dopaminergic system.

Inappropriate activation of the salience network in schizophrenia has been particularly linked to disrupted insula functioning (Uddin, 2015). Beta synchronisation in the bilateral insula is thought to encode task-relevant stimuli information, since this has been observed during relevant stimuli in healthy controls (Liddle et al., 2016). However, schizophrenic patients were found to show this activation during irrelevant stimuli, thus indicating issues in filtering salient information (Liddle et al., 2016).

The ACC is often linked to attention and motivational states (Servan-Schreiber et al., 1998), including lapses in attention (Weissman et al., 2006), and has shown activation changes in the antisaccade task (Jamadar et al., 2015). The ACC is thought to be a hub region involved in the coordination of many cognitive control processes, since it has a broad range of input and output projections within the brain (W. Tang et al., 2019). This includes

projections to the SC and FEF (Leichnetz et al., 1981; Yan Wang et al., 2004), hence it is likely to directly interact with oculomotor and visual attention network processes during pro/antisaccades. Interestingly, single unit recordings of monkey neurons in the ACC and PFC during the pro/antisaccade task reveal that the ACC is more active than the PFC in encoding top-down task-switching mechanisms (Johnston et al., 2007). This directly implicates the ACC and salience network in communicating stimuli relevance, also in the context of the pro/antisaccade task.

The insula receives sensory inputs from a wide range of modalities (Servan-Schreiber et al., 1998), which is believed to aid the sensory processing of encoding relevant information. Although the insula is often considered as a whole region in itself, it can be divided into a larger and smaller portion via the sulcus centralis insulae; the anterior and posterior insula respectively (Shelley & Trimble, 2004). These portions can even be further divided into smaller subdivisions (Mutschler et al., 2009). In particular, the anterior insula is thought to play a large role in interoception, including self-awareness and time passage perception (Craig, 2009). This includes orienting attention and balancing both external and internal perception (Menon & Uddin, 2010).

Moreover, the anterior insula is believed to be more involved in task-focused attentional processes compared to the posterior portion (Nelson et al., 2010). In addition, the anterior insula is thought to communicate directly with the DLPFC and ACC regarding stimuli salience to aid with

cognitive control of attention and working memory functioning (J. Jiang et al., 2015; Menon & Uddin, 2010; Namkung et al., 2017). This further points to how the salience network is involved in the pro/antisaccade task, where it likely plays a role in communicating information regarding the relevance of the stimulus (i.e., prosaccade versus antisaccade target) to the nodes in the oculomotor and visual attention networks.

Additionally, the anterior insula cortex is in close proximity with the inferior/ventrolateral frontal cortex, whereby this region has also been implicated in functions requiring inhibitory control. As reviewed by Aron et al. (2004), the support for this is predominantly from studies of patients with lesions in the right inferior frontal cortex. Patients with these lesions often perform poorly during tasks requiring response inhibition (e.g., Go/No-Go task), task-set switching paradigms and memory retrieval (Aron et al., 2004). A patient lesion study by Hodgson et al. (2007) also found that right ventrolateral frontal cortex lesions were associated with impairments in an oculomotor rule switching task. Interestingly, patients presenting rule-switching task impairments had a lesioned area that overlapped with the right anterior insula cortex, but unimpaired patients did not.

A subset of these patients also completed an antisaccade task, whereby lesions overlapping with the anterior insula were also associated with increased task performance impairments. Hodgson et al. (2007) concluded that lesions in the ventrolateral frontal cortex specific to the right hemisphere predicted impairments in the rule switching task, whereas

lesions in either hemisphere of this region were as likely to exhibit impairments in the antisaccade task. Therefore, these findings support that the anterior insula likely overlaps with inhibitory control functions of the inferior/ventrolateral frontal cortex, whereby the action of the right hemisphere appears more dominant in this domain.

To summarise, the insula and ACC form the salience network and are likely to be hub regions that mediate many functions and processes, from homeostasis and autonomic nervous system interactions, to cognitive control processes like attention. Salience processing links directly to the dopaminergic system, so disrupted salience processing is likely to contribute to attentional problems experienced in ADHD. Therefore, because of the suggested role of the salience network in inhibitory control, the anterior insula and ACC are likely to be implicated in voluntary antisaccadic responses that rely on encoding salience to the opposite location to the target stimulus for making the correct antisaccadic response.

Chapter 3: Methods

3.1. Study overview

This study was an explorative "confidence-in-concept" study designed to provide evidence that RECOGNeyes training would produce beneficial changes in gaze-control in a sample of young adults with ADHD and/or a specific learning difficulty (SpLD), and to delineate ANS and CNS correlates of gaze-control performance and changes in performance.

We recruited a sample of 35 university students and young professionals reporting having ADHD and/or a SpLD. We collected physiological data whilst participants performed the pro/antisaccade task before and after two weeks of RECOGNeyes training. Participants were randomised to undertake different intensities of RECOGNeyes training over the two-week period. This was done firstly to allow as to evaluate compliance with the training protocol, and secondly to provide the potential to investigate dose-related effects. However, our primary aim was to delineate neural correlates of pro/anti-saccade performance, and changes in performance between assessment days.

3.2. Ethics and funding

Prior to commencing the study, ethical approval from the Faculty of Medicine and Health Sciences (FHMS) Research Ethics Committee,

University of Nottingham, was obtained. This included the authorisation of involving healthy human volunteers. In addition, experimenters were only to comprise of staff and students from the University of Nottingham. No major ethical problems were anticipated, but there was a small chance of potentially detecting medical problems after viewing the collected images from magnetic resonance imaging (MRI). The possibility of this happening was communicated to participants in the consent process. If there were any signs for concern in any of the magnetic resonance (MR) images, the Sir Peter Mansfield Imaging Centre (SPMIC) has a standard operating procedure for handling these incidents. The study was funded by the MRC via a Confidence in Concept (CiC) grant from the University of Nottingham.

3.3. Study design

This study builds upon the work from proof-of-concept experiments using RECOGNeyes (see discussion in Chapter 1, Section 1.3.4). This includes the work of García-Baos et al. (2019), whose study compared attention and reading indices of two separate groups before and after behaviourally-distinct interventions. Participants who played RECOGNeyes using mouse responses did not produce significant changes in attention and reading indices compared to the group using eye-tracked responses. This supported the hypothesis that effects of RECOGNeyes attributable to controlling the game using eye movements were more substantial than any generic effects of playing an otherwise similar game.

In this study, we aimed to further investigate specific links between the visual attention system and the RECOGNeyes training intervention by introducing a greater breadth of neural and behavioural measures. Instead of an active control game, we randomly allocated participants to play RECOGNeyes for different numbers of sessions per week. We chose this design to maximise our power to address additional questions regarding the neural correlates of gaze-control, irrespective of any dose-related effects of RECOGNeyes on outcome measures.

Since all participants would have substantial exposure to RECOGNeyes training, we expected to see improvements in gaze control in all participants. This would allow us to investigate not only neural correlates of gaze-control, but also correlates of within-participant variability in gaze control, whether or not it correlated with RECOGNeyes exposure.

Volunteers attended two assessment days spaced two weeks apart at the SPMIC, University of Nottingham. The first visit was approximately three hours and the second totalled around two hours. The structure of each assessment day is depicted in Figure 3 and the measures will be discussed in further detail in Section 3.6. Between assessment days, the participants completed a randomised (single-blind) RECOGNeyes training schedule; this is discussed further in Section 3.5.

Some participants were also invited to attend a third visit to participate in a qualitative, semi-structured interview about the user

experience, facilitators, and barriers of RECOGNeyes training. However, for the scope of this thesis, I will only be discussing experimental procedures pertaining to the two main assessment days.

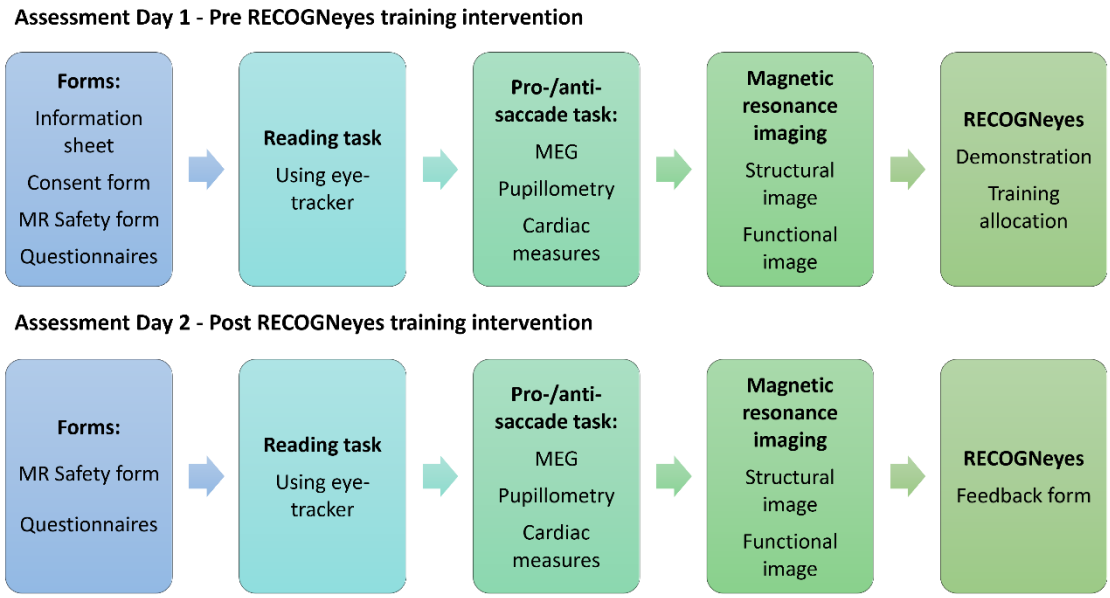

Figure 3: Structure of assessment days.

This schematic presents the order of procedures on each assessment day. Questionnaires included: CAARS-Self report Adult ADHD rating scale (Short Version), TOWRE-II test of word-reading efficiency, General Health Questionnaire – 12 item version (GHQ) and a short questionnaire about ADHD/SpLD diagnoses and current treatments/therapies (please refer to Section 3.6.1.2 for further details regarding these tests/questionnaires).

3.4. Participants

3.4.1. Inclusion criteria

Volunteers were included in this study if they were:

1. Within the age range of 18-30 years.

2. Able to give informed consent.
3. Reported having had a diagnosis of ADHD and/or a SpLD (i.e., dyslexia, dyspraxia, dysgraphia, or dyscalculia).
4. Reported having normal or corrected-to-normal vision, and uncorrected vision sufficient to see medium sized shapes/figures on the screen that are several centimetres in size, roughly an arm's length away.
5. Had the required time available and willingness to complete up to 4 training sessions per week over the two-week interim period, where each training session is 20-30 minutes.

3.4.2. Exclusion criteria

Participants were excluded if:

1. Responses to SPMIC MR Volunteer Safety Screening Questionnaire indicated any safety risks. These mainly pertain to MR safety considerations if there are traces of metals present inside or outside of the body (refer to Appendix A: MR Screening Questionnaire).
2. They had a partial sight or visual field deficit.
3. They were involved in other studies. People who were involved in another study could not participate unless there had been a time lapse of at least 3 months since taking part in the previous study. This is to reduce the possibility of confounding

effects from another study that could influence the outcomes in the current study.

3.4.3. Recruitment

The study was advertised primarily through the Academic Support Services at the University of Nottingham, who sent out emails to students on their mailing list with ADHD or a SpLD (note – this was prior to the Data Protection Act 2018 changes made to the UK General Data Protection Regulation; thus, at the time of recruitment, we were able to send the study advertisement email directly to this mailing list). There were also posters displayed around the university (see Appendix B).

The advertisements gave a brief overview of the study procedures and provided contact information for potential participants to express their interest in taking part. Responders were then sent a study Participant Information Sheet (refer to Appendix C) with further details. If they were still interested, a telephone screening was next conducted to check participation eligibility.

During the telephone screening, volunteers were asked to confirm whether they had a diagnosis of ADHD and/or an SpLD. Further details were acquired during the assessment days regarding the specific conditions they were diagnosed with, and whether this was from a formal diagnosis by a psychologist or doctor or if they self-identified. Volunteers were also asked to disclose information about any medication they were using/prescribed,

but they were not asked to alter their medication schedule to participate in the study.

During screening, potential participants were asked if they were claustrophobic, in case the small environment of the MR scanner might cause them to feel uncomfortable. In addition, participants were asked whether they suffered from tinnitus due to the loud sounds produced by the MR scanner, but that earplugs would be provided to help reduce this noise. Providing this information helped volunteers make an informed decision for if these considerations applied to them.

Volunteers were asked if they had normal or corrected-to-normal vision in the screening process. The reading assessment was conducted in the MEG scanner, but not during the recording of MEG data, so participants could wear glasses for the reading task. However, glasses could not be worn whilst collecting MEG data due to the interference caused by metal objects. They also would pose an MR safety risk (see Exclusion criterion 1). Therefore, participants were asked if they could see medium sized shapes/figures on the screen roughly an arm's length away during the screening process, or alternatively if they could wear contact lenses during the MEG and MRI. If they answered no to this or were unsure, we did not include these individuals in the study.

Participants were then invited to take part if they satisfied the inclusion criteria and did not meet any exclusion criteria (refer to Sections 3.4.1 and 3.4.2). All participants were able to give informed consent and

were aware that they could withdraw at any stage in the study. An inconvenience allowance of £60 was paid to participants in concordance with approval from the University of Nottingham Medical School Ethics Committee. Participants were also emailed a picture of their structural MRI scan to keep for personal interest.

3.4.4. Training randomisation

Participants were each randomly assigned to undertake two, three, or four sessions per week of RECOGNeyes training at home over the two-week period between assessment days. Demographic information, including age, gender, and the nature of SpLD/ADHD, were recorded. Randomisation was stratified by age and gender.

This was a single blind study. To avoid bias in the investigators who conducted the pre- and post-intervention measurements, only the participants were aware of how many RECOGNeyes training sessions they were assigned to complete each week. Moreover, the participants were not informed as to how the intensity of the training schedule they had been assigned compared with other schedules. To maintain blinding in the investigators, participants were given instructions for their particular training schedules in a sealed envelope at the end of the first assessment day. They were asked not to disclose their training instructions to investigators, who were only informed after the data had been analysed. The Chief Investigator, Dr Elizabeth Liddle, was the sole person with access

to the randomisation and training schedule record. Contact details were provided so that participants could contact her directly if they experienced any problems with RECOGNeyes or the training instructions.

3.5. RECOGNeyes training program

3.5.1. Description of RECOGNeyes training

RECOGNeyes software was downloaded onto laptops (Lenovo ThinkPad L560). Each participant was a provided with a laptop and a Tobii 4C eye-tracker to take home. The eye-tracker is mounted by a magnetic strip at the bottom of the laptop screen and connected to the laptop via USB (set-up is depicted in Figure 4).

Participants were asked to space out training times as evenly as possible, with at least one day's rest between training sessions. They were asked to play each RECOGNeyes session for twenty to thirty minutes at their discretion. This was considered a reasonable amount of time to fit into their student schedules. A timer tool was also downloaded onto the laptops with the RECOGNeyes software, which participants were encouraged to use to ensure they trained for an appropriate length of time instead of using another device for a timer that could be a source for distraction. Volunteers were given freedom over how they played RECOGNeyes. For instance, they could play the mini-games in any order (subject to constraints intrinsic to

the game design), play to obtain the minimum score thresholds to unlock as many levels as possible or could repeat mini-games in order to improve their accuracy scores (refer to Section 3.5.2 for gameplay information).

In order to play RECOGNeyes, each participant created an eye-tracker profile specifically calibrated to their eyes, which they selected before opening the RECOGNeyes game software. It was advised to play the game in a quiet room where they would be unlikely to be disturbed and to re-calibrate their eyes before each session to improve eye-tracker response accuracy. An in-game profile also had to be created, which was named according to each participant's subject ID to enable game progress to be saved after each training session.

Figure 4: RECOGNeyes training laptop set-up.

This image depicts the menu screen for the RECOGNeyes program. The image also shows where the eye-tracker attaches to the bottom of the laptop screen.

3.5.2. RECOGNeyes games and tasks

RECOGNeyes comprises of a range of mini-games with different tasks to complete at varying levels of difficulty. Similarly to most video games, as the player progresses they are guided through different levels with changes in gameplay environments. In RECOGNeyes, the player's character is an 'Ice Wizard', where the gaze of the player generates a magical vortex in the game where creatures called 'ice-sprites' live. Throughout the game, the Ice Wizard uses a magical device called an 'Opticke' consisting of a circle of lenses (refer to Figure 5 for examples of gameplay content). The lenses form either ice crystals or fire, with the idea that the player helps the ice-sprites find the ice crystals whilst at the same time helping them to avoid the fire. The mini-games include pro/antisaccade-type tasks to facilitate learning how to hold and control your gaze whilst ignoring any distractors (please refer to Table 2 for the specific mini-game task descriptions).

After completion of each mini-game, there is performance-based feedback that is dependent on accuracy (80%+ accuracy = gold/three stars, 70-79% accuracy = silver/two stars, 60-69% accuracy = bronze/one star, below 60% = no stars). Players must reach a threshold rating in certain mini-games at each environment level to unlock more mini-games at the same level, or to be allowed to progress onto the next environment.

Figure 5: Gameplay images of RECOGNeyes.

The images depict typical gameplay screens in RECOGNeyes. The left image shows the menu screen where the player selects a mini-game, which are chosen via selecting one of the different eye symbols under the central picture. The right image shows an example of in-game content in a mini-game, which illustrates the Opticke apparatus that contains a circle of lenses used by the Ice Wizard. A video of the game in action can be accessed via this link: https://www.youtube.com/watch?v=HRjK8iJbkao (*RECOGNeyesPromotion - YouTube*, 2017).

Table 2: Description of the mini-game tasks in RECOGNeyes.

This table presents the names of each mini-game and a detailed description of the different inhibitory control challenges faced in each one.

Name of mini-game	Description
The Sorcerer's Stare	The player must use their eyes to catch a snowflake, seed, or flake of ash (depending on the environment in the level the player is currently on) and hold the item still in the centre of the screen using their 'Sorcerer's Stare'. This will then draw more of the items into the centre, where the challenge for the player is to hold their gaze without becoming distracted by the surrounding scene and looking away from the centre.
Arcane Abandon	Ice crystals will appear at random in one of the Opticke lenses. The player must quickly look towards the ice crystal to allow an ice-sprite to jump towards it, but if they respond too slowly, the ice crystal will crack. However, sometimes a ring of fire will appear around the

	Opticke, and the player must keep their gaze in the centre in order to protect the ice-sprites from the fire.
Rune of Reversal	An ice crystal circles around the Opticke lenses, but it is surrounded by a shield of fire. The player must keep their gaze in the central vortex whilst the ice crystal moves around the Opticke. However, when the ice crystal changes direction, it becomes released from the fire shield and the player must look towards the ice-crystal at this point to allow the ice-sprite to safely leap towards the crystal. If the player is too slow, the ice crystal cracks, and the ice-sprite cannot reach it in time.
Inverse Incantation	A fire appears in one of the Opticke lenses, and the player must avoid looking towards this lens. Instead, the task for the player is to look at the lens diagonally opposite so the ice-sprite can jump away from the fire. Note – this mini-game in particular encapsulates elements of the antisaccade task.
Delayed Divination	Two ice crystals will appear in succession in the Opticke. The task for the player is to wait and only look at the first ice crystal after the second one has appeared. Otherwise, if the player looks at the first one before the second one appears, the ice-sprite will be attacked by fire. If the player looks at the second ice crystal instead of the first, the crystal breaks.
Clockwork Charm	In one of the Opticke lenses, an ice crystal will gradually form. The player must time their gaze to exactly at the point where the crystal has just formed before looking at it. Looking too early will cause the ice crystal to float away and looking too late will cause the ice crystal to break. Depending on how well the player times their gaze, they will hear one, two or three chimes, with the increasing numbers indicating how successful they are in their response timing.

3.6. Study regimen

3.6.1. Procedures prior to scanning

3.6.1.1. Consent and safety considerations

The structure of the assessment days has been depicted previously in Figure 3. At the start of the first visit, one of the investigators explained the study details and provided volunteers with a Participant Information Sheet (refer to Appendix C), that was also emailed beforehand for participants to go through in their own time. Before providing consent, participants were given the opportunity to ask the investigators any questions they had about the study and were made aware that they could withdraw at any point without having to justify why. If any individual felt that they could not give informed consent, they were not permitted to take part in the study.

Once the participant and the investigator were satisfied that the participant fully understood the study procedures, the participant signed a copy of the consent form; one copy was kept by the investigator, and another was given to the participant to keep for their records. After providing informed consent, participants completed an MR safety form at each visit. This was essential prior to scanning, both for the safety of the participant and to check for the absence of metal on the person for MEG recording sensitivity reasons (as outlined previously in Sections 3.4.2).

3.6.1.2. Questionnaires and RECOGNeyes training demonstration

All questionnaires were self-completed by participants under the supervision of experimenters. All questionnaires and forms (including a copy of the consent form) are stored securely in a participant folder in a locked file cabinet at SPMIC, only accessible to the investigators in the study.

On the first visit, participants completed the multiple-choice self-report Conners' Adult ADHD Rating Scale (CAARS) (Short Version) (Conners et al., 1999) to assess the severity of ADHD symptoms that may be present. Participants also completed a short form to disclose further details regarding the formal/informal SpLDs or ADHD diagnoses they had, and information about any treatments or therapies they were currently receiving.

During both visits, participants completed the Test of Word-Reading Efficiency (TOWRE)-II (Torgesen et al., 2012) to assess any differences between pre-/post-training reading scores. The order of completion of either TOWRE-II form A or B used during the first and second visits respectively was randomised for all participants. The General Health Questionnaire (GHQ) – 12 item version (Goldberg & Williams, 1988) was also completed on both visits to compare any day differences in overall mental health and wellbeing.

The end of the first visit concluded with a demonstration of the RECOGNeyes game and laptop eye-tracker set-up for participants to use at home (further details about RECOGNeyes training are provided in Section 3.5). At this point, participants received their training instructions as part of the randomisation explained in Section 3.4.3. During the follow-up session, experimenters asked participants to complete a brief feedback form about their experience of taking part in the RECOGNeyes study and whether there were any glitches or minor gameplay issues they had noticed, as this would be helpful for any future developments of the game software.

3.6.2. Magnetoencephalography acquisition and assessments during the pro/antisaccade task

3.6.2.1. Participant preparation and head localisation

In preparation for MEG data acquisition, to ensure there were no traces of metal on their person (as outlined in Section 3.4.2), participants were asked to change into disposable scrubs provided by SPMIC and ensure all jewellery and make-up were removed. Subjects had three electromagnetic head position indicator (HPI) coils attached to them as fiducial markers at the nasion, and left and right preauricular points. These fiducial coils were energised throughout the experiment to enable

continuous evaluation of head movement and head localisation in the MEG helmet relative to the MEG sensors.

Next, a three-dimensional (3D) representation of the subject's head shape was then recorded using a 3D digitiser system (Polhemus Inc, Colchester, Vermont, USA). This was to enable the co-registration of their brain anatomy with MEG sensor geometry by surface matching each subject's anatomical MRI head shape with their digitised head shape (explained further in Chapter 7, Section 7.2.3). To enable a smoother surface for the experimenter to trace the digitiser device around the head to record 3D spatial coordinates, this involved temporarily attaching an electroencephalography (EEG) cap to the subject's head. The digitiser was also traced around the eyebrows and nose for a more accurate fit to the individual head shape and facial features during the co-registration process. After completing the digitisation, these coordinates were visualised on a computer. This was then saved, or the digitisation process was repeated if there was insufficient coverage of the head shape.

Electrocardiogram (ECG) electrode wires were also attached at the underside of each forearm and a reference electrode placed behind the ear. Prior to electrode placement, an area of skin at these locations was cleansed with a scrub and alcohol wipe to remove any dead skin which could hinder conductivity. To reduce electrical impedance at the contact point of the electrode with the skin to improve ECG recording quality, a conductive

electrode gel was applied to the ECG electrodes before affixing to the skin with medical tape.

3.6.2.2. Reading task and eye-tracker set-up

After completing these preparation steps, participants completed a short eye-tracked reading task, lasting around five minutes. The task consisted of silently reading three short passages of text, each on a different general knowledge subject. The passages were designed for a reading age of 10. Each subject was randomly assigned three different short passages to read during each assessment day out of a total of nine possible passages. No passage was presented more than once to any one participant. The volunteers sat in the MEG scanner room during the reading task since this is where the projector and eye-tracking equipment were located.

Prior to commencing the task, each participant had their eyes calibrated to the EyeLink® 1000 Plus eye-tracker (SR Research Ltd.). The eye-tracker recorded horizontal and vertical eye movement information to assess saccadic activity during the reading task. After finishing each passage, the volunteers would signal to the experimenters they were ready to continue to the next one. At the end, the experimenters asked a few questions to confirm that the volunteers had focussed on the passages during the task (these responses were not recorded).

3.6.2.3. MEG acquisition set-up

The MEG scanner used during the study was a 275-channel MEG CTF system (Canadian Thin Films, MISL, Coquitlam, BC, Canada) operated in third-order synthetic gradiometer configuration and is contained in a three layer magnetically shielded room. MEG data was acquired at a sampling rate of 600 Hz; thus, over the course of the experiment, each prosaccade and antisaccade block pair had 51000 samples in 85 seconds, totalling 1700 seconds for the MEG data time course (approx. 28 mins). A low-pass anti-aliasing filter at 150 Hz was also applied.

Participants were asked to remain seated in the scanner in an upright position during acquisition and to keep as still as possible during scanning. Experimenters electronically positioned and raised the participant inside the MEG helmet so they could feel the top of it, which enabled close proximity to the sensors to optimise the signal-to-noise ratio (SNR). Padding was also provided to the front, back and sides of the head to enable centralisation of the head in the dewar to the MEG sensors, as well as to provide comfort and limit movement artefacts to benefit all concurrent physiological recordings.

The experimenter explained the pro/antisaccade task to the subjects and inserted the HPI coils to the MEG system and the ECG electrodes into the ECG box (custom made on-site to be MEG compatible). The eye-tracker was recalibrated and when the participant was ready, the experimenters left the shielded room. The MEG operator communicated with the

participant via intercom and monitored them via video camera during the task.

The experiment set-up during MEG scanning is depicted in Figure 6, and the following is a list of the communication steps between all the devices in the set-up:

1. The Display PC was responsible for sending out signals known as 'TTL triggers' from EyeLink® Experiment Builder (SR Research Ltd.) for key events during the task (as presented in Figure 7) simultaneously to:
    a. The overhead projector in the MEG shielded room.
    b. The MEG PC to record this timestamp information in the MEG data file.
2. The projector displayed the Experiment Builder screen in the shielded MEG room via a mirror-projection display.
3. The participant received this visual input from the screen.
4. Saccadic eye movements during the task and pupillometry were recorded (at an acquisition rate of 500 Hz, i.e., 1 sample recorded every 2 msecs) by the eye-tracker simultaneously to MEG and ECG acquisition.
5. This information was sent to the eye-tracker PC that ran the EyeLink® 1000-Plus (SR Research Ltd.) software, which documented saccadic responses and pupillometry data.

6. Information from the eye-tracker was sent back to the display PC, which then initiated the appropriate feedback screen depending on the saccadic response.
7. Concurrently to the task, ECG data was recorded (at the same acquisition rate as MEG of 600 Hz) using surface electrodes placed on the forearm that were connected to an ECG box.
8. The ECG signal was sent to the MEG PC and logged as extra channels within the MEG data file.
9. Electrophysiological signals from the brain were continuously detected during the task by the MEG dewar; this information was sent to the MEG PC to be saved in the MEG data file.

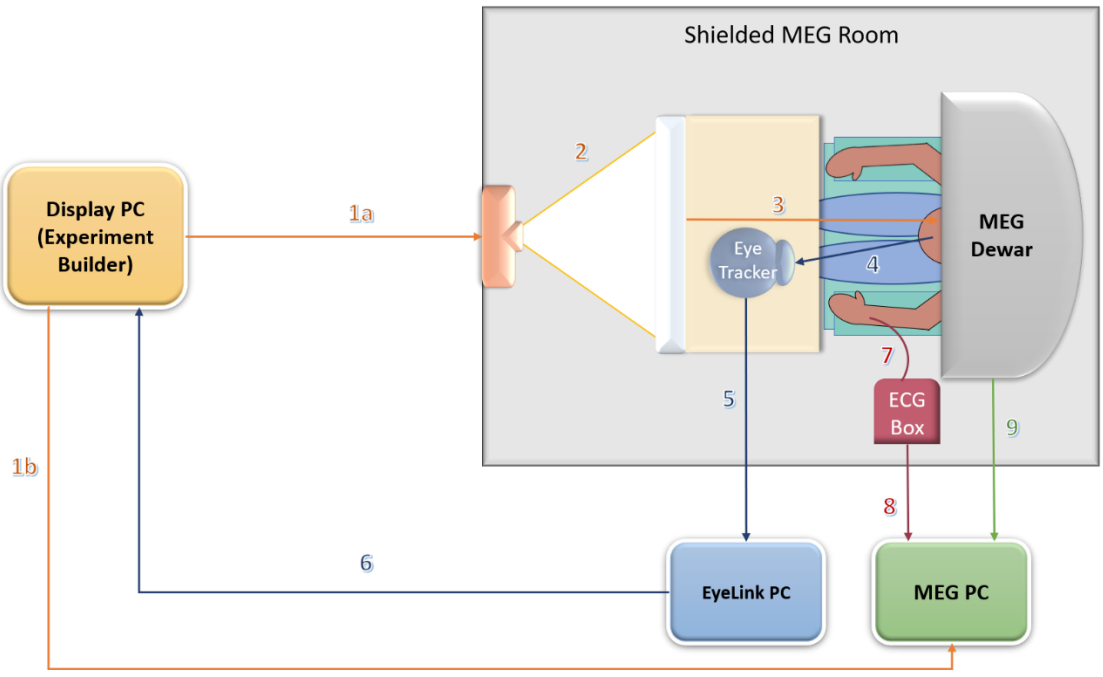

Figure 6: MEG scanning configuration.

This schematic shows how the equipment and computers (PCs) were connected during the pro/antisaccade task.

3.6.2.4. Pro/antisaccade task

During the MEG scan, the volunteers completed a pro/antisaccade task whereby a stimulus is presented in the peripheral vision and the participant performs a voluntary saccade to look either in the same (prosaccade) or opposite (antisaccade) direction of the target (for further information regarding the pro/antisaccade task, refer to Chapter 1, Section 1.2.2). Trials were presented in blocks of six trials that each contained a randomised presentation order of three right and three left target trials. Blocks alternated between prosaccade and antisaccade blocks, which were separated by short rest periods.

The eye-tracker was responsible for recording saccadic responses in the task and changes in pupil dilation (pupillometry). Specific task details are explained fully in Figure 7 and task block design is presented in Figure 8. The task was designed and presented using EyeLink® Experiment Builder (SR Research Ltd.) and projected onto a screen in the shielded MEG room (as depicted in Figure 6).

Participants completed the practice task first, where they had to correctly perform 8 prosaccade and 8 antisaccade trials, completing as many trials as necessary to achieve the minimum number of correct trials. This was to ensure a sufficient understanding of the task, before starting the full task where responses and physiological data were recorded. After completion of the practice task and prior to MEG acquisition, participants

were reminded by the MEG operator when the full task started to remain as still as possible.

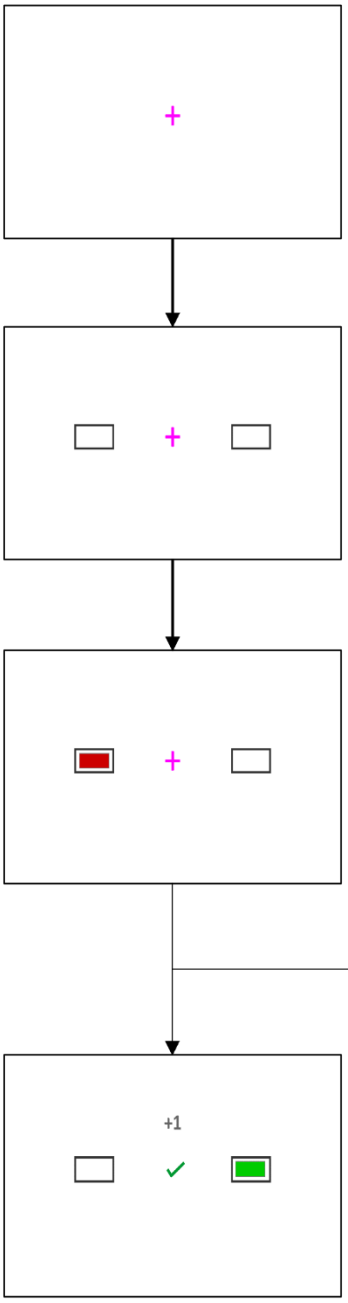

Time: 0 msec, Event: Fixation cross:

A **fixation cross** is presented on the screen at the start of each trial. Fixation cross colour indicates the task type for all trials in that block; in this case a pink cross indicates an antisaccade block. For prosaccade blocks, a blue fixation cross would appear instead.

Time: 300 msecs, Event: Cue:

After 300 msecs have elapsed, the **cue** of two empty rectangular boxes appears.

Time: 1100 msecs, Event: Target:

When the cue has been presented for 800 msecs, one of the empty boxes is filled in red and this is the **target**. The target stays on the screen for a maximum of 1000 msecs, where a correct saccadic response is required within 500 msecs. 'Early response' feedback is given If a saccade is made before the target is presented, 'Slow' feedback if a response is made between 500-1000 msecs and 'No response' feedback after 1000 msecs have elapsed.

Event: Correct Saccadic Response:

On an antisaccade trial like the one pictured, the participant should look away from the red box towards the empty box opposite (alternatively, on a prosaccade trial, the participant would look towards the red box). If successful, a 'correct' feedback screen will appear, with the box that the participant attended to filled in green, a green tick and '+1' indicating a gain of one point.

Event: Incorrect Saccadic Response:

Alternatively, if the participant looks towards the red box on an antisaccade trial (or towards the opposite box on a prosaccade trial), this is an incorrect response. The 'incorrect' feedback screen appears where the box they attend to turns yellow, a yellow cross appears and '-1' indicating to the participant that they had lost a point for that trial.

Figure 7: Description and timings of the pro/antisaccade task used during MEG acquisition.

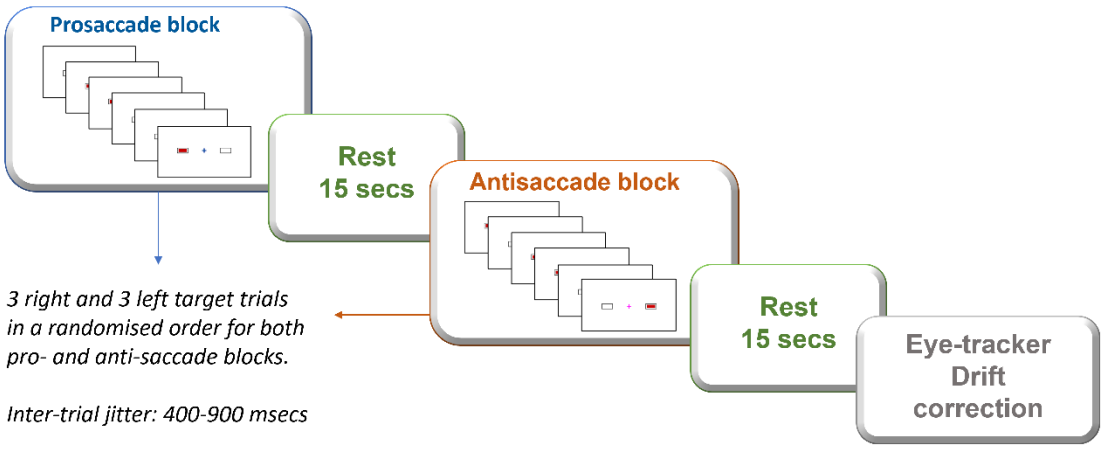

Figure 8: Task block design.

This block sequence is repeated 20 times; resulting in a total of 20 prosaccade and 20 antisaccade blocks, and 120 trials for each type. To enable a smooth transition between trials, the fixation cross was always displayed including rests (i.e., there was never a blank screen). The final score was displayed at the end of the task. MEG and ECG recorded both task and rest data, and only task data was recorded in the pupillometry results.

3.6.3. Magnetic resonance imaging acquisition

3.6.3.1. Type of scanning procedures used

Both structural magnetic resonance imaging (MRI) and resting-state blood-oxygen-level-dependent functional MRI (BOLD fMRI) scans were acquired in the RECOGNeyes study. The reasons for this were twofold: 1) Structural MRIs are an essential component in MEG analysis because individual MRIs are used to co-register MEG information as part of the analytical procedures; 2) Resting-state BOLD fMRI was chosen as a measure to assess possible resting state neurological changes after completing RECOGNeyes training. The resting-state BOLD fMRI data was analysed by another member of the team.

3.6.3.2. Scanning set-up and procedure

Participants always had their MRI scans after their MEG scans, due to the possibility of subtle magnetisation effects that could interfere with the MEG recording if performed in the reverse order (Stapleton-Kotloski et al., 2018). The MRI operator first checked the scanning form filled out by the participant to ensure there were no safety concerns and then explained the scanning procedure. Once satisfied that the participant was ready and all safety precautions had been taken, the MRI operator would take them into the scanning room containing the Philips Achieva 3 Tesla (3T) MR system (Philips Medical Systems, Best, The Netherlands).

Subjects were given ear plugs due to the loud nature of MRI scanning and asked to rest in a supine position on the scanner bed. The head helmet coil was attached, and they were provided with padding, if necessary, to restrict head movement for optimising scanning quality. A hand-operated safety buzzer was provided for the participant to squeeze if they wished to stop the scanning at any point in case of emergency or extreme discomfort. A respiratory belt placed around the subject's middle and a peripheral pulse unit (PPU) attached to their index finger were also set-up for measuring respiration and heart rate respectively during the resting-state fMRI scan. Also, during resting-state fMRI acquisition, participants were required to keep their eyes open and focus on a fixation cross presented to them. This therefore required the set-up of a fixation cross onto a projector screen and to be provided with mirrored glasses to view this from inside the scanner.

Once all the equipment had been set up, the MRI bed was electronically operated into the correct position inside the scanner. The operator left the MRI room and communicated with the subject through an intercom system to check that the participant was comfortable and to prepare them before each scanning program began. This included a reminder to focus on the fixation cross before the resting-state fMRI scan commenced. Total scanning time for both MR scans was approx. 25 minutes. After scanning, the image quality was checked by the operator in case there were large movement artefacts, which would require a repeat MRI scan. Data was saved into the SPMIC database and to a secure university shared drive that can only be accessed by researchers.

3.6.3.3. MRI technical acquisition parameters

A standard MPRAGE sequence protocol was used that is employed in SPMIC for acquiring T1 weighted structural images required for MEG data spatial localisation (details for MEG source localisation can be found in Chapter 7, Section 7.2.3). This has a 1 mm isotropic resolution, 256 x 256 x 160 matrix, and echo time (TE)/repetition time (TR) of 2.2/4.5 msecs, a short interval of 3000 msecs, a flip angle of 8^{o} and a SENSE factor 1 for image registration.

For the resting-state BOLD fMRI scan, echo-planar images (EPIs) were acquired using a 32-channel head coil with SENSE factor 1 in the anterior-posterior direction. The volume dataset at each dynamic time point includes 32 contiguous axial slices in descending order, over a total of 150

time points. Slice thickness of 3.5 mm and in-plane resolution of 3 x 3 mm was used. The TE/TR is 35/2000 msecs, with a flip angle of 85^{o}, and a field of view of 240 x 240 x 112 mm. This is a sequence that produces a T2* image that is sensitive to the local changes in magnetic susceptibility associated with local changes on the level of oxygenation of haemoglobin.

3.7. Data analysis considerations

Unless specified otherwise, IMB SPSS Statistics for Windows, Version 25.0. was used for computing and graphically representing all statistical analyses discussed in the following chapters of this thesis. Significance level was defined as $p < .05$.

Mauchly's test was used to assess sphericity for factors containing more than 2 levels when conducting analysis of variance (ANOVA). Where Mauchly's test indicated a significant violation of the assumption of sphericity, Greenhouse-Geisser correction to the degrees of freedom was used if $\varepsilon < 0.75$, otherwise the Huynh-Feldt estimate was applied (Field, 2013).

I used G*Power 3.1.9.2 (Faul et al., 2007) to compute post-hoc power calculations for the ANOVAs reported in the following results chapters. Cohen's *f* was used to denote effect size, where a small effect size is $f = .10$, medium $f = .25$, and large $f = .40$, and $\alpha = .05$.

Chapter 4: Participant characteristics and behavioural results

In this chapter, I will describe the participant sample and report on the behavioural findings. This includes first establishing sample characteristics and baseline behavioural data for Day 1, then analysing whether there were any significant differences to scores on Day 2. Post-training performance correlates included analysing the pro/antisaccade task reaction time and accuracy to determine whether the participants significantly improved on Day 2 post-RECOGNeyes training. Task performance correlates are hence necessary to establish prior to analysing CNS and ANS correlates of task performance indices.

4.1. Baseline scores and sample characteristics

4.1.1. Recruited sample characteristics

After screening, the final sample recruited were 35 university students (and young professionals) recruited primarily through Academic Support Services at the University of Nottingham. Our specified age range was 18-30; although one participant was aged 31 at the time of the assessment days, all volunteers were within the required age range during recruitment. The sample included 20 females and 15 males aged 19-31 (average age of 24 years).

4.1.2. Subject diagnostic and medication information

A formal diagnosis of ADHD and/or at least one SpLD was reported in all cases. The following diagnostic information provided by the sample were as follows:

- 6 ADHD
    - 1 ADHD-PI type (attention-concentration deficit)
    - 1 with ADD (Attention Deficit Disorder)
    - 1 with dyspraxia
    - 1 with dyspraxia and dyslexia
    - 2 ADHD only
- 18 dyslexia only
- 2 dyspraxia/dyspraxia tendencies only
- 8 dyslexia with dyspraxia
    - 1 stated they also had undiagnosed ADHD
- 1 dyslexia with dysgraphia

We also asked participants about any treatments and interventions they were receiving at the time of the study to help with their ADHD/SpLD. This included details regarding any other regular medications they were taking or any other information they felt would be relevant to disclose. The information provided by the participants included the following:

- 6 participants with an ADHD diagnosis were taking ADHD medication:
    - 1 dextroamphetamine
    - 1 Methylphenidate
    - 1 Concerta XL
    - 1 Elvanse 70mg daily
    - 1 Elvanse 30mg daily and 60mg Strattera (atomoxetine)
    - 1 unspecified and taken irregularly
- 5 had reported receiving academic study support, tutoring and specialist computer software*
- 3 participants were taking medication for depression
    - 1 specified Sertraline 125mg daily for depression and anxiety and took medication for headaches (unspecified). This individual was also taking ADHD medication included in the previous list (30mg Elvanse and 60mg Strattera).
    - 1 taking medication for depression (unspecified) and receiving therapy
    - 1 taking medication for depression only (unspecified)
- 1 participant suffered from chronic fatigue
- 1 person wore corrective glasses for one year after dyslexia diagnosis

* Note, numbers receiving academic support were likely higher since we mainly recruited through the university academic support services. However, these details were not specifically requested in the study, since we were primarily interested in confirmed diagnosis and medications received.

4.1.3. Subject datasets available for analysis

Questionnaire data was collected for all 35 subjects. However, where questions were left blank or it was not clear which answer was selected, these scores were left blank and not included in the subject/category score as appropriate per questionnaire. Prior to statistical analysis of the pupillometry, cardiac and magnetoencephalography performance data, we checked for any missing subject data for each measure after acquisition or cleaning, which are summarised in Figure 9. Each participant was allocated an ID consisting of 'S' followed by a 2-digit number, assigned in order of consent date (1 to 35).

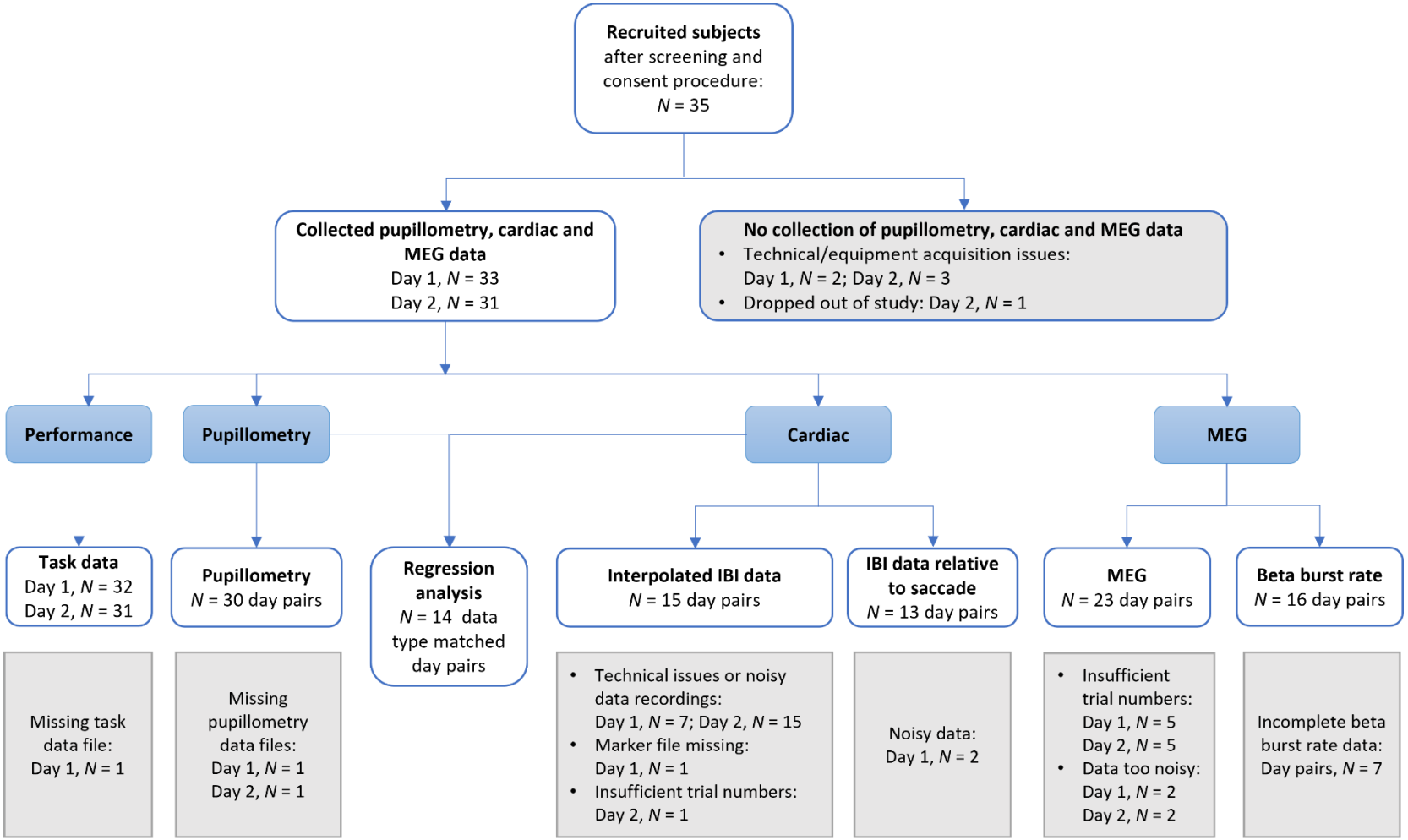

Figure 9: Schematic showing the number of subjects included at each stage of the analysis pipeline.

4.1.4. Short-version CAARS

The multiple-choice self-report CAARS (short version), designed for use in adults, was used to assess ADHD symptoms in our sample. The CAARS questionnaire consists of 26-items where the participant indicates how relevant the statement applies to their symptoms by scoring on a 4-point Likert-type scale (0 = *not at all or never*; 1 = *just a little, once in a while*; 2 = *pretty much, often*; 3 = *very much, very frequently*) (Conners et al., 1999). Raw scores were used to generate *T*-scores (age- and gender-normed scores, scaled to have a mean of 50 and a standard deviation (Std. Dev) of 10) using the scoring sheets from the CAARS manual. The CAARS yields *T*-scores for the following constructs: Inattention/Memory Problems, Hyperactivity/Restlessness, Impulsivity/Emotional Lability, Problems with Self-Concept, and an overall ADHD Index (Conners et al., 1999).

The scale for *T*-scores is constructed so that a higher score indicates more frequent or more severe problems. For example, this means a person with a *T*-score of 60 on one of these items has a score that is one Std. Dev higher than the population mean, i.e., at the 84th percentile, whereas a person with a *T*-score of 70 lies at the 97.7th percentile. Since the scale has a population mean of 50, we can test our sample to see whether their mean score is significantly higher (or lower) than the population mean for each item. Therefore, a one-sample *t*-test was computed for these categories using the population mean of 50 as the test value.

The statistical analysis revealed a significant difference for the Inattention/Memory Problems measure, mean = 59.88, Std. Dev = 10.398; $t(31) = 5.372$, $p = .000$. This indicates that our sample were significantly inattentive, whereby the mean *T*-score in the sample was one Std. Dev higher than the population mean. There was also a significant difference for the Impulsivity/Emotional Lability measure, mean = 45.52, Std. Dev = 8.258; $t(32) = -3.120$, $p = .004$, indicating that the mean Impulsivity/Emotional Lability *T*-score in the sample was significantly lower than the population mean, by nearly half a Std. Dev. No other CAARS measures reached significance. Therefore, our sample was characterised by inattentive, rather than hyperactive/impulsive ADHD symptoms.

4.1.5. TOWRE-II baseline

The TOWRE-II was used to evaluate reading ability to indicate dyslexic traits. This is a single-word reading test that yields three measures of reading efficiency: Sight Word Efficiency (SWE), measuring speed of reading real words; Phonological Decoding Efficiency (PDE), measuring speed of reading pronounceable pseudowords; and Total Word Efficiency (TWE) (Torgesen et al., 2012). Participants are required to read aloud as many words as possible in 45 seconds from a list of real words, and again for a list of pseudowords (i.e., made-up words). To obtain the raw scores, participants were marked on how many words they read correctly in the first list, and how many they pronounced correctly in the second list. The TOWRE provides lookup tables for converting raw scores to Standard scores

normed by age. Standard scores are scaled to have a population mean of 100 and a Std. Dev of 15). A higher TOWRE-II score indicates better reading ability.

A one-sample *t*-test was conducted using the population mean standard score of 100 as the test value. Significance was found for SWE, mean = 89.23, Std. Dev = 12.852; $t(34) = -4.958$, $p = .000$, which indicated the sample mean SWE was significantly below the population mean by nearly 0.75 Std. Devs. There was also a significant finding for the TWE, mean = 93.00, Std. Dev =16.125; $t(34) = -2.568$, $p = .015$, whereby the sample mean for the overall TOWRE score was significantly below the population mean by half a Std. Dev.

Therefore, these findings support that the sample, as a whole, had impaired reading abilities relative to the general population, particularly in the sight word reading domain. Our sample were recruited from the University of Nottingham, which requires a high A-level or equivalent tariff. Thus, we would expect mean scores for university students to be better than population average reading ability scores (above 100). Despite sample mean PDE being non-significantly lower than the population mean (mean = 98.43, Std. Dev = 15.780), this result may nonetheless imply an impairment in phonological decoding, because we would still expect this population to be significantly higher than average for all reading domains. Overall, these findings support that our sample represents a higher than

average prevalence of dyslexia traits, corroborating the high number of dyslexia diagnoses reported by this group of participants (see Section 4.1.1).

4.1.6. GHQ – 12 item version baseline

The GHQ – 12 item version questionnaire is a multiple-choice self-reported questionnaire (Goldberg & Williams, 1988) that has been validated to assess minor mental health symptoms (Hardy et al., 1999). The GHQ questions are phrased to assess recent changes in mental health and in what direction. Raw scores for the responses of each of the 12 items were obtained via a 4-point Likert-type scale. The first response for each item corresponds to better than usual or no impairment being present, so this is assigned a '0'. The next set of responses that are assigned a '1' are for "same as usual" or "no more than usual" responses, which indicate no recent changes in mental health. The remaining answers in the final two columns indicate extent of recent increases in mental health symptoms, scored 2-3, respectively.

The overall GHQ score is the sum of each item score, where a total of '0' is possible that would indicate better than usual/no sign of mental health symptoms present. A score of 12 would indicate an average response of 1 for each item, which infers no recent changes in mental health symptoms. The higher the total, the greater the change in mental health symptoms present.

To assess any significant recent changes in minor mental health symptoms, a one-sample *t*-test was conducted using 12 as the test value.

Statistical analysis did not reach significance, mean = 10.97, Std. Dev = 3.460, $t(34) = -1.759$, $p = .088$. Therefore, this showed that on average our sample had not experienced any recent changes in mental well-being at baseline.

4.2. Behavioural results pre- to post-RECOGNeyes training

4.2.1. Training schedule and compliance

As described in Chapter 3, Section 3.5.1, each participant was assigned to complete 2, 3 or 4 training sessions per week over the 2-week training period. Table 3 summarises the training allocation details and the actual total training time information. If we take a training time of 20 minutes and account for training on average 3 times per week, this equates to an expected average of 120 minutes of total exposure. As shown in Table 3, across groups the mean and Std Dev. total exposure was 129.09 ± 57.71 minutes. Therefore, this supports good RECOGNeyes gaze-control training exposure in our sample.

Table 3: RECOGNeyes training session allocation and total training time details.

No. of sessions per week	No. subjects per group	Actual total training time (mean mins ± Std. Dev)
2	11	94.12 ± 22.82
3	12	137.75 ± 64.14
4	12	152.48 ± 61.70
Total	35	129.09 ± 57.71

4.2.2. Reading assessments and GHQ

The TOWRE-II questionnaire and eye-tracked reading task measures were used to assess the reading ability of the sample and whether there were any changes in the results following RECOGNeyes training. We also administered the GHQ for wellbeing and mental health symptom assessment on both days.

Variables for assessing eye-movement characteristics in reading were selected and computed by other members of our team from standard reading metrics identified in the literature (Rayner, 1998, 2009):

- Mean and Std. Dev of the preferred landing position (PLP), which is the point in the word where the first fixation is made. Typically, this is two or three letters into the start of the word, regardless of word length (Rayner et al., 2001).

- Mean length of words with 0, 1, 2, or 3 fixations. This means having a smaller mean word length with '0' fixations is better to ensure important content words are not being skipped. Having longer mean word lengths with 1-3 fixations may indicate taking in longer words using fewer fixations.

- Mean forwards or backwards saccade size (i.e., regressive saccade from right to left) measured in letter widths (i.e., how many letters into the word the saccade jumped to).

- Proportion of regressive saccades relative to total forward saccades made, excluding saccades made from the end of a line to the beginning of the next.

- Mean and Std. Dev of fixation duration time. This tends to be shorter in more skilled readers (Rayner, 1998).

Paired *t*-tests (in the direction of Day 2 minus Day 1) were computed to assess whether there were any significant changes in these domains on Day 2 compared to Day 1. Results for the reading assessment variables found a significantly lower PLP Std. Dev on Day 2 compared to Day 1, mean = -0.09, Std. Dev = 0.212; $t(26) = -2.195$, $p = .037$. Even though the mean PLP did not change on Day 2, this result indicates that the variance of the PLP significantly reduced; hence, supporting increased reliability about making a saccade to the same point in each new word, which reflects better

saccadic control. The mean length of words with 1 fixation significantly increased on Day 2, mean = 0.13, Std. Dev = 0.212; $t(26) = 3.267$, $p = .003$, meaning that the word size read and processed with one fixation increased, which also points to better saccadic control.

Mean forward saccade size significantly increased on Day 2, mean = 0.86, Std. Dev = 1.664; $t(26) = 2.695$, $p = .012$. This could be an issue if longer words were being skipped, but there were no significant increases in the mean length of words skipped. Therefore, increased forward saccade length is likely to indicate fewer fixations per word on average, implying an increase in perceptual span during reading. In addition, the mean backward saccade size significantly decreased on Day 2, mean = -1.58, Std. Dev = 2.856; $t(26) = -2.881$, $p = .008$. The reduction in backwards saccade size indicates better saccadic control that point to smaller corrective saccades required to re-read previous words again.

Paired *t*-test outcomes for the TOWRE-II score categories found significant improvements on Day 2 for the SWE, mean = 4.15 points improvement, Std. Dev = 6.977; $t(33) = 3.466$, $p = .001$, and TWE, mean = 2.97 points improvement, Std. Dev = 5.531; $t(32) = 3.084$, $p = .004$. This indicates that these reading domain scores that were significantly below average in the general population (as discussed in 1.1.3.) significantly improved on Day 2. Therefore, this could suggest that RECOGNeyes training helped to improve these reading domain scores, particularly for

sight word reading to result in better overall TWE scores. However, it may also simply reflect greater degree of comfort with the task on Day 2.

Paired *t*-test results for the GHQ score between days indicated a significant reduction of the score on Day 2 compared to Day 1, mean = -1.324 points change, Std. Dev = 3.796; $t(33) = -2.033$, $p = .050$. This suggests on average the subjects on Day 2 reported a positive change in recent mental well-being. This is also supported by a one-sample *t*-test using 12 as the test value (as described for baseline Day 1 analysis in Section 4.1.6) showing that the mean sample test score was significantly below this, mean = 9.71, Std. Dev = 3.928; $t(33) = -3.406$, $p = .002$. Therefore, this means the sample on average reported recent improvements in wellbeing on Day 2 and were significantly more likely to report a recent improvement on Day 2 than on Day 1.

4.3. Task performance: Reaction Time

4.3.1. Defining saccade onsets

After each completion of the pro/antisaccade task, performance data and pupillometry data files were generated from EyeLink® 1000-Plus (SR Research Ltd.) software. This included our manually predefined reaction time (RT) variable, which was the elapsed time taken to make a saccadic response after the target was displayed on the screen. Task files also

included data listing the type of response on each trial (i.e., correct, incorrect, early, and late saccadic responses), which was utilised for the task accuracy measures discussed later in Section 4.4).

4.3.2. Express saccade considerations

An additional consideration for saccadic RTs are express saccades; a phenomenon first discovered in monkeys (Fischer & Boch, 1983) and shortly afterwards in humans (Fischer & Ramsperger, 1984). This describes the observation of a bimodal distribution of saccadic RTs, where the first of these peaks corresponds to around 100 msecs in humans, which have been defined as express saccades (Fischer & Ramsperger, 1984; Munoz et al., 1998; C.-A. Wang et al., 2015). Many publications, particularly from Fischer's research group, have studied this phenomenon (as reviewed by Fischer & Weber (1993)), where they believed that express saccades have a different neural network accountable for their production via the 'optomotor reflex'. For instance, this would link directly to discussions in the Chapter 2, Section 2.2.1 regarding the SC mediating such reflexive saccadic responses (Marino et al., 2015). The speed of these saccades would be enabled by by-passing visual and saccadic processing from other cortical regions.

However, the existence of this bimodal distribution has since been contested by other research groups, who have demonstrated that this distribution is influenced by different experimental set-up and task design

parameters, such as increased incidence of express saccades when using gap paradigms (Carpenter, 2001; Kingstone & Klein, 1993; Marino & Munoz, 2009; Schiller et al., 2004). Since a gap paradigm was not used in our pro/antisaccade task for the current study, we expected our task design to limit the number of express saccades. Additionally, other conditions in our task mean there is still the possibility of express saccades to occur, e.g. use of a single target rather than multiple targets (Weber & Fischer, 1994) and training on saccadic tasks can increase the number of express saccades recorded after training than before (Bibi & Edelman, 2009). Since the possibility of express saccades occurring could not be fully ruled out, I decided to exclude trials with RTs of 100 msecs or less in pupillometry, cardiac and magnetoencephalography analyses, because they were likely to be reflexive and not part of the voluntary saccadic pathway we were investigating.

4.3.3. Reaction time data distribution

Saccadic RT was included as one of the measures to assess task performance. As summarised in Figure 9, for task performance data analysis there were a total number of subjects, $N = 32$ for Day 1 and $N = 31$ for Day 2, respectively. Therefore, day-paired task performance data analyses had an N of 31. Summary data for subject RT included computing the median RT for all correct RTs, for prosaccades and antisaccades on Day 1 and Day 2, respectively. This was chosen instead of the mean RT, because the median is less influenced by extremely fast or slow RTs.

Median RT distributions for each day and trial type are represented using histograms, as shown in Figure 10, Figure 11, Figure 12, and Figure 13. These also include summary statistics for each day and trial type combination of the mean, standard deviation (Std. Dev) and *N*. Note that histograms have the same *x*-axis scale for comparison purposes, using a bin width of 20 msecs across a range of 140 to 380 msecs.

The RT data shows that within each day, prosaccade trials had shorter RTs as depicted by more leftward histogram distributions relative to the antisaccade trial distributions. In addition, Day 2 RT distributions are shifted leftwards relative to day 1 histograms, which indicate a higher frequency of shorter RTs. Therefore, this shows that RTs were faster on Day 2 for both trial types, which supports better task performance for both trial types after RECOGNeyes training. Distributions were also narrower for both trial types on Day 2, as supported by smaller Std. Devs. This reduced variation of RT indicates better response consistency after RECOGNeyes training, hence further supporting better performance reliability within saccade type.

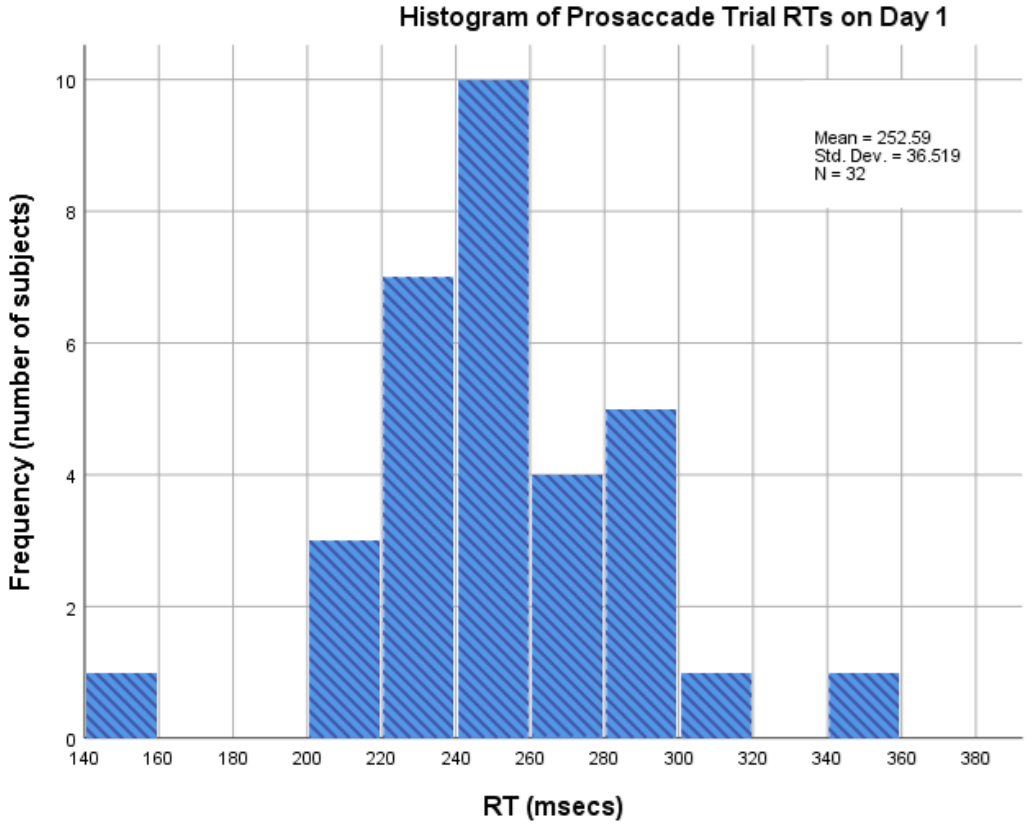

Figure 10: Histogram of RT distribution on Day 1 for prosaccade trials.

Summary statistics (mean, standard deviation (Std. Dev) and number of subjects(N)) are included in the top right-hand corner. Bin width was 20 msecs.

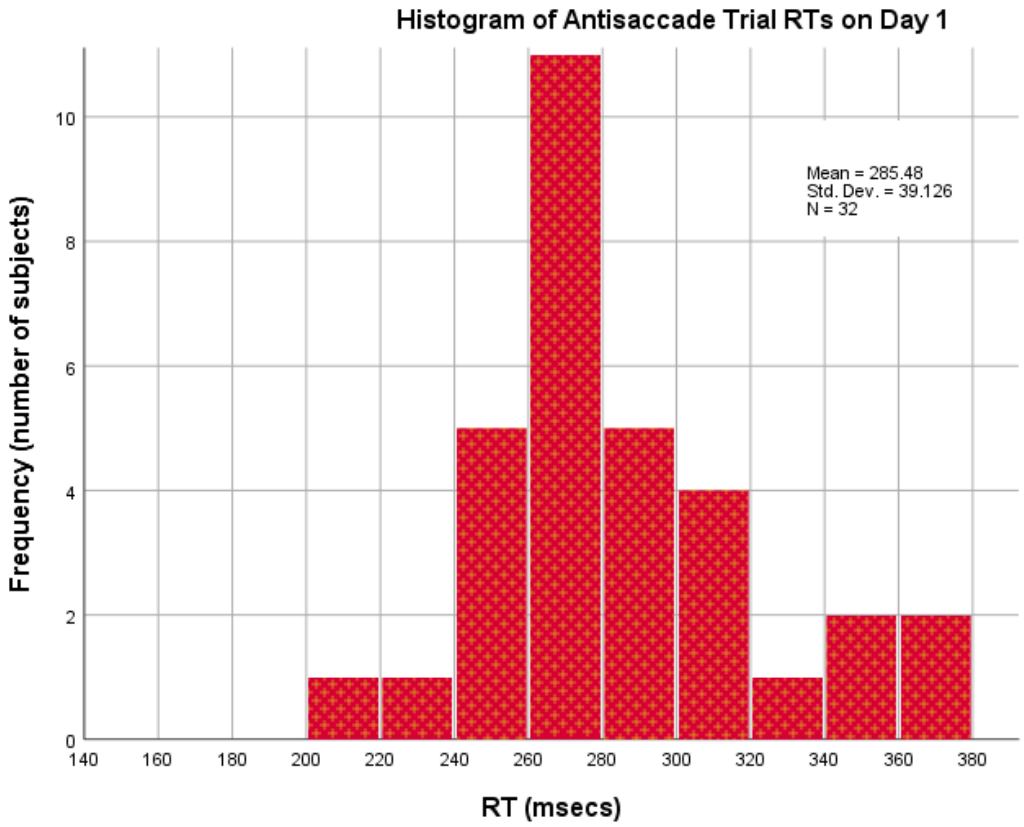

Figure 11: Histogram of RT distribution on Day 1 for antisaccade trials.

Summary statistics (mean, standard deviation (Std. Dev) and number of subjects (N)) are included in the top right-hand corner. Bin width was 20 msecs.

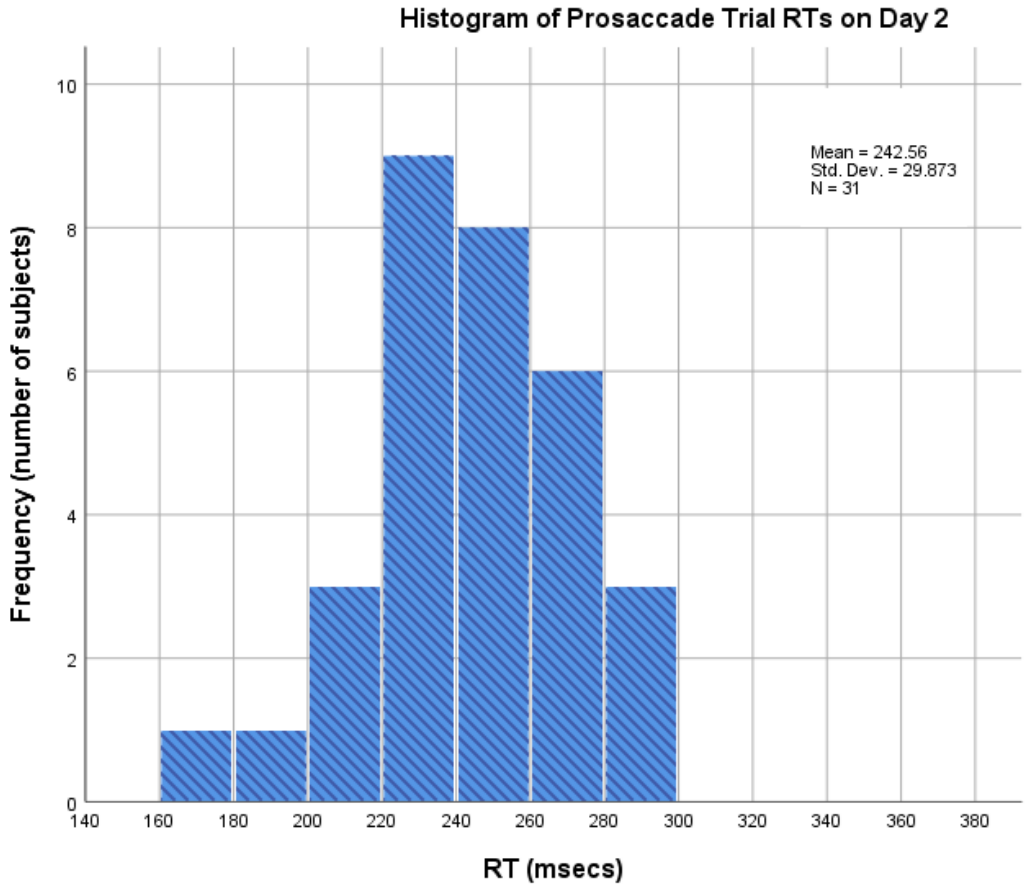

Figure 12: Histogram of RT distribution on Day 2 for prosaccade trials.

Summary statistics (mean, standard deviation (Std. Dev) and number of subjects(N)) are included in the top right-hand corner. Bin width was 20 msecs.

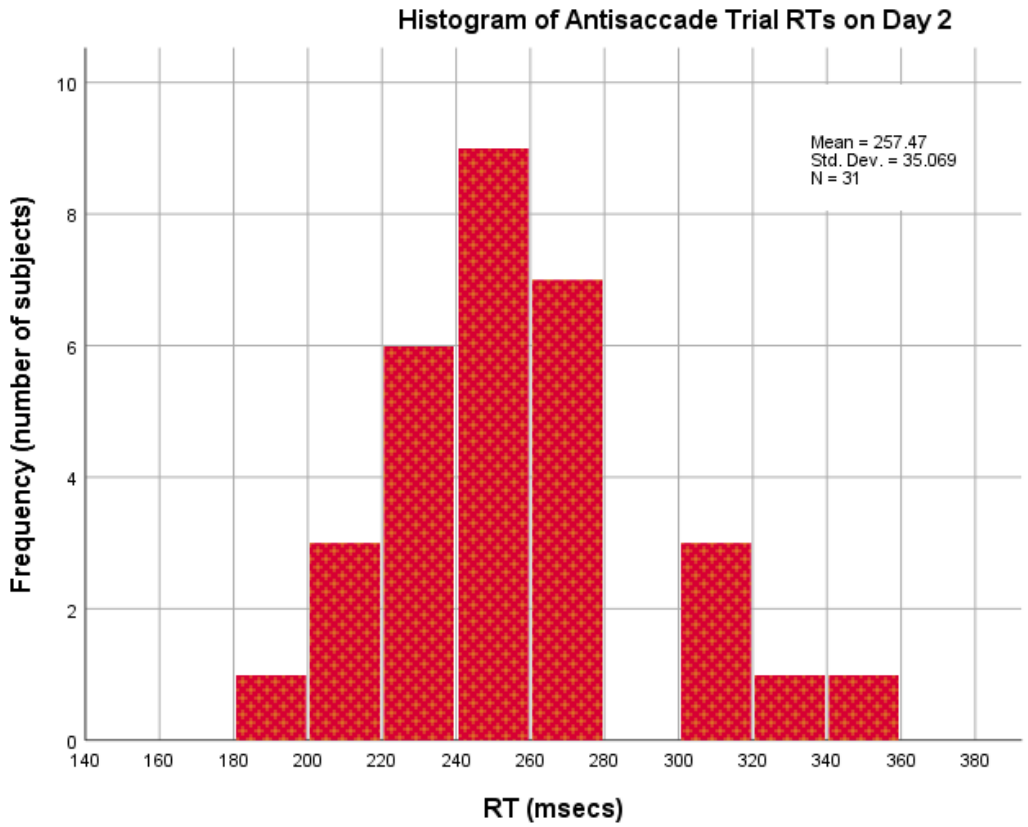

Figure 13: Histogram of RT distribution on Day 2 for antisaccade trials.

Summary statistics (mean, standard deviation (Std. Dev) and number of subjects(N)) are included in the top right-hand corner. Bin width was 20 msecs.

4.3.4. Statistical analysis of reaction times

To analyse whether histogram observations of trial type differences and better performance post-RECOGNeyes training were statistically significant, I conducted a two-way repeated-measures analysis of variance (ANOVA), where each predictor variable had two levels, including Day (Day 1 and Day 2) and Trial Type (prosaccade trials and antisaccade trials). This analysis found a significant effect of Day, $F(1, 30) = 26.236$, $p = .000$,

whereby RTs across trial types were significantly faster on Day 2 than on Day 1. A significant effect of Trial Type, $F(1, 30) = 30.176$, $p = .000$, revealed that RTs were significantly faster for prosaccade trials than for antisaccade trials across days; this is consistent with previous observations that antisaccades take longer to generate than prosaccades (Everling et al., 1998; Munoz et al., 1998; C.-A. Wang et al., 2015). The average RT data across subjects for trial type on each day is illustrated in Figure 14, which are consistent with trends observed in the histogram data.

In addition there was a significant Day by Trial Type interaction, $F(1, 30) = 15.298$, $p = .000$. This interaction was further investigated by calculating the trial type RT differences (median antisaccade RT minus the median prosaccade RT) on each day per subject. The mean ± Std. Dev for the trial type differences on Day 1 was 34.016 ± 32.915 msecs and on Day 2 was 14.903 ± 22.714 msecs. Both are positive, which supports the prior results that antisaccades had longer RTs than prosaccades, and the difference score was larger on Day 1 than on Day 2.

A paired *t*-test revealed that the difference score was significantly less on Day 2 than on Day 1, $t(30) = -3.911$, $p = .000$. Hence, this indicates that despite both trial type RTs being faster on Day 2, there was a much larger improvement for antisaccade trials than for prosaccade trials, which led to a smaller difference between the trial types after training as supported by Figure 14. This striking difference is much more apparent than in the histogram figures, where Figure 14 depicts that the average

antisaccade RT on Day 2 is comparable to the average prosaccade RT on Day 1.

To summarise, RT performance showed improvements for both trial types following RECOGNeyes training, particularly for antisaccade trials. This could be indicative of training improving saccadic control, particularly in the inhibitory control of antisaccadic mechanisms. To ensure that the improved post-training RTs on Day 2 were not the result of a speed-accuracy trade-off, measures of accuracy were analysed; this is discussed in the following section.

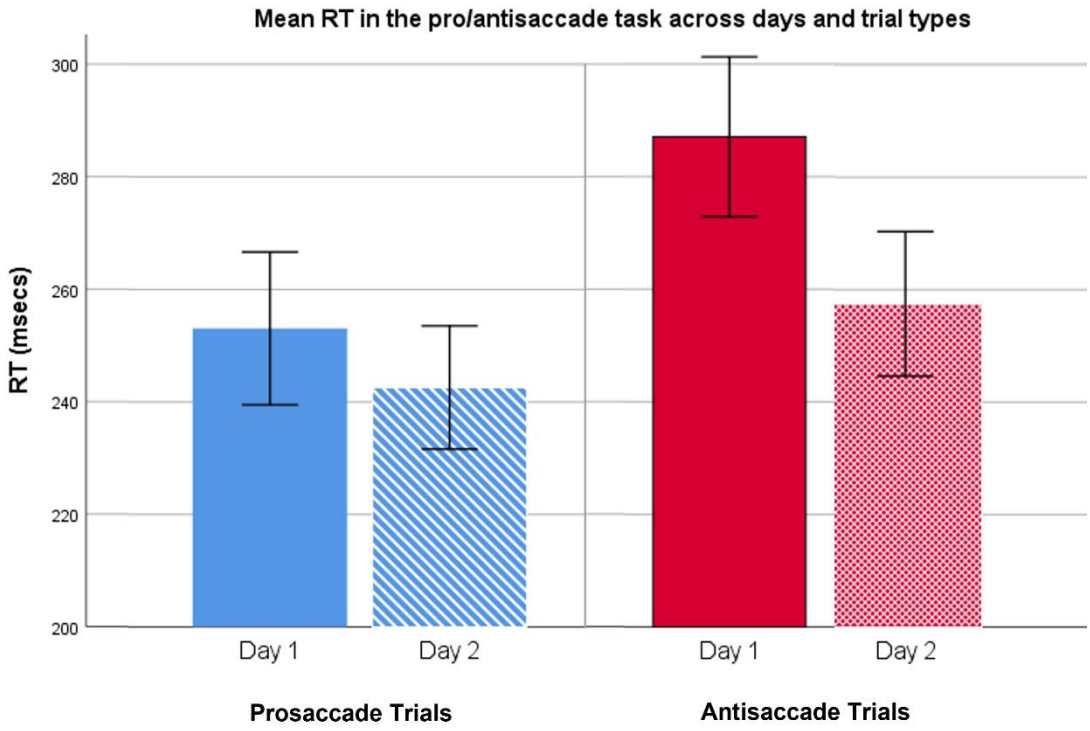

Figure 14: Bar chart of the mean RT for each day and trial type.

Average RTs plotted here are the mean of the subject median RTs for each day and trial type category, including error bars (95% confidence interval).

4.4. Task performance: Accuracy

4.4.1. Using signal detection theory for accuracy and bias measures

It is possible that when participants improve their antisaccade accuracy on a task in which they are sometimes required to make prosaccades that they do so at the cost of making inadvertent antisaccades to prosaccade trials. If so, there may be no net improvement in the ability to "discriminate" between the two trial types – merely a shift in response propensity in the direction of antisaccades. Therefore, to evaluate improvements in task performance accuracy, D-prime (d′) scores were computed as a response discrimination index to reflect how well each subject discriminated between prosaccade and antisaccade trials, and the decision criterion was computed as an index of response bias. The fundamentals of these measures follow the conventions of signal detection theory, where firstly the response types of the task need to be defined; the variables defined in this section are based on similar approaches and theory described in Macmillan & Creelman (2004).

For instance, if there is a single interval (e.g., yes/no) or forced-choice experiment where a signal is either present or not, correctly identifying the presence of a signal is a 'hit' (H), but if this is not detected this is a 'miss'. Alternatively, if a signal is not present and there is no reaction, this is a 'correct rejection' but if the participant responds that a signal is present

when it is not, then this is a 'false alarm' (FA). Since the pro/antisaccade task follows a 2-alternative forced-choice trial format, we can use this classification by basing the responses in relation to the question "is this an antisaccade trial?" being asked of the participant in each trial (refer to Table 4 for the 2 by 2 contingency table of pro/antisaccade task responses).

Table 4: Pro/antisaccade task 2 by 2 contingency table to classify task responses.

Responses were defined based on the participant answering the question "is this an antisaccade trial?".

Participant response:	**Antisaccade trials**	**Prosaccade trials**
YES *(this is an antisaccade trial)*	**Hit rate (H)** = *an antisaccade made on an antisaccade trial*	**False alarm rate (FA)** = *an antisaccade made on a prosaccade trial*
NO *(this is not an antisaccade trial)*	**Miss rate (1-H)** = *a prosaccade made on an antisaccade trial*	**Correct rejection rate (1-FA)** = *a prosaccade made on a prosaccade trial*

Signal detection theory assumes that for each trial type, the decision responses will each have different distributions that are all normally distributed with equal variance. The discrimination index, d′, thus provides a way to measure how close or distinct the trial type distributions are to each other. The less overlap between the distributions and the larger the separation between them, the better the discriminability between response types. Therefore, this penalises a subject that has a default response (e.g., favouring antisaccades at the expense of correctly performing prosaccades),

because there will be less difference between the distributions. The d′ calculation reflects this by computing the difference between the *z*-scored distribution means of 'hit' minus 'false alarm' (i.e., *z*H – *z*FA); thus, better discriminability is indicated by a larger d′ score.

To produce d′ scores for our data, firstly the rate for each type of response outlined in Table 4 was computed (number of responses for each type divided by total number of responses). The total number of trials for the rate calculation only included responded trials with a 'correct' or incorrect' saccade (i.e., trials with late, early or missed responses were excluded from the trial total). The resulting response rates are between 0 and 1. Since response rates are clustered at the top end of the scale, *p*-*z* transform (inverse cumulative standardized normal distribution function, e.g., the NORMSINV function in Excel) is performed to linearise the scale at these high rates.

In our data, there were instances where responses were correct for 100% of trials. However, d′ is not estimable if the rate of correct responses is 100%, since *z*-transforming rates of 0 or 1 result in infinite *z*-score values that cannot be used. Also, a true rate of 100% correct responses is implausible. Since our data provided an estimate of the probability of correct responses derived from a limited number of trials, instances of 100% correct responses in our data indicate that the true error rate is likely to fall between 0 and 1 error in N trials. We therefore adopted the strategy where the number of responded trials was doubled (2N) and a corresponding

correct response rate was calculated from $1 - \frac{1}{2N}$. This assumption truncates the range of possible d′ values in the range where the uncertainty of the estimate is large, while nonetheless setting an upper limit for d′ that increases as confidence increases with increase in N.

The decision criterion was also computed to give an indication of response bias. This is the threshold point of where the subject will respond 'yes' to the decision. For example, a low decision criterion value reflects a more liberal response threshold where the participant is more likely to respond "yes, this is an antisaccade trial", whereas a high decision criterion indicates a stricter threshold where the participant is more likely to respond "no, this is not an antisaccade trial" and favour a prosaccade response. The decision criterion was calculated by averaging the *z*-transformed hit and false alarm rates together and dividing this all by 2 (i.e., (zH + zFA)/2). The convention for this calculation is to multiply by minus 1, but can be computed without (different computational approaches are discussed in Stanislaw & Todorov (1999)). The d′ and decision criterion scores were computed and included in statistical analysis explained in the next section.

4.4.2. Distribution of d′ scores and statistical findings

Prior to statistical analysis, the distributions of the d′ scores were visualised using histograms included in Figure 15 for Day 1 and Figure 16 for Day 2. Both histograms are plotted on the same scale with the same bin width of 0.45 between d′ of 1.40 and 5.45 for ease of comparison between

days. The distribution for d′ scores on Day 2 is shifted leftward relative to the distribution on Day 1, which indicates that response accuracy improved in the task on Day 2.

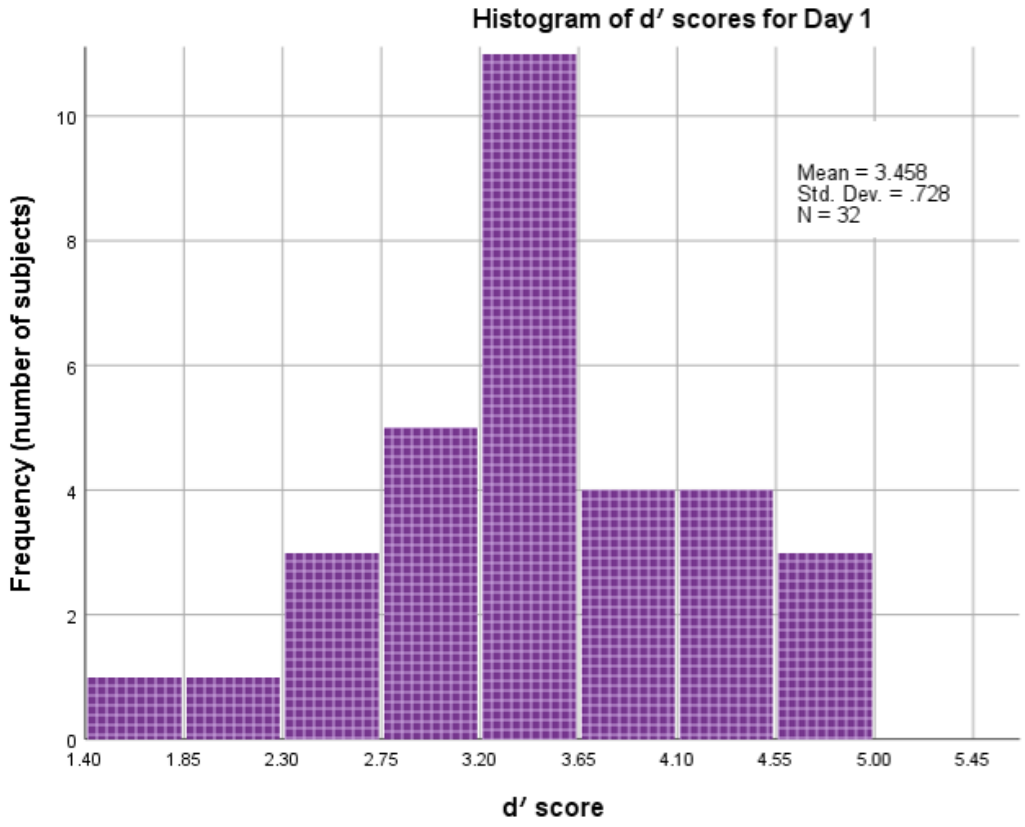

Figure 15: Histogram for d' score distribution across subjects on day 1.

Summary statistics (mean, standard deviation (Std. Dev) and number of subjects (N)) are included in the top right-hand corner of the figure. Bin width was a d' score of 0.45.

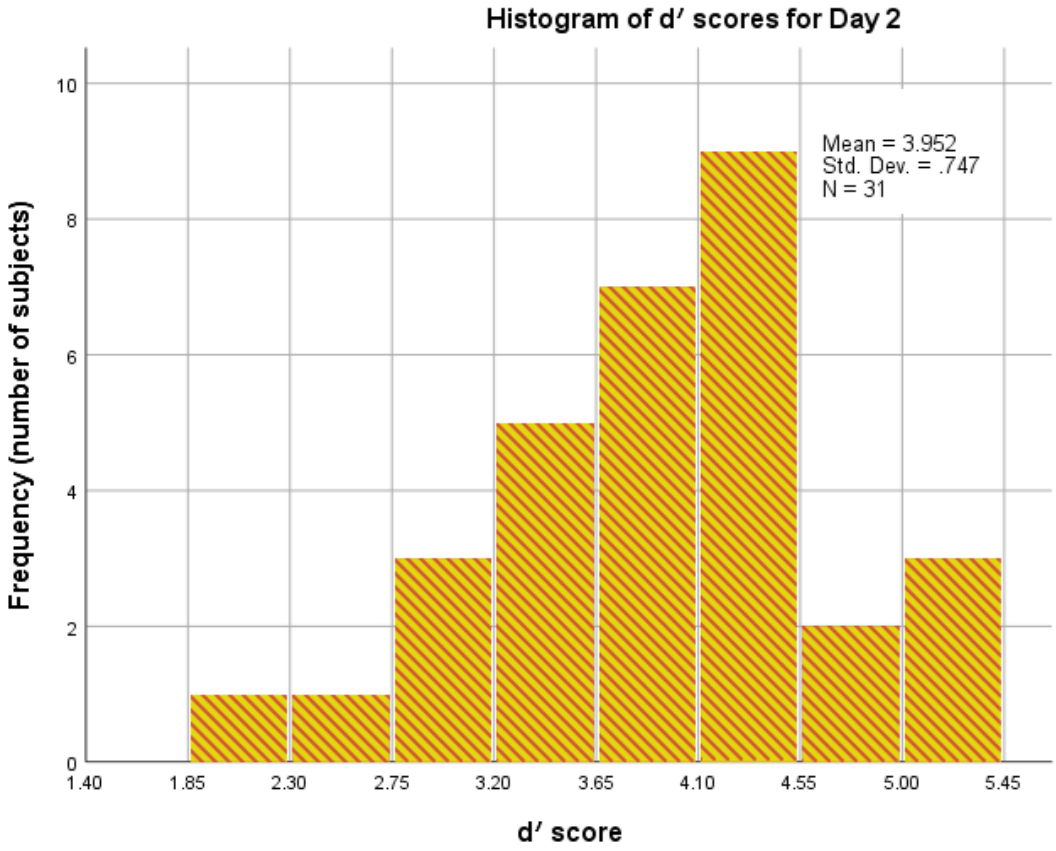

Figure 16: Histogram for d' score distribution across subjects on day 2.

Summary statistics (mean, standard deviation (Std. Dev) and number of subjects (N)) are included in the top right-hand corner of the figure. Bin width was a d' score of 0.45.

Summary statistics of d′ and decision criterion mean, Std. Dev and standard error of the mean (SEM) are included in Table 5. For statistical analysis, paired-sample *t*-tests were computed between the d′ and decision criterion scores across subjects to see if there were any improvements in these accuracy measures on following RECOGNeyes training. These were computed in the order of Day 2 – Day 1 to examine directional change on Day 2. There was a significant difference in d′, $t(30) = 3.811$, $p = .001$,

whereby the positive *t*-value indicates a significant increase in d′ score on Day 2. Therefore, this supports an improvement in the discriminability or sensitivity index between the two trial type responses after RECOGNeyes training, i.e., an improvement in response accuracy.

The summary statistics in Table 5 show that the decision criterion was negative on both days, which indicates a bias towards prosaccades, and that the decision criterion was less negative on Day 2, implying a reduced propensity to make an antisaccade. However, this difference was not significant. Considering that antisaccade trials require the inhibition of a prosaccade, this bias towards prosaccades is not surprising since this is the more reflexive or default response to a stimulus. There were also significant paired correlations between day scores for both d′, $r = 0.563$, $p = .001$, and decision criterion, $r = 0.458$, $p = .010$; thus, supporting good test-retest reliability.

Table 5: Summary statistics for d' and decision criterion scores.

All values are rounded to 3 decimal places (d.p).

	Mean	**Std. Dev**	**SEM**
d′ Day 1	3.481	0.728	0.131
d′ Day 2	3.952	0.747	0.134
Decision criterion Day 1	-0.285	0.279	0.050
Decision criterion Day 2	-0.220	0.192	0.034

4.5. Behavioural results discussion

Our behavioural results at baseline established that the RECOGNeyes sample was characterised by a higher than average prevalence of inattentive rather than hyperactive/impulsive ADHD symptoms. While RECOGNeyes gaze-control is predicated on the idea that inhibitory control of gaze-direction implicates both ADHD symptom types in the control of attention, it was reassuring to find that the sample exhibited impairments on one of these constructs. Our sample was also characterised by poorer than average reading ability (particularly for sight word reading) relative to the general population. As discussed, there is a large overlap between ADHD and SpLDs and 80% of the sample had a dyslexia diagnosis, so this is unsurprising that there were signs of poorer reading abilities.

The sample also did not show significant indications of recent changes in mental health at baseline, making the significant increase in reports of recent beneficial changes on Day 2 reassuring. While it seems unlikely that RECOGNeyes would have had a direct effect on mental well-being, it is nonetheless reassuring that participants do not appear to have found RECOGNeyes deleterious to their mental health, and perhaps indicates that they enjoyed taking part in the study. These results also indicate that there were no co-morbidities of mental health conditions present in the sample.

All subjects engaged in RECOGNeyes training and the mean total playing time indicated good compliance with the assigned protocol. After training, there were significant improvements in various reading skill domains. This included sight word reading ability, which improved overall TOWRE-II scores. In the eye-tracked reading task, after training there were more reliable saccade landing positions into a word, an increase in the word length processed with a single saccade, smaller regressive saccades, and larger forward saccades. These findings indicated overall better top-down visual attention and oculomotor saccadic control processing, supporting a link between reading ability and visual attentional processing.

In regards to pro/antisaccade task performance, both RT and accuracy results established that performance in the pro/antisaccade task significantly improved post-RECOGNeyes training than pre-training levels, and there were differences between trial type responses. Notably, the RT was faster in prosaccade than antisaccade trials regardless of day, but the greatest improvement in RT across days was for antisaccade trials. Since the neural mechanism to produce an antisaccade requires the additional inhibitory control process to suppress the reflexive prosaccade reaction and vector inversion to make a saccade in the opposite direction (as discussed in Chapter 2, Section 2.2.1), this agrees with our results for longer antisaccade production latencies.

Additionally, our results indicate an increase in response accuracy on Day 2 compared to Day 1. This reflects that the faster RTs on Day 2 were

not due to speed-accuracy trade-off, and that instead the faster RTs and greater response accuracy are complementary indices of overall better task performance on Day 2 after training. The larger magnitude of RT improvement in antisaccade trials on Day 2 also corroborates an increased accuracy in performing antisaccades.

It is worth noting that making an antisaccade involves first inhibiting the prepotent motor program for making a prosaccade. This means that faster antisaccade RTs may at least in part reflect more successful inhibition of the prepotent prosaccade motor program. It is possible, therefore, that the more modest decrease in prosaccade RTs reflects a generalised tendency to down-regulate the bottom-up drive to make a saccade to a sudden-onset peripheral stimulus. Alternatively, it may simply reflect the fact that baseline prosaccade RTs are likely to be nearer to the RT lower limit imposed by processing speed.

To summarise, our behavioural findings indicate changes in inhibitory control and saccadic processes between assessment days, as well as task performance findings supporting day and trial type differences. The following chapters will investigate ANS and CNS measures during the pro/antisaccade task and whether these relate to task performance outcomes.

Chapter 5: ANS effects as measured by pupillometry

5.1. Background and Rationale

In the RECOGNeyes study, we aimed to assess neural correlates of cognitive control in the pro/antisaccade task. This chapter reports an investigation into arousal effects as measured by pupillometry. I will examine changes in pupil size in response to both the cue that signals an upcoming target stimulus and to the target stimulus itself. Both are likely to reflect the alerting response component of the preparatory processes in the pro/antisaccade task. I will also investigate the relationship between pupil dilation responses and task performance as measured by reaction times. As pro/antisaccade task performance, indexed by both accuracy and reaction time, improved on Day 2 after RECOGNeyes training compared with Day 1, I will investigate correlates of performance as measured by RT, and how these may differ between Day 1 and Day 2.

Pupillometry is the technique of measuring pupil size and was first established in the 1960s (Hess & Polt, 1960, 1964; Kahneman & Beatty, 1966). Since these pioneering studies, pupillometry has been a widely used tool for psychological and cognitive neuroscience research topics ranging from attentional processing, arousal, emotion, perception, language, working memory, and decision making (further information regarding the

history of pupillometry is reviewed by Laeng et al. (2012); Sirois & Brisson (2014)).

Recently, applications of pupillometry have focused on assessing changes in pupil size as an indirect measure of arousal, alerting and cognitive functioning. The key region involved in mediating these arousal mechanisms is the brainstem nucleus locus coeruleus (LC); the singular source of cortical norepinephrine (NE), which has an array of central and peripheral nerve projections to cortical regions, midbrain, brainstem and spinal cord (Berridge & Waterhouse, 2003; Foote et al., 1983; Samuels & Szabadi, 2008a). For further details regarding arousal, alerting and the autonomic nervous system, refer to Chapter 2, Section 2.1.2).

Support for the relationship between LC-NE activity, arousal and pupil dilation originated from neurophysiological studies recording directly from monkey LC neurons. These studies found that increased LC firing correlated with increased cognitive task load and responding to salient stimuli (Aston-Jones et al., 1994; Rajkowski et al., 2004), pupil dilation (Aston-Jones & Cohen, 2005) and both (Joshi et al., 2016; Varazzani et al., 2015).

Changes in pupil dilation are thought to largely reflect changes in LC neuronal firing (Aston-Jones & Cohen, 2005), although as pupil size responds to parasympathetic activity by constricting, concurrent parasympathetic activity may somewhat modulate the rate of pupil dilation. Nonetheless, pupillometry is increasingly being adopted as a non-invasive

method to directly assess phasic and tonic changes of LC-NE activity in humans in studies of arousal (Cheadle et al., 2014; Einhäuser et al., 2008, 2010; Eldar et al., 2013; Gilzenrat et al., 2010; Hayes & Petrov, 2016a; Jepma & Nieuwenhuis, 2011).

Furthermore, in line with Aston-Jones and Cohen's model (see further discussion in Chapter 2, Section 2.1.2) in which phasic LC firing reflects an "exploitation" mode, task-related pupil dilation has been established to index cognitive effort and task engagement (Beatty, 1982a, 1982b; da Silva Castanheira et al., 2021; Gilzenrat et al., 2010; Richer & Beatty, 1987). A review by van der Wel & van Steenbergen (2018) concludes that pupil dilation increases with greater task demands. Evidence specifically regarding the pro/antisaccade task indicates increased preparatory pupil dilation in antisaccade trials than prosaccade trials (Karatekin et al., 2010; C.-A. Wang et al., 2015, 2016), and that preparatory pupil dilation is correlated with faster RTs on antisaccade trials (C.-A. Wang et al., 2015, 2016). As antisaccades are likely to demand more effort, this suggests that more effortful tasks elicit greater preparatory arousal, as indexed by pupil dilation.

Geva et al. (2013) investigated the time courses of pupil dilation during the Attentional Network Task (ANT) used by Posner's group to delineate Posner's proposed Alerting, Orienting and Executive attentional networks. The ANT is a modified flanker task performed under four cuing conditions: no cue; a spatially informative cue (one that both "alerts" and

"orients"; and two kinds of "alerting only" cues that predict the time, but not the location, of the upcoming stimulus. Geva et al. (2013) found that even a non-spatially informative "alerting only" cue (presented 500 msecs prior to the target) elicited significant phasic pupil dilation, which was followed by continued pupil dilation following target onset.

In our version of the pro/antisaccade task, the target is preceded by an "alerting-only" cue 800 msecs earlier. This cue provides only temporal information; it does not inform the participant of the location of the upcoming target. While it provides information regarding trial type, this is merely a reminder, as the trials are arranged in blocks of the same trial type, and information is additionally provided before each block as to which kind of trials it will contain. Our paradigm therefore allowed us to investigate both cue-elicited and target-elicited phasic pupil dilation.

We measured pupil dilation rate in response to task-relevant stimuli to assess phasic arousal as an index of task effort, before and after the RECOGNeyes training intervention, and to evaluate whether pupil dilation rate predicted task performance trial-by-trial. We measured pupil dilation in relation to key trial events (e.g., cue, target, saccade onset, etc.) in order to investigate specific mechanistic changes at within-trial timescales.

Given that increased pupil dilation should index greater arousal and cognitive effort during the pro/antisaccade task, our research questions were:

- Does anticipatory task-related arousal, as indexed by mean pupil size and rate of change in pupil size over the anticipatory period between cue and target differ between prosaccade and antisaccade trials and/or after RECOGNeyes training?
- Does the rate of phasic pupil dilation elicited by the temporal cue (i.e., during the cue-target anticipatory period) differ from dilation rates elicited by the target, and do these effects differ by trial type and/or after RECOGNeyes training?
- Does greater pupil dilation rate (cue-elicited or target-elicited) predict faster pro/antisaccade RTs, trial-by-trial, and do these effects differ by trial type and/or after RECOGNeyes training?

5.2. Methods

5.2.1. Choice of data pre-processing parameters

Pupil size measurements are conventionally reported as diameter in millimetres. However, the EyeLink® 1000-Plus (SR Research Ltd.) eye-tracker that we used during the RECOGNeyes study records pupil size in terms of the number of pixels within the area of the detected pupil region in arbitrary units. The *EyeLink® 1000 Plus User Manual* recommends for their eye-tracker that: "since pupil size is recorded in arbitrary units that is not calibrated across participants, measures of pupil size are best recorded

as percent change relative to a baseline period" (SR Research, 2017, p.110); this is taken into consideration during the normalisation procedure used for our data, described in Section 5.2.3.3.

Pupillometry recordings are subject to high frequency noise from drift, microsaccades and tremor (Duchowski, 2017) and variation between trials and subjects. Additionally, there are blinks and artefacts (see Figure 17), which if removed introduce periods of missing data points. Data pre-processing methods are therefore required to clean the data signal, correct for blinks and artefacts, and to normalise trial and subject variation in the signal.

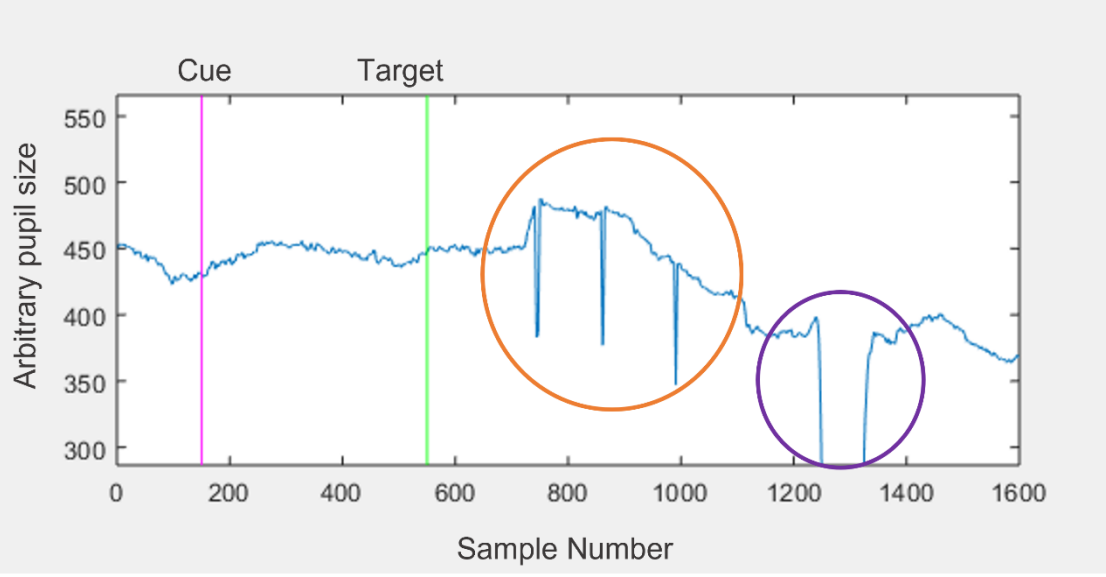

Figure 17: Raw trace blinks and artefacts.

This figure depicts the raw pupillometry trace in a typical trial. The purple circle on the right highlights a blink, where pupil size reaches zero and there is a gap of no signal detected. The orange circle on the left encloses a part of the trace containing artefacts of abrupt drops in the signal that appear as 'spikes'.

Procedures for pre-processing pupillometry data to remove artefacts and adjust for potentially confounding sources of variance remain a topic of debate. A PubMed search using the terms “pupillometry and MEG” or “pupillometry and EEG” revealed 50 potentially relevant papers. However, the lack of detail in the reported methods, diversity of equipment employed and inconsistencies between studies, makes it difficult to draw definite conclusions. Nonetheless, review of these papers suggested the following guidelines:

Since pupil size was measured as the number of pixels in the eye-tracked pupil region, blinks (as illustrated in Figure 17) corresponded to parts of the signal that dropped out entirely where there are no pupil pixels detected. The pupil size reaches zero, followed by a gap in the trace before the eye-tracker detected the pupil again. Transient artefacts in the signal can also occur that do not necessarily reach zero that could be due to half blinks, which is why they obscure the number of pixels detected but are shorter than blinks. The majority of studies in my literature search included procedures for identifying blinks and extreme values, where the most common approach was to exclude samples that are ±3 standard deviations (Std. Dev) from the mean pupil data per epoch/trial or subject (Ásgeirsson & Nieuwenhuis, 2017; Hjortkjær et al., 2020; Miles et al., 2017).

After removing blinks and artefacts, it is common practice to reject trials exceeding a threshold of corrupted data points. This proportion ranges between 15 % (Miles et al., 2017), 20 % (Hjortkjær et al., 2020), 30 % (Babo-

Rebelo et al., 2016, 2019) and 33 % (Kamp & Donchin, 2015). Linear interpolation is then the standard correction approach applied to combat missing data points after removing blinks or artefacts (Babo-Rebelo et al., 2016, 2019; Hjortkjær et al., 2020; Kamp & Donchin, 2015; Kostandyan et al., 2019; Miles et al., 2017; Murphy et al., 2011; Scharinger et al., 2015; Siegle et al., 2008; Zekveld et al., 2010).

A handful of these studies included more specific details pertaining to the interpolation procedure, including the extension of missing data segments to ensure all blink or spurious data points were removed. For instance, Hjortkjær et al. (2020) interpolated 350 msecs before the blink segment to 700 msecs afterwards. Alternatively, Miles et al. (2017) used 66 msecs prior to and 132 msecs after the blink segment and justified their choice by citing previous studies that used a similar approach (Siegle et al., 2008; Zekveld et al., 2010).

Pupillary dilation and constriction occur at low frequencies (McLaren et al., 1992), thus filters to remove high frequency noise can be applied without affecting the validity of the pupillometry data signal. I found the methods most often used to remove high frequency noise from pupillometry data were to apply a 4^{th}-order low-pass Butterworth filter with a 10 Hz cut-off frequency (Babo-Rebelo et al., 2016, 2019) and the moving average approach (Hjortkjær et al., 2020; Kamp & Donchin, 2015; McMahon et al., 2016). However, the Butterworth filtering approach preserves the sample number and temporal resolution of the original dataset compared to a

moving average. The Butterworth filter also has advantages over other low-pass filters such as the Chebyshev Type I and elliptic filters, because it is smoother and does not have a passband ripple (*Butterworth Filter Design - MATLAB Butter - MathWorks United Kingdom*, n.d.).

Normalisation is a common approach to control for individual trial and subject variances when comparing across datasets. In the literature I reviewed, the two normalisation approaches most commonly utilised were baseline correction relative to a pre-stimulus event (Donhauser et al., 2018; Kamp & Donchin, 2015; Kostandyan et al., 2019; Miles et al., 2017; Murphy et al., 2011; Wessel et al., 2011) or *z*-scoring (Ásgeirsson & Nieuwenhuis, 2017; Babo-Rebelo et al., 2016, 2019; Kluge et al., 2011) so that measures are scaled to within-subject variances and centred on each participant's own mean.

Taking account of these guidelines, I developed the procedure for pre-processing the RECOGNeyes pupillometry data as described in the following section.

5.2.2. Exporting trial data

EyeLink® Data Viewer (SR Research Ltd.) software package was used to export time-series pupillometry data. The Data Viewer reports include pupil metrics such as the time course of average pupil area (in arbitrary units), timestamps for each sample relative to the start of the trial

(in msecs), and sample messages for key trial events (e.g., trial start, target, and saccade onset).

Variable extraction and data pre-processing of the outputs from these sample reports were conducted using custom scripts I wrote in MATLAB R2021a (MathWorks Inc.). Any data from practice trials or error trials (including early and late responses) were removed, leaving only data from correct trials. Trial data was extracted from the trial start marker to 500 msecs after the target presentation marker. This time range was chosen to include the anticipatory period (cue to target) and a response period (target to maximum response time).

The pre-processing techniques described in the following section were applied to each trial individually for each subject and day dataset.

5.2.3. Data pre-processing parameters

5.2.3.1. Blinks and artefacts

Blinks and artefacts were identified and removed by excluding samples ±3 Std. Devs from the mean trial pupil size. To ensure the removal of spike artefacts (as illustrated in Figure 17), I also calculated pupil size differences between every 4th sample and removed samples where the difference was 15 or greater. I then extended these periods of missing data by 66 msecs prior to and 132 msecs after each missing data segment (Miles et al., 2017). Trials were excluded if the proportion of empty data samples

was greater than 30 %; this threshold was derived by taking the median of the percentages outlined in Section 5.2.1.

5.2.3.2. Interpolation methods

Most studies in my literature search adopted a linear interpolation; however, this could underestimate pupil dilation changes where changes are non-monotonic. Therefore, I employed the pchip interpolation method instead, a "shape-preserving piecewise cubic interpolation" (*1-D Data Interpolation (Table Lookup) - MATLAB Interp1 - MathWorks United Kingdom*, n.d.). This polynomial interpolation preserves the overall slope shape of the trial data and replaces missing data points based on fitting a cubic interpolation. Unlike similar methods such as spline, pchip does not overshoot and introduces fewer artificial oscillations into the interpolated portions. The example in Figure 18 displays the result of pchip interpolation with our pupillometry data.

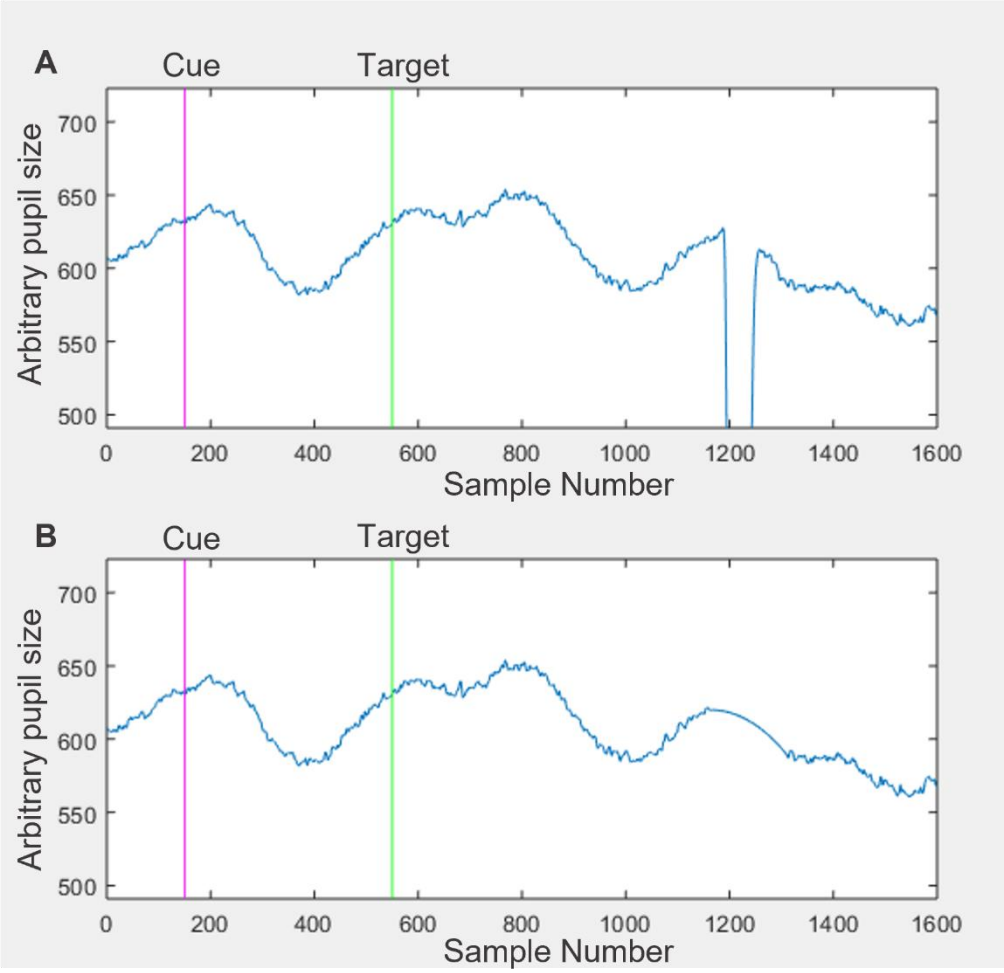

Figure 18: Example of pchip interpolation before and after it was applied.

In 2A) there is a prominent blink artefact present in the data at around 1200 samples. In 2B) this shows how the artefact has been replaced with an interpolation that fits the curved shape of the trial trace. Note that interpolations at the beginning or end of the trial used the nearest real data point for fitting the interpolation.

5.2.3.3. Filtering and normalising data

To remove high frequency noise (as evidenced in Figure 17 and Figure 18), and smooth the data signal, I applied a 4th-order low-pass Butterworth filter using a 4 Hz cut-off frequency (more effective than the aforementioned 10 Hz cut-off). This was chosen to retain temporal

resolution in the RECOGNeyes data to ensure accurate marker information for analysis of specific trial events and to facilitate cross-comparability to the cardiac and MEG modalities, compared to using a moving average approach. An example of the filtered signal is illustrated in Figure 19.

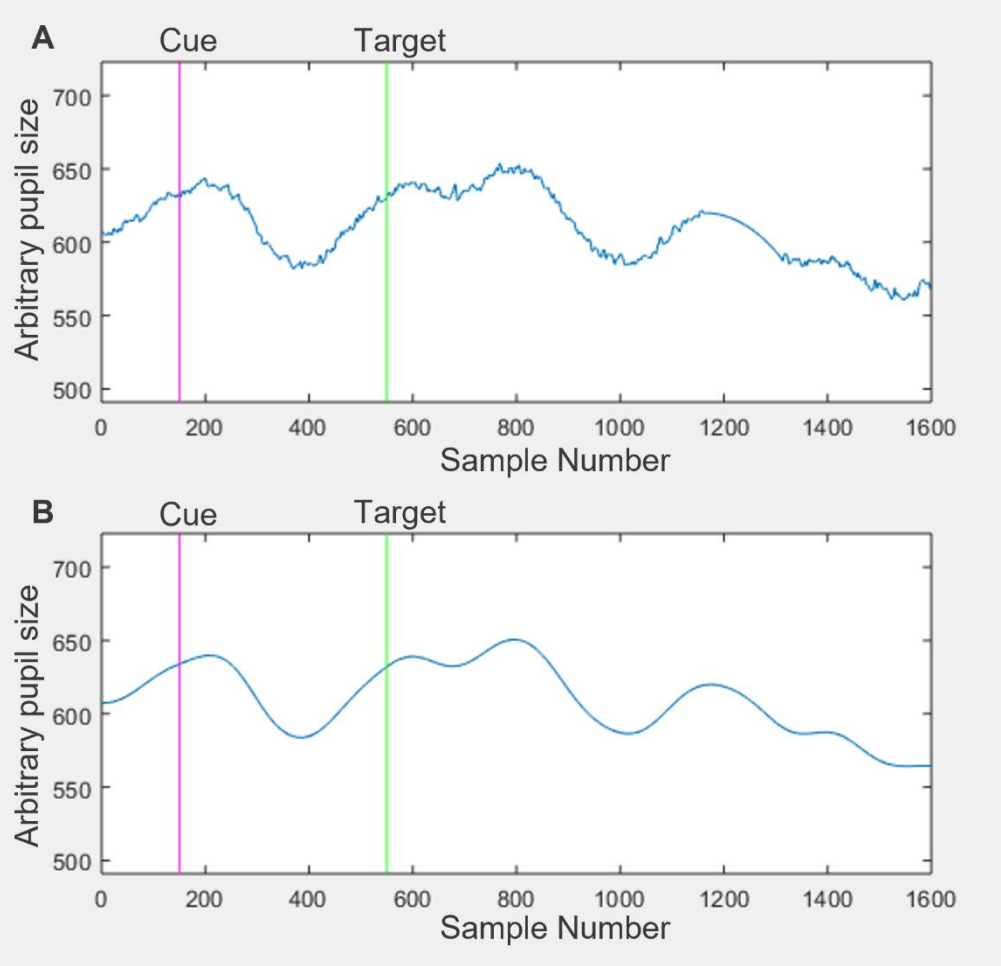

Figure 19: Application of Butterworth filter before and after.

3A) This shows the raw trace after interpolation of blinks and artefacts. 3B) This depicts how the filter has smoothed the high frequency noise in the signal, whilst maintaining the overall shape in the trial data.

I used the baseline correction method to normalise trial data, which was more frequently reported from my literature search and is advised by

the *EyeLink® 1000 Plus User Manual* for analysing arbitrary pupil size data (as mentioned in Section 5.2.1). A 200 msecs baseline period was chosen (Wessel et al., 2011), whereby pupil sizes were expressed as percentages of the mean pre-cue baseline period of 250 to 50 msecs prior to cue onset for each trial.

5.2.4. Defining periods of interest and trial variables

Trial event markers can vary in temporal accuracy depending on time lags between triggers sent to different computers and equipment in the experiment set-up (as illustrated in Chapter 3, Figure 6). To standardise trial anticipatory periods, the timing of all events were defined relative to the target marker. Cue onset was deemed to have occurred 800 msecs prior to target onset. Saccade onset was calculated as target time plus reaction time (RT); for RT derivation, refer to Chapter 4, Section 4.3.1.

The full length of the extracted trial data was used for visualising general data trends and quality. However, only data from cue onset to saccade onset was included in statistical analysis. This is because response period data may be confounded by the pupil foreshortening effect after the saccade, as well as luminance changes and gaze deviations after receiving on-screen response feedback (see discussion about this limitation further in Section 5.4.4). For binned data, only cue to target data was used in statistical analysis to assess anticipatory period phasic changes in pupil size.

Rate of change in pupil size within the three periods of interest were calculated. This included the pre-target anticipatory period rate in the cue to target interval (i.e., cue-elicited dilation rate). Post-target intervals in the response period included target plus 100 msecs and target to saccade onset (i.e., target-elicited dilation rates). Rate of pupil dilation in each period of interest was calculated by:

$$Rate\ of\ pupil\ dilation = \frac{Pupil\ size\ at\ event\ 2 - Pupil\ size\ at\ event\ 1}{Period\ of\ interest\ duration\ (msecs)}$$

Rather than assessing the difference in pupil size at two time points, computing the rate of dilation in this way enables the comparison between different rate period durations. This was important for examining the relationship between dilation rate and reaction time (RT), and this method has presented growing interest (Kurniawan et al., 2020). I computed the median rate for each period of interest separately for trial types in each subject day dataset.

To evaluate the relationship between pupil dilation rate and task performance, Spearman's rank correlations were computed between pupil dilation rate and RT. Spearman's was used because RT distributions tend to be positively skewed, and Pearson's correlation would may give undue weighting to long RT values. Within-participant correlations between dilation rates and RT were computed across all trials of each trial type for each of the three rate periods of interest. The correlation coefficients were linearised using the Fisher r- to z-transformation.

To investigate time courses over the whole trial period, I binned pupil size data into 13 bins of 100 msecs duration from the start of the anticipatory period (cue) to the end of the response period (target plus 500 msecs). This was done for each participant, for each day and trial type.

To estimate the change in pupil size between bins, I subtracted pupil size at each time point from the value at the corresponding time point in the previous bin. As there were 50 samples per bin, using '*n*' to represent the sample number, I computed the differences (*diff*):

$$diff_n = Sample_{n+50} - Sample_n$$

Following this, we grouped every 50 consecutive sample diffs. The means of these groups were calculated, resulting in 12 bin differences. Using this procedure preserves information about the gradient between bins.

5.3. Results

5.3.1. Analysis considerations and sensitivity analysis

As reported in Chapter 4, Figure 9, there were a total of *N*=30 day-paired subject datasets available for pupillometry statistical analysis. Further analysis considerations are described in Chapter 3, Section 3.7.

After completing data pre-processing steps, some participants only yielded a low number of correct trials containing clean data. This included two participants with fewer than 30/120 usable trials on day 1. When examining graphical representations of individual subject data, one participant was a visual outlier on both days. Therefore, I performed a sensitivity assessment by repeating statistical analyses with these participants omitted. Removal of these subjects did not affect the statistical significance of the results, so they were not removed from statistical analysis.

5.3.2. Phasic pupil size changes across trial time course

To examine task-related phasic changes in pupil size across the anticipatory period, I conducted a three-way repeated-measures ANOVA (2 x 2 x 8) with three within-subjects factors: Day (2 levels: Day 1 and Day 2); Trial Type (2 levels: prosaccade and antisaccade trials) and Time Bin (8 levels: mean pupil size values in each of the eight 100 msecs time bins).

There was a significant main effect of Time Bin across all factors, $F(1.254, 36.368) = 64.292$, $p < .001$. Polynomial contrasts indicated a significant linear trend across Time Bins, $F(1, 29) = 72.454$, $p < .001$. This is illustrated in Figure 20, which depicts a steady monotonic increase in pupil size across time bins. Figure 21 also shows a consistent increase in average pupil size across key trial events. Therefore, this confirms a phasic increase in pupil size following cue onset throughout the anticipatory cue-

target period, when averaged across both trial types and days. An interaction between Day by Time Bin was also close to significance, $F(2.026, 58.744) = 3.047$, $p = .054$, indicating a trend for the rate of phasic arousal during the anticipatory period to be lower on Day 2 than on Day 1.

However, there was also a significant main effect of Trial Type, $F(1, 29) = 4.174$, $p = .050$, whereby pupil size in the anticipatory period was significantly larger in prosaccade trials than in antisaccade trials. As there was no significant Trial Type by Time Bin interaction ($F<1$), this indicates a significantly higher level of tonic arousal during the prosaccade blocks than during antisaccade blocks, but does not indicate any trial type differences in the degree of phasic arousal elicited by the cue.

Figure 20 and Figure 21 suggest this trend may reverse after target presentation to target plus 500 msecs, where pupil dilation rate appears greater in antisaccade trials compared to prosaccade trials in the response period than in the anticipatory period. This effect was investigated by comparing pupil dilation rates before and after target onset (see Section 5.3.3 below).

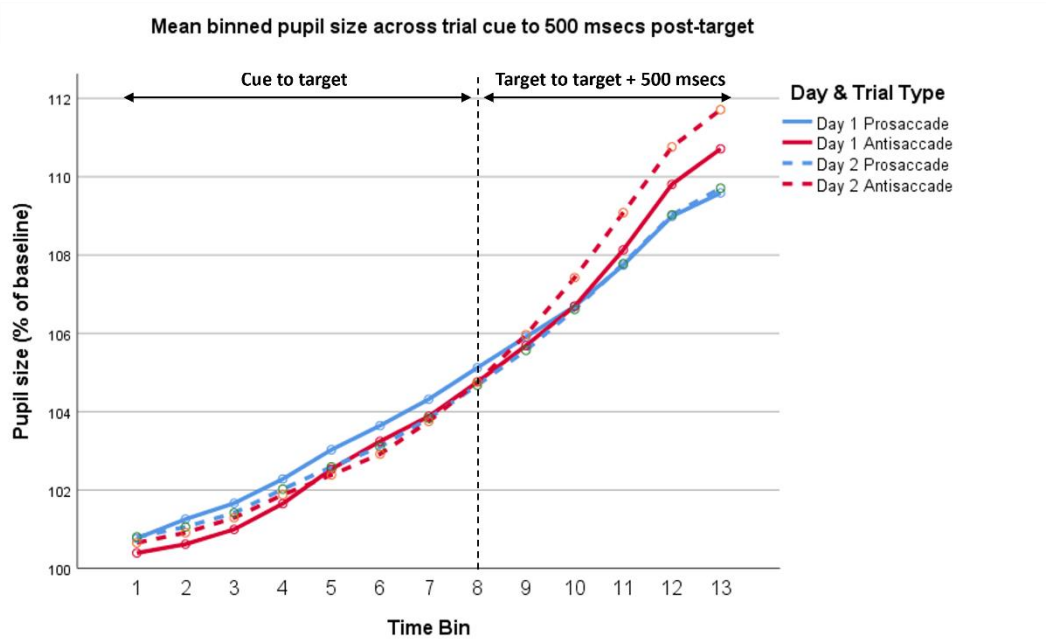

Figure 20: Binned pupil size data across trial time course at 100 msec bin intervals.

This figure depicts the mean of the subject mean binned pupillometry data for each day and trial type. Bin 1 starts from the cue onset, the end of bin 8 is the target presentation, and bin 13 is to 500 msecs post-target. Only time bins in the cue to target period, to the left of the dotted line, were entered into the 2x2x8 ANOVA.

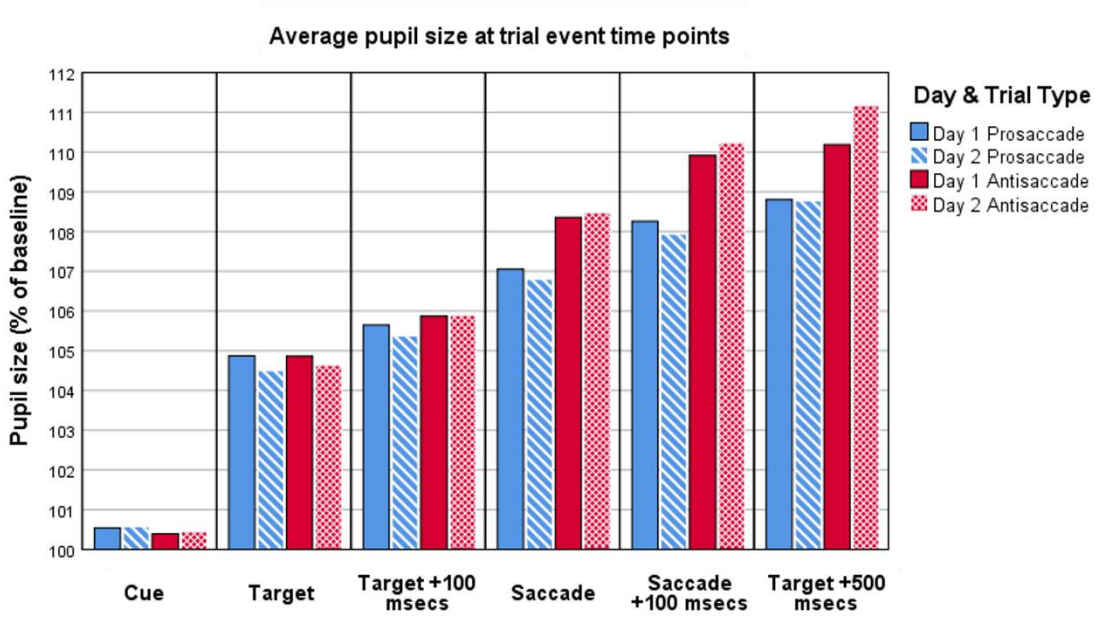

Figure 21: Pupil size at key events during the trial time course.

The following key trial event time points were selected: cue, target, target plus 100 msecs, saccade onset, saccade plus 100 msecs and target plus 500 msecs (end of the response period). The addition of the target and saccade markers plus 100 msecs were to focus on pupil dilatory changes occurring around the saccade onset. For each subject day dataset, the median size at these events were extracted separately per trial type to avoid the influence of extreme values in this measure of central tendency. This figure depicts the mean of the median pupil sizes at chosen trial events across subjects at each trial type and day combination.

5.3.3. Phasic pupil dilation rate before and after target onset

In Figure 22, I have plotted the changes in pupil size between successive 100 msecs time bins from cue onset to 500 msecs following target onset; thus, depicting how the rate of phasic dilation varied across the trial time course. All values are positive, reflecting the monotonic increase in pupil size across the trial reported above and illustrated in Figure 20. The greatest rates of change in pupil size were observed after target onset,

where the peak phasic dilation rate was observed between bins 11 and 12, i.e., between 300 and 400 msecs after target onset. As mean saccade latencies were around 250 msecs, this suggests that phasic dilation continued to increase in rate following the saccade.

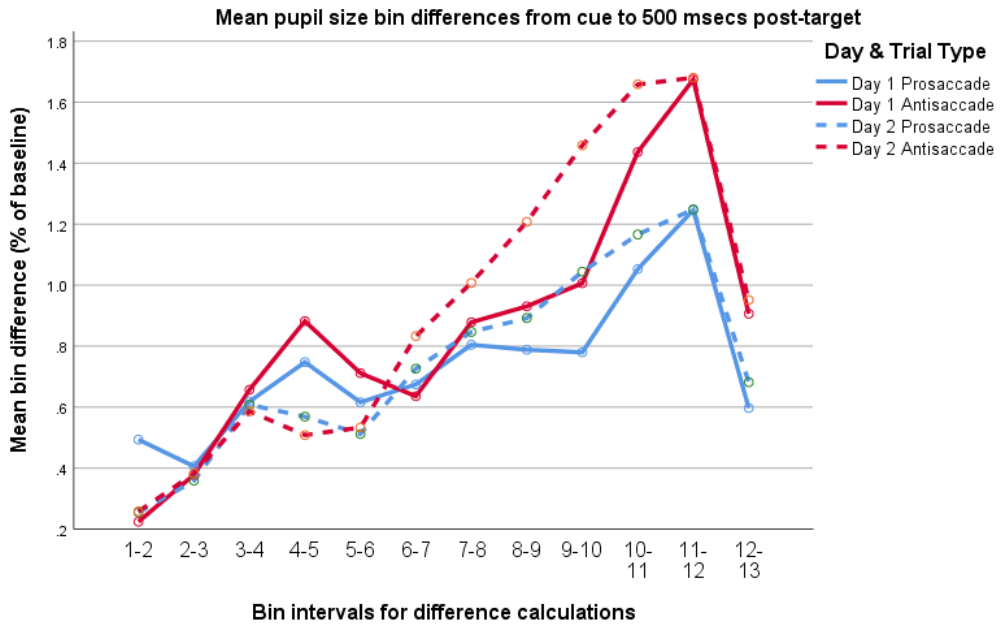

Figure 22: Mean bin differences of pupil size change across trial time course.

This figure reflects the gradient of pupil size change across the trial, where the change is the increase in pupil size (% baseline) per 100 msecs (bin width).

However, observations following saccadic activity must be interpreted with caution, due to confounds of the pupil foreshortening effect (refer to Section 5.4.4). Nevertheless, these pupil size data trends support the conclusion that phasic pupil dilation rate continues to increase following

target presentation, and that target-elicited pupil dilation rates are higher than cue-elicited rates.

To investigate this, I computed cue-elicited pupil dilation rates between cue and target, and target-elicited pupil dilation rates both between target and 100 msecs later (target + 100 msecs) and between target and saccade onset (which varied from trial to trial) as described previously (see Section 5.3.2). Neither measure of target-elicited phasic pupil dilation rates are likely to be affected by foreshortening. However, the target to target + 100 msecs interval may capture less of the target-elicited phasic dilation, while the target to saccade onset interval is potentially confounded by effects of RT. Note, however, that by computing *rate* between two time points, rather than total dilation, such confounding is minimised.

To compare cue-elicited dilation rate with target-elicited dilation rate and to determine whether this comparison differed between days, and/or trial types, I conducted two three-way repeated-measures ANOVAs. These ANOVAs had three within-subject factors: Day (two levels: Day 1 and Day 2); Trial Type (2 levels: prosaccade and antisaccade trials); and Time Period (2 levels: cue-elicited pupil dilation; target-elicited pupil dilation). In the first ANOVA (ANOVA 1) the target-elicited pupil dilation rate was evaluated between target onset and 100msecs later, while in the second (ANOVA 2), the target-elicited pupil dilation rate was evaluated between target onset and saccade onset.

For both ANOVAs, there was a significant main effect of Time Period (ANOVA 1: $F(1, 29) = 18.967$, $p < .001$; ANOVA 2: $F(1, 29) = 37.361$, $p < .001$), reflecting significantly greater target-elicited dilation rates than cue-elicited dilation rates when these were averaged over trial type and day. This is illustrated in Figure 23, where dilation rate is lowest between cue to target, greater between target plus 100 msecs, and the greatest between target and saccade.

Both ANOVAs also had a significant main effect of Trial Type (ANOVA 1: $F(1, 29) = 24.576$, $p < .001$; ANOVA 2: $F(1, 29) = 54.437$, $p < .001$), reflecting greater overall phasic dilation for antisaccade trials than for prosaccade trials when these rates were averaged across the two time periods (see Figure 23).

However, for both ANOVAs, there were additional Trial Type by Time Period interactions (ANOVA 1: $F(1, 29) = 20.810$, $p < .001$; ANOVA 2: $F(1, 29) = 41.512$, $p < .001$), and significant Day by Time Period interactions (ANOVA 1: $F(1, 29) = 11..594$, $p = .002$; ANOVA 2: $F(1, 29) = 7.423$, $p = .011$). To interpret these interactions, I conducted separate two-way ANOVAs for pupil dilation rates computed over each time period (cue-target; target-target + 100 msecs; target to saccade), where the within-subjects factors were Day (2 levels: Day 1 and Day 2); and Trial Type (2 levels: prosaccade and antisaccade trials).

For the anticipatory cue-target period, there were no significant effects of Trial Type or Day, indicating similar degrees of cue-elicited pupil

dilation between trial types and between days. However, for the target to target + 100 msecs time period, there was a significant main effect of Trial Type, $F(1, 29) = 27.665$, $p < .001$, where target-elicited pupil dilation rate was significantly greater for antisaccades than for prosaccades. There was also a significant main effect of Day, $F(1, 29) = 5.777$, $p = .023$, where target-elicited dilation rate was significantly greater on Day 2 than on Day 1, regardless of trial type (no significant interaction between Day and Trial Type, $p > .05$). For the target to saccade onset period, results were similar; target-elicited pupil dilation rate was significantly greater for antisaccades than prosaccades, $F(1, 29) = 61.218$, $p < .001$, while an overall increase in dilation rate on Day 2 was significant at trend level, $F(1, 29) = 3.731$, $p = .063$.

Taken together, these results show that target-elicited pupil dilation rates were significantly greater than cue-elicited dilation rates. Also, target-elicited pupil dilation rates were greater for antisaccade trials than for prosaccade trials; this effect of trial type being significantly greater than the (non-significant) effect of trial type on cue-elicited pupil dilation. These findings replicate the findings by Karatekin et al. (2010) and Wang et al. (2015, 2016) of greater phasic dilation on antisaccade trials than on prosaccade trials and clarifies that this effect is significantly greater for target-elicited pupil dilation rates than for cue-elicited phasic dilation rates.

The results also provide evidence for an increase in target-elicited pupil dilation rates on Day 2 compared to Day 1; a result that reached

statistical significance in the target to target + 100 msecs period. This could be a result of RECOGNeyes training, or, more generally, an effect associated with improved task performance (greater accuracy and faster RTs especially on antisaccade trials) observed on Day 2 compared to Day 1. If so, it suggests that improved gaze control following practice on inhibitory gaze control task may involve increased phasic alerting to the stimulus. This interpretation would be consistent with the finding by Wang et al. (2015, 2016) of faster RTs on antisaccade trials being associated with greater phasic pupil dilation.

I therefore investigated within-subject trial-by-trial correlations between phasic pupil dilation rates and RT. This included comparing correlations between RT and cue-elicited pupil dilation rate, correlations between RT and target-elicited pupil dilation rate, and the relationship between these effects and trial type, as well as effects of RECOGNeyes training.

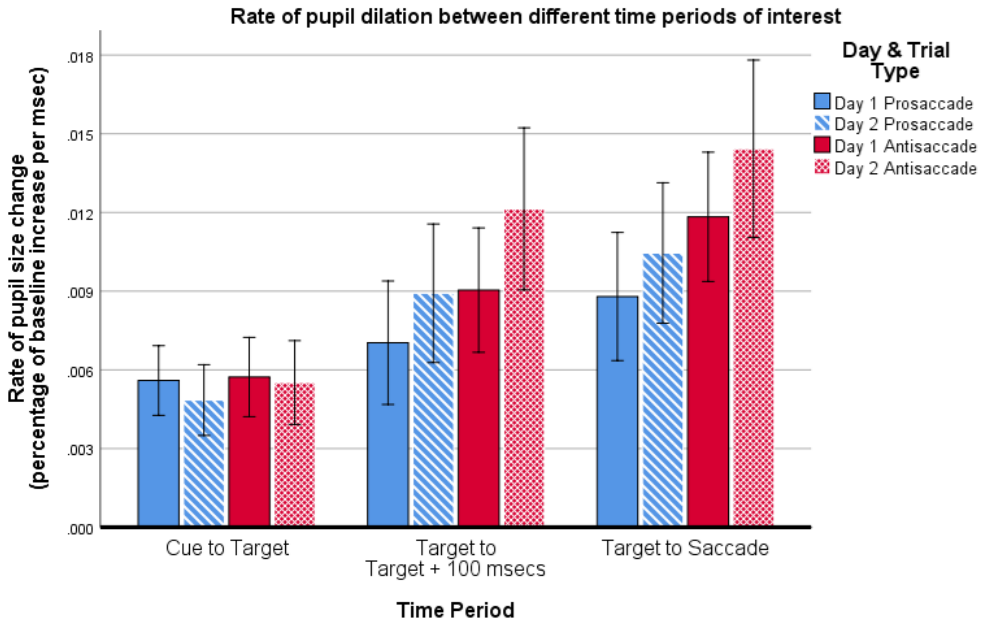

Figure 23: Cue-elicited and target-elicited pupil dilation rates.

The average rates plotted in this figure are the means of the median pupil dilation rates across subjects for these time periods of interest for each day and trial type. Error bars are plotted as 95% confidence intervals (CI).

5.3.4. Spearman's rank correlations between pupil dilation rate and reaction time

To investigate whether pupil dilation rate correlated with performance, I examined the Spearman's correlation coefficient (*z* transformed) between RT and pupil dilation rate, either observed in the cue-target interval or in one of the intervals following target onset. To test whether these correlation values differed between days, trial types and the pupil dilation period used in the correlation, I conducted two three-way repeated-measures ANOVAs. The dependent variable was the within-subjects correlation between RT and pupil dilation rate, and the within-

subjects factors were Day (2 levels: Day 1 and Day 2); Trial Type (2 levels: prosaccade and antisaccade) and Time Period (2 levels: whether the correlation was computed between RT and cue-elicited pupil dilation rate, or between RT and target-elicited pupil dilation rate). In ANOVA 1, the time period used for the target-elicited pupil dilation rate was the interval between target onset and 100 msecs later, and in ANOVA 2, it was the interval between target onset and saccade onset.

The *F*-test for the between-subjects intercept for these ANOVAs tests the null hypothesis that the mean value of the RT and pupil dilation rate correlation coefficients, when averaged across all conditions, is not significantly different from zero. In other words, it provides an omnibus test of the hypothesis that across participants, RT will tend to be correlated with phasic pupil dilation in the same direction.

This *F*-test was significant in both ANOVAs (ANOVA 1: $F(1, 29) = 162.927$, $p < .001$; ANOVA 2: $F(1, 29) = 87.474$, $p < .001$). Hence, this indicates that across participants and periods of interest, the mean of these correlation coefficients was significantly different from zero. The signs of each of the mean correlation values were all negative, despite being small in magnitude (Figure 24). This indicates that as predicted, and consistent with Wang et al. (2015, 2016), faster pupil dilation rates were associated with faster RTs; notably, unlike Wang and colleagues, this finding is for both trial types in our data and not only for antisaccade trials. Hence, this supports the hypothesis that greater phasic pupil dilation indexes greater

effort. One-sample *t*-tests confirmed that all mean correlation values were significantly below zero, as indicated by the error bars in Figure 24.

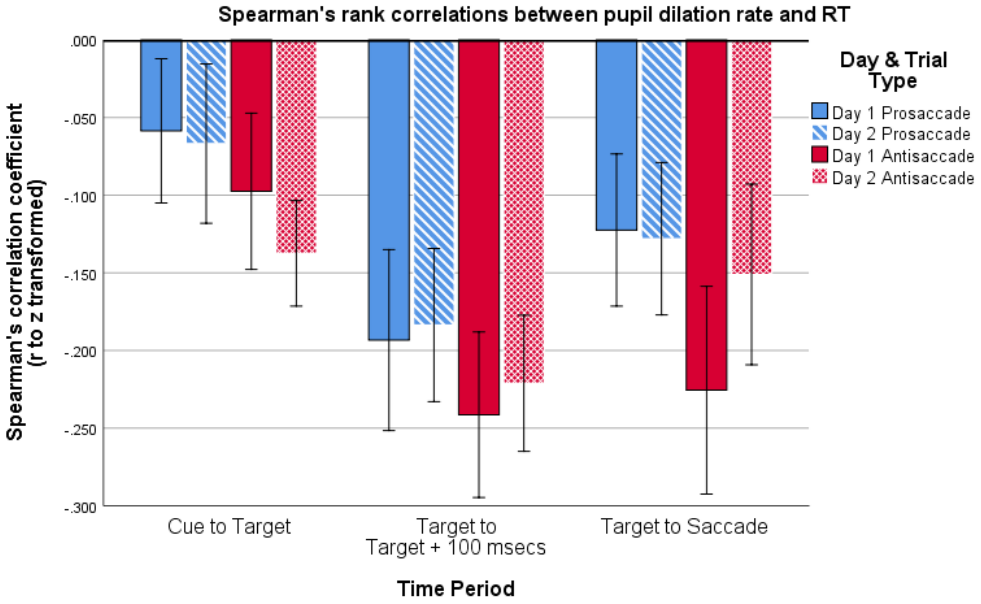

Figure 24: Spearman's rank correlations between pupil dilation rate and RT.

Plotted are the subject correlation coefficient r to z transformed mean averages for each day, trial type and time period, including error bars (95% CI).

Both ANOVAs indicated a significant main effect of Time Period (ANOVA 1: $F(1, 29) = 67.353$, $p < .001$; ANOVA 2: $F(1, 29) = 12.713$, $p = .001$), reflecting in both comparisons significantly more negative correlations between RT and target-elicited pupil dilation rate than between RT and cue-elicited dilation rate, when these are averaged over day and trial type.

There was also a significant main effect of Trial Type in both ANOVAs (ANOVA 1: $F(1, 29) = 6.863$, $p = .014$; ANOVA 2: $F(1, 29) = 10.417$, $p = .003$), whereby correlation coefficients were significantly more negative in antisaccade trials than in prosaccade trials on both days (as depicted in Figure 24). This indicates that pupil dilation rate was more strongly correlated with RT on antisaccade trials than on prosaccades when averaged across pupil dilation periods used in the correlation, and days.

However, in ANOVA 2, there was also a significant three-way Day by Trial Type by Time Period interaction, $F(1, 29) = 6.200$, $p = .019$. To interpret this interaction, I computed a two-way repeated-measures ANOVA for each trial type in which the factors were Day (2 levels: Day 1 and Day 2) and Time Period (2 levels: correlation values between RT and cue-elicited pupil dilation rate; correlation values between RT and target-elicited pupil dilation rate).

For prosaccade trials, this ANOVA indicated a significant main effect of Time Period, $F(1, 29) = 10.091$, $p = .004$, reflecting more negative RT correlations for target-elicited pupil dilation rates than for cue-elicited pupil dilation rates. There were no other main effects or interactions with Day, consistent with what can be observed in Figure 24. For antisaccades, the ANOVA indicated a significant main effect of Time Period, $F(1, 29) = 6.469$, $p = .017$, indicating more negative correlations between RT and target-elicited pupil dilation rates than between cue-elicited pupil dilation rates. However, for this ANOVA, there was also a significant Day by Time Period

interaction $F(1, 29) = 8.954$, $p = .006$. Simple effects ANOVAs conducted on antisaccade RT pupil dilation correlations for each Time Period indicated that while RT correlations with cue-elicited pupil dilation did not differ significantly between days, RT correlations with target-elicited pupil dilations in the target to saccade period (but not the target to target + 100 msecs period) were significantly less negative on Day 2 than on Day 1, $F(1, 29) = 6.298$, $p = .018$.

To summarise these results: firstly, these analyses of the patterns of within-subject correlations between RT and phasic pupil dilation show that phasic pupil dilation strongly predicts RT, whether the correlation is computed between RT and cue-elicited phasic dilation, or between RT and either of the target-elicited phasic dilation measures. In all cases, greater phasic dilation predicts faster RT on a trial-by-trial basis. This is consistent with the hypothesis that phasic pupil dilation indexes not simply phasic arousal, but also the cognitive effort associated with that trial.

Secondly, correlations were consistently more negative for antisaccade trials than for prosaccade trials. This indicates that trial-by-trial variation in cognitive effort plays a greater role in predicting reaction speed on the trial type requiring greater cognitive control (antisaccades) than for the less demanding trial type (prosaccades), and consistent with the findings of greater target-elicited pupil dilation rates on antisaccade trials.

Thirdly, correlations between phasic pupil dilation rate and RT were consistently stronger for target-elicited pupil dilation than for cue-elicited pupil dilation.

Lastly, the results do not indicate that either RECOGNeyes training or simple practice effects strengthen the link between phasic pupil dilation and RT; indeed, for antisaccade trials, there was a reduction in the strength of the correlation between RT and target-elicited pupil dilation on day 2. Figure 24 however does illustrate that the preparatory cue-elicited phasic dilation RT correlations were somewhat stronger on day 2 than on day 1 (despite this result not reaching significance).

5.4. Discussion

5.4.1. Question 1

> Does anticipatory task-related arousal, as indexed by mean pupil size and rate of change in pupil size over the anticipatory period between cue and target differ between prosaccade and antisaccade trials and/or after RECOGNeyes training?

Our data shows clear evidence of monotonic task-related phasic pupil dilation over the anticipatory period, indicating anticipatory phasic arousal in response to a temporally informative cue. Pupil size increased monotonically relative to baseline across the 1300 msecs period from cue

onset to the post-saccadic period (as supported by Figure 20 and Figure 21). Bin difference data also supported a steady increase in pupil dilation rate across the anticipatory period (see Figure 22), reaching a maximum after saccade onset.

However, our data do not indicate any effect of trial type or effects of RECOGNeyes training on the increase in pupil size over the anticipatory period. Instead, mean pupil size was larger throughout the anticipatory period for prosaccade trials than for antisaccade trials. This may reflect greater tonic arousal during the prosaccade blocks. Alternatively, it may be that during antisaccade blocks, pupil dilation was tonically reduced by greater vagal activity during these blocks. This hypothesis will be explored further in the following chapter.

5.4.2. Question 2

> Does the rate of phasic pupil dilation elicited by the temporal cue (i.e., during the cue-target anticipatory period) differ from dilation rates elicited by the target, and do these effects differ by trial type and/or after RECOGNeyes training?

Comparison between cue-elicited pupil dilation rates and target-elicited pupil dilation rates revealed significantly greater target-elicited dilation rates for antisaccade trials than for prosaccade trials. This was despite overall smaller pupil size during the anticipatory period for

antisaccade trials, suggesting reduced tonic arousal. The findings of greater rates of pupil dilation for antisaccade trials than for prosaccade trials replicates the finding by Karatekin et al. (2010) and Wang et al. (2015, 2016) of greater phasic dilation for antisaccade trials, and further clarifies that this effect is significantly greater for target-elicited pupil dilation than for cue-elicited pupil dilation, which were not significantly affected by trial type. Since antisaccade production involves the recruitment of additional neural processes to actively inhibit a reflexive prosaccade and execute a saccade in the opposite direction to the stimulus (as described in Chapter 2, Section 2.2.1), this finding is consistent with the hypothesis that greater arousal/effort is elicited on antisaccade trials.

Analysis of pupil dilation rate relative to trial events also revealed significantly greater target-elicited pupil dilation rates than cue-elicited pupil dilation rates (as depicted in Figure 23), with the greatest pupil dilation rates being target-elicited pupil dilation on antisaccade trials. Target-elicited pupil dilation rates tended to be greater on Day 2 than on Day 1, an effect that was statistically significant when computed between target onset and 100 msecs later. This could be interpreted as increased phasic arousal elicited by the target stimuli after RECOGNeyes training, but could also simply be the result of greater task familiarity on Day 2. Whether or not improved performance on Day 2 was a result of RECOGNeyes training, it is consistent with the interpretation that the improved performance on Day 2 was related to greater target-induced phasic arousal.

5.4.3. Question 3

> Does greater pupil dilation rate (cue-elicited or target-elicited) predict faster pro/antisaccade RTs, trial-by-trial, and do these effects differ by trial type and/or after RECOGNeyes training?

Our finding of consistently negative correlations between phasic pupil dilation rate and RT replicate the findings by Wang et al. (2015, 2016) of a negative correlation between pupil dilation rate and RT for antisaccade trials. Moreover, our results indicate that phasic pupil dilation rate predicts RT regardless of trial type, or whether the correlation is computed between RT and cue-elicited pupil dilation rate or RT and target-elicited pupil dilation. Nonetheless, we found the strongest correlations for antisaccade trials, and with target-elicited pupil dilation rates rather than for cue-elicited dilation rates (as depicted in Figure 24).

We found little evidence that these correlations were affected by RECOGNeyes training. However, cue-elicited pupil dilation rate and RT correlations were slightly stronger for antisaccade trials on Day 2 compared to Day 1 (although this observational finding did not reach significance). This could indicate favoured 'preparatory' processes and less 'reactive' responses occurring on Day 2 than on Day 1 that contributed to better task performance in antisaccade trials. Also, given the finding of increased phasic pupil dilation rates on Day 2, coupled with behavioural evidence of faster RTs on Day 2, this suggests that training-related (or task-familiarity related) improvements in RT on Day 2 were mediated by the same process

that resulted in greater target-elicited pupil dilation rates on Day 2, but leaving the correlations between RT and pupil dilation rate largely unchanged. The following Chapter 6 will address event-locked cardiac data to assess vagal (PNS) effects, where it will be investigated whether these results relate to the SNS-mediated arousal findings that have been presented in the current chapter.

5.4.4. Acquisition considerations and limitations

I will now describe some of the limitations experienced during acquisition, how these were mitigated and suggested improvements on the pupillometry methodology.

Pupillometry recordings are sensitive to confounds from the pupillary light reflex (refer to Chapter 2, Section 2.1.1 for ANS background describing pupil reflexes). This means luminance changes from task stimuli appearing and disappearing from the screen could cause dilatory and constrictor effects related only to reflexive responses to light stimulation rather than from cognitive processing of the task stimuli itself. To limit this in our study, the task was projected at the same luminance level onto the screen. Also, our anticipatory period of interest had unchanging stimuli on the screen, namely the cue of two empty boxes and the consistently presented fixation cross.

However, the response period in our task included the target presentation of a filled box, which could slightly reduce luminance and confound increased dilation measured in prosaccade trials. For antisaccades, looking towards the empty box would increase luminance exposure to the pupils due to the white background, which could cause pupil constriction. Conversely, our data shows that pupil size after target presentation in antisaccade trials dilates and does not constrict, and maximum dilation is greater compared to prosaccade trials. Therefore, this supports that our data has had limited impact of luminance confounds.

Another major consideration when collecting pupillometry data is the pupil foreshortening error (PFE), which is not often sufficiently controlled for (Hayes & Petrov, 2016b). This is where deviations in eye gaze relative to the stationary eye-tracker occludes the pupil to appear more elliptical in shape, causing an apparent reduction in pupil size. This was prevented through our use of a fixation cross that had to be fixated upon between the start of the trial and the saccade onset, as facilitated by calibration to a set area for monitoring fixation, as described in *EyeLink® 1000 Plus User Manual* (SR Research, 2017, p.41). This ensured we minimised the issue of the PFE up to the point of the saccade onset, because the trial was classed as an 'early' response and not included in the final dataset if the gaze deviated from the fixation cross location. We also re-calibrated after every pro/antisaccade block pair (see task timeframe in Chapter 3, Figure 8) to increase the precision in detecting pupil size and when the eye gaze deviated from the fixation cross.

However, the response period data may be confounded by the PFE after the saccadic response, as well as luminance changes and gaze deviations after receiving on-screen response feedback. Therefore, the full length of the extracted trial data was used for visualising general data trends, whereas statistical analysis only included data up to the point of the saccade onset. Observations for data trends corresponding to events after the saccade onset were thus interpreted with caution.

An improvement upon the experiment design includes measuring the exact distance from the screen to enable the calculation of pupil size conversion into millimetres. Also, recording during rest periods and having a longer, or using different anticipatory period lengths, could enable us to study different preparatory mechanisms occurring at different timeframes.

Chapter 6: ANS effects as measured with heartrate data

6.1. Background and Rationale

In the RECOGNeyes study, we were interested in autonomic correlates of anticipatory cognitive control processes in the pro/antisaccade task. In this chapter, I will investigate anticipatory and post-saccadic heartrate changes, as heartrate changes at this timescale are likely to be largely mediated by changes in parasympathetic activity. Specifically, I will investigate anticipatory cardiac deceleration to examine the role of the 'vagal brake' in preparing to respond to an upcoming target stimulus. I will relate this measure to trial-by-trial performance as indexed by reaction time. I will also report an investigation into whether phasic PNS activity as indexed by cardiac deceleration accounts for separate, or the same, variance in reaction time to that accounted for by phasic SNS activation, as indexed by pupil dilation rate.

6.1.1. Measuring heartrate

Changes in electrical activity during the cardiac waveform cycle is measured using electrocardiography. Recordings were first attempted by Waller in the late 19th century, but Einthoven is considered to be the founder of the modern electrocardiogram (ECG) also known under the 'EKG'

abbreviation from his original Dutch translation “elektrokardiogramm” (Barold, 2003); usually measured via electrodes placed onto the skin.

The cardiac waveform has characteristic elements, each referred to by a letter of the alphabet. The P wave signifies atrial depolarisation, the QRS complex corresponds to atrial repolarisation and ventricular depolarisation, and finally the T wave represents ventricular repolarisation (Ingale et al., 2020; Kher, 2019). An example of the PQRST waveform pattern is displayed in Figure 25. As can be seen, the R wave typically has the biggest amplitude in the potential difference of the electrical signal and a characteristically sharp peak. This makes it easy to detect on the ECG, and it provides a useful and precise cardiac cycle marker for the purposes of measuring heartrate (HR).

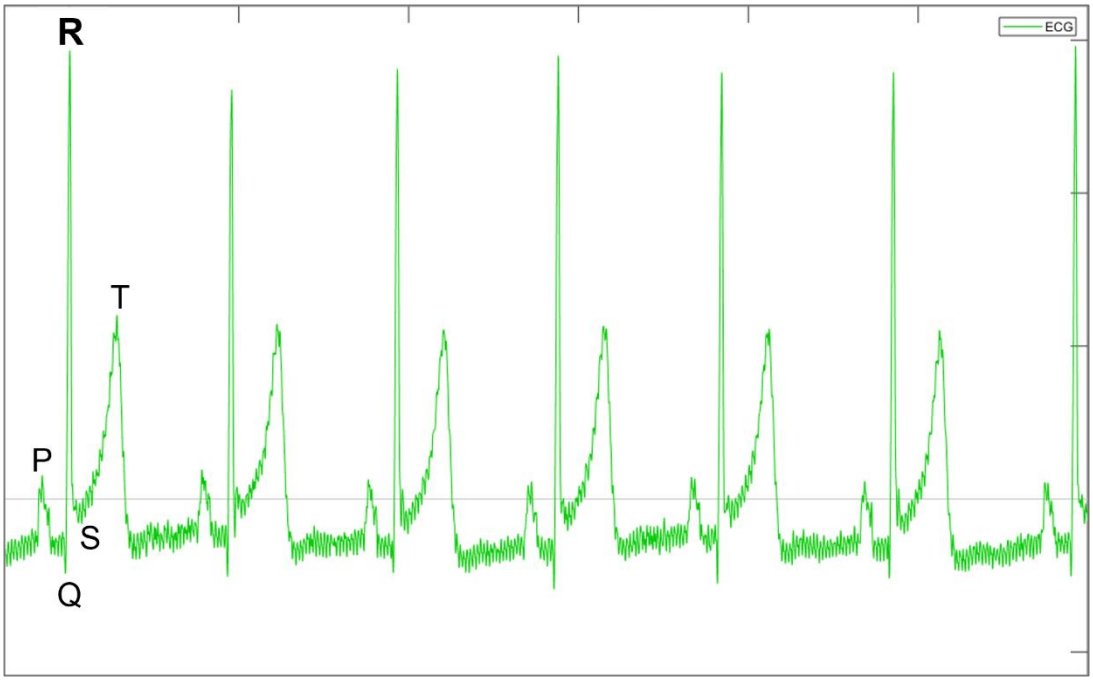

Figure 25: Raw ECG trace with PQRST waveform identification.

This ECG trace example is from a subject dataset in the RECOGNeyes study. The signal time course is plotted where the x-axis is time (msecs) and signal voltage (mV) is on the y-axis. QRS complex reflects ventricular depolarisation, and the largest deflection denoted by the R wave (labelled in bold) is the element required for HRV analysis.

6.1.2. Relating heartrate to arousal and cognitive performance

The vagal nerve is the principle nerve of the parasympathetic nervous system that influences cardiac function and synapses directly onto the heart. Vagal activation of the heart causes immediate HR slowing (cardiac deceleration), whilst vagal withdrawal (cessation of vagal activation) results in immediate HR acceleration (for more background information regarding vagal and ANS cardiac effects, refer to Chapter 2,

Sections 2.1.1 and 2.1.2). This means that over short timescales typical of anticipatory responses to salient stimuli, changes in HR are largely mediated by the PNS, although overall HR evaluated over a longer period, e.g., 10s of seconds, may be modulated by fluctuations in sympathetic activation.

Since the latter half of the 20th century, links have been established between changes in HR and cognitive performance. Cardiac deceleration is proposed to be a component of the orienting response (Graham & Clifton, 1966); as discussed in more detail in Chapter 2, Section 2.1.1. Anticipatory cardiac deceleration is observed in response to a cue signalling an upcoming target stimulus, followed by cardiac acceleration after the motor response (Jennings & van der Molen, 2005; Jennings & Wood, 1977; Lacey & Lacey, 1974, 1978; Reyes del Paso et al., 2015). This anticipatory cardiac deceleration was proposed to reflect preparatory mechanisms related to reaction timings (Jennings, 1992; Somsen et al., 2002), which is supported by findings of direct correlations between greater anticipatory cardiac deceleration with faster reaction time (Jennings et al., 1998; Reyes del Paso et al., 2015).

The phenomena of stimulus-elicited cardiac deceleration thus relates to the intricate mechanisms of arousal that govern our attentive state (Porges, 2007; Wass et al., 2015). The parasympathetic slowing of HR observed in humans when exposed to threatful and negative stimuli may be a trait retained in our evolution of the 'freeze' mechanism observed in many

animals species in response to threat and dangerous situations, and co-opted in mammals as a feature of the orienting response to new and behaviourally salient stimuli (Gladwin et al., 2016; Hermans et al., 2013; Porges, 2007; Roelofs, 2017). Greater preparatory cardiac deceleration is associated with more effective motor responses, which is exhibited in sports professionals compared to novices in that sport, e.g., golf (Cooke et al., 2014), pistol shooting (Tremayne & Barry, 2001) and balance beam gymnastics (Cottyn et al., 2008), suggesting that it serves an important function in readying the body for action.

Although PNS and SNS branches of the ANS tend to have opposing effects on the organs they govern, and typically work reciprocally, the processes underlying the orienting response appear to involve concurrent activation of both the SNS, observed as phasic pupil dilation, and the PNS system, observed as cardiac deceleration (Libby et al., 1973; van der Molen et al., 1989). This suggests that attentional orienting involves not a single "global" preparatory process, but one that involves coordination of multiple systems, including both branches of the ANS (Jennings et al., 1998, 2009; Jennings & van der Molen, 2005; Ribeiro & Castelo-Branco, 2019). See Shaffer et al. (2014) for a review regarding these complex reciprocal relationships between cognitive, motor and autonomic processes of the heart.

In Chapter 5, I reported robust evidence that anticipatory phasic pupil dilation rate is negatively correlated, within-subjects, with saccadic

RTs in our cued pro/antisaccade task. Using a simple manual RT task with no temporal cue to predict target onset, Jennings et al. (1998) found a negative correlation between cardiac deceleration and RT, but not between pupil dilation rate and RT. Interestingly, they found no significant trial-by-trial correlation between pupil dilation and cardiac deceleration, suggesting that these effects, though concurrent, are independent rather than part of a "global" anticipatory process that elicits correlated activity in both branches of the ANS.

In the RECOGNeyes study, we acquired ECG recordings from participants as well as pupillometry data in order to investigate ANS correlates of anticipatory processes involved in inhibitory control during the pro/antisaccade task. In this chapter, I will address the following research questions:

- Does anticipatory vagal activation indexed by HR deceleration occur in preparation for a saccadic response, and, if so, does the deceleration differ between pro- and antisaccade trials, and/or after RECOGNeyes training?
- Are rates of pupil dilation and cardiac deceleration positively or negatively correlated with each other within-subjects, trial-by-trial, and what light does this relationship shed on the role of the ANS in anticipatory processes?
- Does cardiac deceleration rate (cue-elicited or target-elicited) account for additional or shared within-subject variance in RT,

trial-by-trial to that accounted for by pupil dilation rate, and do these effects differ by trial type and/or after RECOGNeyes training?

6.2. Methods

6.2.1. Filtering and R wave extraction

To extract the R wave timestamps from the ECG data, I used the MATLAB application Brainstorm (Version: 3.200615) (Tadel et al., 2011, 2019), using MATLAB R2018a (MathWorks Inc.). Figure 25 depicts an example of a raw ECG trace in Brainstorm. Brainstorm also has an automated R wave detection function for extracting R wave timestamps, which is necessary for heartrate variability analysis.

To clean the data, I applied a 50 Hz notch filter to remove noise from AC mains electricity, and a 7-70 Hz band-pass filter to remove high and low frequency artefacts. This includes low frequency artefacts from respiration, and baseline wander (Eckberg, 2000; Ingale et al., 2020; Kher, 2019) and high frequency noise from muscle artefacts (Christov et al., 2017; Christov & Daskalov, 1999; Ingale et al., 2020).

Further cleaning methods were then required to remove artefactual peaks remaining in the signal. I visually identified and manually selected any remaining artefacts in each dataset to be labelled as 'bad segments' to

be omitted from the ECG signal before running the automated R wave detection function. These 'bad segments' were defined as the presence of excessive movement noise, poor recording quality, or ectopic beats where R waves were too close together.

For running the automated R wave detection procedure, I set the event detection filter to 7 to 30 Hz, which our lab has found by trial and error produces more reliable R wave detection than the default bandpass filter of 10 to 40 Hz. I used an amplitude threshold of 2 standard deviations (Std. Devs) for the filtered signal to exceed for an R event to be identified and set the threshold for the minimum duration between two events, i.e., the smallest latency between two R waves, to 300-400 msecs.

Following this, I visually inspected the labelled R waves on every subject's ECG timeseries. This allowed me to ensure they had been detected correctly and to add any missed R waves or delete incorrectly identified ones as necessary. Timestamps for the R waves, bad segment markers and trial markers (including saccade onset time) were then exported to an Excel spreadsheet.

6.2.2. IBI variable extraction

To study the HR around the saccade onset in each trial, IBI values were extracted from the exported spreadsheets using custom MATLAB scripts. IBI_0 was defined as the R-R interval encompassing the saccade

onset marker. Using this IBI_0 as the reference point, the two preceding IBIs and the two succeeding IBIs were also extracted for each trial, giving a series of five successive IBIs, denoted: IBI_{-2}, IBI_{-1}, IBI_0, IBI_{+1} and IBI_{+2}. Where the perisaccadic ECG contained missing data due to artefact removal, the IBI was not computed.

For each subject, for each trial type and for each day, IBI values for each trial with usable data were tabulated in an N row by 5 column matrix, where N is the number of trials with useable data, and the 5 columns represent IBI_{-2} to IBI_{+2}. These matrices were then summarised across trials by taking the median of each column, ignoring missing values. Medians, rather than means, were used to summarise the values across trials to avoid undue influence from outlying values.

6.2.3. Interpolated "instantaneous HR" values

To provide a way to evaluate short-term HR change over the trial event intervals used in the pupillometry analysis, we used an interpolation method to produce "instantaneous" HR and IBI values at the same sampling frequency as the pupillometry data. Using in-house MATLAB scripts and functions, for each subject's session dataset, each IBI value calculated from the timestamps of the detected R waves (Brainstorm output) was plotted against the timestamp of the R wave that terminated the IBI. This gave a chart of vertical bars in which the vertical axis represents the duration of

the IBI, and the horizontal axis represents the time of the terminal R wave (illustrated in the top panel of Figure 26).

Where intervals between successive R waves gave implausibly large intervals, due to missing data segments or missed R waves, these were easily visible as much taller bars on the plot. Similarly, any remaining artefactual R waves occurring mid-cycle were visible as much smaller bars. The plots were then visually inspected, and spuriously long or short peaks were manually cropped from the time series, giving a time series of plausible IBIs, each "sampled" at the time of their terminal R wave.

A pchip interpolation (refer to Chapter 5, Section 5.2.3.2) was then applied to this cleaned IBI time series to derive a “virtual” instantaneous IBI value at a regular sampling rate. In our case, we chose 500 Hz to match the sampling rate of the pupillometry data. This interpolated time series was then divided into 60,000 to give a plot of “instantaneous” HR at a higher and more regular sampling rate than the HR itself. Interpolating in this way between R wave times allows the rates of HR change to be computed between any events of interest, regardless of when the next or most recent R waves occurred, and is one of the techniques used to derive frequency domain measures of HRV (not used in this study). An example of the interpolated instantaneous HR timeseries is displayed in bottom panel of Figure 26.

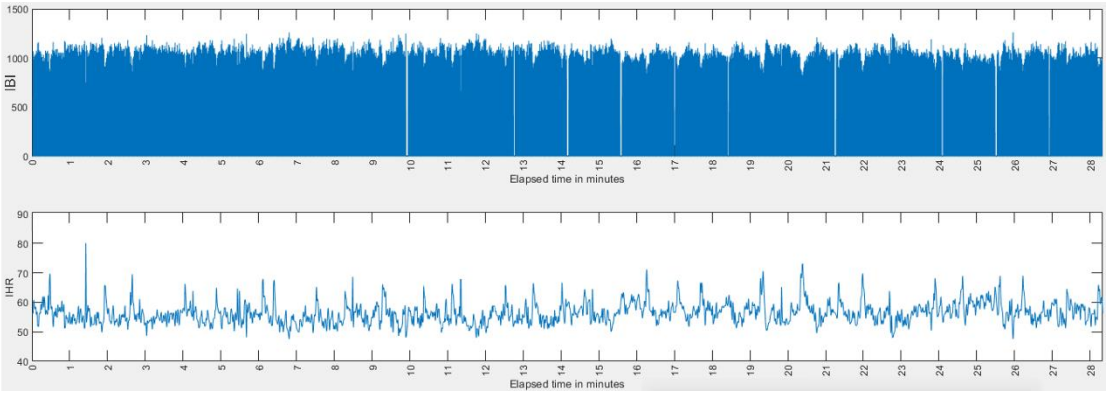

Figure 26: Example subject timeseries data of IBI and interpolated instantaneous heartrate.

The top panel shows the IBI plotted vertically (in msecs) across the whole task timeseries (in minutes). Gaps are where an IBI has been removed because it was too long, due to missing data segments or missed R waves in the data. The bottom panel depicts the result of the interpolated instantaneous HR, equating to a sampling rate of 500 Hz.

6.2.4. Event-related cardiac deceleration rates

The interpolated IBI time series enabled the computation of similar task-related analytic methods to that applied to the pupillometry (described in Chapter 5) as well as to the MEG data (described in Chapter 7). First, trials were excluded if there were more than 30 % of samples in the trial where data had been interpolated during periods of missing consecutive IBIs (the same threshold was also used for missing pupillometry data, see Chapter 5, Section 5.2.3.2).

Rates of change in "virtual" interpolated IBI were evaluated over the same trial periods as for the pupillometry data (cue to target; target to target + 100 msecs; target to saccade onset). Within-subjects trial-by-trial Spearman's correlations with RT were also computed and converted to *z*

values using the Fisher *r-z* transform. In addition, where sufficient trials with good HR data and good pupillometric data were available, within-participant trial-by-trial Pearson's correlation matrices were computed for RT (natural log), pupil dilation rates, and cardiac deceleration rates for the cue to target and target to target + 100 msecs time periods. This enabled multiple regression coefficients to be extracted for the prediction of RT from both pupil dilation rate and cardiac deceleration rate.

6.3. Results

6.3.1. Analysis considerations

For full details regarding data analysis considerations, refer to Chapter 3, Section 3.7. Statistical analysis follows a similar format to those conducted for the pupillometry data in Chapter 5. Additional analysis includes correlations between RT, rate of cardiac deceleration and rate of pupil dilation.

Interpolated instantaneous IBI data for event-related cardiac deceleration rates included a total of N=15 subjects for day-paired analyses. There were a total of N=13 day-paired subjects for IBI variable data relative to saccade onset. The within-subjects correlations between cardiac deceleration rate, pupil dilation rate and RT required subjects to have sufficient numbers of correctly responded-to trials with both valid

pupillometry and cardiac data, where there were N=14 data type matched and day-paired subjects. Further details regarding missing subject data for different analyses is included in Chapter 4, Figure 9.

6.3.2. IBI changes relative to saccade onset

Analysis of IBI variables across the time course of individual trials rather than across the whole experiment were conducted to investigate changes in HR occurring over smaller timescales.

To assess IBI changes before and after saccade onset and whether this differed between days or trial types, a three-way ANOVA was conducted with three within-subjects factors: Day (2 levels: Day 1 and Day 2); Trial Type (2 levels: prosaccade and antisaccade); and IBI relative to saccade onset (5 levels: IBI_{-2} to IBI_{+2}). Across days and trial types, there was a significant main effect of IBI, $F(1.750, 21.000) = 22.822$, $p < .001$. Polynomial contrasts indicated a significant quadratic component $F(1,12) = 23.893$, $p < .001$, reflecting a rise and fall across the five IBIs, peaking at IBI_0, as can be seen the values plotted in Figure 27. IBI durations increase from IBI_{-1} to IBI_0, indicating cardiac deceleration, followed by a decrease from IBI_0 to IBI_{+2}, where HR accelerates back to the level observed at IBI_{-1}. In other words, this reflects preparatory cardiac deceleration prior to saccade onset, followed by cardiac acceleration after saccade execution.

There was also a significant main effect of Trial Type, $F(1, 12) = 7.588$, $p = .017$, indicating that antisaccade trials overall have significantly

greater IBIs (i.e., slower HR) than prosaccade trials (as seen in Figure 27). However, there was no significant Trial Type by IBI interaction, suggesting greater tonic parasympathetic activity during antisaccade trials. Interestingly, this parallels the observation of smaller tonic pupil size during antisaccade blocks reported in Chapter 5, Section 5.3.2.

Although Figure 27 suggests this difference between trial types was greater on Day 2 than on Day 1, and that IBIs appear shorter on Day 2 than on Day 1 across trial types, there were no significant main effects of Day (Day 1, mean: 862.165, SEM: 17.946; Day 2, mean: 836.061, SEM: 28.471; $F(1, 12) = 6.46$, $p = .437$), nor any interactions with Day. Post-hoc power calculations revealed a 95 % chance of finding a medium effect size, but only a 19 % chance of finding a small effect size. This implies that a large or medium effect were unlikely to be missed, but a significant small effect size cannot be ruled out.

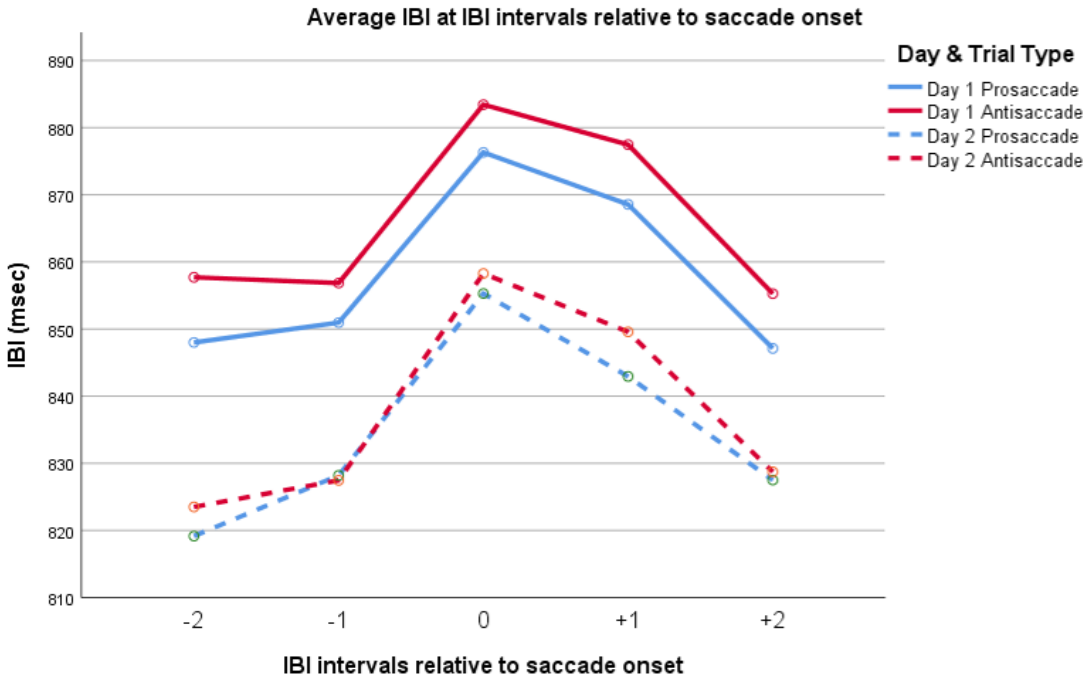

Figure 27: Average IBI across the trial time course for intervals relative to saccade onset (at IBI_0).

The means of the subject median IBIs are depicted in this figure for each day and trial type.

6.3.1. Cardiac deceleration rates

Due to IBIs being ~600–1000 msecs in duration, the onset of the saccade relative to the beginning of IBI_0 can vary widely between trials. Figure 28 shows the interpolated time course of these "virtual" instantaneous IBI values and show that deceleration (as measured by increasing IBI values) is apparent between the cue and target, but even more so after target onset. I therefore used these interpolated instantaneous IBI time series values to compute deceleration rates between cue and target and between target and saccade onset, to delineate more

precisely the cardiac deceleration dynamics associated with saccadic response preparation. Results from this investigation are reported in the following.

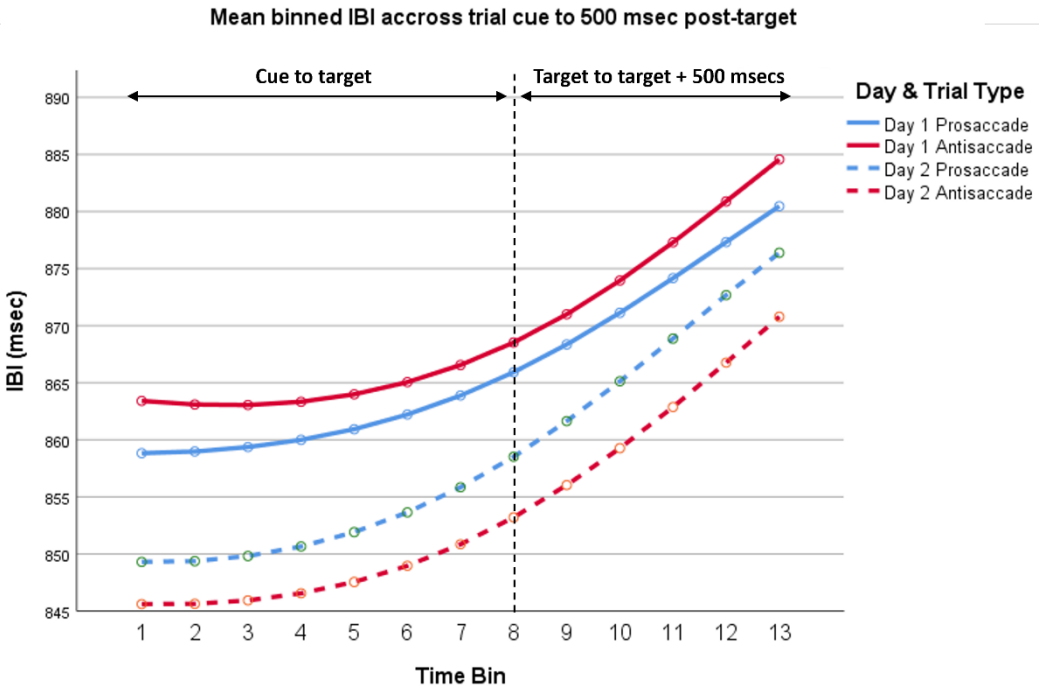

Figure 28: Instantaneous IBI values across trial time courses for each day and trial type averaged into 100 msec bins.

Bin 1 starts from the cue onset, the end of bin 8 is the target presentation, and bin 13 is to 500 msecs post-target. Note that values were not binned prior to computing the deceleration rates.

To compare rate of cardiac deceleration between the anticipatory cue to target period and post-target periods (target to target +100 msecs or target-saccade), three-way ANOVAs were conducted with three within-subjects factors: Day (2 levels: Day 1 and Day 2); Trial Type (2 levels: prosaccade and antisaccade); and Time Period (2 levels: cue-target

deceleration rate and post-target deceleration rate (ANOVA 1: target to target + 100 msecs and ANOVA 2: target-saccade).

There was a significant main effect of Time Period in both ANOVAs (ANOVA 1: $F(1, 14) = 52.802$, $p < .001$; ANOVA 2: $F(1, 14) = 48.484$, $p < .001$) where post-target deceleration rate was significantly greater than anticipatory cue-target deceleration rate. There were no other significant main effects, or interactions; although, there was a trend for deceleration rates to be greater on Day 2 than on Day 1 across trial types (Main effect of Day – ANOVA 1: $F(1, 14) = 3.722$, $p = .074$; ANOVA 2: $F(1, 14) = 4.092$, $p = .063$). Mean rate values are illustrated in Figure 29.

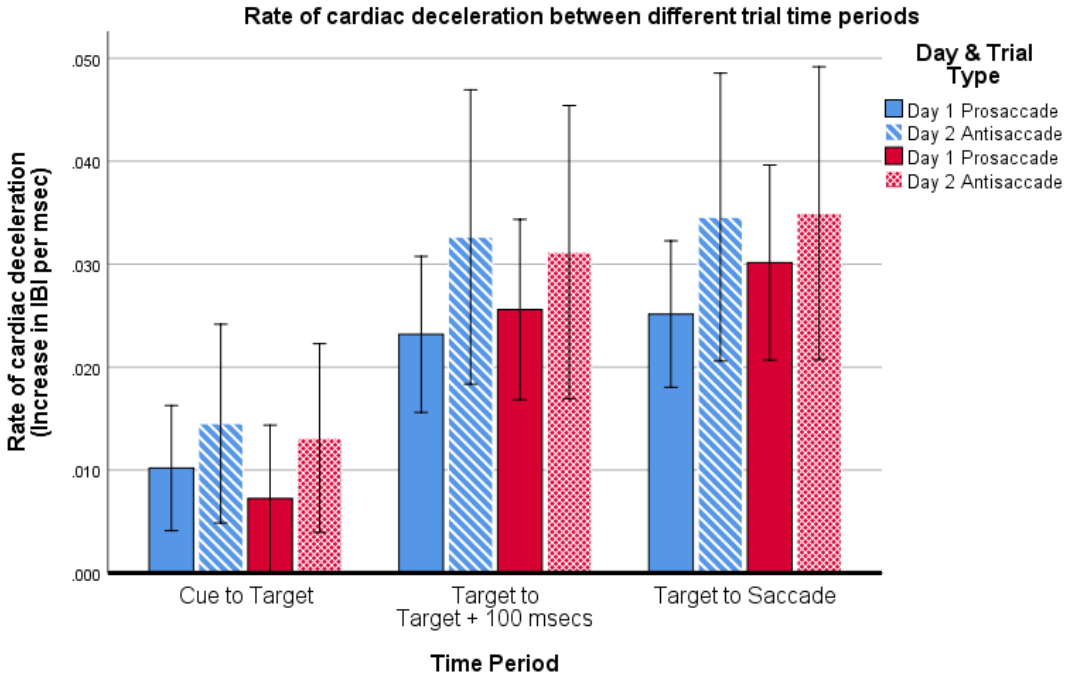

Figure 29: Rate of cardiac deceleration for cue to target and post-target time periods.

Plotted are the mean of the median cardiac deceleration rates at these time periods across subjects for each day and trial type. Error bars are 95% CI.

6.3.2. Cardiac deceleration rate correlations with RT

As with the pupil dilation rates, I computed within-subjects trial-by-trial Spearman's correlations between cardiac deceleration rates and RT. I used two three-way repeated-measures ANOVAs to compare RT correlations between the cue-target and post-target deceleration rate periods (target to target +100 msecs or target-saccade, respectively). The three within-subjects factors included: Day (2 levels: Day 1 and Day 2); Trial Type (2 levels: prosaccade and antisaccade); and Time Period (2 levels: cue-target deceleration rate and post-target deceleration rate (ANOVA 1: target to target + 100 msecs and ANOVA 2: target-saccade).

The *F*-test for the between-subjects intercepts were significant for both ANOVAs, (ANOVA 1: $F(1, 14) = 20.750$, $p < .001$; ANOVA 2: $F(1, 14) = 17.394$, $p = .001$), which as discussed previously shows that the mean of the correlation coefficients averaged across all conditions was significantly different from zero. Since the signs of the mean correlation coefficients were negative, therefore greater cardiac deceleration rate was correlated with faster RT (as seen in Figure 30).

There were no significant within-subjects main effects or interactions in these ANOVAs. However, I reasoned that any effects of Day and/or Trial Type might nonetheless be more marked in the cue-target anticipatory period than the post-target response periods, even if not significantly so. I therefore conducted two-way ANOVAs, containing two within-subjects factors of Day (2 levels: Day 1 and Day 2) and Trial Type (2 levels:

prosaccade and antisaccade) to examine effects for each rate time period individually. This revealed that in the cue-target anticipatory period, RT correlations with cardiac deceleration were significantly more negative for antisaccade trials than for prosaccade trials, $F(1, 14) = 5.773$, $p = .031$, but not in post-target periods. This suggests that preparatory cardiac deceleration is more predictive of RT in antisaccade trials than in prosaccade trials.

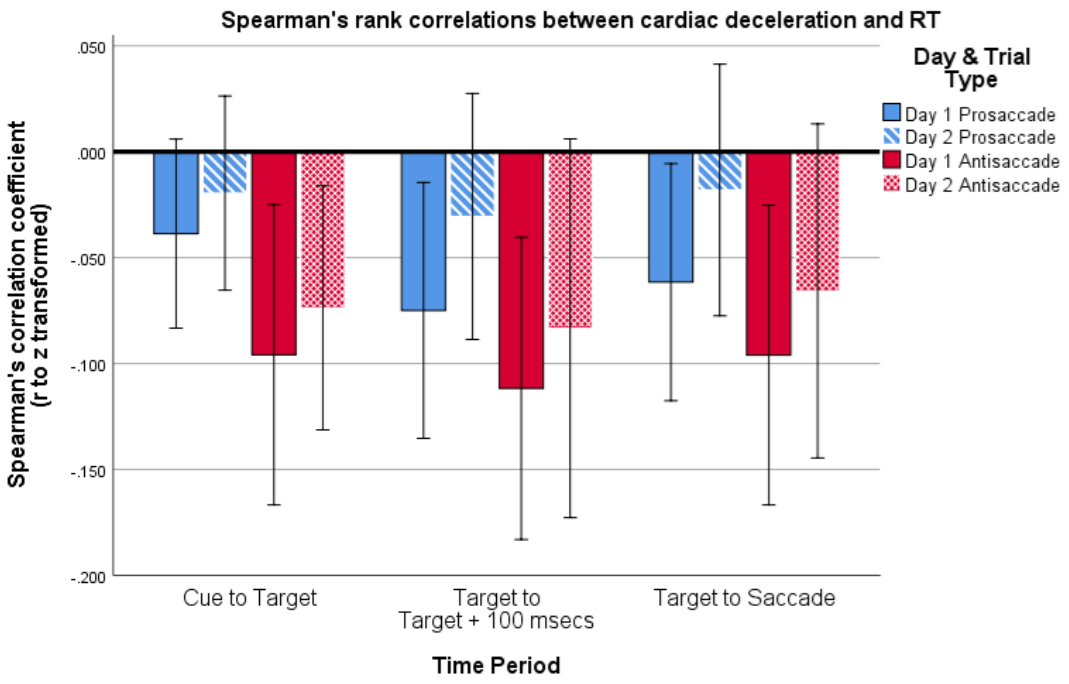

Figure 30: Spearman's rank correlations between cardiac deceleration rate and RT at different trial time periods.

Plotted are the subject correlation coefficient r to z transformed mean averages for each day and trial type. Error bars are 95% CI.

6.3.3. Do pupil dilation rates and cardiac deceleration rates account for different variance in RT?

The RECOGNeyes study data provide robust evidence that that both anticipatory SNS activation, as measured by pupil dilation rate, and PNS activation, as measured by cardiac deceleration rate predict RT on a trial-by-trial basis. This raises the question of whether rates of pupil dilation and cardiac deceleration account for the same variance in RT, which would suggest that faster RTs are the result of more efficient deployment of a single cognitive process that coactivates both ANS branches to a similar extent on each trial. Alternatively, do they account for separate variance, which would suggest that PNS and SNS anticipatory processes are activated by separate cognitive systems that may vary independently from trial to trial.

Correlations between RT and pupil dilation/cardiac deceleration rates computed between target and saccade onset are potentially confounded by the fact that the time period of interest is itself the length of the saccade latency. However, we observed significant correlations between RT and both pupil dilation rate and cardiac deceleration rate even when rates were calculated over the short target to target + 100 msecs period. I therefore restricted the following analysis to rates calculated over the anticipatory period between cue and target, and the immediate post-target period (target to target + 100 msecs).

I first computed within-subjects correlation matrices between pupil dilation rates and cardiac deceleration rates, respectively, over the two time-periods of interest (cue-target; target to target + 100 msecs) and RT. This resulted in a 5 x 5 matrix for each participant for each trial type and day. For these correlations, I used Pearson's correlation coefficients, as they give a more precise estimate of fit and using the natural log of the RT controls for excess leverage from long RTs.

Firstly, to determine whether pupil dilation and cardiac deceleration rates were correlated with one another, I conducted two-way repeated-measures ANOVAs using within-subjects factors of Day (2 levels: Day 1 and Day 2) and Trial Type (2 levels: prosaccade and antisaccade) for each of the trial time periods. The dependent measures were the Fisher-transformed correlation values for pupil dilation rate and cardiac deceleration rate.

For the cue and target anticipatory period ANOVA, there was a statistically significant between-subjects intercept, $F(1, 13) = 11.710$, $p = .005$, and the mean correlation value was negative. This indicated that pupil dilation rate and cardiac deceleration rates were negatively correlated over the anticipatory period: more rapid pupil dilation rate was associated with less steep cardiac deceleration, and vice versa. There was no significant overall correlation, either positive or negative, between pupil dilation rate and cardiac deceleration rate when computed over the target to target + 100 msecs period.

To answer the question as to whether our indices of phasic autonomic activation account for the same or different variance in RT, we used the correlation matrix to compute regression coefficients for two multiple regression models (one for each period of interest) in which pupil dilation rate and cardiac deceleration rate were the predictor variables, and RT the dependent variable.

A Pearson's correlation matrix can be used to derive standardised regression coefficients by solving simultaneous equations. This was done for each of the two time periods of interest to derive regression parameters for the regression model:

$$RT_i = b_1 pupil\ dilation\ rate_i + b_2 cardiac\ deceleration\ rate_i + error$$

Whereby i is for a given subject, and beta b is the regression coefficient for each predictor variable. This yields two standardised regression coefficients, one for pupil dilation rate (b_1) and one for cardiac deceleration rate (b_2), respectively. They provide an estimate of how much each one predicts RT after controlling for the prediction made by the other. Figure 31 shows the mean values for the regression coefficients across subjects for each predictor, trial type, time period, and day.

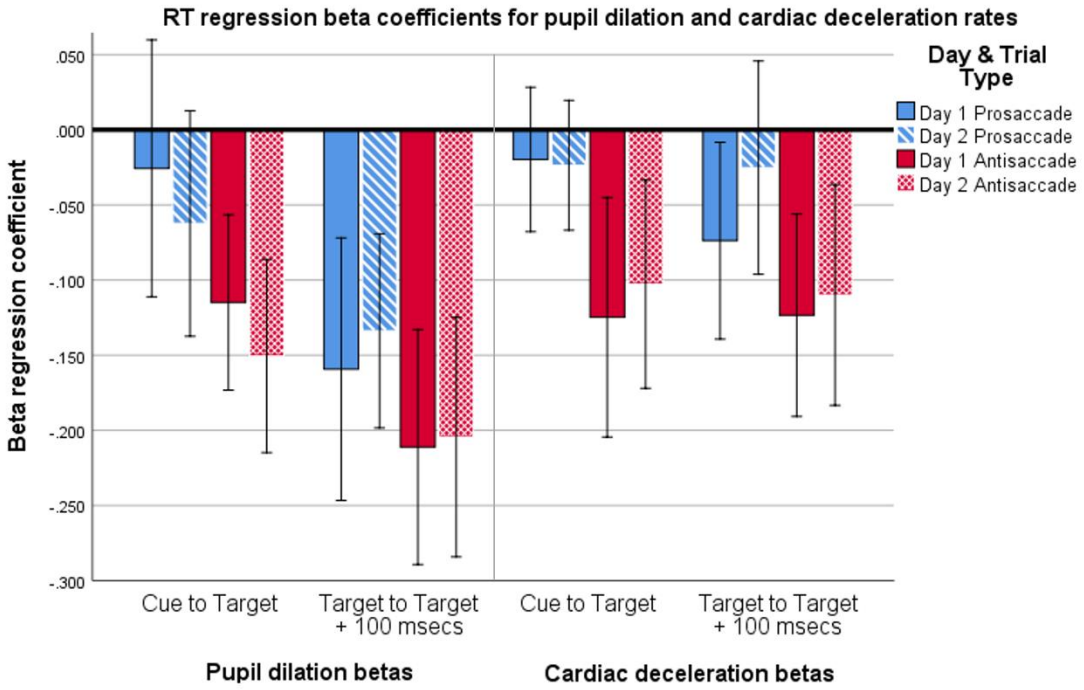

Figure 31: RT regression beta coefficients between pupil dilation rate and cardiac deceleration rate.

Betas are divided so that the left side include the pupil dilation betas and the right side include the cardiac deceleration betas. These are the mean betas across subjects for each day and trial type. Error bars are 95% CI.

I then used repeated-measures ANOVAs to compare these standardised regression coefficients between Predictors (pupil dilation rate and cardiac deceleration rate), Days, Trial Type and Time Period. I entered the standardised regression coefficients into an initial four-way repeated-measures ANOVA for the following factors: Day (2 levels: Day 1 and Day 2), Time Period (2 levels: cue to target; target to target + 100 msecs), Trial Type (2 levels: prosaccade and antisaccade) and Predictor (2 levels: pupil dilation rate and cardiac deceleration rate).

There was a significant main effect of Predictor, $F(1, 13) = 7.930$, $p = .015$, which indicated that pupil dilation rate had more negative regression coefficients than cardiac deceleration rate coefficients. A significant main effect of Time period, $F(1, 13) = 14.458$, $p = .002$, also indicated that target to target + 100 msecs regression coefficients were more negative than cue-target regression coefficients. Additionally, a main effect of Trial Type, $F(1, 13) = 24.691$, $p < .001$, indicated there were significantly more negative regression coefficients for antisaccade trials than for prosaccade trials.

However, there was a significant Predictor by Time Period interaction, $F(1, 13) = 6.919$, $p = .021$, indicating that the regression coefficients were more similar in the cue-target anticipatory period than in the target to target + 100 msecs period (see Figure 32).

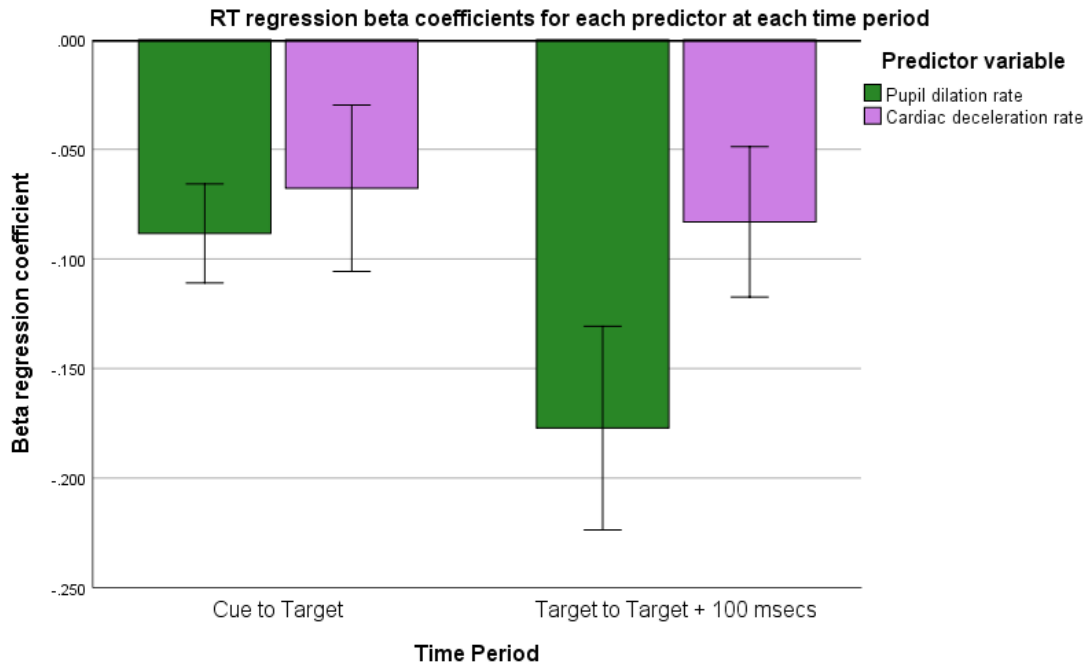

Figure 32: RT regression beta coefficients collapsed over day and trial type for each predictor and time period.

This figure presents the mean betas across subjects. Error bars are plotted as 95% CI.

To interpret this interaction, I conducted follow-up ANOVAs on each time period separately. For the anticipatory cue-target interval, again, there was a significant main effect of Trial Type, $F(1, 13) = 20.424$, $p < .001$, whereby regression coefficients were significantly more negative for antisaccades than for prosaccades. However, there was no main effect of Predictor, indicating no significant difference in the predictive power of the two ANS measures in the cue-target anticipatory period. The between-subjects intercept was significant, $F(1, 13) = 55.204$, $p < .001$, indicating that regression coefficients averaged over day and trial type were

significantly negative, and indeed even for prosaccades separately, this effect reached statistical significance, $F(1, 13) = 5.059$, $p = .042$.

For the target to target + 100 msecs ANOVA, there was a significant main effect of Predictor, $F(1, 13) = 10.724$, $p = .006$, indicating a significantly more negative pupil dilation regressor than cardiac deceleration regressor. There was also a significant effect of Trial type, $F(1, 13) = 15.120$, $p = .002$, again reflecting more negative regression coefficients for antisaccade trials. In addition, the between-subjects intercept was significant $F(1, 13) = 112.288$, $p < .001$, indicating across all factors that the regression coefficients were significantly negative.

There were no significant main effects or interactions involving Day in these ANOVAs. However, it is important to note that while for Day 1 there were 25 participants with data from both measures containing a sufficient number of trials to compute a full correlation matrix, only 14 of these participants had enough good trials on Day 2 for a day-to-day comparison. I therefore re-computed the aforementioned ANOVAs with Day 1 data only to see whether these findings remained robust with more within-subjects statistical power, which obtained similar results.

6.4. Discussion

6.4.1. Question 1

> Does anticipatory vagal activation indexed by HR deceleration occur in preparation for a saccadic response, and, if so, does the deceleration differ between pro- and antisaccade trials, and/or after RECOGNeyes training?

Overall, our results showed that significant preparatory cardiac deceleration precedes the saccadic response in the pro/antisaccade task and is followed by significant acceleration. Despite a plethora of evidence for preparatory cardiac deceleration prior to a motor response followed by cardiac acceleration (as discussed in Section 6.1.2), to our knowledge, this is the first time pre-motor deceleration and post-motor acceleration have been reported in relation to a saccadic eye-movement.

While IBIs were significantly longer overall (i.e., slower HR) for antisaccade trials than prosaccade trials, there were no differences between trial types in the rate of deceleration. This mirrors the finding in Chapter 5 of overall smaller pupil size during antisaccade blocks and may reflect lower tonic SNS mediated arousal during these blocks. Alternatively, and perhaps more interestingly, it may reflect greater tonic vagal (i.e., PNS) activation throughout antisaccade blocks, reducing the mean pupil size and resulting in lower mean HR during these trials. If so, it may indicate that the

antisaccade task blocks that require greater inhibition induced greater overall application of the “vagal brake”.

6.4.2. Question 2

> Are rates of pupil dilation and cardiac deceleration positively or negatively correlated with each other within-subjects, trial-by-trial, and what light does this relationship shed on the role of the ANS in anticipatory processes?

There was no indication in our data of a positive correlation, trial-by-trial, between anticipatory pupil dilation and anticipatory cardiac deceleration, suggesting independent processes. Indeed, during the cue to target anticipatory period, the two were negatively correlated – greater pupil dilation on a trial was associated with less cardiac deceleration and vice versa. This may indicate a trace of reciprocal PNS-SNS coordination, even when the two systems are co-active.

Alternatively, it may simply indicate that they are independently invoked, but exert opposing effects on their respective organs. For instance, trials where there is high SNS activation would counteract cardiac deceleration, whereas trials with high PNS activation would depress the rate of pupil dilation. Essentially, the effects of phasic SNS and PNS activation may be additive when it comes to facilitating reaction time, but subtractive regarding their effects on the relevant organs.

6.4.3. Question 3

> Does cardiac deceleration rate (cue-elicited or target-elicited) account for additional or shared within-subject variance in RT, trial-by-trial to that accounted for by pupil dilation rate, and do these effects differ by trial type and/or after RECOGNeyes training?

Our results showed that greater anticipatory cardiac deceleration rate is significantly correlated with faster RT, which supports previous findings (Jennings et al., 1998; Reyes del Paso et al., 2015). Arguably, the most fascinating finding from the current analyses is that our study is the first to establish that greater anticipatory rates of cardiac deceleration and pupil dilation are not only both associated with faster RT together, but that these predictor variables account for separate variance of RT.

Previous findings by Jennings et al. (1998) studied both cardiac deceleration and pupil dilation correlations with RT, but only cardiac deceleration correlations were significant. Jennings et al. (1998) did report negative correlations indicating increased pupil dilation correlated with faster RT; however, these were too weak to reach statistical significance. Although greater pupil dilation has been correlated with faster saccadic RT on antisaccade trials (C.-A. Wang et al., 2015, 2016), this has never been confirmed together with cardiac deceleration. This idea is not well established in the literature, whereby recent studies still report Jennings et al. (1998) to support that only cardiac deceleration and not pupil dilation

is correlated with RT (Ribeiro & Castelo-Branco, 2019). Our findings may differ to that of Jennings and colleagues due to differences in their experimental design compared to ours, such as different pupillometry equipment, the use of an auditory instead of visual stimulus, and use of a manual response lever rather than saccadic responses. Therefore, this warrants further investigation of concurrent pupillometry and ECG to assess the joint contributions of pupil dilation and cardiac deceleration in predicting RT to validate our findings, as this is lacking in the literature.

Our data showed that pupil dilation and cardiac deceleration rates contribute to separate variance of RT, which indicates that it is the underlying autonomic drives accounting for faster RT, rather than cardiac deceleration or pupil dilation per se. This thus supports the hypothesis that phasic arousal “alerting” processes and phasic vagal “orienting” processes, while both serving to prepare the organism for action in response to a stimulus, are invoked by independent cognitive processes. In other words, this suggests that the effect of the preparatory "accelerator” (i.e., LC-NE arousal indexed by pupil dilation) plus vagal brake have an antagonistic physiological modulation on the respective organs, but have an additive or synergistic effect on performance.

Additionally, pupil dilation rate contributed more to predicting RT than cardiac deceleration rate, particularly for target-elicited rates. This may indicate that increased SNS phasic arousal in response to the target is more predictive of task performance, due to enhanced alerting responses to

the visual target stimulus, with less reliance of modulation by the vagal break; however, our results still support that both contribute to better task performance together than separately.

Moreover, our evidence from both data types suggests that more of the RT variance is accounted for by these processes in antisaccade responses than prosaccade responses. This indicates both greater phasic pupil dilation arousal responses are applied for alerting to the stimulus, together with a stronger vagal brake to prevent orienting reflexes to reduce directional errors, are particularly important for antisaccadic performance. Therefore, this suggests these ANS processes are important in modulating top-down inhibitory control mechanisms.

Although the current analyses did not find strong effects of day, powered analysis for day effects were low. This means future research with increased number of participant datasets available for both days would be needed to fully evaluate any day effects of cardiac deceleration and pupil dilation in correlational analyses.

Overall, these measures of arousal reflect joint contributions of sympathetic and parasympathetic activation prior to making a saccadic response that are indicative of performance. This is supported to be accounted for by simultaneous activation of the alerting response and phasic arousal indexed by sympathetic pupillary dilation, and the orienting response from parasympathetic cardiac deceleration (vagal brake) working together in attentional inhibitory control mechanisms. However, more

research is required in this area to confirm and validate these findings. Next, I will discuss the CNS brain correlates measured using magnetoencephalography.

6.4.4. Cardiac data limitations

The primary limitation affecting the analysis of cardiac data was the lack of day-paired subject datasets. This reduced the power of all analyses described in this chapter, which could account for the lack of significant findings of day effects, despite some figures pertaining to a difference between days. To improve the ECG data acquisition, the battery powered ECG box could be replaced by a mains supply option to limit any disruptions to power from flat batteries. Additionally, more time allocated in the scanner room may have enabled time to check the ECG signal quality and amend the placement of electrode fixtures to the skin if necessary or replace faulty electrodes.

Furthermore, collecting related cardiac measures such as blood pressure could capture the broader autonomic influences on different cardiac mechanisms (e.g., assessing whether parasympathetic effects are generalised across all cardiac indices at the same time). Additionally, respiratory measures are closely related to the cardiovascular system, thus recording respiratory measures could help us to interpret wider dynamics of autonomic nervous system drive.

Chapter 7: CNS effects as measured with magnetoencephalography

7.1. Background and rationale

The RECOGNeyes study was designed to investigate neural correlates of performance on the pro/antisaccade task, and the effects of gaze-control training on these measures in an inattentive sample. In Chapters 4 and 5, I have presented autonomic correlates of performance as measured by anticipatory pupillometric and heartrate changes during the pro/antisaccade task. In this chapter, I will present our investigation of CNS correlates using magnetoencephalography (MEG). We aimed to test the general hypothesis that gaze-control training using RECOGNeyes is associated with changes in function of the brain mechanisms underlying inhibitory control. We investigated the time courses of oscillatory amplitude during the anticipatory period between cue and target onset.

A cued version of the pro/antisaccade task was specifically chosen to elucidate top-down inhibitory control mechanisms of response anticipation (refer to Chapter 1, Section 1.2.2). During the period between the cue and target, this task activates regions within the visual attention and oculomotor networks (as discussed in Chapter 2, Section 2.2 and illustrated in Figure 2). These cognitive control processes of attention and cognitive control are governed by specific oscillatory neurodynamics to facilitate the

relevant activation and inhibition patterns in brain regions of the visual attention/oculomotor network (Hwang et al., 2014, 2016; Munoz & Everling, 2004).

7.1.1. Frequency-band oscillations, inhibitory control, and visual attention/oculomotor network regions

The oscillatory rhythms of brain activity were first discovered by Hans Berger, the inventor of electroencephalography (EEG) (H. Berger, 1929). Oscillatory frequencies range from very slow (minutes per cycle) to very fast (up to 600 Hz) (Curio et al., 1994). Oscillations from 0.5 Hz upwards are traditionally divided into five bands, each named after a Greek letter of the alphabet (delta, 0.5 – 4 Hz; theta, 4 – 8 Hz; alpha, 8 – 12 Hz; beta, 12 – 30 Hz; gamma, >30 Hz) (Buzsáki, 2006). Each of these bands are believed to serve specific functions. This includes lower frequencies being more likely to facilitate long-range coordination of brain networks, whilst fast oscillations in the gamma-band are implicated in local activity and information processing (Buzsáki, 2006). We focussed on the role of the four lower frequency bands in anticipatory processes during the cue-target interval in the pro/antisaccade task.

Alpha waves were the first electrophysiological oscillations to be discovered during the invention of the EEG (H. Berger, 1929). Alpha waves consist of prominent oscillations around 8-12 Hz, especially over the visual cortex when the eyes are closed (Buzsáki, 2006). However, they are also

ubiquitous in the brain, and are thought to indicate "idling" or inhibition/suppression of brain regions (Händel et al., 2011).

In studies investigating cognitive control, alpha-band oscillations are associated with top-down inhibition (Klimesch et al., 2007) and preparatory processing prior to responding to a stimulus, particularly in fronto- and occipitoparietal regions (Capotosto et al., 2009; Cooke et al., 2014; Fu et al., 2001; Hamm et al., 2012; Hanslmayr et al., 2007; Simonet et al., 2019). Findings from non-human primates have shown increased alpha-band power to be observed with reduced neuronal spiking and firing rates (Haegens et al., 2011). Electrophysiological studies also using EEG have found decreased posterior alpha-band power during periods of focus and tasks engaging attentional control (Chen et al., 2008; van Driel et al., 2012), including prior to antisaccadic responses (van Noordt et al., 2017). EEG findings also support a long-range top-down frontoparietal network that is mediated by preparatory alpha-band (Phillips et al., 2014). Following an intensive computer-training paradigm, Barnes et al. (2016) found significant improvements in the working memory of children and detected increased alpha and gamma band coupling (16 and 90 Hz, respectively) using MEG between the superior frontal and parietal cortices with the inferior temporal cortex, respectively. This endorses the idea that top-down alpha modulates gamma bottom-up cognitive processing.

Furthermore, MEG findings have shown increased preparatory alpha-band activity in the frontal eye field (FEF) is associated with

successful antisaccade performance, suggesting a role in inhibiting reflexive prosaccades (Hwang et al., 2014, 2016). These findings are consistent with MEG work by Jensen and colleagues, who have an extensive body of work regarding alpha-band oscillations in mediating important visuospatial attentional processes. Research from this group has focussed particularly on posterior and occipitoparietal cortical alpha, which they propose is involved in processing the level of salience/relevance of visual information, which modulates phase-locked gamma-band activity (O. Jensen et al., 2012). In turn, Marshall et al. (2015) provide evidence supporting a role for bilateral FEF in the top-down control of anticipatory occipitoparietal cortical alpha (as well as gamma-band activity); thus, directly linking to Hwang's findings for top-down FEF alpha in the pro/antisaccade task discussed previously. Additionally, Jensen's group propose that preparatory alpha-band oscillations during visuospatial attentional processes 'gate by inhibition' to modulate processing in a given region (O. Jensen & Mazaheri, 2010; van Dijk et al., 2008). Zhigalov & Jensen (2020) confirmed this idea recently in the vicinity of the parieto-occipital sulcus, but not for visual gain control in the primary visual cortex.

In addition, a MEG study Popov et al. (2019) revealed that posterior alpha is generated in a retinotopic fashion for mediating visuospatial attentional processes. The general findings from Jensen's team support the role of the PEF in the oculomotor control of saccadic activity that was outlined in Chapter 2, Section 2.2.4, as alpha-band power could mediate the proposed visuospatial and vector transformation processes, whereby this is

influenced by top-down control from the FEF. Interestingly, Jensen et al. (2021) has proposed that the phase-coding of alpha oscillation may be the key to how current and upcoming visual stimuli are processed (e.g., including for reading mechanisms) and that saccades are mediated by alpha phase-coding. This theory requires validation from future research, but does provide a mechanism to tie together why problems in reading coincide directly with attentional issues, thus implicating disturbances in parietal alpha modulations in dyslexia and ADHD.

Beta-band oscillations occur in the 13 – 30 Hz range (Buzsáki, 2006). Although the entire range of functions that beta oscillations serve are not fully understood, they are believed to play an important role in sensorimotor responses and voluntary movements (Neuper & Pfurtscheller, 2001). This includes motor response timing and adapting bottom-up and top-down cognitive control mechanisms (Arnal, 2012). Additionally, beta is hypothesised by Engel & Fries (2010) to "maintain the status quo" of the current cognitive or sensorimotor processing state, rather than in changing situations. In the context of saccadic control, there is support for preparatory increases in beta-band oscillations in the right dorsolateral prefrontal cortex (R DLPFC) in the top-down processing of antisaccade responses (Hwang et al., 2014, 2016). Hwang et al. (2014) also proposes that beta could mediate saccadic control mechanisms via the thalamocortical section of the visual attention oculomotor network (Hikosaka et al., 2000).

Exposure to a stimulus initially causes an event-related desynchronisation (ERD), whereby there is a reduction in beta amplitude, followed by elevated beta band power following a motor response. This beta rebound or event-related synchronisation (ERS) (Neuper & Pfurtscheller, 2001) is a well-established phenomenon, also known as post-movement beta rebound (PMBR) (Jurkiewicz et al., 2006), which usually has an above-baseline rebound. Beta rebound has been found to be affected by task complexity and the type of learning mechanisms employed (Haar & Faisal, 2020). Also, even in the absence of a motor response, exposure to a stimulus still results in an ERS that returns to baseline levels, rather than exceeding baseline as with PMBR (Briley et al., 2021; Liddle et al., 2016).

However, these findings are observed in trial-averaged data. Work by Stephanie Jones and colleagues (Jones, 2016; Sherman et al., 2016; Shin et al., 2017) observed that when analysing individual trials, the beta-band reveals bursting behaviour, which has been termed "beta bursts". This finding is also corroborated by other research groups (Briley et al., 2021; Feingold et al., 2015; Little et al., 2019; Lundqvist et al., 2016).

Moreover, Shin et al. (2017) collected MEG data during a tactile detection task, whereby they reported that increased temporal proximity of beta bursts to stimulus presentation led to decreased stimulus detection responses. This directly implicates the timing of beta burst occurrence in perception and suggests that beta bursts could mediate inhibitory mechanisms by switching off incoming sensory information processing.

Spitzer & Haegens (2017) further propose beta bursts to activate and re-activate specific neural assemblies in the context of relevant information processing, rather than just "maintaining the status quo" (Engel & Fries, 2010). Therefore, analysing the bursting properties of beta could reveal different information about its functionality compared to just using trial averaged data.

Theta oscillations in the 4 – 8 Hz range (Buzsáki, 2006) are supported to be involved in cognitive control mechanisms within the frontal cortex (Cavanagh et al., 2012; Cavanagh & Frank, 2014; Cooper et al., 2017; Sauseng et al., 2007). Theta is also thought to play a key role in mediating hippocampal memory systems, such as navigation and integrating spatial memory information with episodic and semantic memories (i.e., for building internal maps) (Buzsáki, 2002, 2005). Additionally, theta-band activity has been implicated in saccadic eye movement processing, including mediating phase reset to improve reaction timing mechanisms (Diederich et al., 2014). This includes evidence for successful antisaccade trials presenting greater preparatory theta power in the prefrontal cortex and midbrain regions (Cornwell et al., 2012) as well as in the medial frontal cortex (van Noordt et al., 2017). Additionally, theta oscillations in frontoparietal regions are thought to facilitate sensorimotor processing by resolving top-down and bottom-up processing conflicts (Fiebelkorn & Kastner, 2019).

Delta oscillations occur in the 0.5 – 4 Hz range (Buzsáki, 2006) and have traditionally been the focus of sleep research (Amzica & Steriade,

1998; Borbély et al., 1984). However, there has been growing interest in task-based studies regarding the wider implications of the delta-band in cognitive functioning. This includes response timing (Gillary & Niebur, 2016; Stefanics et al., 2010), decision making (Nácher et al., 2013), the degree of abstraction in task rules (Riddle et al., 2020), gating bottom-up sensory input (Harmony, 2013), and internal time keeping for temporal response dynamics (Arnal & Kleinschmidt, 2017). Coupling between delta and beta oscillations is also associated with accuracy (Arnal et al., 2015) and attentional processing (Morillas-Romero et al., 2015).

Additionally, lower frequency-bands of theta and delta oscillations have been implicated in various cardiac effects. For example, reduced delta-band activity is associated with cardiac deceleration (Patron et al., 2019), and increased heart rate variability (HRV) is associated with increased frontal delta-band power (Machetanz et al., 2021). Frontal increases in theta-band power are also observed with increased HRV (Kubota et al., 2001; Machetanz et al., 2021). This provides support for the involvement of lower frequency band oscillations in mediating arousal mechanisms. Further discussion regarding arousal and the LC-NE model mediating arousal mechanisms in the ANS and CNS can be found in Chapter 2, Section 2.1.2.

7.1.2. MEG background

Brain oscillations can be detected non-invasively using MEG or EEG, which both have high temporal resolution. However, more accurate spatial location of the oscillatory signal can be achieved using MEG. This is aided by MEG having the advantage of less smearing in spatial topography of the signal, due to avoiding scalp and biological tissue conductivity interference experienced with EEG, since the conductivity equivalent for magnetic fields (permittivity) remains the same from scalp to sensor (Baillet, 2017).

Understanding the basis of MEG originates from knowledge regarding neuronal communication in the brain via electrochemical signals. When neuronal receptors are activated, there is a series of intracellular processes resulting in the influx and efflux of charged ions. This alters the membrane potential and results in action potential events that propagate intracellular currents to flow along the axons of neurons. The summation of electrical currents from synchronous neuronal signalling induces magnetic fields that disperse throughout the brain to the scalp surface. Pyramidal cells located in the outer layers of the cerebral cortex contain particularly long axonal and dendritic structures, which aids the propagation of electrical currents and magnetic fields resulting from the depolarisation of these neurons that can be detected externally (Baillet, 2017; Baillet et al., 2001; Okada et al., 1997).

Complex cortical folding in the brain structure gives rise to sulci and gyri, thus electrical currents flow either parallel to or perpendicular to the

skull. The flow of tangential dipole currents (parallel to skull) induce magnetic fields that can be detected externally from the head in comparison to radial dipole currents (perpendicular to skull) (Hämäläinen et al., 1993; Vrba & Robinson, 2001). Although, the head is not a perfect sphere, which means there is some contribution of radial signals to the external magnetic fields (Baillet et al., 2001).

However, magnetic fields produced from the brain are in the range of several picotesla (equivalent to $1x10^{-12}$ T), which is extremely small compared to the Earth's magnetic field of 0.5 millitesla (0.0005 T) and urban magnetic noise that is 1 million – 1 billion times greater than brain magnetic fields (Vrba & Robinson, 2001). Therefore, technology that enables highly sensitive detection of magnetic fields is required to record magnetic field changes from the brain.

The first magnetoencephalography (MEG) recording from the brain was achieved by Cohen (1968), whereby magnetic fields from neuronal activity induce electrical currents in pick-up coils, which is proportional to the amplitude of the original magnetic induction. These coils are coupled to superconducting quantum interference device (SQUID) magnetometers (Cohen, 1972) that enable the sensitive detection of the small magnitude electrical currents induced in the pick-up coils. The superconductors in the SQUID magnetometers require the operation of the machinery at extremely low temperatures, typically attained by using a cryogen of liquid helium in a thermally insulated dewar container (Baillet, 2017). Current MEG

apparatus configurations involve hundreds of pick-up coils (channels) arranged in a helmet system attached to the dewar, all operated within a magnetically shielded room (Baillet, 2017; Hämäläinen et al., 1993; Vrba & Robinson, 2001).

7.1.3. Aims

In this study we were specifically interested in the neural processes involved in preparing to respond to a target requiring a pro- or antisaccade, and how they might be modulated by gaze-control training. In MEG studies of a similar cued pro/antisaccade task, Hwang et al. (2014, 2016) found that during the anticipatory period between cue and target, antisaccade preparation was associated with increased alpha power in the FEF and beta power in the right dorsolateral prefrontal cortex (R DLPFC), compared with prosaccade trials. This suggests that top-down anticipatory inhibition is associated with increased alpha and beta power in these regions.

However, as discussed above, theta and delta oscillations are also implicated in inhibitory and preparatory processes, so power time-courses in these bands were also investigated. Moreover, as reviewed in Chapter 2, visual attention also involves top-down modulation of activity in primary visual cortex (V1), parietal eye fields (PEF) and the salience network in addition to the FEF and DLPFC. We therefore investigated anticipatory oscillatory processes in the following cortical ROIs from the visual attention network identified in Chapter 2: V1; bilateral PEF; bilateral FEF; bilateral

anterior insula; bilateral DLPFC. To do this, I first reviewed the brain imaging literature to compute average brain coordinates of each of these regions. I then used a beamformer method (Brookes et al., 2008) to extract the time courses of signals from the brain from each of these locations (see details regarding this process in Section 7.2.3).

We set out to delineate power-time courses of each frequency band in each ROI during the anticipatory period and to determine whether these were modulated by trial type (prosaccade trials vs antisaccade trials) and by training (Day 1 vs Day 2). We also investigated transient beta bursts in single trial data to delineate any effects of beta bursts on trial-by-trial performance, and to help characterise ERD and ERS effects.

We predicted that effects associated with anticipatory inhibition, (namely effects associated with antisaccade trials as compared with prosaccade trials) would be enhanced following training in inhibitory gaze-control. Given the findings of Hwang et al. (2014, 2016), we specifically predicted that preparatory alpha power in FEF and beta power in DLPFC would be greater for antisaccades than for prosaccades in frontal regions, and were likely to also be greater on Day 2 (following training) than on Day 1. This prediction was also supported by the finding by Hwang et al. (2016) of reduced anticipatory alpha in the FEF in adolescents compared to young adults, and that greater alpha power was associated with more accurate task performance. We also predicted that beta burst rate would be greater

for antisaccades than for prosaccades, and that this would tend to increase on Day 2.

7.1.4. Research questions

My research questions therefore were:

- Are antisaccades associated with greater anticipatory alpha in the FEFs and greater anticipatory beta in the R DLPFC, as found by Hwang et al.? If so, are these effects enhanced after RECOGNeyes training?
- What are the characteristic time courses of oscillatory amplitude over the anticipatory period between cue and target in each of the delta, theta, alpha and beta bands, and are they modulated by trial type and/or RECOGNeyes training?
- Since beta amplitude, averaged over trials, is likely to reflect the probability distribution of transient beta bursts, are beta burst probabilities modulated by time, trial type and/or RECOGNeyes training?

7.2. Methods

7.2.1. Source localisation and visual attention network regions of interest

MEG poses an inverse problem of how to determine the exact physiological sources of the observed signals. This is fundamentally an ill-posed problem, due to the infinite models that could fit the source data (Baillet, 2017; Ferree et al., 2000; Gonçalves et al., 2000). The neural activity and signal detected by each MEG sensor will change over the experiment time course, but assuming the head remains stationary, the physiological source weighting of the electrophysiological signal from each sensor will remain constant. Therefore, beamforming can be used as a forward solution source localisation technique that applies adaptive spatial filtering to estimate source power in a co-variance matrix of time course by frequency band (S. E. Robinson & Vrba, 1999; Van Veen et al., 1997). Beamforming hence offers a way to determine cortical electrophysiological activity from a range of networks and ROIs.

Beamforming requires the specification of spatial locations to extract electrophysiological time-frequency series information from. Locations can be defined in standardised coordinate systems including Talairach (Talairach & Tournoux, 1988) and Montreal Neurological Institute (MNI) space (D. L. Collins et al., 1998). These locations can be selected from peak activation coordinates in functional neuroimaging studies. Alternatively, in

more recent years, there is increased use of atlases containing pre-defined parcellation regions (Destrieux et al., 2010; Fischl, 2012; Fischl, Sereno, & Dale, 1999; Fischl, Sereno, Tootell, et al., 1999; Gong et al., 2009; Tzourio-Mazoyer et al., 2002); however, these parcellated cortical areas cannot be customised.

Since we are interested in studying the neural activity in brain regions implicated in the cognitive control of gaze, I selected cortical regions from the visual attention network (outlined in Chapter 2, Section 2.2 and Figure 2) to use as regions of interest (ROIs). The final ROIs included were: frontal eye field (FEF), parietal eye field (PEF), dorsolateral prefrontal cortex (DLPFC), primary visual cortex (V1), and anterior insula (Ant Ins). The reasons for selecting these regions were two-fold. Firstly, cortical regions rather than subcortical regions of the network are recruited in top-down control processes of anticipation and preparation during the pro/antisaccade task (refer to Chapter 2, Section 2.2 for discussion regarding the functionality of each region). Secondly, subcortical areas in the midbrain and brainstem are deeper in the brain, meaning that these regions have low signal-to-noise ratio (SNR) in MEG recordings that yield poorer data quality (Hämäläinen et al., 2010). Hwang et al. (2014) found poor SNR in the supplementary eye field (SEF) and anterior cingulate cortex (ACC) regions compared to other lateral ROIs, thus these regions were not included in later studies (Hwang et al., 2016). Therefore, we decided not to include the SEF and anterior cingulate as ROIs in the current MEG analysis.

To obtain centroid coordinates to use in source localisation analysis, I conducted an independent literature search to collate peak activation coordinates reported in functional brain imaging literature on gaze control and visual attention; this is reported in Appendix D. The final coordinates are listed in Table 6 and illustrated in Figure 33.

7.2.2. MEG data pre-processing

Unix computer system programs, as well as customised MATLAB and Bash scripts were used to pre-process MEG data. Using trial block markers, the raw MEG files for each subject on each acquisition day were divided up into three separate dataset files that contained prosaccade trials, antisaccade trials, and rest periods, respectively. Trial type datasets were further epoched into individual trials of three seconds in length. Correct/incorrect response markers were inserted to ensure only correct trials were included in MEG data analysis. For each individual dataset, trials were removed if the recorded head motion deviated more than 2.5 mm from the mean calculated head motion.

We used DataEditor software (Release: 5.2.1-linux-20060623, VSM MedTech Systems Inc., Coquitlam, BC, Canada) to filter the MEG datasets and visually inspect the data for artefacts. DC offset was applied to remove possible noise from electric mains signals. A 1 Hz high-pass filter and 150 Hz low-pass filter were used to remove noise from extremely low and high frequencies in the signal, respectively. During acquisition, gradiometers are

used as a reference to record the signal from magnetic fields passing through the scanner only, whereas the direct sensors record all magnetic fields detected within the wider scanner environment. Therefore, third-order synthetic gradiometers were applied to subtract from the direct sensors to limit environmental magnetic noise and localise neural magnetic activity detected by the scanner sensors. For all MEG datasets, trained members of our team visually inspected each individual trial to manually remove those containing artefacts from muscle movements or large deviations in the signal from blinking.

7.2.3. Co-registration and source localisation procedure

To assess neural activity from specific ROIs in MEG data analysis, the co-registration procedure first involves aligning anatomical information from each participants' MRI with their digitised 3D head shape and fiducial coil positions (details of MRI acquisition and Polhemus digitisation procedure described in Chapter 3). MRI Viewer from the CTF software package (Release: 5.2.1-linux-20060809, VSM MedTech Systems Inc., Coquitlam, BC, Canada) was used to concatenate the series of DICOM MPRAGE files (one image per slice) into a single reconstructed 256 x 256 x 256 MRI file. Next, a head shape file was generated that contained an outline of the head and face shape without the neck region, ensuring the nose was included as an essential reference point on the digitised head shape. This MRI head shape file was co-registered with the digitised Polhemus head shape file by using in-house MATLAB scripts and MRI

Viewer to remove any spurious points until reaching a satisfactory fit. Then the recorded positions of the nasion, left ear and right ear fiducials were uploaded onto the finalised co-registered head shape.

We used custom MATLAB scripts with functions from the FieldTrip software toolbox (Oostenveld et al., 2011) and applied a similar data processing pipeline to that developed by O'Neill et al. (2017) for conducting the source localisation procedure. Anatomical MRIs were segmented by removing the skull and scalp so that only the brain remained in the image. Each subjects' anatomy from their individual MRI was warped into standard MNI space and divided into a volumetric grid of 4 mm voxels prior to performing registration between the template and subject space. During this normalisation procedure, a transformation matrix was computed to select the closest voxels in the MNI grid that match the average ROI coordinate locations determined in Figure 33 and Table 6 (see Appendix D) across all subject datasets.

A scalar linearly constrained minimum variance (LCMV) beamforming method (S. E. Robinson & Vrba, 1999; Van Veen et al., 1997) was applied to reconstruct source data using adaptive spatial filtering. The dipole approximation for the forward model was based on the single-shell method by Nolte (2003), to represent a shape more akin to a brain than a sphere. At each location, three dipoles in the x, y and z axes are modelled, whereby an eigenvalue decomposition is used to concatenate the three axes into one to optimise the SNR (Sekihara et al., 2004). The Tikhonov

regularisation method was employed, using a regularisation parameter of 1 % of the difference between the maximum and minimum eigenvalues of the covariance. This heavy regularisation parameter ensures the time course is representative of the area centred on the ROI coordinate.

Beamformer weights that represented the electrophysiological signal between 1 – 150 Hz at each of the pre-defined centroid ROI coordinates were generated as a covariance matrix across the whole MEG time series for each dataset (Brookes et al., 2008). This resulted in calculating 36 single time courses of electrophysiological data for each subject, corresponding to the 9 different ROIs, the 2 pro/antisaccade trial types and the 2 experiment acquisition days. The single virtual electrode time series data is therefore used to model the electrophysiological data recorded if there was an 'electrode' placed into each ROI in the brain.

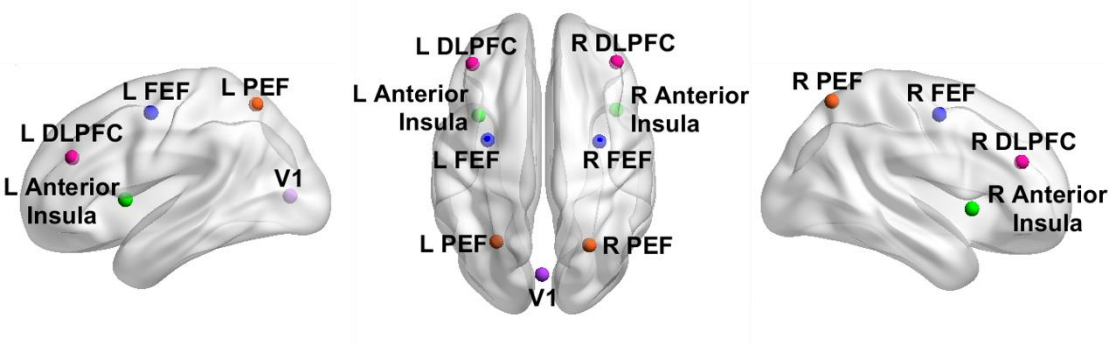

Figure 33: Visual attention network loci used as seed ROI centroids for MEG source localisation analysis.

From left to right, loci are presented on the left sagittal, axial, and right sagittal brain views respectively. These loci are specialised in MNI space and visualised on an ICBM (International Consortium for Brain Mapping) 152 template brain (Mazziotta et al., 2001) using BrainNet Viewer (http://www.nitrc.org/projects/bnv/) (Xia et al., 2013).

Table 6: MNI coordinates for ROI seed centroid locations.

These are the median MNI coordinates derived from the coordinate tables generated from the literature search in Appendix D.

ROIs	MNI co-ordinates		
	x	*y*	*z*
R DLPFC	40.5	38.5	25
L DLPFC	-39.5	37.5	26.5
R FEF	31.15	-5.5	50.45
L FEF	-31	-4.7	50.5
R Anterior Insula	40.5	12	0
L Anterior Insula	-36	9	4
R PEF	25.5	-63	57.5
L PEF	-26	-61	55
V1	-0.82	-79.25	5.93

7.2.4. Derivation of variables for statistical analysis

Using MATLAB R2021a (MathWorks Inc.), functions composed by Briley et al. (2020) were applied to extract time-frequency amplitude envelope spectrograms between the frequencies of 0.1 – 40 Hz in 0.1 Hz increments using Continuous Wavelet Transform, and to identify beta-frequency burst events from the single-channel electrophysiological data. From the time-frequency spectrogram (TFS), I averaged amplitude values within the following discrete, non-overlapping frequency bands (discussed in Section 7.1.1): delta (0.5 – 3 Hz), theta (4 – 8 Hz), alpha (10 – 12 Hz) and beta (13 – 30 Hz). Note: MEG data was high-pass filtered from 1 Hz, but

using 0.5 Hz for the delta band is within the one octave shoulder allowance in the filter calculation. Anticipatory trial data was extracted from the cue to the target onset and response period data from the target onset onwards was not included. This is because for the purposes of this thesis, I have elected to confine MEG analysis to the anticipatory period, as this period allows the examination of cognitive control processes uncontaminated by any lateralised effects occurring due to the hemifield in which the target stimulus was presented.

Only correct trials with responses within 500 msecs were included in the analyses. For beta burst analyses, a 100 msecs sliding window with a slide interval of 3.5 msecs was used to compute beta burst probability across trials over the anticipatory period, using Briley's *slideWins* function. This yields a continuous estimate of beta burst probability over the 800 msecs anticipatory period. The first 200 sliding burst rate data points were used so each 100 msecs bin consisted of the same number of 25 data points in each. Further custom-made MATLAB scripts were used for deriving trial and subject averaged data.

TFS oscillatory amplitude data was truncated to remove the highest and lowest 5 % of data points to mitigate the effect of any extreme or spurious data samples. For each ROI and frequency band, oscillatory amplitude was normalised within subjects by *z*-scoring across acquisition day datasets and trial types. Time series data were then averaged over 100

msecs bins using the same approach used for pupillometry and cardiac data analysis, as described in Chapter 5, Section 5.2.4.

7.3. Results

7.3.1. MEG analysis considerations

There was a total of N=23 day-paired subjects for MEG data analysis, and day-paired subjects totalled N=16 for sliding beta burst rate data (refer to Chapter 4, Figure 9). Details regarding missing data and analysis considerations are included in Chapter 3, Section 3.7.

Due to the large number of measures included in ANOVA tests, there was good power in the following analyses to find small effect sizes. For delta-band and theta-band analyses, there was a 96 % chance and 94 % chance of finding a small effect size for binned data and bin difference ANOVAs, respectively. For alpha- and beta-bands, there was a high chance of ~99% in bin and bin difference ANOVAs of finding a small effect size. In beta burst analysis, there was a 95 % chance of finding a small effect size. This incurs a very high chance of finding an effect of any size, and it is highly unlikely that a small effect size was missed in factors that did not reach a significance of $p < .05$. However, as for many of the investigations I did not have a strong *a priori* hypothesis, thus p-values should be taken as indicative evidence of an effect rather than as a strong rejection of the null.

7.3.2. General data trends

As an initial scoping analysis of the time courses of oscillatory amplitudes across the anticipatory period, I conducted a five-way repeated-measures ANOVA (9 x 4 x 2 x 2 x 8) with five within-subjects factors: ROI (9 levels: V1, L PEF, R PEF, L Ant Ins, R Ant Ins, L FEF, R FEF, L DLPFC and R DLPFC); Frequency Band (4 levels: delta, theta, alpha and beta bands); Day (2 levels: Day 1 and Day 2); Trial Type (2 levels: prosaccade and antisaccade trials) and Time Bin (8 levels: mean *z*-scored oscillatory amplitude values in each of the eight 100 msecs time bins).

Statistically significant interactions included an interaction between Frequency Band by Bin, $F(4.219, 92.828) = 34.029$, $p < .001$, indicating that time courses were significantly different between bands. Time courses for each band, averaged across ROIs, trial types and days, are plotted in Figure 34. This shows a characteristic time course for each frequency band:

- Delta amplitude shows a "hockey stick" time course, starting high and tending to fall throughout the majority of the anticipatory period, ending with a small upwards deflection.
- Theta shows a sinusoidal time course, reaching a maximum early in the period, and a minimum before the end of the period.
- Alpha shows a monotonic rise throughout the anticipatory period.

- Beta shows a fall in amplitude followed by a rise. This is consistent with the well-known pattern of event-related beta desynchronisation (ERD) following a behaviourally salient stimulus, followed by a "rebound" event-related synchronisation (ERS) to above baseline levels following a movement (Neuper & Pfurtscheller, 2001), or to at least baseline levels if no motor response is made (Briley et al., 2021; Liddle et al., 2016).

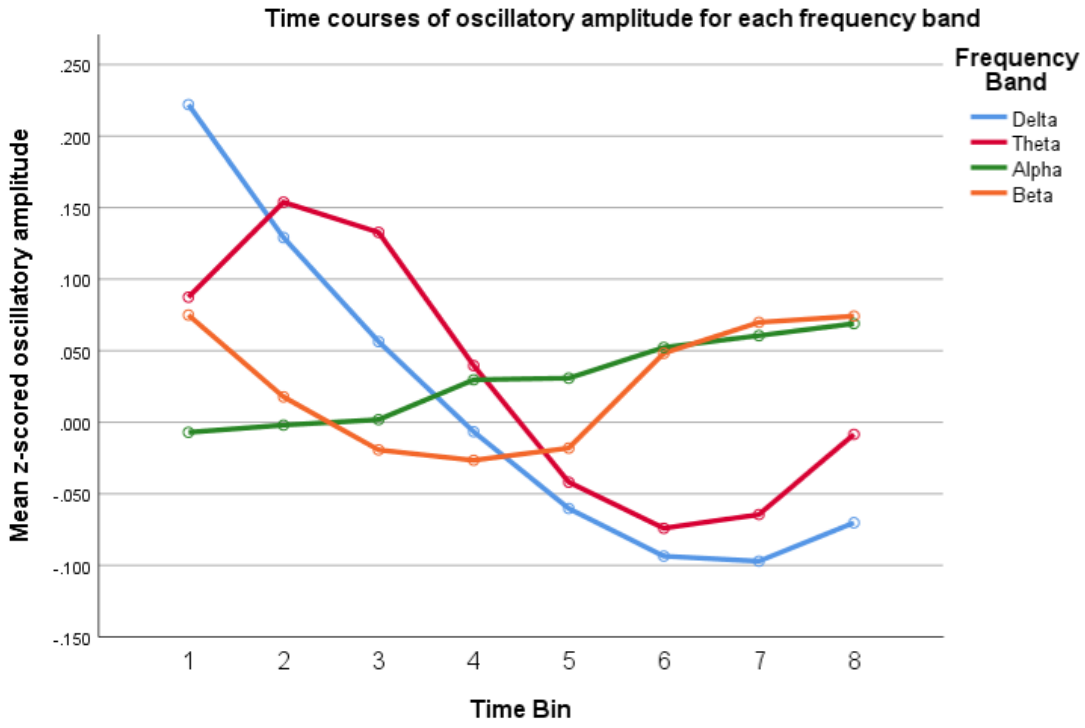

Figure 34: Time courses of oscillatory amplitudes for each frequency band, collapsed across days, trial types and ROIs.

There was a significant main effect of Trial Type, $F(1, 22) = 6.246$, $p = .020$, whereby oscillatory amplitudes in the anticipatory period were significantly larger in prosaccade trials than in antisaccade trials. In addition, there was a trend for a main effect of Day, $F(1, 22) = 4.273$, $p = .051$, which would indicate greater overall oscillatory amplitude on Day 2 after RECOGNeyes training compared to Day 1.

To interpret these effects further, I analysed each frequency band separately.

7.3.3. Delta-band

To investigate changes in delta-band amplitude across the anticipatory period, I first checked for any hemispheric effects across the eight ROIs for which we had data from both hemispheres. I achieved this by conducting a four-way (2 x 4 x 2 x 8) repeated-measures ANOVA with Hemisphere (2 levels: left and right), ROI homotopic pair (4 levels: PEF, Ant Ins, FEF, DLPFC), Day (2 levels), Trial type (2 levels) and Bins (8 levels) as factors. As there were no significant main effects of hemisphere, nor interactions, I averaged values across hemispheres for further analysis.

I conducted a four-way repeated-measures ANOVA (5 x 2 x 2 x 8) with four within-subjects factors: ROI (5 levels: V1, PEF, Ant Ins, FEF, and DLPFC); Day (2 levels: Day 1 and Day 2); Trial Type (2 levels: prosaccade and antisaccade trials) and Time Bin (8 levels: mean *z*-scored TFS values in each of the eight 100 msecs time bins).

There was a significant main effect of Trial Type, $F(1, 22) = 7.183$, $p = .014$, whereby delta amplitude in antisaccade trials was significantly less than in prosaccade trials. This is illustrated in Figure 35.

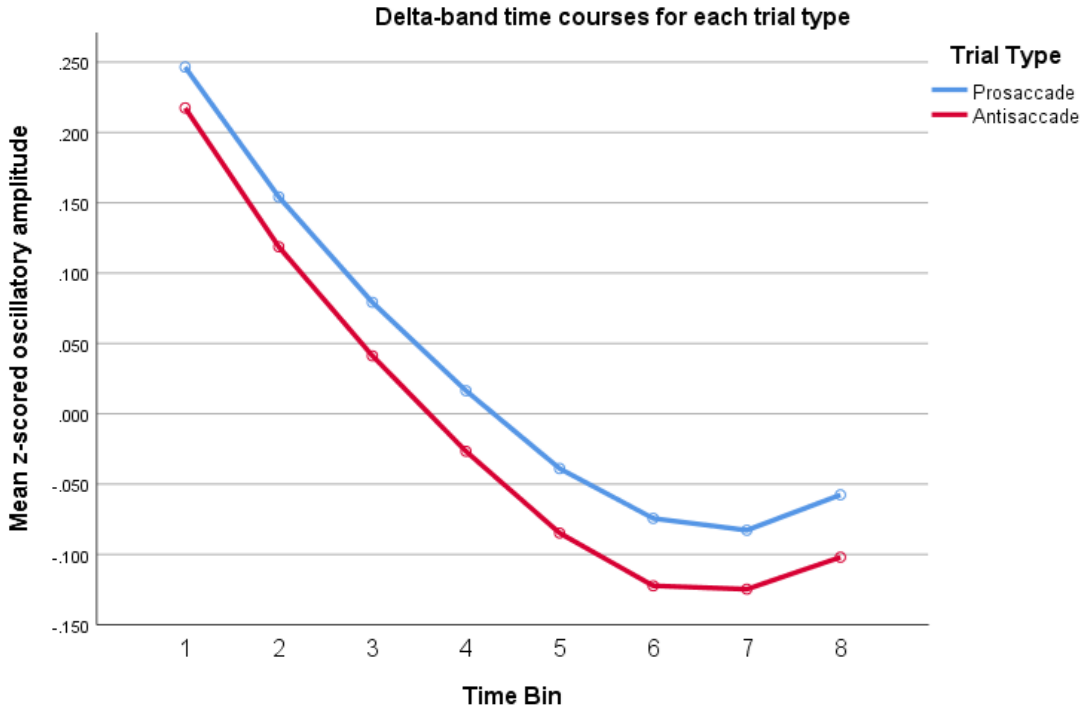

Figure 35: Delta amplitude across the trial time course for prosaccade and antisaccade trials.

Data is collapsed across day and ROIs. This presents a lower delta amplitude in antisaccade trials compared to prosaccade trials.

In addition, there was a significant main effect of Time Bin, $F(1.235, 27.164) = 84.846$, $p < .001$, as shown in the delta line plotted previously in Figure 34, whereby delta amplitude tends to start high and decrease over the course of the anticipatory period, the rate of decrease slowing towards the end of the period, and amplitude starting to rise at the end.

There was also a significant ROI by Time Bin interaction, $F(28, 616) = 15.136$, $p < .001$, as shown in Figure 36. This shows the "hockey stick" pattern for delta-band amplitude to start high (particularly in posterior ROIs of V1 and PEF), which decreases across bins until around bin 6, then most ROIs show a slight inflection of increased amplitude in the latter bins (particularly anterior ROIs of DLPFC, FEF and Ant Ins). This general downward trend and inflection in the latter bins across the anticipatory period is further supported by a significant overall quadratic trend, $F(1, 22) = 80.910$, $p < .001$ when amplitudes are averaged across ROIs.

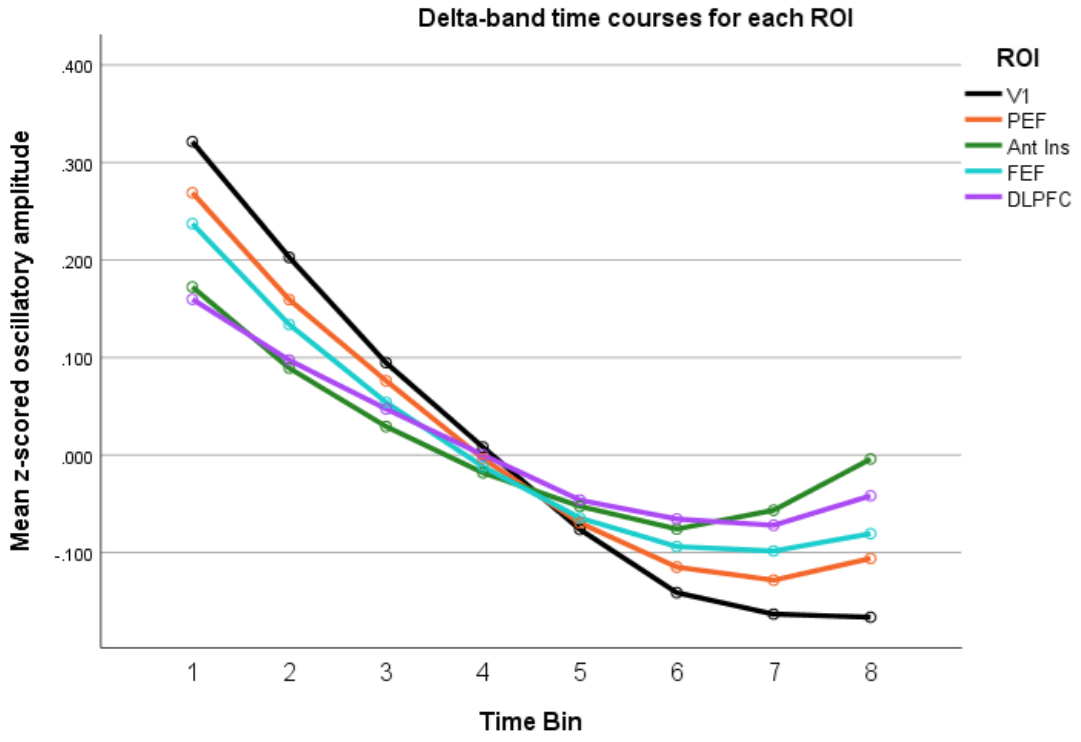

Figure 36: Delta band time courses plotted by ROI across the anticipatory period.

Time courses are collapsed over days and trial types. Note that the more anterior ROIs tend to start lower and show a more upward deflection towards the end of the anticipatory period.

There was also a significant ROI x Day x Time Bin interaction, $F(28, 616) = 2.306$, $p < .001$. This was investigated by conducting separate three-way repeated-measures ANOVAs for each ROI. These ANOVAs had three within-subjects factors: Day (two levels: Day 1 and Day 2); Trial Type (2 levels: prosaccade and antisaccade trials); and Time Bin (8 levels). V1 was the only ROI to have a Day by Time Bin interaction, $F(1.500, 32.997) = 6.196$, $p = .009$. This interaction is plotted in Figure 37 and shows that delta power was higher at the beginning of the trial on Day 2 than on Day 1 and fell more steeply. Polynomial contrasts for the interaction indicated a significant linear trend, $F(1, 22) = 7.760$, $p = .011$, confirming a significant linear decrease in the Day difference over the trial time course. There was no additional significant main effect of Day ($p > .05$).

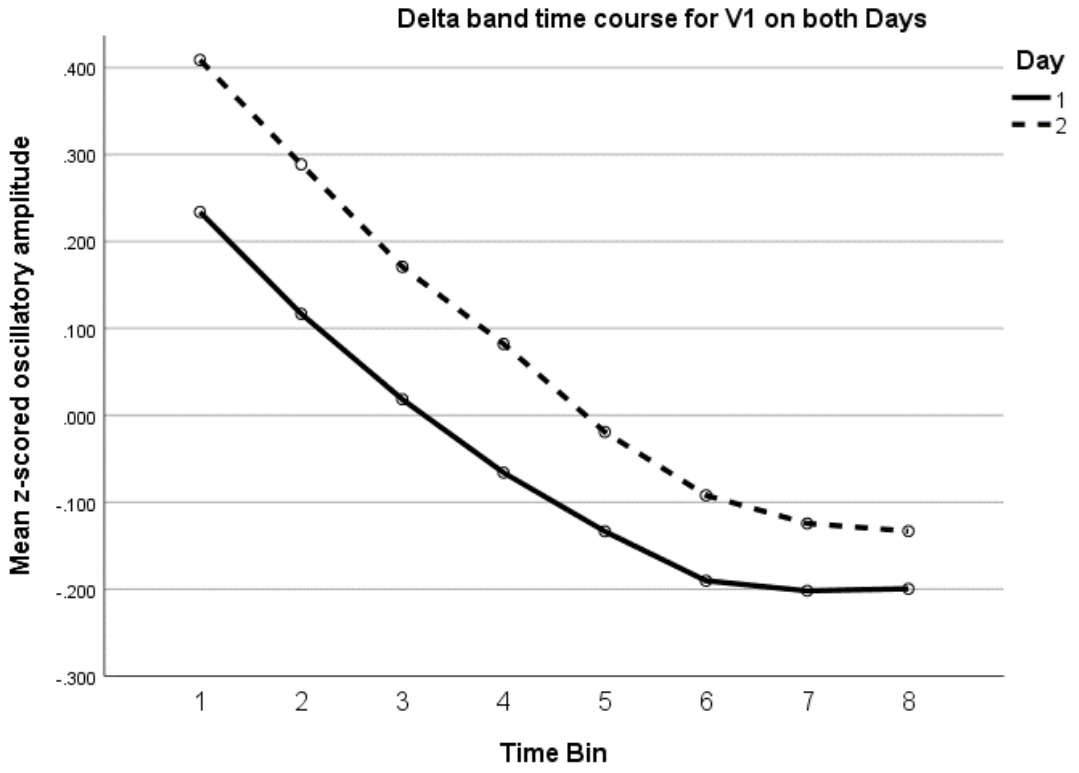

Figure 37: Delta amplitude time course in V1 on Day 1 compared with Day 2.

This depicts the higher V1 delta amplitude on Day 2, whereby there is also a sharper reduction across the trial time course compared to on Day 1.

To help visualise the pattern of delta modulation over time across ROIs and Days, I plotted the gradients (differences between successive binned amplitudes) in Figure 38. Note the negative gradient for all ROIs until late in the trial. The gradients become less negative over the time course of the trial, becoming positive for all ROIs by the end of the trial on Day 1, and for all except V1 on Day 2.

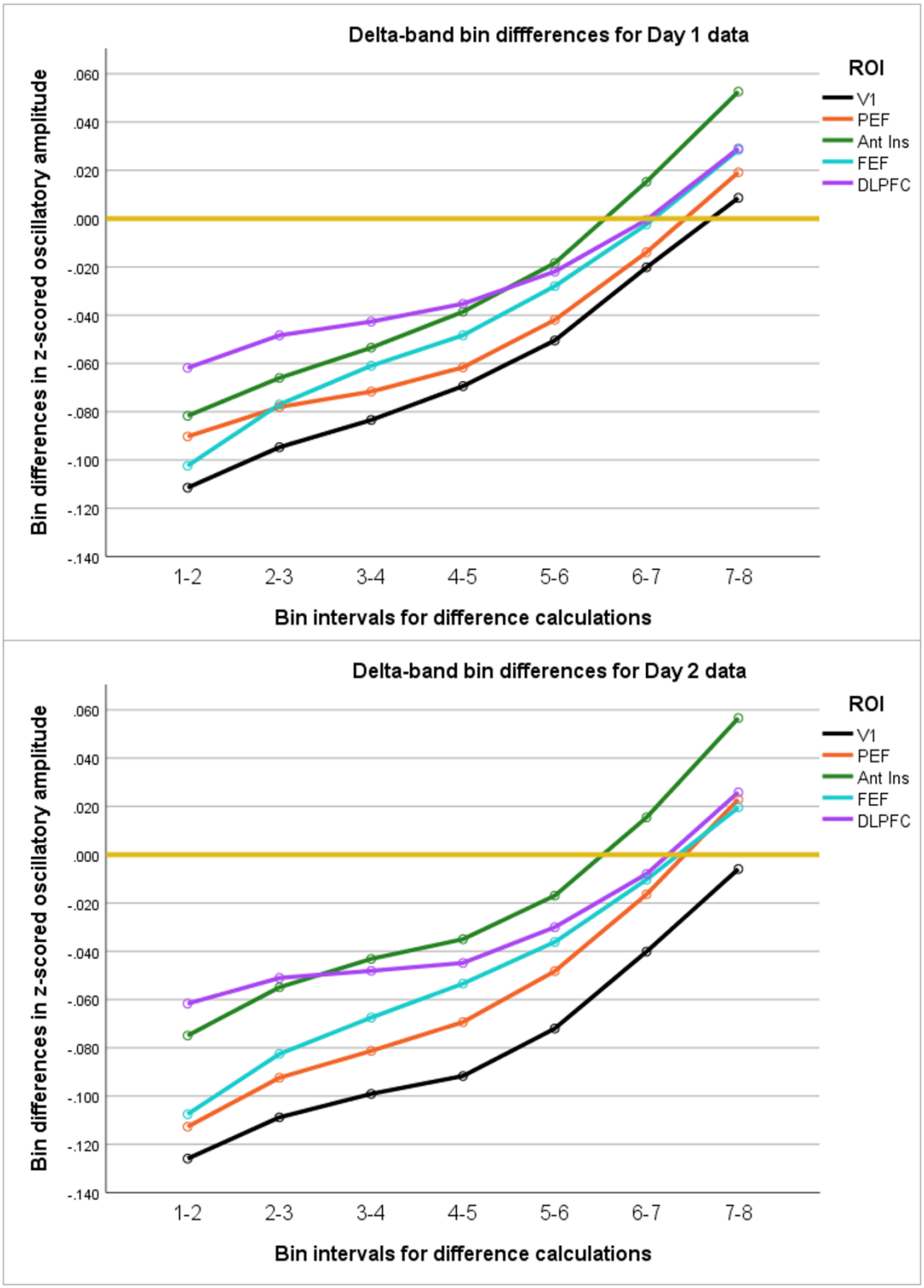

Figure 38: Delta-band amplitude bin differences showing the gradient change in the trial time course for each ROI.

Average data is collapsed over trial types, plotted separately for each day, whereby the top panel is day 1 data, and the bottom panel is day 2 data. The same y-axis scale is used to plot data in both panels to compare day differences.

To summarise these delta findings:

- Delta amplitude had a "hockey stick" time course across the anticipatory period in all ROIs. The highest amplitude was at the start of the trial (i.e., cue onset) particularly in posterior ROIs, where amplitude declined across the trial and was followed by a flattening or upward deflection at the end of the period. This upward deflection was more marked in more anterior ROIs, indicating an anteriorisation of delta towards the end of the anticipatory period.
- Delta amplitude was lower overall for antisaccade trials than for prosaccade trials.
- In V1, delta change over time was more marked on Day 2 than on Day 1, starting higher and reducing more steeply.

7.3.4. Theta-band

To study changes in theta-band oscillatory amplitude across the anticipatory period, as with the delta band, I checked for hemisphere effects in the four homotopic pairs of ROIs. While there were significant hemisphere by ROI differences, the overall sinusoidal shape of the time course was similar across hemispheres, but was wider in amplitude range in the left hemisphere than in the right. As with delta, I therefore averaged amplitudes across hemispheres, and conducted the same four-way (5 x 2 x

2 x 8) repeated measures ANOVA as for delta, with four within-subjects factors: ROI (5 levels: V1, PEF, Ant Ins, FEF, and DLPFC); Day (2 levels: Day 1 and Day 2); Trial Type (2 levels: prosaccade and antisaccade trials) and Time Bin (8 levels).

There was a significant main effect of Time Bin, $F(1.907, 41.964) = 29.560$, $p < .001$. Polynomial contrasts indicated a significant cubic trend, $F(1, 22) = 64.795$, $p < .001$, capturing the two directional changes in the data, which is visible in the sinusoidal time course for theta band plotted above in Figure 34. In addition, there was a significant main effect of Day, $F(1, 22) = 7.121$, $p = .014$, whereby there was significantly more theta power on Day 2 than on Day 1.

However, there was also a significant ROI by Time Bin interaction, $F(28, 616) = 6.762$, $p < .001$. As can be seen in Figure 39, while the sinusoidal pattern is apparent for all ROIs (and was statistically significant in all ROIs), the amplitude of the sinusoid is larger for the posterior ROIs (V1 and PEF), and the maximum tends to occur slightly later for the more anterior ROIs (DLPFC, FEF and Ant Ins).

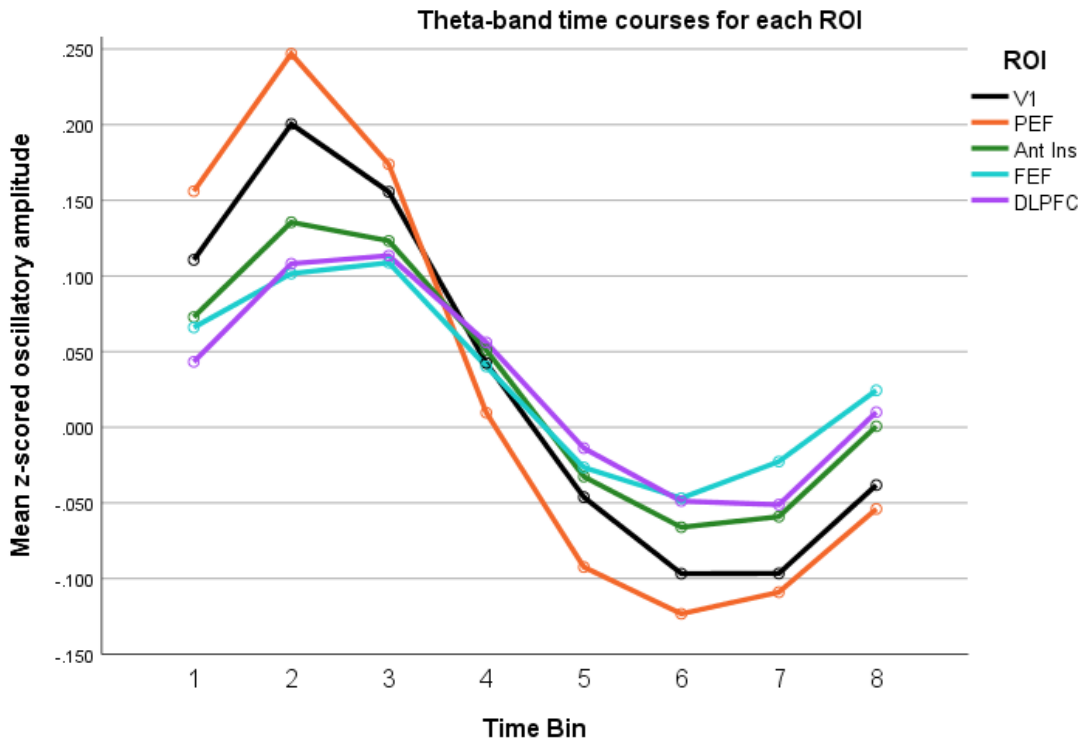

Figure 39: Theta amplitude time courses plotted by ROI across the anticipatory period.

Time courses are collapsed over days and trial types. Note that the more anterior ROIs have greater amplitude magnitudes across the anticipatory period. They have an earlier maxima peak than anterior ROIs, reflecting an anteriorisation effect across the time course.

This effect is illustrated further in Figure 40, which is a plot of the gradients computed as the differences between successive bins. The amplitude gradient is positive in all ROIs at the start of the anticipatory period but does reach zero. This indicates that at this point in the time course an amplitude maximum has been reached, which appears later for more anterior ROIs.

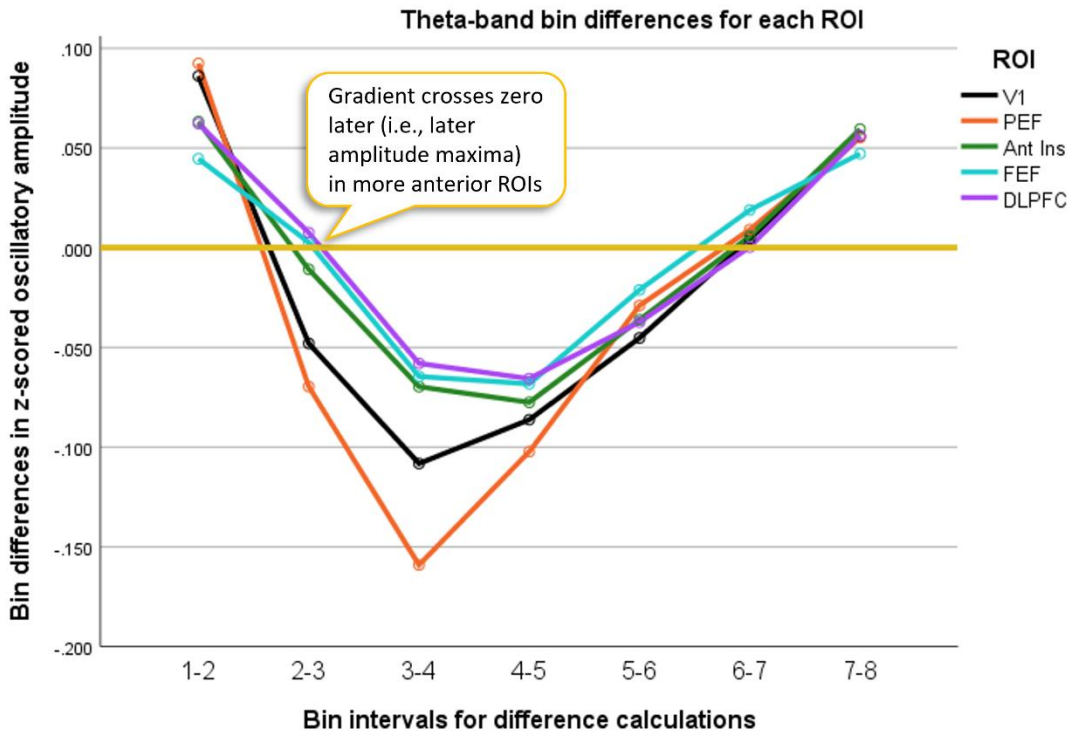

Figure 40: Theta-band oscillatory amplitude bin differences for each ROI, averaged across days and trial types.

Note the positive gradient in all ROIs at the beginning of the anticipatory period, which reaches zero (corresponding to maximum theta amplitude) later for more anterior ROIs.

To summarise these theta findings:

- Theta amplitude shows a characteristic sinusoidal time course during the anticipatory period, reaching a maximum near the beginning after cue onset, and a minimum towards the end close to target onset.
- The timing of the early maximum has an anteriorised effect, whereby the maxima occur later in more anterior ROIs.

- Theta amplitudes were overall significantly higher on Day 2 than on day 1.

7.3.5. Alpha-band

The time course of alpha, when averaged across all ROIs as plotted in Figure 34 previously, showed an overall upward trajectory in the anticipatory period. However, alpha amplitude time courses plotted for each ROI separately, as depicted in Figure 41, revealed much more heterogeneity between hemispheres of the homotopic ROI pairs than was apparent for either delta or theta. Notably, the pattern of a monotonic increase in alpha power over the course of the anticipatory period, as shown in Figure 34, was only apparent in the FEFs where they reach a higher amplitude by target onset compared to the other ROIs; although, this only starts from Bin 3 (300 msecs to 400 msecs post-cue) onwards.

Moreover, at least one homotopic pair (i.e., PEFs) showed a noticeable difference between left and right hemisphere time course patterns. For the alpha investigations, I therefore did not average across homotopic pairs of ROIs.

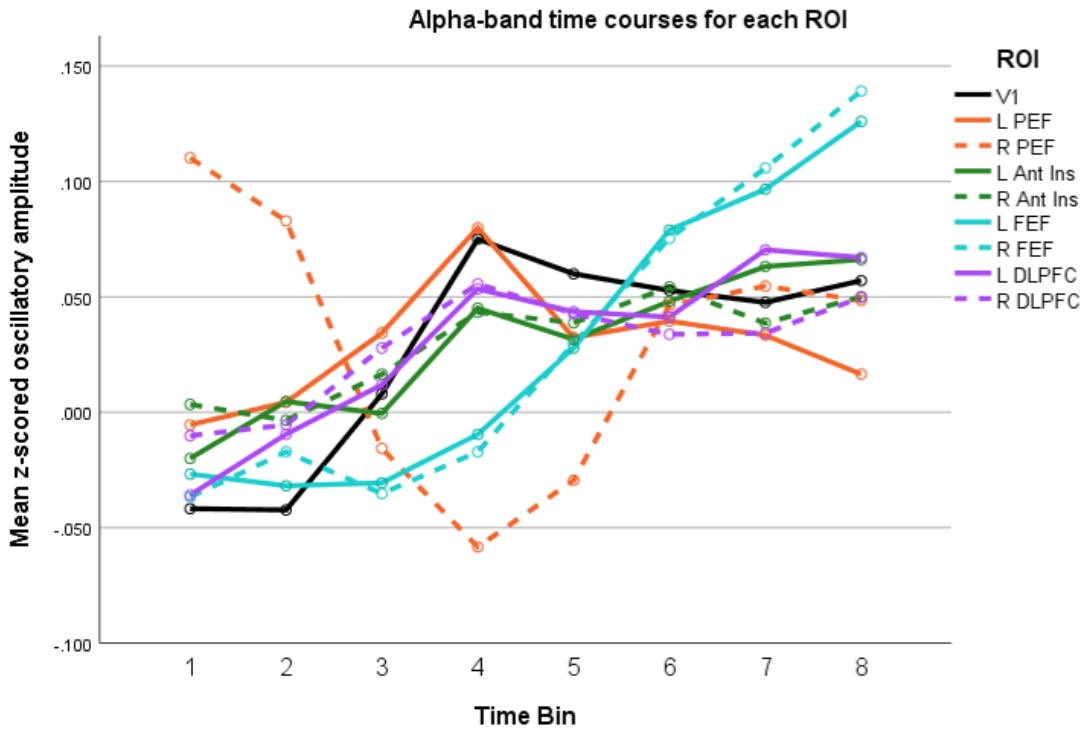

Figure 41: Alpha amplitude time courses by ROI, averaged across days and trial types.

Hwang et al. (2014, 2016) proposed a top-down inhibitory role for FEF alpha, as evidenced by a greater anticipatory alpha amplitude in the FEFs for antisaccades than for prosaccades. I therefore first investigated alpha amplitude time courses in the FEFs by conducting a four-way repeated measures ANOVA (2 x 2 x 2 x 8) where the within-subjects factors were Hemisphere (2 levels); Day (2 levels); Trial Type (2 levels) and Time Bin (8 levels). This gave a significant main effect of Time Bin, $F(2.384, 52.446) = 12.513$, $p < .001$. Polynomial contrasts confirmed a significant linear term, $F(1, 22) = 20.664$, $p < .001$), reflecting the trend for FEF alpha power to increase approximately linearly over the course of the anticipatory period.

However, there were no significant main effects or interactions of Trial Type, thus our data do not replicate Hwang's finding of increased anticipatory alpha for antisaccade trials. Although, our results do broadly replicate the finding of increasing alpha power over the anticipatory period. There were no significant effects of Day, nor of Hemisphere, and no significant interactions. Time courses for each trial type are shown in Figure 42.

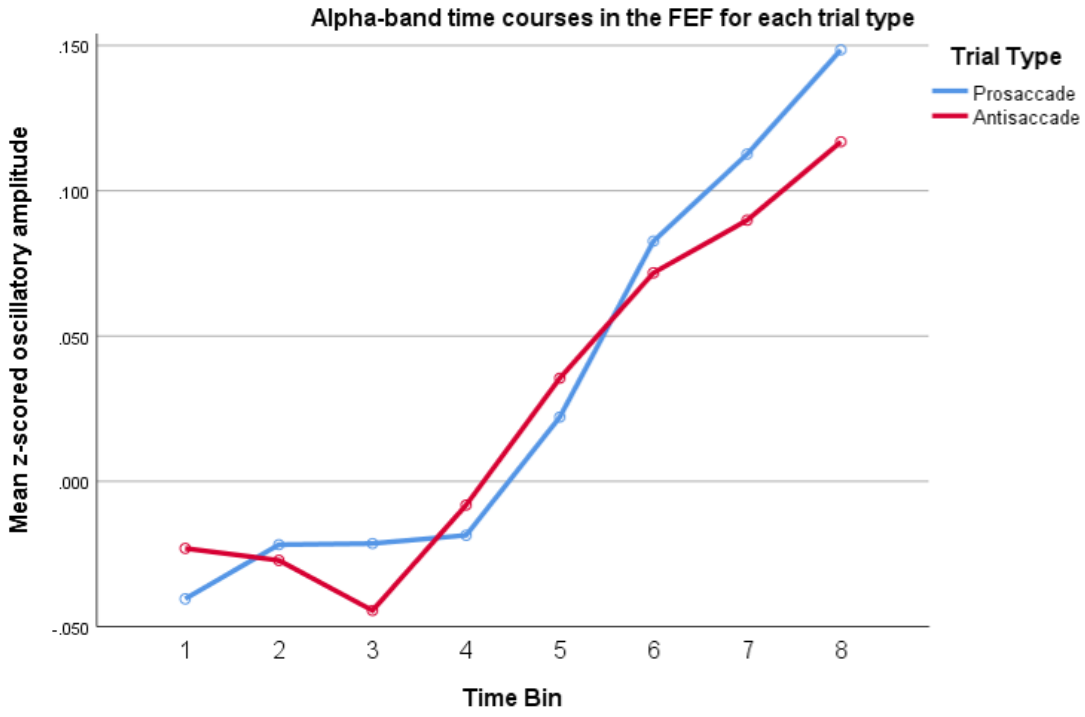

Figure 42: Alpha amplitude time courses in the FEF for each trial type, averaged over day and hemisphere.

There was no significant difference in mean alpha power between trial types, nor were the time course trajectories significantly different for the two trial types.

I repeated this ANOVA for each of the other homotopic ROI pairs, and for V1 (without the hemisphere factor). For the Ant Ins, there was a

significant Trial Type by Time Bin effect, indicating a significantly different time course for the two trial types, $F(3.390, 74.576) = 2.753$, $p = .042$. Inspection of the two trial type time courses plotted in Figure 43 suggests a less marked rise in alpha for antisaccades than for prosaccades. In fact, in the final bins around 200 msecs prior to target, there is a reduction in alpha in antisaccades whilst it continues to rise for prosaccades. This could indicate that this difference between trial types is only valid in the final bins prior to target, which infers an alpha suppression in the Ant Ins during the final bins prior to target. However, ANOVAs conducted for each trial type separately indicated no significant systematic modulation of alpha over time for either trial type, so this may be a spurious finding and should be interpreted with caution.

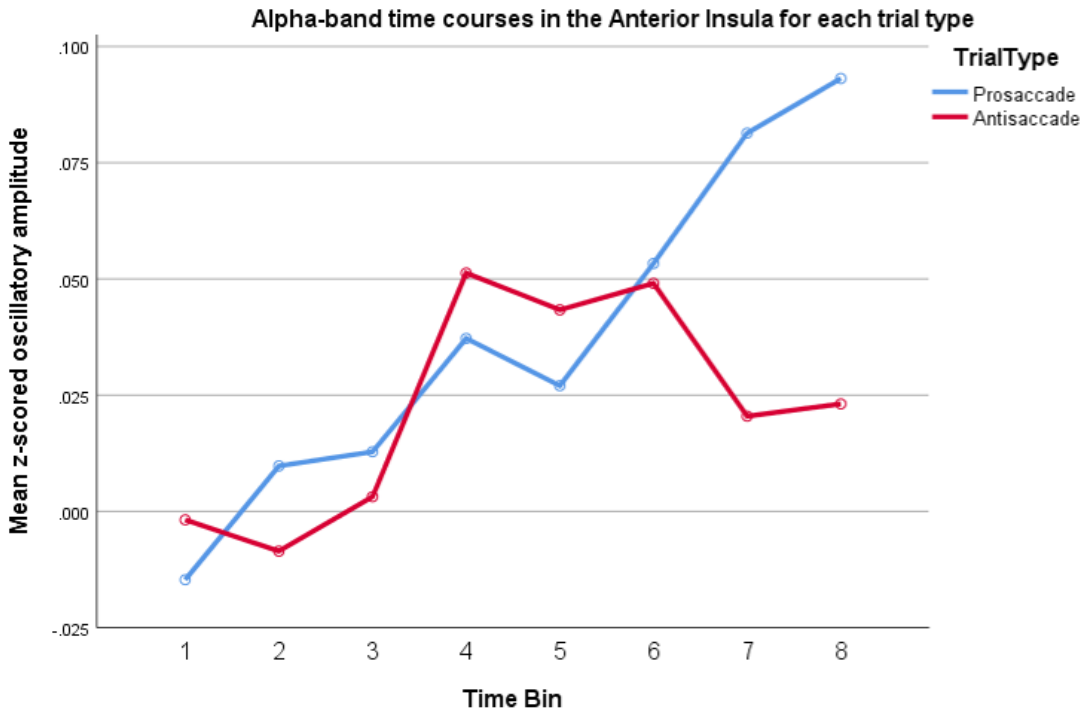

Figure 43: Alpha amplitude time course in the Anterior Insula for each trial type, averaged across hemispheres and days.

This indicates visually that the trial types are most disparate in the final two bins of the anticipatory period.

For the PEF, there was a significant Hemisphere by Time Bin interaction, $F(2.811, 61.840) = 7.182$, $p < .001$. This reflects the very different time courses observed for left and right PEF plotted earlier in Figure 41 and plotted alone in Figure 44. ANOVAs conducted on the PEF in each hemisphere separately indicated no significant systematic modulation of alpha amplitude over time in the L PEF, but a significant main effect of time on the right. As indicated in Figure 44, R PEF alpha amplitude decreases initially, then rises again from midway through to levelling off at the end of the anticipatory period. This fall-then-rise pattern was confirmed by polynomial contrast that indicated a significant

quadratic, $F(1, 22) = 12.521$, $p = .002$, and quartic $F(1, 22) = 12.417$, $p = .002$ terms in the polynomial fit. These results could indicate alpha suppression of the R PEF in the middle of the anticipatory period.

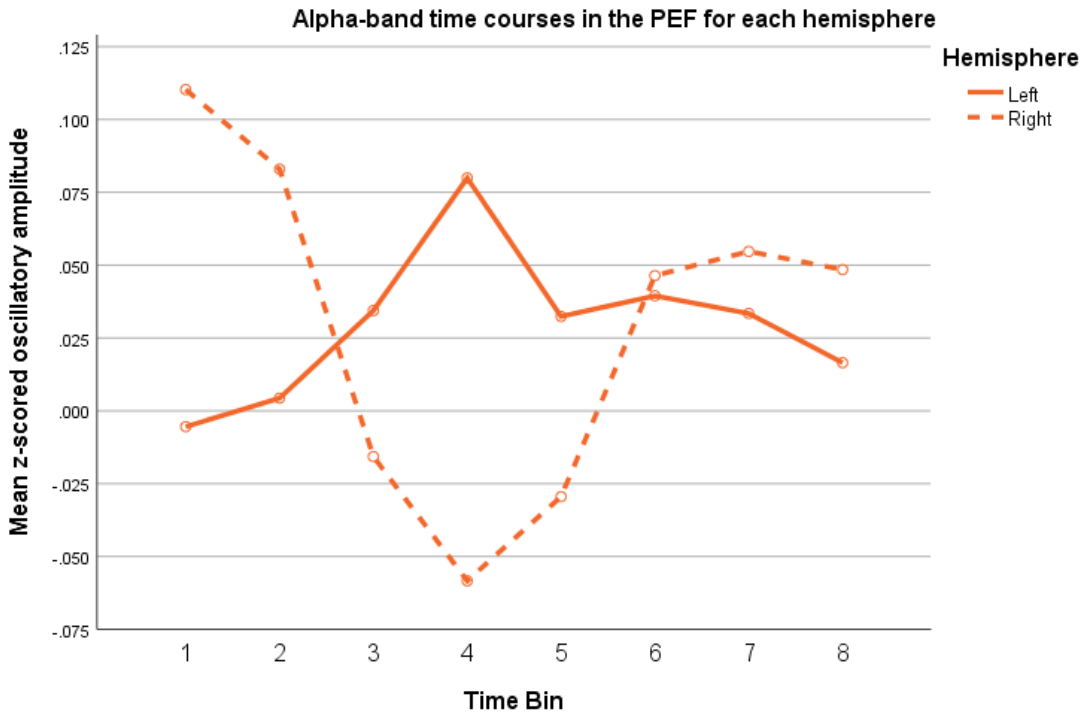

Figure 44: Alpha amplitude time courses for the PEF by hemisphere, averaged across trial type and day.

Interestingly, the R PEF was also the only ROI to present a significant main effect of Day, $F(1, 22) = 4.839$, $p = .039$, whereby alpha power in the R PEF significantly increased on Day 2. There were also significant Trial Type by Time Bin interactions in the R PEF, $F(3.964, 87.199) = 2.870$, $p = .028$. Polynomial contrasts analysis showed a significant linear trend in the R PEF, $F(1, 22) = 13.889$, $p = .001$, This indicated that

the difference in R PEF alpha power between trial types increased across the time course (see Figure 45), whereby there was greater alpha power in prosaccade trials than in antisaccade trials, particularly in the latter bins.

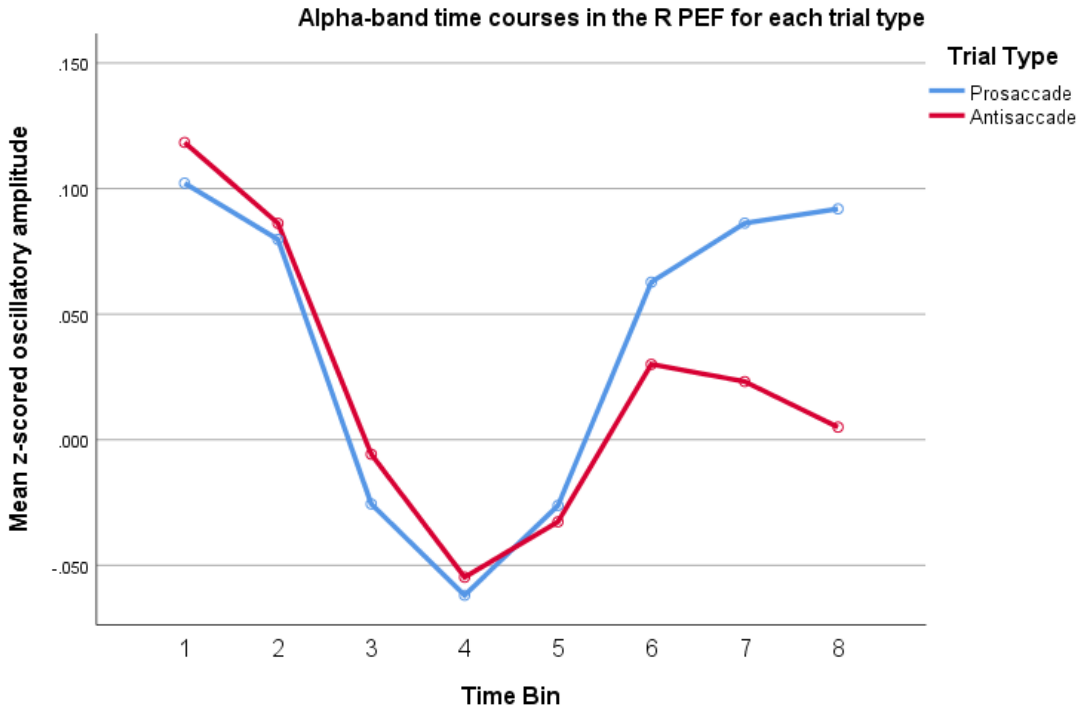

Figure 45: Alpha time courses in the R PEF for prosaccades and antisaccades separately. Time courses are averaged across days.

To summarise these alpha findings:

- We did not replicate Hwang's finding of greater anticipatory FEF alpha amplitude on antisaccade trials. However, we did broadly replicate their finding of rising alpha as target onset approaches. We also found no effect of Day on FEF alpha. We therefore have no evidence to suggest that greater inhibition on antisaccade trials was associated with greater anticipatory

alpha, nor that the improved task performance on Day 2 was associated with an increase in anticipatory FEF alpha.

- The time course of alpha in the right PEF differed markedly from the time course in left PEF, in which alpha amplitude falls for the first half of the anticipatory period following the cue, then rises again as target onset approaches.
- Trial type effects were observed in the R PEF and Ant Ins, whereby there is an indication for a reduction in alpha in antisaccade trials compared to prosaccade trials, particularly in the latter bins.
- Day effects were observed only in the R PEF, whereby there was greater alpha amplitude on Day 2 compared to Day 1.

7.3.6. Beta-band

Beta amplitude time courses for each ROI are plotted in Figure 46. All except V1 show the broad pattern of beta ERD-ERS seen in the ROI averaged time course in Figure 34.

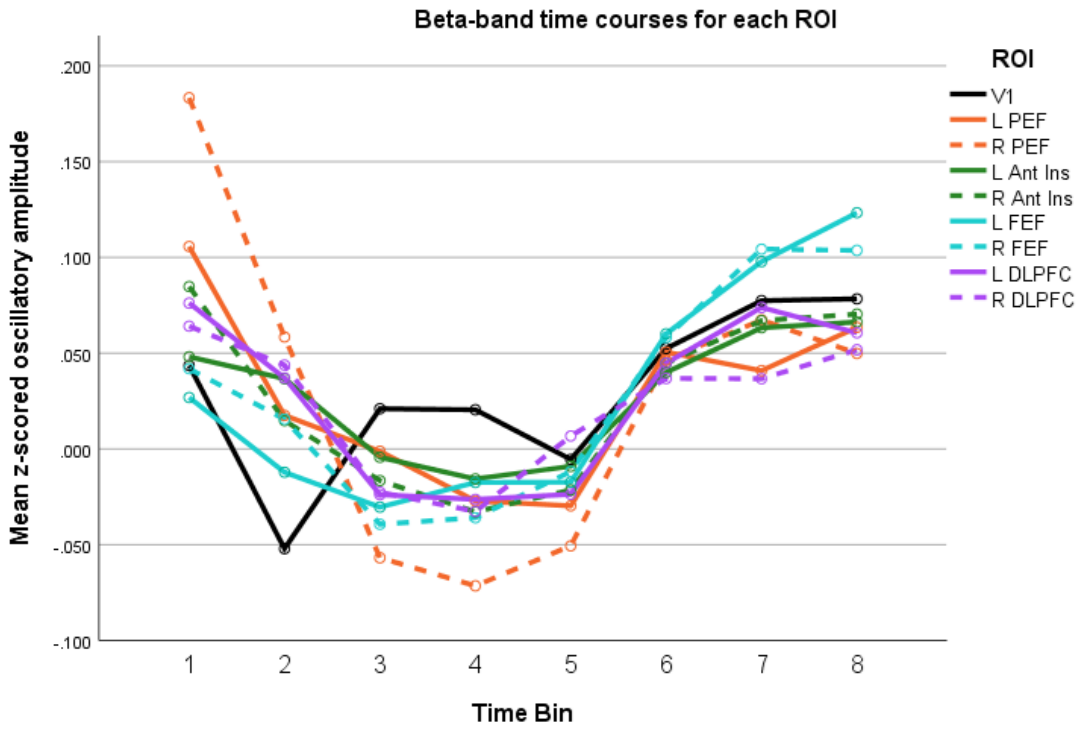

Figure 46: Beta amplitude time courses for all ROIs, collapsed across days and trial types.

However, with as alpha, we had an *a priori* hypothesis about anticipatory beta in the R DLPFC, which Hwang et al. (2014) had found to be greater for antisaccade trials than for prosaccade trials. I therefore started my investigation of anticipatory beta with analysis of the time course of beta amplitude in R DLPFC.

I conducted a three-way repeated-measures ANOVA (2 x 2 x 8) with three within-subjects factors: Day (2 levels: Day 1 and Day 2); Trial Type (2 levels: prosaccade and antisaccade trials) and Time Bin (8 levels). There was no significant main effect of Trial Type but there was a significant Trial Type by Time Bin interaction, $F(3.574, 78.626) = 2.820$, $p = .036$. The time courses for each trial type are plotted in Figure 47. The plot indicates that the beta time courses for the two trial types tend to diverge over the course of the anticipatory period, with prosaccade beta power exceeding antisaccade beta power towards the end of the trial. Polynomial contrasts confirmed that this divergence was significantly linear, $F(1, 22) = 11.159$, $p = .003$, suggesting that the divergence increased linearly toward the end of the anticipatory period. However, it does not replicate the Hwang finding and, if anything, ERS is reduced for antisaccades compared with prosaccades.

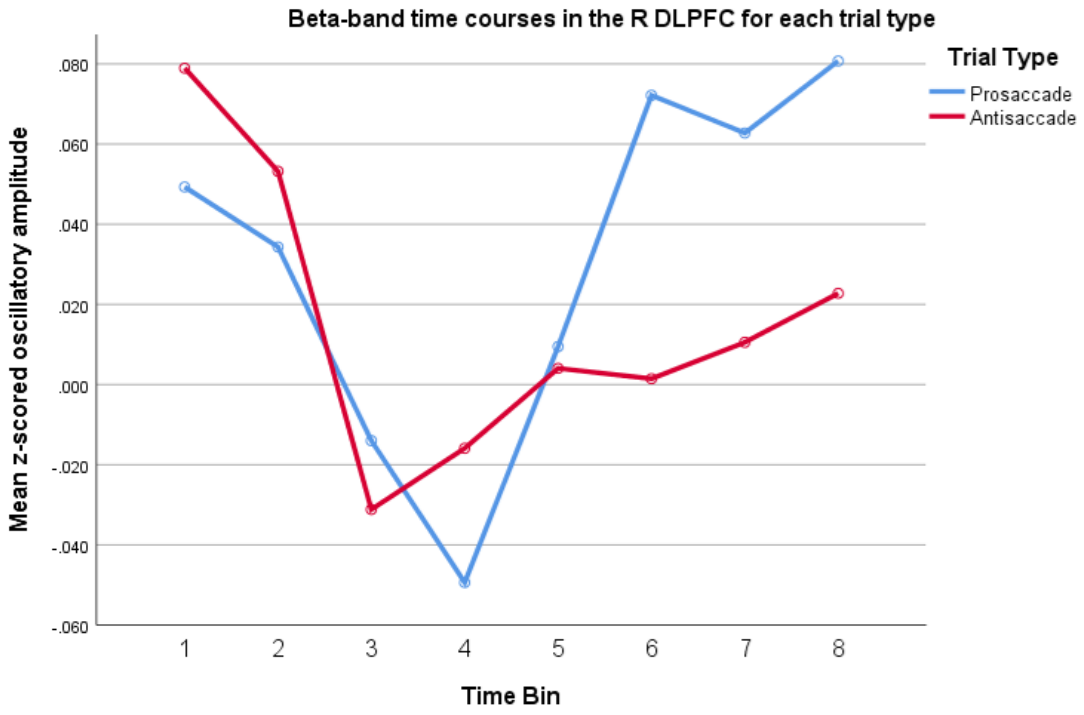

Figure 47: Beta amplitude time course in the R DLPFC for each trial type, collapsed across days.

Note the increased trial type amplitude differences in the latter time bins.

Additionally, Hwang et al. (2014, 2016) also found that increases in R DLPFC beta preceded that of FEF alpha. Figure 48 shows the time courses for FEF alpha and R DLPFC beta for each trial type. This indicates that within trial types, FEF alpha and R DLPFC beta reach their minima around Bin 3 for antisaccades, and Bin 4 for prosaccades. Moreover, the increase in FEF alpha appears to be steeper than R DLPC beta, particularly for antisaccade trials. Our data therefore does not indicate a similar finding to that from Hwang and colleagues, whereby both increases appear to occur around the same time within trial types. However, we did not compute cross-frequency coupling analysis, so this cannot be qualified further.

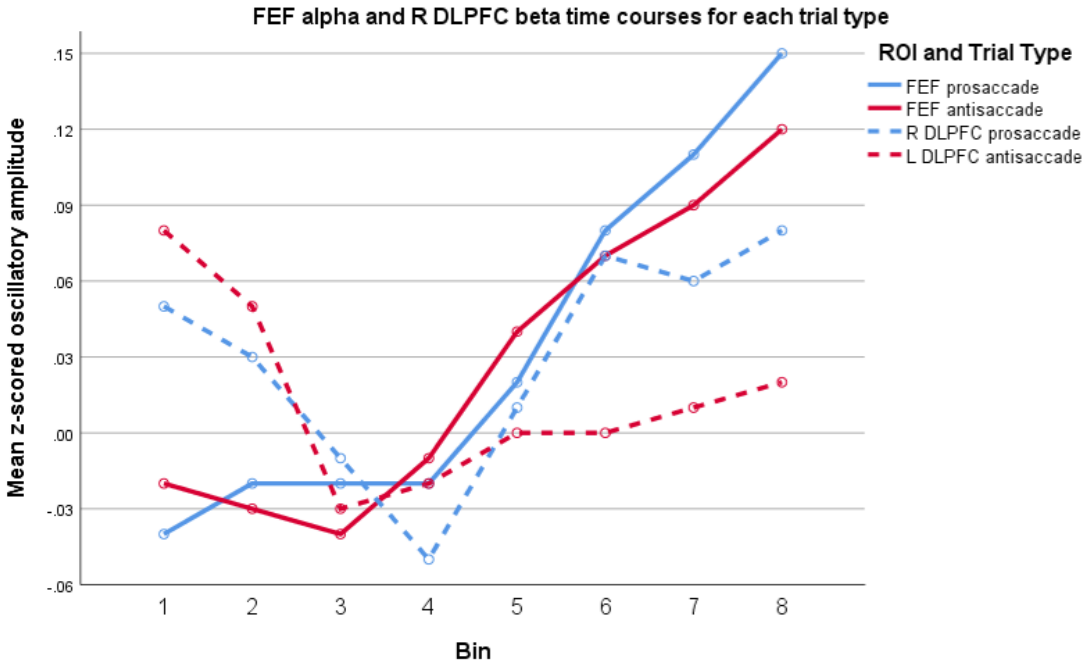

Figure 48: FEF alpha and R DLPFC beta time courses, plotted separately for prosaccade and antisaccade trial types.

To investigate beta time courses across all ROIs, I conducted a four-way repeated-measures ANOVA (9 x 2 x 2 x 8) with four within-subjects factors: ROI (9 levels: V1, L PEF, R PEF, L Ant Ins, R Ant Ins, L FEF, R FEF, L DLPFC and R DLPFC); Day (2 levels: Day 1 and Day 2); Trial Type (2 levels: prosaccade and antisaccade trials) and Time Bin (8 levels: mean *z*-scored TFS values in each of the eight 100 msecs time bins).

There was a significant main effect of Time Bin, $F(3.079, 67.733) = 8.611$, $p < .001$, where this also had a significant quadratic trend, $F(1, 22) = 20.265$, $p < .001$, reflecting the ERD-ERS pattern already noted.

Additionally, there was a significant main effect of Trial Type, $F(1, 22) = 6.549$, $p = .018$, where there was significantly less overall beta

amplitude in antisaccade trials than for prosaccade trials. However, there was also a significant ROI by Trial Type interaction, $F(8, 176) = 2.083$, $p = .040$, indicating that the differences between trial types was greater in some ROIs than others, as well as a significant ROI by Time Bin interaction, $F(56, 1232) = 4.314$, $p < .001$.

To investigate the specific patterns for each ROI of the anticipatory beta time courses, I examined each ROI or homotopic ROI pair separately. As with the alpha amplitude data, I entered beta amplitude data into four-way ANOVAs for each of the homotopic ROI pairs, and a three-way ANOVA for V1, for which there was no hemisphere factor (see alpha results section above for ANOVA specification).

There were significant main effects of Trial Type for the Anterior Insula, $F(1, 22) = 4.703$, $p = .041$ and PEF, $F(1, 22) = 9.432$, $p = .006$, whereby the mean beta amplitude was significantly lower for antisaccade trials than for prosaccade trials in both ROIs. For the Anterior Insula there was also a significant Hemisphere by Trial Type interaction, $F(1, 22) = 5.562$, $p = .028$, whereby this effect of Trial Type was significantly greater in the right Anterior Insula than the left.

For PEF there was a significant Hemisphere by Time Bin interaction, $F(3.796, 83.522) = 6.900$, $p < .001$; the ERD-ERS pattern being more marked in the right hemisphere than in the left (refer to Figure 49). Additionally, alpha and beta time courses in the R PEF appear to follow very similar patterns in the amplitude across the anticipatory period (see Figure 50).

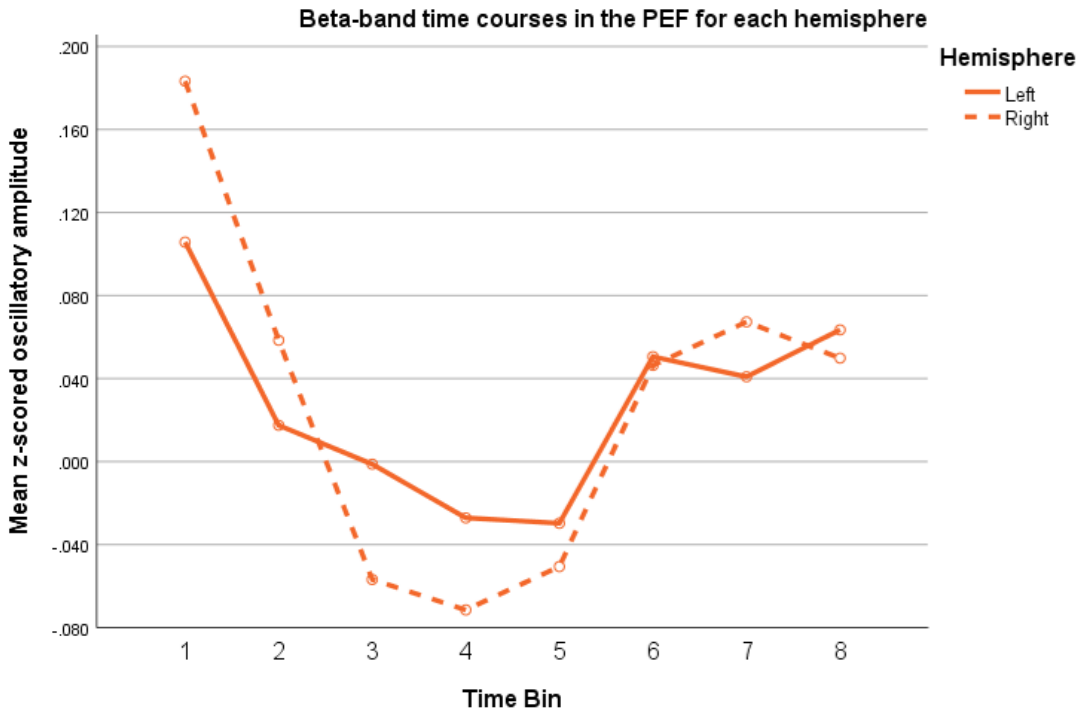

Figure 49: Beta PEF amplitude time courses in each hemisphere, averaged across trial types and days.

Mean PEF beta was significantly lower for antisaccade trials (not shown), but there was no significant interaction between trial type and time bin or hemisphere.

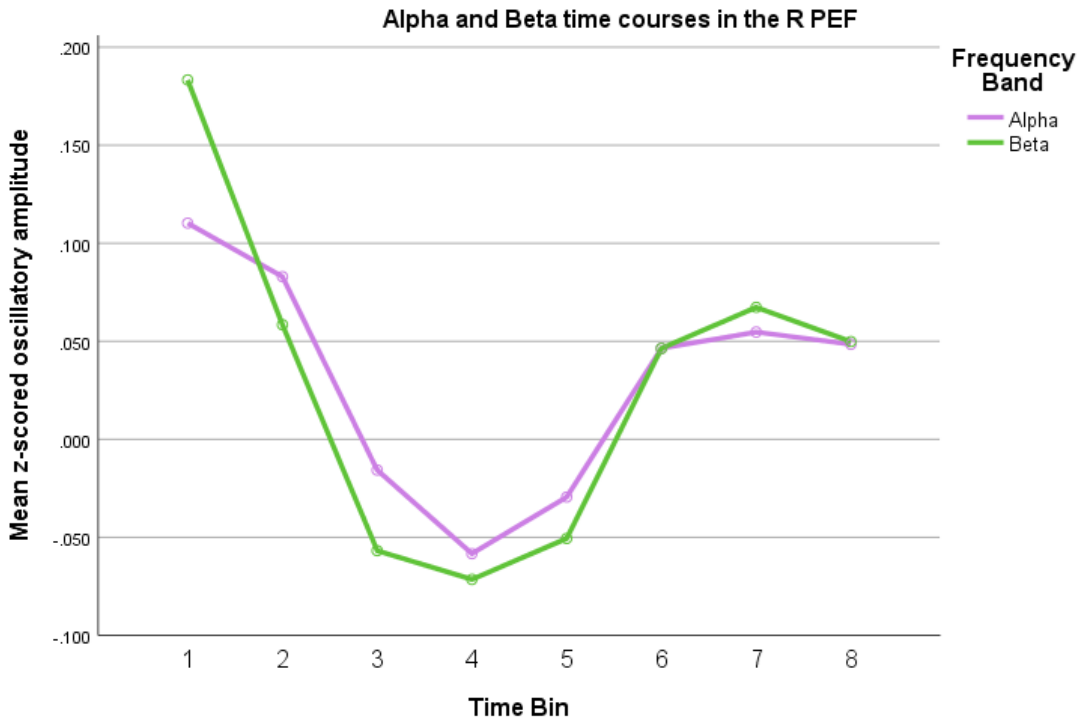

Figure 50: Alpha and Beta time courses in the R PEF, averaged across days and trial types.

Note the striking similarities between the two frequency band time courses in the R PEF, which is not observed in the other ROIs.

Figure 51 shows the beta time courses for each ROI averaged across Days (panels A and B) and Trial Types (panels C and D). Inspection of the plots seems to indicate that while the pattern of ERD is broadly similar over trial types and days, the pattern of ERS seems to differ: The ERS peak for antisaccade trials appears to be prior to the end of the anticipatory period and followed by what may be an anticipatory ERD immediately prior to target onset. Moreover, a similar pattern appears to differentiate beta time courses on Day 1 from Day 2. When data are averaged over trial types, an ERD immediately prior to target onset is more marked on Day 2 than Day

1. Notably, comparing the plots in Figure 51 shows remarkable similarity between the shapes of Day 1 and Prosaccade trials (panels A and C) and Day 2 and Antisaccade trials (panels B and D).

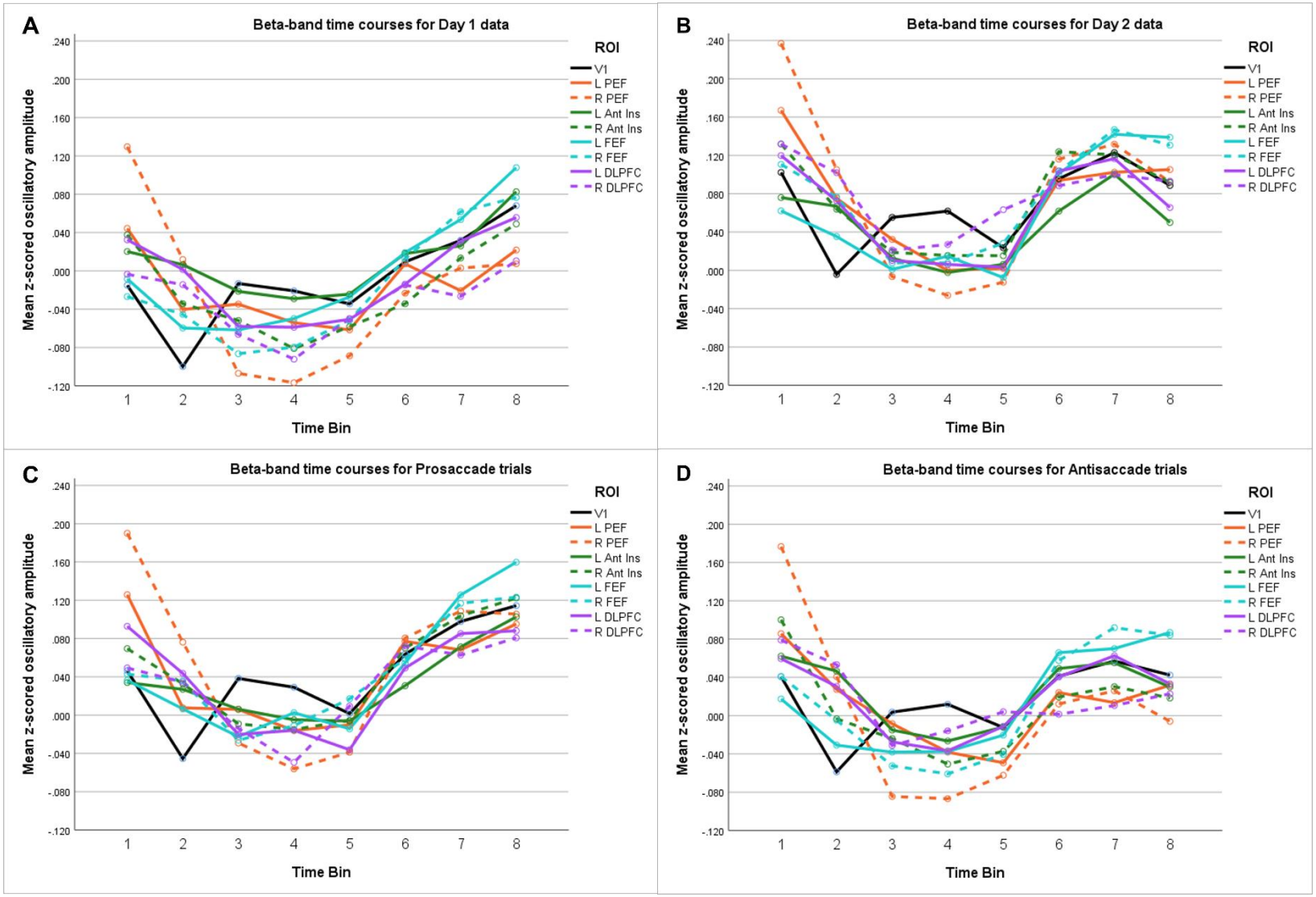

Figure 51: Beta amplitude time courses for each Day (panels A and B) and Trial Type (panels C and D) across ROIs.

As ERS and ERD are likely to reflect probability distributions of transient beta bursts rather than smoothly changing beta amplitudes (refer to beta bursts description in Section 7.1.1), I further investigated these ERD-ERS patterns using beta bursts rates, binned into 100 msecs bins. I conducted a four-way repeated-measures ANOVA (9 x 2 x 2 x 8) with four within-subjects factors: ROI (9 levels: V1, L PEF, R PEF, L Ant Ins, R Ant Ins, L FEF, R FEF, L DLPFC and R DLPFC); Day (2 levels: Day 1 and Day 2); Trial Type (2 levels: prosaccade and antisaccade trials) and Time Bin (8 levels: mean burst rate in each of the eight 100 msecs time bins).

There was a main effect of ROI, $F(3.708, 55.615) = 5.315$, $p = .001$, indicating significant differences between beta burst rates in different ROIs. Deviation contrasts indicated that beta burst rate in the L Ant Ins was significantly higher than the mean across all other ROIs, $F(1, 15) = 15.764$, $p = .001$. However, there were no significant interactions with ROI, indicating similar effects of Time Bin, Trial Type and Day across all ROIs. Beta burst rate across the trial time course for each ROI is depicted in Figure 52, lower panel.

There was a significant main effect of Time Bin, $F(2.799, 41.989) = 6.739$, $p = .001$. Polynomial contrasts also indicated a significant quadratic trend across Time Bins, $F(1, 15) = 26.047$, $p < .001$, as illustrated in Figure 52 upper panel, reflecting the ERS-ERD pattern observed in the binned beta amplitude data.

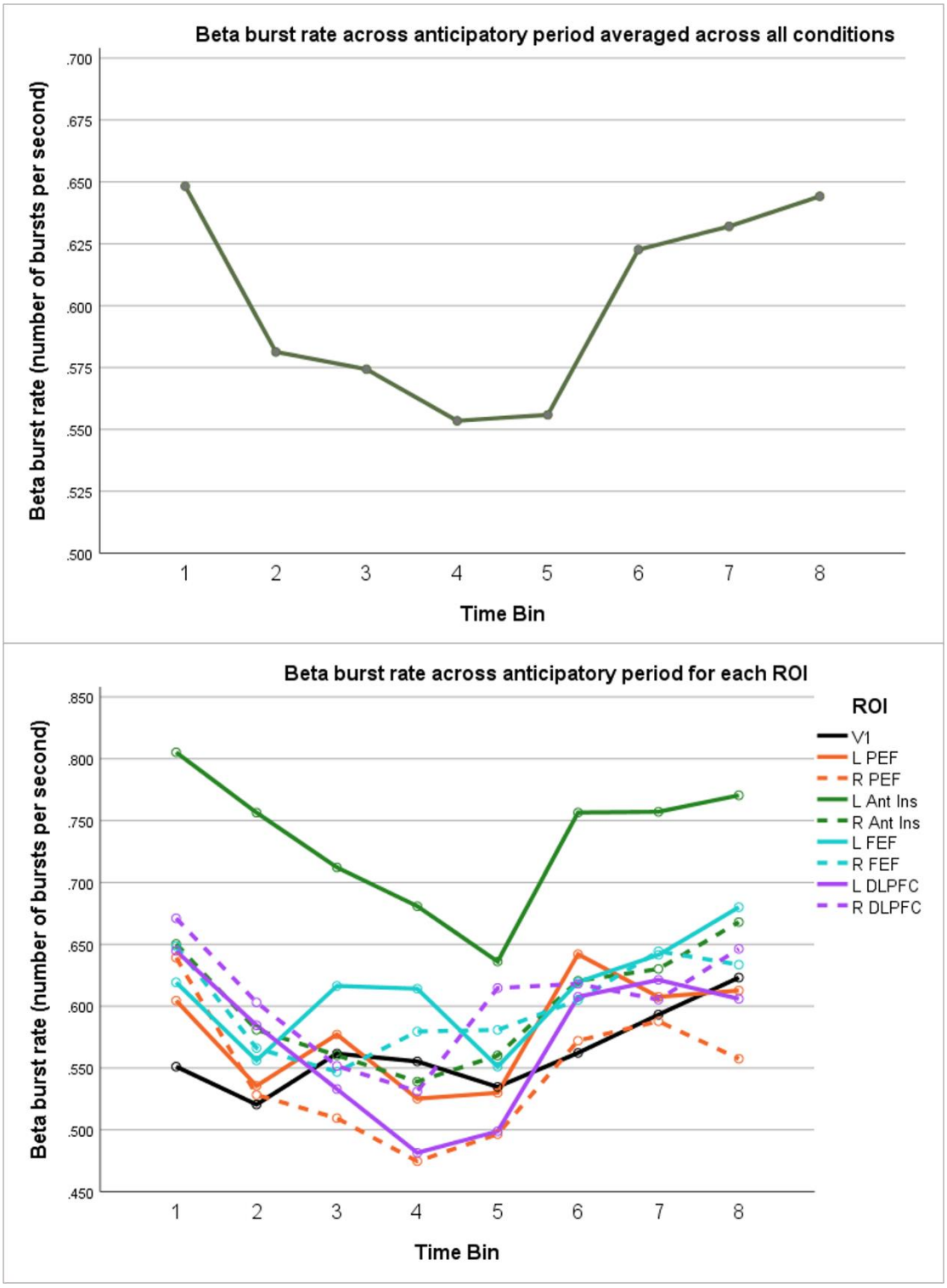

Figure 52: Beta burst rate across the anticipatory period collapsed across days and trial types.

The upper panel is also collapsed across ROIs, whereas the lower panel shows the burst rate for each ROI.

To investigate effects of Trial Type and Day on ERS-ERD patterns, I conducted separate ANOVAs on the first 5 bins, to evaluate effects of Day and Trial Type on cue-related ERD, and the 3 last bins, to evaluate effects of Day and Trial Type on cue-related ERS, together with any "anticipatory" ERD in the final bin prior to target onset.

For the first 5 bins reflecting cue-related ERS, there was a significant main effect of Time Bin, $F(2.670, 45.385) = 13.418$, $p < .001$, and polynomial contrasts indicated a significant linear term, $F(1, 17) = 29.906$, $p < .001$, reflecting the downward linear trend in beta burst probability over the first 600 msecs following the cue; i.e., the ERS. There was also a significant quadratic term, reflecting the flattening of the downward trend between Bins 4 and 5 (Figure 52 upper panel). However, there were no significant effects of Trial Type or Day.

For the ANOVA conducted on the last three bins, there was a significant Day by Time Bin interaction, $F(2, 40) = 9.770$, $p < .001$, as shown in Figure 53. On Day 1, burst rate continues to increase towards the end of the anticipatory period, while on Day 2 it reaches a peak in the 600-700 msecs bin, and then declines, indicating an "anticipatory" ERD just prior to target onset. The polynomial contrast had a significant quadratic term, $F(1, 20) = 21.845$, $p < .001$, reflecting this pattern of differences between days.

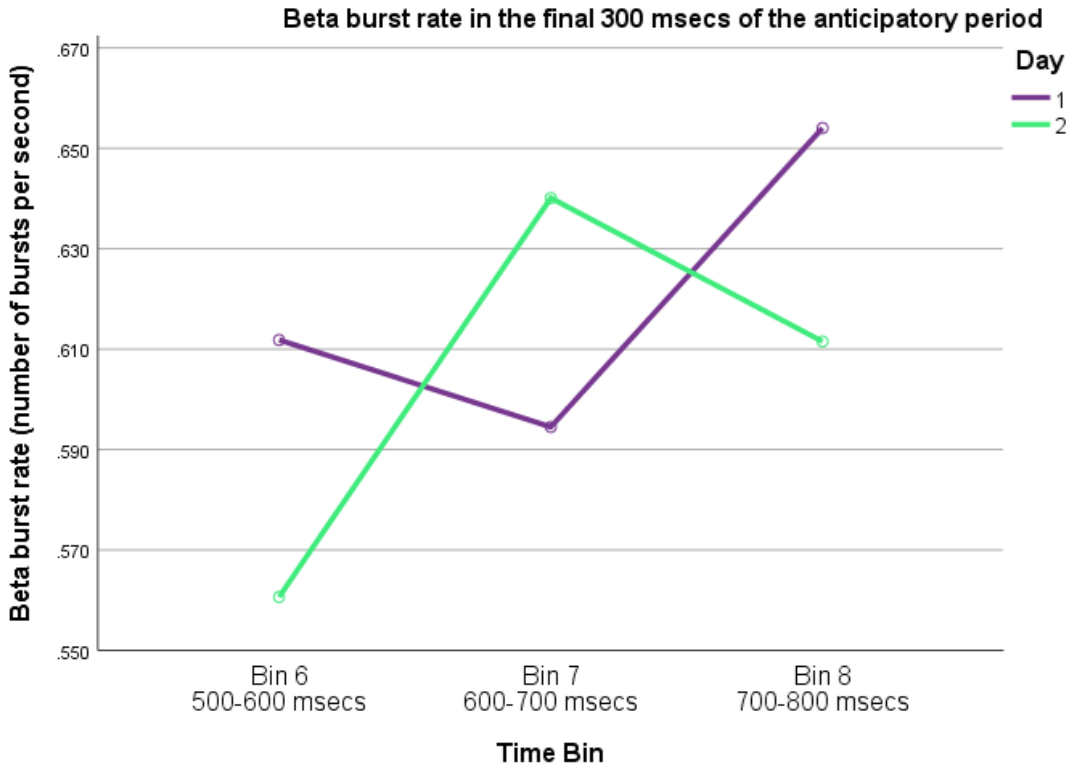

Figure 53: Beta burst rate in the last 300 msecs of the anticipatory period, showing the different pattern on Day 2 compared to on Day 1.

There was also a significant effect of Trial Type, $F(1, 20) = 4.462$, $p = .047$, indicating lower burst probability in this part of the anticipatory period for antisaccades than for prosaccades; thus reflecting reduced ERS for antisaccades than for prosaccades. For reference, beta burst rates throughout the anticipatory period are plotted for each day, for each ROI in Figure 54.

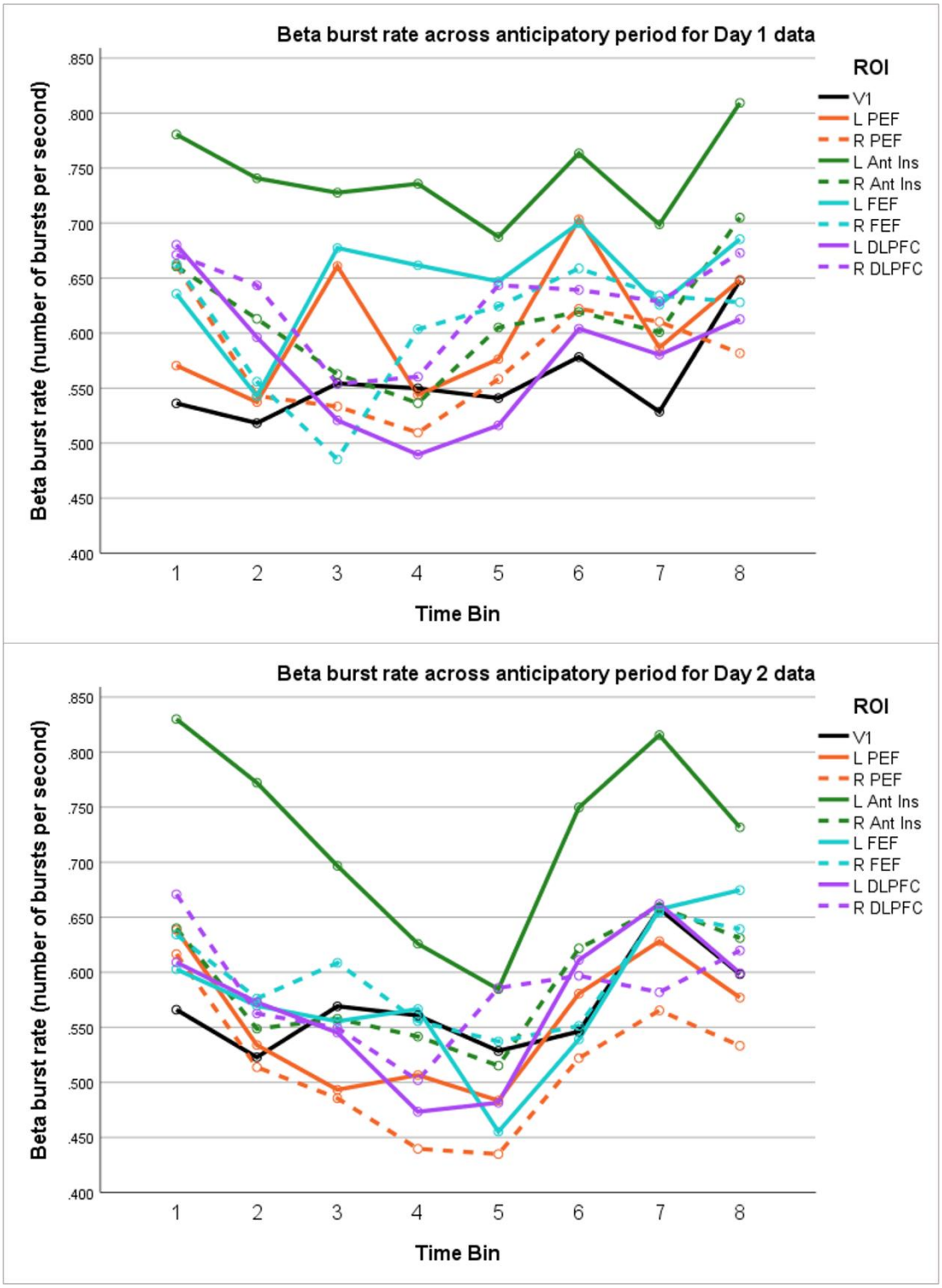

Figure 54: Beta burst rate across the anticipatory period for each ROI on each Day.

Average data is collapsed over trial types, plotted separately for each day, whereby the top panel is Day 1 data, and the bottom panel is Day 2 data. Each time bin represents 100 msecs of data. The same y-axis scale is used to plot data in both panels to compare differences between days.

Occurrence of beta bursts per trial in any one ROI was too low to be able to compute meaningful trial-by-trial RT correlations with rate or timing of beta bursts.

To summarise the beta band findings:

- We did not replicate the finding by Hwang et al. of lower mean anticipatory beta amplitude in the R DLPFC on antisaccade trials than on prosaccade trials. On the contrary, while the time courses of beta over the course of the anticipatory period significantly diverged, the trend was for beta to rise to a higher amplitude on prosaccade trials than on antisaccade trials.
- Where we found effects of trial type in the Anterior Insula and the PEF, beta amplitudes were lower rather than higher on antisaccade trials compared to prosaccade trials. Mean beta burst rate across all ROIs also indicated reduced ERS for antisaccade trials during the final 300 msecs of the anticipatory period.
- As with alpha, there were significant differences in the time courses of beta between the left and right PEF, whereby the ERS-ERD pattern was larger in amplitude in the R PEF than in the L PEF. Notably, alpha and beta time courses in the R PEF were extremely similar.

- Beta burst rate analyses suggest that after RECOGNeyes training, an "anticipatory" ERD occurs just prior to target onset, which follows an ERS peak occurring at 600-700 msecs. A related pattern distinguishes antisaccades from prosaccades, where overall ERS is reduced in antisaccade relative to prosaccades. This may suggest that the anticipatory inhibitory processes associated with antisaccade trials on both days is generalised across trial types on Day 2.

7.4. Discussion

7.4.1. Question 1

- Are antisaccades associated with greater anticipatory alpha in the FEFs and greater anticipatory beta in the R DLPFC, as found by Hwang et al.? If so, are these effects enhanced after RECOGNeyes training?

FEF alpha and R DLPFC beta did increase in amplitude during the anticipatory period; however, we found no evidence that antisaccade trials were associated with either greater anticipatory alpha amplitude in the FEFs nor with greater anticipatory beta amplitude in the R DLPFC. If anything, beta ERS was less for antisaccade trials than for prosaccade trials. Analysis of the time course of beta burst rates showed clear evidence

of a cue-related ERD over the first 500 msecs of the anticipatory period, followed by an ERS over the final 300 msecs. On Day 1, this ERS was greatest in the final 100 msecs, while on Day 2, peak ERS was reached between 600 and 700 msecs post-cue, followed by a second "anticipatory" ERD during the final 100 msecs prior to the target. Our predictions based on Hwang et al. (2014) were therefore not confirmed. Moreover, our prediction based on Hwang et al. (2014, 2016) that anticipatory alpha would increase on Day 2 was not confirmed.

Also in regards to the findings by Hwang et al. (2014, 2016), we may have also expected an increase in R DLPFC beta to precede that of FEF alpha. Despite observing a rise in both ROI frequency band time courses, our data plotted in Figure 48 does not support the findings by Hwang and colleagues, whereby the rise in both ROI frequency bands occur at the same time within trial types (Bin 3 prosaccades and Bin 4 antisaccades). However, we did not compute cross-frequency analyses to analyse these observations in the data, so it is not possible to evaluate this fully.

Moreover, we must take into consideration the differences between the design of the studies used in RECOGNeyes and that used by Hwang and colleagues. For instance, Hwang used a longer anticipatory period in their pro/antisaccade task of 1500 msecs, whereas ours was 800 msecs. They also adopted slightly different definitions of the alpha band (10-18 Hz, compared to 10-12 Hz used in our study) and beta band (18-38 Hz, compared to 13-30 Hz used in our study). They also used a different method for

locating regions of interest, namely with the Destrieux automated atlas approach (Destrieux et al., 2010). In summary, these factors may have contributed to differences in the observed effects in both studies. Therefore, future research is required to further validate and explore these findings.

7.4.2. Question 2

- What are the characteristic time courses of oscillatory amplitude over the anticipatory period between cue and target in each of the delta, theta, alpha and beta bands, and are they modulated by trial type and/or RECOGNeyes training, and do these effects differ between ROIs?

We found distinct time course shapes across the anticipatory period for each of the frequency bands (as illustrated in Figure 34). Delta presented a "hockey stick" shape, starting high in amplitude, decreasing across the time course, and finishing with a slight upwards inflection prior to target onset. Theta was depicted to have a sinusoidal shape, peaking in amplitude around 200 msecs after the cue, where it decreases and shows a final increase in amplitude just prior to the target. Alpha showed a general monotonic increase across the time course. Beta presented an initial ERD after cue presentation, followed by an ERS up to the point of target onset.

Notably, slow-wave oscillatory frequency bands of delta and theta presented anteriorised effects across their time courses. In the delta-band, posterior ROIs of V1 and PEF had greater amplitude peaks at cue onset, and anterior ROIs of the DLPFC, FEF and Ant Ins presented greater inflections at the end of the period prior to target onset. V1 showed the least inflection at the end, whereby this was the only ROI where the gradient in the final amplitude change was in fact negative on Day 2. In the theta-band, anterior ROIs reached later maxima than posterior ROIs. Since posterior regions are activated earlier within the oculomotor network during visual attention processing (see Chapter 2, Section 2.2.1), bottom-up early visual processing occurring in V1 and PEF could be communicated to frontal regions in the visual attention network, which may account for our observed anteriorised effects in these frequency bands.

V1 also showed day effects, whereby there was higher delta amplitude at cue onset and a steeper reduction in amplitude across the time course on Day 2 than on Day 1. Delta is implicated in internal time keeping and response timing mechanisms (Arnal & Kleinschmidt, 2017; Gillary & Niebur, 2016; Stefanics et al., 2010), thus the anteriorisation in delta amplitude time courses could implicate the involvement of posterior regions in mediating temporal and response timing mechanisms, as well as sensory bottom-up gating processes (Harmony, 2013). Therefore, the effect of day in V1 could indicate more efficiency in these processes.

Furthermore, reduced delta power is associated with heartrate slowing (Patron et al., 2019), thus the general reduction in delta across the anticipatory period could be related to our results of cardiac deceleration in the anticipatory period. Furthermore, the reduced delta amplitude in antisaccade trials compared to prosaccade trials could relate to our findings indicating increased tonic PNS indices of smaller pupil size (Chapter 5) and greater cardiac deceleration (Chapter 6) in antisaccade trials. Therefore, this could link with delta possibly mediating effects of autonomic arousal, whereby reduced delta is observed with increased tonic PNS effects.

There were also modulations of day in the theta-band, whereby there were higher theta amplitudes across ROIs and Trial Types on Day 2. Since theta is supported to be involved with mediating phase reset (Diederich et al., 2014) and balancing top-down and bottom-up processes (Fiebelkorn & Kastner, 2019), more theta power on Day 2 could reflect better orchestration of these cognitive control processes after RECOGNeyes training.

Towards the middle of the anticipatory period, most ROIs present an increase in alpha-band power, which is likely to reflect increased top-down inhibition to prevent premature saccades. Despite our bilateral FEF findings not supporting our predictions based on Hwang and colleagues outlined in Question 1, FEF alpha did present the largest linear increases in alpha-band amplitude across the anticipatory period, also reaching the highest amplitude by target onset compared to other ROIs in the network. This does support previous suggestions that bilateral FEF is the primary

source for mediating top-down inhibitory control via increased alpha-band suppression effects over visual attention/oculomotor network regions for successful saccadic performance (Hwang et al., 2014, 2016; Marshall et al., 2015).

The PEF showed hemispheric effects, whereby the R PEF was the only region to show a reduction in alpha-band amplitude during the middle of the anticipatory period, and alpha amplitude was lower in antisaccades compared to prosaccade trials. Since alpha primarily is supported to exert inhibitory influences (see alpha background in Section 7.1.1), this could reflect less inhibitory top-down signals via alpha being sent to the R PEF to enable preparatory visuospatial processing, particularly in antisaccade trials for mediating vector inversion transformation processes (as discussed for the role of the PEF in Chapter 2, Section 2.2.4).

However, alpha-power increased in the R PEF on Day 2, which was the only ROI to show this effect. One possibility is that this reflects increased top-down alpha-mediated inhibitory control influence in the R PEF on Day 2. Alternatively, this could indicate less overall alpha-mediated suppression required to facilitate the computation of visuospatial processes during the pro/antisaccade task, inferring more efficient inhibitory control processing. Also, lateralisation of these effects to the R PEF is interesting, given support in the literature for right hemispheric dominance in visual attention, alerting and orienting responses more so than the left, discussed in detail by Spagna et al. (2020). Additionally, there is evidence showing

significant fMRI activations in the right parietal lobe for orienting (Spagna et al., 2020). Thus, reduced alpha suppression could indicate more efficient preparatory processes relating to orienting in the R PEF.

The anterior insula also presented trial type effects in the alpha-band, whereby there was lower alpha amplitudes in antisaccade trials compared to prosaccade trials, and this was particularly apparent in the latter bins of the anticipatory period. This could possibly be reflecting reduced top-down inhibition in this region, particularly just prior to target onset, to increase salience processing for antisaccade trial stimulus relevance (as discussed in Chapter 2, Section 2.2.5). However, time course modulations in each trial type did not present significant effects of time bin, so this should be interpreted with caution.

In the beta-band, most ROIs (except for V1) showed a reduction in amplitude in the middle of the anticipatory period (ERD), followed by an increase in beta-band amplitude and beta burst rate towards the final 300 msecs of the anticipatory period (ERS). At the beginning of the anticipatory period, there was a notable increase in beta-band amplitude for V1 that was not observed in any other ROIs. This could possibly reflect a temporally informative initial alerting response to cue presentation, which could reset the preparatory period 'internal clock' that initiates phase-locking processes. This could also potentially link to modulations in the slow wave oscillations described previously, including theta phase reset and delta internal clock processes in this preparatory period.

There were also different modulations in beta time courses for each trial type, whereby the Ant Ins and PEF demonstrated lower beta amplitudes on antisaccade trials compared to prosaccade trials. This modulation of trial type differences was stronger in the R Ant Ins compared with the L Ant Ins. This reduction in beta-band modulation could be related to differences in salience processing on antisaccade trials compared to prosaccade trials.

Furthermore, differences in the degree of beta modulation between trial types in the R and L Ant Ins could indicate lateralisation of different effects mediated by each hemisphere. For instance, the right inferior/ventrolateral cortex, which is in the same vicinity as the anterior insula, has been strongly implicated in inhibition as discussed in Chapter 2, Section 2.2.5 (Aron et al., 2004; Hodgson et al., 2007). Thus, these hemispheric differences could reflect the differential inhibitory control requirements for antisaccade trials compared to prosaccade trials.

In addition, these hemispheric findings could relate to differential ANS processing, whereby the R Ant Ins is involved in mediating SNS effects and the L Ant Ins mediating PNS effects (Cechetto & Shoemaker, 2009; Craig, 2005). More recent support for this includes a study by DiNuzzo et al. (2019), who found R Ant Ins activation with increased pupil diameter (an index of sympathetic drive; see Chapter 5 and Chapter 2, Section 2.1.2). Therefore, not only could this reflect increased salience processing, but

could also directly link to mediating arousal changes and the ANS responses we see from our pupillometry and cardiac data.

Trial type modulations in the PEF also implicate this region in regards to extra visuospatial and vector transformation processing required for antisaccade trials compared to prosaccade trials. The PEF also had hemispheric time course differences in the beta-band, including a larger ERS-ERD amplitude in the R PEF than in the L PEF. Interestingly, both alpha and beta R PEF time courses follow a very similar pattern (refer to Figure 50). This links back to the previous discussed ideas regarding this lateralisation, whereby the R PEF may be particularly important in mediating visuospatial processing compared to the L PEF. Future research investigating the functions of these regions of the visual attention network across these frequency band ranges are required to build our understanding of the entirety of the roles these network regions serve.

7.4.3. Question 3

- Since beta amplitude, averaged over trials, is likely to reflect the probability distribution of transient beta bursts, are beta burst probabilities modulated by time, trial type and/or RECOGNeyes training?

Beta burst rate analysis across the anticipatory period reflected similar modulation patterns observed in beta amplitude data, which supported the idea that the ERS and ERD reflect probability distributions of transient beta bursts. We found that after RECOGNeyes training, there was an ERS peak occurring at 600-700 msecs followed by an additional "anticipatory" ERD prior to target onset, which was not observed for Day 1 data. Moreover, trial types differed in a similar pattern to days, whereby prosaccades presented a continuous ERS to target onset, but the ERS was dampened in antisaccade trials. This could be interpreted as the inhibitory control mechanisms underlying processes in antisaccade trials being generalised on Day 2 across both trial types. A preparatory ERD could also indicate better motor response timing and inhibitory control of processing sensory input (i.e., balancing top-down and bottom-up mechanisms) (Arnal, 2012; Spitzer & Haegens, 2017).

Notably, the L Ant Ins had more beta bursts compared to any other region. This could possibly be indicative of salience network processing, or autonomic effects since there is support for the L Ant Ins in mediating PNS actions (Cechetto & Shoemaker, 2009; Craig, 2005).

Overall, these findings therefore build upon previous beta burst research (see Section 7.1.1), whereby bursting activity presents distinct patterns following a stimulus. However, our results suggest that these patterns may reflect distinct cognitive processes and mechanisms recruited. For example, preparation to 'reflexively react' in a prosaccade trial presents

beta ERS that continues to the actual target presentation. Conversely, a preparatory ERD following the ERS in antisaccade trials before the actual target stimulus could reflect additional top-down inhibitory control processes that mediate both the inhibition of the reflexive saccade and preparing to voluntary look away from the target.

7.4.4. MEG limitations

There were some limitations for the MEG data collected in this study. Beta bursts enable a single trial measure for use in trial-by-trial correlational analysis with performance; however, our data had low numbers of beta bursts occurring on most trials in the anticipatory period of our data, where many did not have any. Therefore, there were not enough bursts to compute meaningful trial-by-trial RT correlational analysis, but using longer time periods in trial data that includes the response period may enable future analyses for performance correlates. We also did not compute phase analysis, which could be considered in future analysis paradigms. This may also allow us to conduct trial-by-trial task performance correlations with phase. Ipsilateral and contralateral ROI analyses relative to the stimulus or saccade were not computed and may be a potential direction for future analyses for analysing post-saccade and response period effects. We also did not study gamma-band oscillatory activity. However, gamma was excluded from MEG data analysis because

of poorer signal-to-noise-ratio for high frequencies in the gamma-band (Boto et al., 2016; Dalal et al., 2009; Jerbi et al., 2009).

Chapter 8: Final discussion and concluding remarks

The RECOGNeyes research project is the first study of its kind to measure ANS indices of pupillometric and heartrate data concurrently with CNS neural correlates using MEG on the pro/antisaccade task, before and after an inhibitory control training paradigm. Collectively, these findings highlight CNS and ANS correlates of inhibitory control, and changes in correlates following RECOGNeyes gaze-control training. In this Chapter, I will summarise these key findings and their possible impact and implications on the wider scientific, educational, and clinical communities, as well as the potential benefits of future developments of RECOGNeyes. I will also suggest possible study limitations and ideas for future research directions.

8.1. Summary of findings

8.1.1. Behavioural and task performance findings

Behavioural and task performance results were addressed in Chapter 4. Baseline sample characteristics showed that our sample on average had greater inattentive ADHD traits and poorer reading ability, compared to the general population. Therefore, our study participants were the ideal target audience to undertake RECOGNeyes training, since

inattentive individuals should benefit the most from gaze-control training. All subjects also had good exposure to the RECOGNeyes training program to compare pre- and post-effects of our behavioural findings, ANS, and CNS measures between assessment days.

Our behavioural findings indicated that reading ability indices improved following RECOGNeyes training. This included improvements in the sight-word reading domain, more accurate fixation landing positions, smaller sizes of regressive saccades, larger forward saccades without increasing the size of skipped words, and increased word length with only a single fixation. These findings all support the idea that RECOGNeyes training could potentially result in better top-down saccadic control mechanisms that contribute to these improved reading features observed on Day 2.

Our results also revealed better pro/antisaccade task performance after RECOGNeyes training, as reflected by better response accuracy and RT on Day 2 compared to on Day 1. Furthermore, there was enhanced performance improvements in RT, particularly for antisaccade trials compared with prosaccade trials, without any indication of this resulting from a speed-accuracy trade-off. This also supports better inhibitory control processing on Day 2 compared to Day 1.

Furthermore, additional analyses conducted in Appendix E showed that increased time spent playing RECOGNeyes was associated with smaller standard deviation of first landing place; shorter mean length of

skipped words; shorter fixation durations; smaller proportion of regressive saccades; reduced antisaccade cost; higher d´ accuracy scores. Change measures of antisaccade cost and fixation duration also reached statistical significance in the univariate analysis. This supports that our findings of Day effects in reading and task performance data are likely to be attributed to RECOGNeyes training, rather than purely test-retest effects.

8.1.2. ANS correlates

ANS measures of pupillometry (Chapter 5) and cardiac data (Chapter 6) reflected changes in the anticipatory period of pupil dilation and cardiac (heartrate) deceleration, respectively. These results corroborate previous findings that pupil dilation indexes greater LC-NE arousal, whereby in our study we observed phasic dilation in preparation for alerting responses to the target stimulus. In addition, our results support the idea that cardiac deceleration reflects an increase in the "vagal brake" to control preparations for orienting responses to the target stimulus. Also, our findings showed reduced mean pupil dilation and reduced mean heartrate in antisaccade trials compared to prosaccade trials, supporting the idea for overall increases in tonic PNS/vagal tone during antisaccade blocks.

Both increased rates of pupil dilation and cardiac deceleration correlated with better performance. Moreover, our study is the first to demonstrate that increased pupillary dilation and cardiac deceleration contribute to better task performance together. This reflects simultaneous

action of the sympathetic 'accelerator' that augments the LC-NE arousal system, as indexed by pupil dilation, working together with the parasympathetic 'vagal brake' for better preparatory inhibitory control processes that contribute to better performance.

Additionally, preparatory rate of pupil dilation was found to be a significantly larger factor than the rate of cardiac deceleration in our performance regression model, particularly target-elicited dilation. This could mean there a greater reliance on visual alerting mechanisms in order to perform more efficient responses compared to the action of the vagal brake, but that both are important to occur simultaneously in preparation to a stimulus. There was also no indication that the two measures were positively correlated, but instead the opposite whereby anticipatory cue-target pupil dilation and cardiac deceleration rates were negatively correlated with one another. Hence, the branches have additive effects on performance but subtractive effects on the respective organ, i.e., vagal activation limits pupil dilation, and increased phasic pupil dilation reduces the extent of the vagal brake. Therefore, this represents a positively-coupled relationship with RT, but a reciprocal relationship with respect to each other.

Furthermore, these correlations of ANS measures with RT revealed key trial type differences. Both individual and combined correlations of pupil dilation and cardiac deceleration rates with RT were stronger for antisaccade trials than for prosaccade trials. These findings support the

requirement of stronger inhibitory control and arousal processes to be recruited in preparation of voluntary antisaccade production combined with active prosaccade inhibition, than the mechanisms required for just making a reflexive prosaccade.

8.1.3. CNS correlates

MEG was used to assess the CNS correlates of cognitive control, which revealed a series of complex neurodynamics that mediate preparatory inhibitory control processes coordinated between regions of the visual attention network during the pro/antisaccade task. Stronger modulations of slow-frequency band delta and theta activity in posterior regions, compared to frontal regions, indicate a possible anteriorised mechanism for relaying bottom-up visual information to the frontal cortex. Also, timing mechanisms and phase resets have been previously attributed to these slow-wave frequency bands, so these findings could indicate these processes occurring across the visual attention network as well.

Our results of FEF alpha and R DLPFC beta time courses showed they positively increased in amplitude across the anticipatory period, but they did not replicate Hwang's findings for stronger modulation in antisaccade trials compared to prosaccade trials. However, our alpha FEF results still indicated significant increases in this region more than other ROIs in the visual attention network; thus, supporting previous findings for its role in facilitating top-down inhibitory control mechanisms.

Interestingly, the R PEF region showed alpha suppression, which indicated less inhibition of this region. Additionally, R PEF beta showed a very similar pattern to alpha-band data, whereby there was a larger beta ERD-ERS pattern in the R PEF compared to the L PEF. This supported previous reports of the PEF in playing an active role in preparing visuospatial processing, but that this is particularly lateralised to the right PEF, linking to stronger lateralisation of the right attentional network. This effect was greater in antisaccade trials, which indicated more preparatory action and extra resources required for vector inversion.

Observations of beta ERD and ERS from beta-band amplitude data and beta burst data revealed modulations of Day and Trial Type, whereby there was an additional late or "anticipatory" ERD prior to the target in antisaccades compared to prosaccade trials, and on Day 2 compared to Day 1. This could reflect the inhibitory control processing for antisaccade trials being generalised to overall increased inhibitory control processing on Day 2.

There were also bilateral Ant Ins decreases in the alpha and beta bands for antisaccade trials compared to prosaccade trials. Lateralised differences were observed in Ant Ins beta, whereby the L Ant Ins had the highest rate of beta bursts compared to all other visual attention network regions, and the R Ant Ins had greater trial type differences. Therefore, these modulations could link to salience network processing, which is particularly more important during antisaccadic processing, and

lateralisation effects may reflect differences in modulating ANS mechanisms.

Additional analyses, described in Appendix E, showed that greater exposure to RECOGNeyes training was associated with reduced FEF alpha and DLPFC beta. There were also task improvements associated with a larger reduction in DLPFC beta, which was associated with a reduction in in antisaccade RT cost. These results indicated reduced DLPFC beta was associated with improved gaze control. Moreover, resting-state connectivity fMRI analyses of these regions (also in Appendix E) found that increased RECOGNeyes exposure was associated with reduced homotopic connectivity, i.e., increased independence of hemispheric visual attention networks, as well as increased within-hemispheric connectivity in the left hemisphere. These are not CNS correlates per se, but correlates of cognitive control capacity, i.e., correlates of change-induced strengthening of the visual attention network. This reflects that RECOGNeyes could mediate plastic changes in brain regions associated with gaze-control, which is even present at rest when not actively engaging these network regions.

8.2. Implications and impact

8.2.1. Scientific research impact

This is the first study to utilise this novel experimental design, combining a cognitive control training paradigm with two assessment days consisting of MEG, autonomic measures, and reading assessment. Our ANS measures have discovered task performance correlations with both pupil dilation and cardiac deceleration rates, revealing valuable insights about the SNS and PNS balance within arousal mechanisms, alerting and orienting responses. Furthermore, our MEG findings outline preparatory neurodynamics across a range of frequency bands and propose a mechanism between different visual attention/oculomotor network regions that also mediate inhibitory control processes. This is one of the first studies to investigate neurodynamic activity of these frequency bands for this range of cortical visual attention and oculomotor network regions.

In addition, we have established key differences in trial type mechanisms, including differences in tonic and phasic arousal mechanisms, whereby both phasic LC-NE arousal indicated by pupil dilation rate and preparatory “vagal brake" cardiac deceleration rate for the orienting response are more corelated to antisaccade trial performance than prosaccade performance. There is also an indication for greater tonic PNS modulation (or less tonic SNS modulation) in antisaccade trials compared with prosaccade trials.

Moreover, CNS inhibitory control mechanisms reflected less inhibition of R PEF on antisaccade trials, indicating increased preparation for vector transformation processing. The Ant Ins also showed reduced alpha and beta amplitudes in antisaccade trials compared to prosaccade trials, which could be reflecting salience network and ANS processing differences between trial types. The findings from this study have therefore developed our understanding about preparation and anticipation for responding to a stimulus and the differences in the production of pro- and antisaccades.

In regards to changes between assessment days, the most notable CNS correlate of day change includes an additional "anticipatory" beta ERD during the anticipatory period just prior to target onset, after RECOGNeyes training. There was also increased overall amplitudes in the theta-band on Day 2, and specifically increased delta amplitude in V1 on Day 2. These findings were suggested to reflect stronger inhibitory control and top-down and bottom-up processes following RECOGNeyes training. Improvements in reading correlates across days was also a positive indicator of increased top-down inhibitory control due to better reading saccadic control responses. These day effect observations are unlikely to be solely due to test-retest effects, since RECOGNeyes exposure analysis supported that task performance, reading, and CNS correlates related with amount of exposure to RECOGNeyes training (see Appendix E). Overall, these findings provide support that top-down attentional networks can be trained with gaze-control RECOGNeyes training using oculomotor tasks.

In summary, this multimodal study has shown the value of using a wide range of measures, particularly for assessing CNS and ANS measures together. Therefore, these ideas could be used to aid the design of future research studies. Using a paradigm such as the pro/antisaccade task has shown its value in revealing specific physiological timing changes in the cue to target anticipatory period, so we can further understand the components involved in preparation and inhibitory control mechanisms. Therefore, these techniques and measures could be beneficial to utilise in future research, particularly for developing our understanding regarding top-down inhibitory processing, attention, and arousal.

8.2.2. Educational impact

Using RECOGNeyes as a gaze-control training tool for the inhibitory control of attention means it could be developed to be utilised as a unique educational tool specifically for ADHD and for other disorders affecting attention. RECOGNeyes has the advantages over first-line mediation treatments of avoiding medication-related side-effects in developing children, which would appeal to those parents who have hesitations about their children taking stimulant medications. Also, RECOGNeyes does not have the same barrier of requiring a medical prescription.

Due to the ease of its usability, set-up, and affordability of the technology, this means RECOGNeyes has the potential to be widely distributed in schools and be used by children with and without formal

diagnoses at school or at home. This means teachers could utilise this training tool to improve the engagement of inattentive children, who may experience problems with attention in the classroom and have traits of ADHD, but may not satisfy the full ADHD diagnostic criteria. Moreover, RECOGNeyes also has the capability to be adapted for different ages and abilities, since we found good engagement from an inattentive adult sample.

8.2.3. Diagnostic and clinical impact

The development of the RECOGNeyes training program has the potential for it to be offered as a first-line intervention for ADHD/SpLDs, and/or as an adjunct to medication. Furthermore, this study has highlighted the importance of the role of the ANS in arousal mechanisms for inhibitory control performance, thus implicating its role in attentional processing. Therefore, RECOGNeyes could be utilised in clinical settings to reveal autonomic profiles for attentional difficulties by simultaneously measuring ANS indices, like pupillometry and heartrate. This could be investigated further to develop diagnostic markers as well as using RECOGNeyes as a attention training tool for combatting ADHD symptoms.

Incorporating ANS measures could help us to tailor treatment interventions for different individuals who may have heterogeneous symptoms. Profiling atypical autonomic processes could also identify new targets for developing medication treatments that stabilise any imbalances in ANS drive. Overall, this study has examined the importance of exploring

non-pharmacological options that provide more treatment choices to help a wider range of individuals who may experience attentional problems. Therefore, there is a lot of scope for RECOGNeyes to be used in a clinical setting for ameliorating attentional problems and could even be potentially utilised as a diagnostic tool.

8.3. Limitations

There are limitations of the RECOGNeyes study that should be taken into consideration. Individual results chapters have outlined the specific methodological and experimental limitations relevant to that particular measure. A general limitation across the study though is the sample size, whereby not all participants completed all parts of each assessment, and some participants were excluded in final analyses. This means some analyses were underpowered, including day comparisons and cross-modality comparisons. It should be noted that this is an inattentive sample only including people with ADHD/SpLDs, so we cannot conclude that all of these findings apply to the wider population. Also, heterogeneity within each type of diagnosis/combination of diagnoses could have impacted the overall findings. This includes not screening for other common cooccurring neurodevelopmental disorders such as autism, so it may have been helpful to assess autistic symptoms as it may be a confounder for observed behavioural/physiological findings.

There could also be sample bias from recruiting mostly university level students, who are high-functioning and may not present all elements of ADHD/SpLD diagnoses. This should therefore be taken into account when developing RECOGNeyes training for use in school children, who are likely to be our main target in future developments of RECOGNeyes. Despite this, we still observed marked improvement in performance even in this current sample, who are likely to have developed effective strategies to manage their symptoms to some extent. Therefore, if benefits are observed in this cohort, individuals with greater impairment may have even greater gains from RECOGNeyes training.

8.4. Future directions and ideas

There are currently research proposals underway to develop the RECOGNeyes software and test the program more robustly in schoolchildren. This includes the idea of implementing biofeedback within the training by using autonomic measures of pupillometry and heartrate and portable EEG to detect neural activity, which modulate the game soundtrack. This would enable the player to learn how to modulate their physiological state to enhance their attention for optimal performance. Developing RECOGNeyes further could lead to larger scale availability of the training program and distribution to schools/parents of children with attentional difficulties. It would also be beneficial to conduct more longitudinal studies to establish the long-term effects and benefits of RECOGNeyes.

In conclusion, RECOGNeyes has helped to establish the benefits of using gaze-control training to target attentional difficulties. Hence, this could pave the way for the development of other types of games, training platforms for attentional training, and targeting other cognitive functions. For instance, this could include developing smartphone app versions and linking to personal devices such as smart watches that can record biometrics including heartrate, blood pressure, etc. RECOGNeyes could also be expanded in the future for different neurodevelopmental conditions such as autism, psychiatric conditions, or individuals without any formal diagnoses. This could involve incorporating suitable game features for different diagnoses, e.g., different sensory features more suited to people with autism.

More generally, our multimodal approach could be applied to a wider range of studies to assess other cognitive processes and neurodevelopmental changes. Moreover, further research could be undertaken to understand the different autonomic profiles and biomarkers for ADHD and SpLDs in terms of arousal and CNS function and how this relates to symptomology.

References

1-D data interpolation (table lookup) - MATLAB interp1 - MathWorks United Kingdom. (n.d.). MathWorks. Retrieved September 1, 2021, from https://uk.mathworks.com/help/matlab/ref/interp1.html?searchHighlight=interp1&s_tid=srchtitle#btwp6lt-1-xq

Achtman, R. L., Green, C. S., & Bavelier, D. (2008). Video games as a tool to train visual skills. *Restorative Neurology and Neuroscience*, *26*(4–5), 435–446. https://www.ncbi.nlm.nih.gov/pmc/articles/PMC2884279/

Agnew-Blais, J. C., Polanczyk, G. V., Danese, A., Wertz, J., Moffitt, T. E., & Arseneault, L. (2018). Young adult mental health and functional outcomes among individuals with remitted, persistent and late-onset ADHD. *British Journal of Psychiatry*, *213*(3), 526–534. https://doi.org/10.1192/bjp.2018.97

Aksayli, N. D., Sala, G., & Gobet, F. (2019). The cognitive and academic benefits of Cogmed: A meta-analysis. *Educational Research Review*, *27*, 229–243. https://doi.org/10.1016/j.edurev.2019.04.003

Al-Shathri, A., Al-Wabil, A., & Al-Ohali, Y. (2013). Eye-controlled games for behavioral therapy of attention deficit disorders. *In: Stephanidis C. (Eds) HCI International 2013 - Posters' Extended Abstracts. HCI 2013. Communications in Computer and Information Science*, *373*(PART I),

574–578. https://doi.org/10.1007/978-3-642-39473-7_114

Amador, N., Schlag-Rey, M., & Schlag, J. (2004). Primate Antisaccade. II. Supplementary Eye Field Neuronal Activity Predicts Correct Performance. *Journal of Neurophysiology*, *91*(4), 1672–1689. https://doi.org/10.1152/jn.00138.2003

American Psychiatric Association. (2013). *Diagnostic and Statistical Manual of Mental Disorders: DSM-5* (5th ed.). American Psychiatric Association. https://doi.org/10.1176/APPI.BOOKS.9780890425596

Amzica, F., & Steriade, M. (1998). Electrophysiological correlates of sleep delta waves. *Electroencephalography and Clinical Neurophysiology*, *107*(2), 69–83. https://doi.org/10.1016/S0013-4694(98)00051-0

Andersen, R. A., Brotchie, P. R., & Mazzoni, P. (1992). Evidence for the lateral intraparietal area as the parietal eye field. *Current Opinion in Neurobiology*, *2*(6), 840–846. https://doi.org/10.1016/0959-4388(92)90143-9

Androulakis, X. M., Krebs, K., Peterlin, B. L., Zhang, T., Maleki, N., Sen, S., Rorden, C., & Herath, P. (2017). Modulation of intrinsic resting-state fMRI networks in women with chronic migraine. *Neurology*, *89*(2), 163–169. https://doi.org/10.1212/WNL.0000000000004089

Antshel, K. M., & Barkley, R. (2008). Psychosocial Interventions in Attention Deficit Hyperactivity Disorder. *Child and Adolescent Psychiatric Clinics of North America*, *17*(2), 421–437.

https://doi.org/10.1016/j.chc.2007.11.005

Antzaka, A., Lallier, M., Meyer, S., Diard, J., Carreiras, M., & Valdois, S. (2017). Enhancing reading performance through action video games: The role of visual attention span. *Scientific Reports*, *7*(14563), 1–10. https://doi.org/10.1038/s41598-017-15119-9

Armstrong, I. T., & Munoz, D. P. (2003). Inhibitory control of eye movements during oculomotor countermanding in adults with attention-deficit hyperactivity disorder. *Experimental Brain Research*, *152*(4), 444–452. https://doi.org/10.1007/s00221-003-1569-3

Arnal, L. H. (2012). Predicting "when" using the motor system's beta-band oscillations. *Frontiers in Human Neuroscience*, *6*(225), 1–3. https://doi.org/10.3389/fnhum.2012.00225

Arnal, L. H., Doelling, K. B., & Poeppel, D. (2015). Delta-beta coupled oscillations underlie temporal prediction accuracy. *Cerebral Cortex*, *25*(9), 3077–3085. https://doi.org/10.1093/cercor/bhu103

Arnal, L. H., & Kleinschmidt, A. K. (2017). Entrained delta oscillations reflect the subjective tracking of time. *Communicative & Integrative Biology*, *10*(5–6), e1349583. https://doi.org/10.1080/19420889.2017.1349583

Arnsten, A. F. T., & Pliszka, S. R. (2011). Catecholamine influences on prefrontal cortical function: Relevance to treatment of attention deficit/hyperactivity disorder and related disorders. *Pharmacology*

Biochemistry and Behavior, *99*(2), 211–216. https://doi.org/10.1016/j.pbb.2011.01.020

Aron, A. R., Robbins, T. W., & Poldrack, R. A. (2004). Inhibition and the right inferior frontal cortex. *Trends in Cognitive Sciences*, *8*(4), 170–177. https://doi.org/10.1016/j.tics.2004.02.010

Arora, I., Bellato, A., Ropar, D., Hollis, C., & Groom, M. J. (2021). Is autonomic function during resting-state atypical in Autism: A systematic review of evidence. *Neuroscience and Biobehavioral Reviews*, *125*, 417–441. https://doi.org/10.1016/j.neubiorev.2021.02.041

Ásgeirsson, Á. G., & Nieuwenhuis, S. (2017). No arousal-biased competition in focused visuospatial attention. *Cognition*, *168*, 191–204. https://doi.org/10.1016/j.cognition.2017.07.001

Astle, D. E., Barnes, J. J., Baker, K., Colclough, G. L., & Woolrich, M. W. (2015). Cognitive training enhances intrinsic brain connectivity in childhood. *Journal of Neuroscience*, *35*(16), 6277–6283. https://doi.org/10.1523/JNEUROSCI.4517-14.2015

Aston-Jones, G., & Cohen, J. D. (2005). An integrative theory of locus coeruleus-norepinephrine function: Adaptive gain and optimal performance. *Annual Review of Neuroscience*, *28*(1), 403–450. https://doi.org/10.1146/annurev.neuro.28.061604.135709

Aston-Jones, G., Rajkowski, J., Kubiak, P., & Alexinsky, T. (1994). Locus coeruleus neurons in monkey are selectively activated by attended cues

in a vigilance task. *Journal of Neuroscience*, *14*(7), 4467–4480. https://doi.org/10.1523/jneurosci.14-07-04467.1994

Babo-Rebelo, M., Buot, A., & Tallon-Baudry, C. (2019). Neural responses to heartbeats distinguish self from other during imagination. *Neuroimage*, *191*, 10. https://doi.org/10.1016/J.NEUROIMAGE.2019.02.012

Babo-Rebelo, M., Richter, C. G., & Tallon-Baudry, C. (2016). Neural Responses to Heartbeats in the Default Network Encode the Self in Spontaneous Thoughts. *The Journal of Neuroscience*, *36*(30), 7829. https://doi.org/10.1523/JNEUROSCI.0262-16.2016

Baillet, S. (2017). Magnetoencephalography for brain electrophysiology and imaging. *Nature Neuroscience*, *20*(3), 327–339. https://doi.org/10.1038/nn.4504

Baillet, S., Mosher, J. C., & Leahy, R. M. (2001). Electromagnetic brain mapping. *IEEE Signal Processing Magazine*, *18*(6), 14–30. https://doi.org/10.1109/79.962275

Banaschewski, T., Roessner, V., Dittmann, R. W., Santosh, P. J., & Rothenberger, A. (2004). Non-stimulant medications in the treatment of ADHD. *European Child and Adolescent Psychiatry, Supplement*, *13*(1), i102–i116. https://doi.org/10.1007/s00787-004-1010-x

Barkley, R. A. (1997). Behavioral inhibition, sustained attention, and executive functions: Constructing a unifying theory of ADHD.

Psychological Bulletin, *121*(1), 65–94. https://doi.org/10.1037/0033-2909.121.1.65

Barkley, R. A. (2002). Psychosocial treatments for attention-deficit/hyperactivity disorder in children. *Journal of Clinical Psychiatry*, *63*(Suppl. 12), 36–43. https://www.psychiatrist.com/jcp/neurodevelopmental/adhd/psychosocial-treatments-attention-deficit-hyperactivity

Barnes, J. J., Nobre, A. C., Woolrich, M. W., Baker, K., & Astle, D. E. (2016). Training working memory in childhood enhances couplinbetween frontoparietal control network and task-related regions. *Journal of Neuroscience*, *36*(34), 9001–9011. https://doi.org/10.1523/JNEUROSCI.0101-16.2016

Barold, S. S. (2003). Willem Einthoven and the birth of clinical electrocardiography a hundred years ago. *Cardiac Electrophysiology Review*, *7*(1), 99–104. https://doi.org/10.1023/A:1023667812925

Barry, R. J., Clarke, A. R., & Johnstone, S. J. (2003). A review of electrophysiology in attention-deficit/hyperactivity disorder: I. Qualitative and quantitative electroencephalography. *Clinical Neurophysiology*, *114*(2), 171–183. https://doi.org/10.1016/S1388-2457(02)00362-0

Basak, C., Boot, W. R., Voss, M. W., & Kramer, A. F. (2008). Can Training in a Real-Time Strategy Video Game Attenuate Cognitive Decline in

Older Adults? *Psychology and Aging*, *23*(4), 765–777. https://doi.org/10.1037/a0013494

Bast, N., Poustka, L., & Freitag, C. M. (2018). The locus coeruleus–norepinephrine system as pacemaker of attention – a developmental mechanism of derailed attentional function in autism spectrum disorder. *European Journal of Neuroscience*, *47*(2), 115–125. https://doi.org/10.1111/ejn.13795

Bavelier, D., & Green, C. S. (2019). Enhancing Attentional Control: Lessons from Action Video Games. *Neuron*, *104*(1), 147–163. https://doi.org/10.1016/j.neuron.2019.09.031

Baweja, R., Hale, D. E., & Waxmonsky, J. G. (2021). Impact of CNS Stimulants for Attention-Deficit/Hyperactivity Disorder on Growth: Epidemiology and Approaches to Management in Children and Adolescents. *CNS Drugs*, *35*(8), 839–859. https://doi.org/10.1007/S40263-021-00841-W

Bear, M. F., Connors, B. W., & Paradiso, M. A. (2007). *Neuroscience: Exploring the brain* (3rd ed.). Lippincott Williams & Wilkins Publishers.

Beatty, J. (1982a). Task-evoked pupillary responses, processing load, and the structure of processing resources. *Psychological Bulletin*, *91*(2), 276–292. https://doi.org/10.1037/0033-2909.91.2.276

Beatty, J. (1982b). Phasic Not Tonic Pupillary Responses Vary With

Auditory Vigilance Performance. *Psychophysiology*, *19*(2), 167–172. https://doi.org/10.1111/j.1469-8986.1982.tb02540.x

Beck, S. J., Hanson, C. A., Puffenberger, S. S., Benninger, K. L., & Benninger, W. B. (2010). A controlled trial of working memory training for children and adolescents with ADHD. *Journal of Clinical Child and Adolescent Psychology*, *39*(6), 825–836. https://doi.org/10.1080/15374416.2010.517162

Beissner, F., Meissner, K., Bär, K. J., & Napadow, V. (2013). The autonomic brain: An activation likelihood estimation meta-analysis for central processing of autonomic function. *Journal of Neuroscience*, *33*(25), 10503–10511. https://doi.org/10.1523/JNEUROSCI.1103-13.2013

Belchior, P., Marsiske, M., Sisco, S. M., Yam, A., Bavelier, D., Ball, K., & Mann, W. C. (2013). Video game training to improve selective visual attention in older adults. *Computers in Human Behavior*, *29*(4), 1318–1324. https://doi.org/10.1016/j.chb.2013.01.034

Bellato, A., Arora, I., Hollis, C., & Groom, M. J. (2020). Is autonomic nervous system function atypical in attention deficit hyperactivity disorder (ADHD)? A systematic review of the evidence. *Neuroscience and Biobehavioral Reviews*, *108*, 182–206. https://doi.org/10.1016/j.neubiorev.2019.11.001

Bellato, A., Arora, I., Kochhar, P., Hollis, C., & Groom, M. J. (2020). Atypical electrophysiological indices of eyes-open and eyes-closed resting-state

in children and adolescents with ADHD and autism. *Brain Sciences*, *10*(5), 272. https://doi.org/10.3390/brainsci10050272

Bellato, A., Arora, I., Kochhar, P., Ropar, D., Hollis, C., & Groom, M. J. (2021). Heart Rate Variability in Children and Adolescents with Autism, ADHD and Co-occurring Autism and ADHD, During Passive and Active Experimental Conditions. *Journal of Autism and Developmental Disorders*. https://doi.org/10.1007/s10803-021-05244-w

Bellato, A., Norman, L., Idrees, I., Ogawa, C. Y., Waitt, A., Zuccolo, P. F., Tye, C., Radua, J., Groom, M. J., & Shephard, E. (2021). A systematic review and meta-analysis of altered electrophysiological markers of performance monitoring in Obsessive-Compulsive Disorder (OCD), Gilles de la Tourette Syndrome (GTS), Attention-Deficit/Hyperactivity disorder (ADHD) and Autism. *Neuroscience & Biobehavioral Reviews*, *131*, 964–987. https://doi.org/10.1016/J.NEUBIOREV.2021.10.018

Bellocchi, S., Muneaux, M., Bastien-Toniazzo, M., & Ducrot, S. (2013). I can read it in your eyes: What eye movements tell us about visuo-attentional processes in developmental dyslexia. *Research in Developmental Disabilities*, *34*(1), 452–460. https://doi.org/10.1016/j.ridd.2012.09.002

Bells, S., Isabella, S. L., Brien, D. C., Coe, B. C., Munoz, D. P., Mabbott, D. J., & Cheyne, D. O. (2020). Mapping neural dynamics underlying saccade preparation and execution and their relation to reaction time and direction errors. *Human Brain Mapping*, *41*(7), 1934–1949.

https://doi.org/10.1002/hbm.24922

Belyusar, D., Snyder, A. C., Frey, H. P., Harwood, M. R., Wallman, J., & Foxe, J. J. (2013). Oscillatory alpha-band suppression mechanisms during the rapid attentional shifts required to perform an anti-saccade task. *NeuroImage*, *65*, 395–407. https://doi.org/10.1016/j.neuroimage.2012.09.061

Benoit, J. J., Roudaia, E., Johnson, T., Love, T., & Faubert, J. (2020). The neuropsychological profile of professional action video game players. *PeerJ*, *8*, e10211. https://doi.org/10.7717/peerj.10211

Berger, H. (1929). Über das Elektroenkephalogramm des Menschen. *Archiv Für Psychiatrie Und Nervenkrankheiten*, *87*, 527–570. http://www.citeulike.org/user/Philibikus/article/3907383

Berger, I., Dor, T., Nevo, Y., & Goldzweig, G. (2008). Attitudes toward attention-deficit hyperactivity disorder (ADHD) treatment: Parents' and children's perspectives. *Journal of Child Neurology*, *23*(9), 1036–1042. https://doi.org/10.1177/0883073808317726

Berntson, G. G., Cacioppo, J. T., Quigley, K. S., & Fabro, V. T. (1994). Autonomic space and psychophysiological response. *Psychophysiology*, *31*(1), 44–61. https://doi.org/10.1111/j.1469-8986.1994.tb01024.x

Berridge, C. W., Devilbiss, D. M., Andrzejewski, M. E., Arnsten, A. F. T., Kelley, A. E., Schmeichel, B., Hamilton, C., & Spencer, R. C. (2006). Methylphenidate Preferentially Increases Catecholamine

Neurotransmission within the Prefrontal Cortex at Low Doses that Enhance Cognitive Function. *Biological Psychiatry*, *60*(10), 1111–1120. https://doi.org/10.1016/j.biopsych.2006.04.022

Berridge, C. W., & Waterhouse, B. D. (2003). The locus coeruleus-noradrenergic system: Modulation of behavioral state and state-dependent cognitive processes. *Brain Research Reviews*, *42*(1), 33–84. https://doi.org/10.1016/S0165-0173(03)00143-7

Bertoni, S., Franceschini, S., Puccio, G., Mancarella, M., Gori, S., & Facoetti, A. (2021). Action video games enhance attentional control and phonological decoding in children with developmental dyslexia. *Brain Sciences*, *11*(2), 1–18. https://doi.org/10.3390/brainsci11020171

Bibi, R., & Edelman, J. A. (2009). The influence of motor training on human express saccade production. *Journal of Neurophysiology*, *102*(6), 3101–3110. https://doi.org/10.1152/jn.90710.2008

Bigger, J. T., Albrecht, P., Steinman, R. C., Rolnitzky, L. M., Fleiss, J. L., & Cohen, R. J. (1989). Comparison of time- and frequency domain-based measures of cardiac parasympathetic activity in Holter recordings after myocardial infarction. *The American Journal of Cardiology*, *64*(8), 536–538. https://doi.org/10.1016/0002-9149(89)90436-0

Bikic, A., Leckman, J. F., Christensen, T., Bilenberg, N., & Dalsgaard, S. (2018). Attention and executive functions computer training for attention-deficit/hyperactivity disorder (ADHD): results from a

randomized, controlled trial. *European Child and Adolescent Psychiatry*, *27*(12), 1563–1574. https://doi.org/10.1007/s00787-018-1151-y

Bikic, A., Leckman, J. F., Lindschou, J., Christensen, T. O., & Dalsgaard, S. (2015). Cognitive computer training in children with attention deficit hyperactivity disorder (ADHD) versus no intervention: study protocol for a randomized controlled trial. *Trials*, *16*(1). https://doi.org/10.1186/S13063-015-0975-8

Bilbao, C., & Piñero, D. P. (2020). Diagnosis of oculomotor anomalies in children with learning disorders. *Clinical and Experimental Optometry*, *103*(5), 597–609. https://doi.org/10.1111/cxo.13024

Biotteau, M., Danna, J., Baudou, É., Puyjarinet, F., Velay, J. L., Albaret, J. M., & Chaix, Y. (2019). Developmental coordination disorder and dysgraphia: Signs and symptoms, diagnosis, and rehabilitation. *Neuropsychiatric Disease and Treatment*, *15*, 1873–1885. https://doi.org/10.2147/NDT.S120514

Birbaumer, N., Veit, R., Lotze, M., Erb, M., Hermann, C., Grodd, W., & Flor, H. (2005). Deficient fear conditioning in psychopathy: A functional magnetic resonance imaging study. *Archives of General Psychiatry*, *62*(7), 799–805. https://doi.org/10.1001/archpsyc.62.7.799

Biscaldi, M., Fischer, B., & Hartnegg, K. (2000). Voluntary saccadic control in dyslexia. *Perception*, *29*(5), 509–521. https://doi.org/10.1068/p2666a

Blaser, E., Eglington, L., Carter, A. S., & Kaldy, Z. (2014). Pupillometry reveals a mechanism for the Autism Spectrum Disorder (ASD) advantage in visual tasks. *Scientific Reports*, *4*(1), 1–5. https://doi.org/10.1038/srep04301

Boot, W. R., Kramer, A. F., Simons, D. J., Fabiani, M., & Gratton, G. (2008). The effects of video game playing on attention, memory, and executive control. *Acta Psychologica*, *129*(3), 387–398. https://doi.org/10.1016/j.actpsy.2008.09.005

Borbély, A. A., Tobler, I., Loepfe, M., Kupfer, D. J., Ulrich, R. F., Grochocinski, V., Doman, J., & Matthews, G. (1984). All-night spectral analysis of the sleep EEG in untreated depressives and normal controls. *Psychiatry Research*, *12*(1), 27–33. https://doi.org/10.1016/0165-1781(84)90135-5

Boto, E., Bowtell, R., Krüger, P., Fromhold, T. M., Morris, P. G., Meyer, S. S., Barnes, G. R., & Brookes, M. J. (2016). On the potential of a new generation of magnetometers for MEG: A beamformer simulation study. *PLoS ONE*, *11*(8), e0157655. https://doi.org/10.1371/journal.pone.0157655

Bradley, M. M., Keil, A., & Lang, P. J. (2012). Orienting and Emotional Perception: Facilitation, Attenuation, and Interference. *Frontiers in Psychology*, *0*(NOV), 493. https://doi.org/10.3389/FPSYG.2012.00493

Breukelaar, I. A., Antees, C., Grieve, S. M., Foster, S. L., Gomes, L.,

Williams, L. M., & Korgaonkar, M. S. (2017). Cognitive control network anatomy correlates with neurocognitive behavior: A longitudinal study. *Human Brain Mapping*, *38*(2), 631–643. https://doi.org/10.1002/hbm.23401

Brier, M. R., Thomas, J. B., Snyder, A. Z., Benzinger, T. L., Zhang, D., Raichle, M. E., Holtzman, D. M., Morris, J. C., & Ances Dr., B. M. (2012). Loss of intranetwork and internetwork resting state functional connections with Alzheimer's disease progression. *Journal of Neuroscience*, *32*(26), 8890–8899. https://doi.org/10.1523/JNEUROSCI.5698-11.2012

Briley, P. M., Liddle, E. B., Groom, M. J., Smith, H. J. F., Morris, P. G., Colclough, G. L., Brookes, M. J., & Liddle, P. F. (2018). Development of human electrophysiological brain networks. *Journal of Neurophysiology*, *120*(6), 3122–3130. https://doi.org/10.1152/jn.00293.2018

Briley, P. M., Liddle, E. B., Simmonite, M., Jansen, M., White, T. P., Balain, V., Palaniyappan, L., Bowtell, R., Mullinger, K. J., & Liddle, P. F. (2021). Regional Brain Correlates of Beta Bursts in Health and Psychosis: A Concurrent Electroencephalography and Functional Magnetic Resonance Imaging Study. *Biological Psychiatry: Cognitive Neuroscience and Neuroimaging*, *6*(12), 1145–1156. https://doi.org/10.1016/j.bpsc.2020.10.018

Brodde, O. E., Bruck, H., Leineweber, K., & Seyfarth, T. (2001). Presence,

distribution and physiological function of adrenergic and muscarinic receptor subtypes in the human heart. *Basic Research in Cardiology*, *96*(6), 528–538. https://doi.org/10.1007/s003950170003

Brodde, O. E., & Michel, M. C. (1999). Adrenergic and muscarinic receptors in the human heart. *Pharmacological Reviews*, *51*(4), 651–689. https://pharmrev.aspetjournals.org/content/51/4/651.short

Brookes, M. J., Vrba, J., Robinson, S. E., Stevenson, C. M., Peters, A. M., Barnes, G. R., Hillebrand, A., & Morris, P. G. (2008). Optimising experimental design for MEG beamformer imaging. *NeuroImage*, *39*(4), 1788–1802. https://doi.org/10.1016/j.neuroimage.2007.09.050

Brown, K. A., Samuel, S., & Patel, D. R. (2018). Pharmacologic management of attention deficit hyperactivity disorder in children and adolescents: A review for practitioners. *Translational Pediatrics*, *7*(1), 36–47. https://doi.org/10.21037/tp.2017.08.02

Brown, M. R. G., Goltz, H. C., Vilis, T., Ford, K. A., & Everling, S. (2006). Inhibition and generation of saccades: Rapid event-related fMRI of prosaccades, antisaccades, and nogo trials. *NeuroImage*, *33*(2), 644–659. https://doi.org/10.1016/j.neuroimage.2006.07.002

Brown, M. R. G., Vilis, T., & Everling, S. (2007). Frontoparietal activation with preparation for antisaccades. *Journal of Neurophysiology*, *98*(3), 1751–1762. https://doi.org/10.1152/jn.00460.2007

Bruce, C. J., & Goldberg, M. E. (1985). Primate frontal eye fields. I. Single

neurons discharging before saccades. *Journal of Neurophysiology*, *53*(3), 603–635. https://doi.org/10.1152/jn.1985.53.3.603

Brunoni, A. R., & Vanderhasselt, M. A. (2014). Working memory improvement with non-invasive brain stimulation of the dorsolateral prefrontal cortex: A systematic review and meta-analysis. *Brain and Cognition*, *86*(1), 1–9. https://doi.org/10.1016/j.bandc.2014.01.008

Bueno, V. F., Kozasa, E. H., Da Silva, M. A., Alves, T. M., Louzã, M. R., & Pompeiá, S. (2015). Mindfulness meditation improves mood, quality of life, and attention in adults with attention deficit hyperactivity disorder. *BioMed Research International*, *2015*(Article ID: 962857), 1–14. https://doi.org/10.1155/2015/962857

Butterworth filter design - MATLAB butter - MathWorks United Kingdom. (n.d.). MathWorks. Retrieved August 31, 2021, from https://uk.mathworks.com/help/signal/ref/butter.html?s_tid=doc_ta#bucsinx

Buzsáki, G. (2002). Theta oscillations in the hippocampus. *Neuron*, *33*(3), 325–340. https://doi.org/10.1016/S0896-6273(02)00586-X

Buzsáki, G. (2005). Theta rhythm of navigation: Link between path integration and landmark navigation, episodic and semantic memory. *Hippocampus*, *15*(7), 827–840. https://doi.org/10.1002/hipo.20113

Buzsáki, G. (2006). *Rhythms of the Brain*. Oxford University Press. https://doi.org/10.1093/acprof:oso/9780195301069.001.0001

Cameron, I. G. M., Riddle, J. M., & D'Esposito, M. (2015). Dissociable roles of dorsolateral prefrontal cortex and frontal eye fields during saccadic eye movements. *Frontiers in Human Neuroscience*, *9*(613), 1–14. https://doi.org/10.3389/fnhum.2015.00613

Capotosto, P., Babiloni, C., Romani, G. L., & Corbetta, M. (2009). Frontoparietal cortex controls spatial attention through modulation of anticipatory alpha rhythms. *Journal of Neuroscience*, *29*(18), 5863–5872. https://doi.org/10.1523/JNEUROSCI.0539-09.2009

Carpenter, R. H. S. (2001). Express saccades: is bimodality a result of the order of stimulus presentation? *Vision Research*, *41*(9), 1145–1151. https://doi.org/10.1016/S0042-6989(01)00007-4

Cavanagh, J. F., & Frank, M. J. (2014). Frontal theta as a mechanism for cognitive control. *Trends in Cognitive Sciences*, *18*(8), 414–421. https://doi.org/10.1016/j.tics.2014.04.012

Cavanagh, J. F., Zambrano-Vazquez, L., & Allen, J. J. B. (2012). Theta lingua franca: A common mid-frontal substrate for action monitoring processes. *Psychophysiology*, *49*(2), 220–238. https://doi.org/10.1111/j.1469-8986.2011.01293.x

Cechetto, D. F., & Shoemaker, J. K. (2009). Functional neuroanatomy of autonomic regulation. *NeuroImage*, *47*(3), 795–803. https://doi.org/10.1016/j.neuroimage.2009.05.024

Chamorro, Y., Betz, L. T., Philipsen, A., Kambeitz, J., & Ettinger, U. (2021).

The Eyes Have It: A Meta-analysis of Oculomotor Inhibition in Attention-Deficit/Hyperactivity Disorder. *Biological Psychiatry: Cognitive Neuroscience and Neuroimaging*. https://doi.org/10.1016/j.bpsc.2021.05.004

Chan, E., Fogler, J. M., & Hammerness, P. G. (2016). Treatment of attention-deficit/hyperactivity disorder in adolescents: A systematic review. *JAMA - Journal of the American Medical Association*, *315*(18), 1997–2008. https://doi.org/10.1001/jama.2016.5453

Chang, C., & Glover, G. H. (2010). Time-frequency dynamics of resting-state brain connectivity measured with fMRI. *NeuroImage*, *50*(1), 81–98. https://doi.org/10.1016/j.neuroimage.2009.12.011

Cheadle, S., Wyart, V., Tsetsos, K., Myers, N., DeGardelle, V., HerceCastañón, S., & Summerfield, C. (2014). Adaptive gain control during human perceptual choice. *Neuron*, *81*(6), 1429–1441. https://doi.org/10.1016/j.neuron.2014.01.020

Chen, A. C. N., Feng, W., Zhao, H., Yin, Y., & Wang, P. (2008). EEG default mode network in the human brain: Spectral regional field powers. *NeuroImage*, *41*(2), 561–574. https://doi.org/10.1016/j.neuroimage.2007.12.064

Christov, I. I., & Daskalov, I. K. (1999). Filtering of electromyogram artifacts from the electrocardiogram. *Medical Engineering and Physics*, *21*(10), 731–736. https://doi.org/10.1016/S1350-4533(99)00098-3

Christov, I. I., Neycheva, T., & Schmid, R. (2017). Fine tuning of the dynamic low-pass filter for electromyographic noise suppression in electrocardiograms. *Computing in Cardiology*, *44*, 1–4. https://doi.org/10.22489/CinC.2017.088-007

Cieslik, E. C., Zilles, K., Caspers, S., Roski, C., Kellermann, T. S., Jakobs, O., Langner, R., Laird, A. R., Fox, P. T., & Eickhoff, S. B. (2013). Is there one DLPFC in cognitive action control? Evidence for heterogeneity from Co-activation-based parcellation. *Cerebral Cortex*, *23*(11), 2677–2689. https://doi.org/10.1093/cercor/bhs256

Coe, B. C., & Munoz, D. P. (2017). Mechanisms of saccade suppression revealed in the anti-saccade task. *Philosophical Transactions of the Royal Society B: Biological Sciences*, *372*(1718), 20160192. https://doi.org/10.1098/rstb.2016.0192

Coe, B. C., Tomihara, K., Matsuzawa, M., & Hikosaka, O. (2002). Visual and Anticipatory Bias in Three Cortical Eye Fields of the Monkey during an Adaptive Decision-Making Task. *Journal of Neuroscience*, *22*(12), 5081–5090. https://doi.org/10.1523/jneurosci.22-12-05081.2002

Coe, B. C., Trappenberg, T., & Munoz, D. P. (2019). Modeling saccadic action selection: Cortical and basal ganglia signals coalesce in the superior colliculus. *Frontiers in Systems Neuroscience*, *13*(3), 1–22. https://doi.org/10.3389/fnsys.2019.00003

Cohen, D. (1968). Magnetoencephalography: Evidence of magnetic fields

produced by alpha-rhythm currents. *Science*, *161*(3843), 784–786. https://doi.org/10.1126/science.161.3843.784

Cohen, D. (1972). Magnetoencephalography: Detection of the brain's electrical activity with a superconducting magnetometer. *Science*, *175*(4022), 664–666. https://doi.org/10.1126/science.175.4022.664

Colavita, F. B. (1974). Human sensory dominance. *Perception & Psychophysics*, *16*(2), 409–412. https://doi.org/10.3758/BF03203962

Cole, M. W., & Schneider, W. (2007). The cognitive control network: Integrated cortical regions with dissociable functions. *NeuroImage*, *37*(1), 343–360. https://doi.org/10.1016/j.neuroimage.2007.03.071

Collins, D. L., Zijdenbos, A. P., Kollokian, V., Sled, J. G., Kabani, N. J., Holmes, C. J., & Evans, A. C. (1998). Design and construction of a realistic digital brain phantom. *IEEE Transactions on Medical Imaging*, *17*(3), 463–468. https://doi.org/10.1109/42.712135

Collins, P. (2016). *The remediation of oculomotor and attentional deficits of children with ADHD: identifying and training control mechanisms based on ocular data* [Doctoral Thesis, University of Nottingham]. http://eprints.nottingham.ac.uk/31898/

Conners, K. C., Ehrhard, D., & Sparrow, E. P. (1999). *Conners' adult ADHD rating scales (CAARS): technical manual.* North Tonawanda, NY: Multi-Health Systems.

Connolly, J. D., Goodale, M. A., Goltz, H. C., & Munoz, D. P. (2005). fMRI activation in the human frontal eye field is correlated with saccadic reaction time. *Journal of Neurophysiology*, *94*(1), 605–611. https://doi.org/10.1152/jn.00830.2004

Connor, D. F., Steeber, J., & McBurnett, K. (2010). A review of attention-deficit/hyperactivity disorder complicated by symptoms of oppositional defiant disorder or conduct disorder. *Journal of Developmental and Behavioral Pediatrics*, *31*(5), 427–440. https://doi.org/10.1097/DBP.0b013e3181e121bd

Cooke, A., Kavussanu, M., Gallicchio, G., Willoughby, A., Mcintyre, D., & Ring, C. (2014). Preparation for action: Psychophysiological activity preceding a motor skill as a function of expertise, performance outcome, and psychological pressure. *Psychophysiology*, *51*(4), 374–384. https://doi.org/10.1111/psyp.12182

Cooper, P. S., Wong, A. S. W., McKewen, M., Michie, P. T., & Karayanidis, F. (2017). Frontoparietal theta oscillations during proactive control are associated with goal-updating and reduced behavioral variability. *Biological Psychology*, *129*, 253–264. https://doi.org/10.1016/j.biopsycho.2017.09.008

Corbetta, M., Patel, G., & Shulman, G. L. (2008). The Reorienting System of the Human Brain: From Environment to Theory of Mind. *Neuron*, *58*(3), 306–324. https://doi.org/10.1016/j.neuron.2008.04.017

Corbetta, M., & Shulman, G. L. (2002). Control of goal-directed and stimulus-driven attention in the brain. *Nature Reviews Neuroscience*, *3*(3), 201–215. https://doi.org/10.1038/nrn755

Cornwell, B. R., Mueller, S. C., Kaplan, R., Grillon, C., & Ernst, M. (2012). Anxiety, a benefit and detriment to cognition: Behavioral and magnetoencephalographic evidence from a mixed-saccade task. *Brain and Cognition*, *78*(3), 257–267. https://doi.org/10.1016/j.bandc.2012.01.002

Cortese, S., Ferrin, M., Brandeis, D., Buitelaar, J., Daley, D., Dittmann, R. W., Holtmann, M., Santosh, P., Stevenson, J., Stringaris, A., Zuddas, A., & Sonuga-Barke, E. J. S. (2015). Cognitive training for attention-deficit/hyperactivity disorder: Meta-analysis of clinical and neuropsychological outcomes from randomized controlled trials. *Journal of the American Academy of Child and Adolescent Psychiatry*, *54*(3), 164–174. https://doi.org/10.1016/j.jaac.2014.12.010

Cottyn, J., De Clercq, D., Crombez, G., & Lenoir, M. (2008). The role of preparatory heart rate deceleration on balance beam performance. *Journal of Sport and Exercise Psychology*, *30*(2), 159–170. https://doi.org/10.1123/jsep.30.2.159

Coull, J. T., Frith, C. D., Büchel, C., & Nobre, A. C. (2000). Orienting attention in time: Behavioural and neuroanatomical distinction between exogenous and endogenous shifts. *Neuropsychologia*, *38*(6), 808–819. https://doi.org/10.1016/S0028-3932(99)00132-3

Coull, J. T., Nobre, A. C., & Frith, C. D. (2001). The noradrenergic α2 agonist clonidine modulates behavioural and neuroanatomical correlates of human attentional orienting and alerting. *Cerebral Cortex*, *11*(1), 73–84. https://doi.org/10.1093/cercor/11.1.73

Craig, A. D. (2005). Forebrain emotional asymmetry: A neuroanatomical basis? *Trends in Cognitive Sciences*, *9*(12), 566–571. https://doi.org/10.1016/j.tics.2005.10.005

Craig, A. D. (2009). How do you feel - now? The anterior insula and human awareness. *Nature Reviews Neuroscience*, *10*(1), 59–70. https://doi.org/10.1038/nrn2555

Craven, M. P., & Groom, M. J. (2015). Computer Games for User Engagement in Attention Deficit Hyperactivity Disorder (ADHD) Monitoring and Therapy. *Proceedings - 2015 International Conference on Interactive Technologies and Games, ITAG 2015*, 34–40. https://doi.org/10.1109/iTAG.2015.9

Crawford, S. G., Kaplan, B. J., & Dewey, D. (2006). Effects of coexisting disorders on cognition and behavior in children with ADHD. *Journal of Attention Disorders*, *10*(2), 192–199. https://doi.org/10.1177/1087054706289924

Critchley, H. D., Corfield, D. R., Chandler, M. P., Mathias, C. J., & Dolan, R. J. (2000). Cerebral correlates of autonomic cardiovascular arousal: A functional neuroimaging investigation in humans. *Journal of*

Physiology, *523*(1), 259–270. https://doi.org/10.1111/j.1469-7793.2000.t01-1-00259.x

Critchley, H. D., Mathias, C. J., Josephs, O., O'Doherty, J., Zanini, S., Dewar, B. K., Cipolotti, L., Shallice, T., & Dolan, R. J. (2003). Human cingulate cortex and autonomic control: Converging neuroimaging and clinical evidence. *Brain*, *126*(10), 2139–2152. https://doi.org/10.1093/brain/awg216

Critchley, H. D., Nagai, Y., Gray, M. A., & Mathias, C. J. (2011). Dissecting axes of autonomic control in humans: Insights from neuroimaging. *Autonomic Neuroscience: Basic and Clinical*, *161*(1–2), 34–42. https://doi.org/10.1016/j.autneu.2010.09.005

Critchley, H. D., Tang, J., Glaser, D., Butterworth, B., & Dolan, R. J. (2005). Anterior cingulate activity during error and autonomic response. *NeuroImage*, *27*(4), 885–895. https://doi.org/10.1016/j.neuroimage.2005.05.047

Curio, G., Mackert, B. M., Burghoff, M., Koetitz, R., Abraham-Fuchs, K., & Härer, W. (1994). Localization of evoked neuromagnetic 600 Hz activity in the cerebral somatosensory system. *Electroencephalography and Clinical Neurophysiology*, *91*(6), 483–487. https://doi.org/10.1016/0013-4694(94)90169-4

Curtis, C. E., & D'Esposito, M. (2003). Persistent activity in the prefrontal cortex during working memory. *Trends in Cognitive Sciences*, *7*(9), 415–

423. https://doi.org/10.1016/S1364-6613(03)00197-9

da Silva Castanheira, K., LoParco, S., & Otto, A. R. (2021). Task-evoked pupillary responses track effort exertion: Evidence from task-switching. *Cognitive, Affective and Behavioral Neuroscience*, *21*(3), 592–606. https://doi.org/10.3758/s13415-020-00843-z

Dalal, S. S., Baillet, S., Adam, C., Ducorps, A., Schwartz, D., Jerbi, K., Bertrand, O., Garnero, L., Martinerie, J., & Lachaux, J. P. (2009). Simultaneous MEG and intracranial EEG recordings during attentive reading. *NeuroImage*, *45*(4), 1289–1304. https://doi.org/10.1016/j.neuroimage.2009.01.017

Davidson, M. C., & Marrocco, R. T. (2000). Local infusion of scopolamine into intraparietal cortex slows covert orienting in rhesus monkeys. *Journal of Neurophysiology*, *83*(3), 1536–1549. https://doi.org/10.1152/jn.2000.83.3.1536

De Luca, M., Di Pace, E., Judica, A., Spinelli, D., & Zoccolotti, P. (1999). Eye movement patterns in linguistic and non-linguistic tasks in developmental surface dyslexia. *Neuropsychologia*, *37*(12), 1407–1420. https://doi.org/10.1016/S0028-3932(99)00038-X

Deen, B., Pitskel, N. B., & Pelphrey, K. A. (2011). Three systems of insular functional connectivity identified with cluster analysis. *Cerebral Cortex*, *21*(7), 1498–1506. https://doi.org/10.1093/cercor/bhq186

Destrieux, C., Fischl, B., Dale, A., & Halgren, E. (2010). Automatic

parcellation of human cortical gyri and sulci using standard anatomical nomenclature. *NeuroImage*, *53*(1), 1–15. https://doi.org/10.1016/j.neuroimage.2010.06.010

Diamond, A. (2013). Executive functions. *Annual Review of Psychology*, *64*, 135–168. https://doi.org/10.1146/annurev-psych-113011-143750

Diederich, A., Schomburg, A., & Van Vugt, M. (2014). Fronto-central theta oscillations are related to oscillations in saccadic response times (SRT): An EEG and behavioral data analysis. *PLoS ONE*, *9*(11), e112974. https://doi.org/10.1371/journal.pone.0112974

DiNuzzo, M., Mascali, D., Moraschi, M., Bussu, G., Maugeri, L., Mangini, F., Fratini, M., & Giove, F. (2019). Brain Networks Underlying Eye's Pupil Dynamics. *Frontiers in Neuroscience*, *13*(965), 1–13. https://doi.org/10.3389/fnins.2019.00965

Dockree, P. M., Barnes, J. J., Matthews, N., Dean, A. J., Abe, R., Nandam, L. S., Kelly, S. P., Bellgrove, M. A., & O'Connell, R. G. (2017). The Effects of Methylphenidate on the Neural Signatures of Sustained Attention. *Biological Psychiatry*, *82*(9), 687–694. https://doi.org/10.1016/j.biopsych.2017.04.016

Donhauser, P. W., Florin, E., & Baillet, S. (2018). Imaging of neural oscillations with embedded inferential and group prevalence statistics. *PLoS Computational Biology*, *14*(2), e1005990. https://doi.org/10.1371/journal.pcbi.1005990

Donohue, S. E., Woldorff, M. G., & Mitroff, S. R. (2010). Video game players show more precise multisensory temporal processing abilities. *Attention, Perception, and Psychophysics*, *72*(4), 1120–1129. https://doi.org/10.3758/APP.72.4.1120

Dosenbach, N. U. F., Fair, D. A., Miezin, F. M., Cohen, A. L., Wenger, K. K., Dosenbach, R. A. T., Fox, M. D., Snyder, A. Z., Vincent, J. L., Raichle, M. E., Schlaggar, B. L., & Petersen, S. E. (2007). Distinct brain networks for adaptive and stable task control in humans. *Proceedings of the National Academy of Sciences of the United States of America*, *104*(26), 11073–11078. https://doi.org/10.1073/pnas.0704320104

Dosenbach, N. U. F., Visscher, K. M., Palmer, E. D., Miezin, F. M., Wenger, K. K., Kang, H. C., Burgund, E. D., Grimes, A. L., Schlaggar, B. L., & Petersen, S. E. (2006). A Core System for the Implementation of Task Sets. *Neuron*, *50*(5), 799–812. https://doi.org/10.1016/j.neuron.2006.04.031

Duchowski, A. T. (2017). *Eye tracking methodology: Theory and practice* (3rd ed.). Springer International Publishing. https://doi.org/10.1007/978-3-319-57883-5

DuPaul, G. J., & Stoner, G. (2014). *ADHD in the schools : assessment and intervention strategies* (3rd ed.). Guilford Publications.

DuPaul, G. J., Weyandt, L. L., & Janusis, G. M. (2011). ADHD in the Classroom: Effective Intervention Strategies. *Theory into Practice*,

50(1), 35–42. https://doi.org/10.1080/00405841.2011.534935

Dye, M. W. G., Green, C. S., & Bavelier, D. (2009). Increasing speed of processing with action video games. *Current Directions in Psychological Science*, *18*(6), 321–326. https://doi.org/10.1111/j.1467-8721.2009.01660.x

Ebitz, R. B., & Moore, T. (2017). Selective modulation of the pupil light reflex by microstimulation of prefrontal cortex. *Journal of Neuroscience*, *37*(19), 5008–5018. https://doi.org/10.1523/JNEUROSCI.2433-16.2017

Ebitz, R. B., & Moore, T. (2019). Both a gauge and a filter: Cognitive modulations of pupil size. *Frontiers in Neurology*, *10*(1190), 1–14. https://doi.org/10.3389/fneur.2018.01190

Eckberg, D. L. (2000). Physiological basis for human autonomic rhythms. *Annals of Medicine*, *32*(5), 341–349. https://doi.org/10.3109/07853890008995937

Eden, G. F., & Vaidya, C. J. (2008). ADHD and developmental dyslexia: Two pathways leading to impaired learning. *Annals of the New York Academy of Sciences*, *1145*(1), 316–327. https://doi.org/10.1196/annals.1416.022

Einhäuser, W., Koch, C., & Carter, O. L. (2010). Pupil dilation betrays the timing of decisions. *Frontiers in Human Neuroscience*, *4*, 18. https://doi.org/10.3389/fnhum.2010.00018

Einhäuser, W., Stout, J., Koch, C., & Carter, O. (2008). Pupil dilation reflects perceptual selection and predicts subsequent stability in perceptual rivalry. *Proceedings of the National Academy of Sciences of the United States of America*, *105*(5), 1704–1709. https://doi.org/10.1073/pnas.0707727105

Eldar, E., Cohen, J. D., & Niv, Y. (2013). The effects of neural gain on attention and learning. *Nature Neuroscience*, *16*(8), 1146–1153. https://doi.org/10.1038/nn.3428

Engel, A. K., & Fries, P. (2010). Beta-band oscillations-signalling the status quo? *Current Opinion in Neurobiology*, *20*(2), 156–165. https://doi.org/10.1016/j.conb.2010.02.015

Everling, S., & Fischer, B. (1998). The antisaccade: A review of basic research and clinical studies. *Neuropsychologia*, *36*(9), 885–899. https://doi.org/10.1016/S0028-3932(98)00020-7

Everling, S., & Munoz, D. P. (2000). Neuronal correlates for preparatory set associated with pro-saccades and anti-saccades in the primate frontal eye field. *Journal of Neuroscience*, *20*(1), 387–400. https://doi.org/10.1523/jneurosci.20-01-00387.2000

Everling, S., Spantekow, A., Krappmann, P., & Flohr, H. (1998). Event-related potentials associated with correct and incorrect responses in a cued antisaccade task. *Experimental Brain Research*, *118*(1), 27–34. https://doi.org/10.1007/s002210050252

Ewe, L. P. (2019). ADHD symptoms and the teacher–student relationship: a systematic literature review. *Emotional and Behavioural Difficulties*, *24*(2), 136–155. https://doi.org/10.1080/13632752.2019.1597562

Fair, D. A., Cohen, A. L., Power, J. D., Dosenbach, N. U. F., Church, J. A., Miezin, F. M., Schlaggar, B. L., & Petersen, S. E. (2009). Functional brain networks develop from a "local to distributed" organization. *PLoS Computational Biology*, *5*(5), e1000381. https://doi.org/10.1371/journal.pcbi.1000381

Fan, J., Gu, X., Guise, K. G., Liu, X., Fossella, J., Wang, H., & Posner, M. I. (2009). Testing the behavioral interaction and integration of attentional networks. *Brain and Cognition*, *70*(2), 209–220. https://doi.org/10.1016/j.bandc.2009.02.002

Fan, J., McCandliss, B. D., Fossella, J., Flombaum, J. I., & Posner, M. I. (2005). The activation of attentional networks. *NeuroImage*, *26*(2), 471–479. https://doi.org/10.1016/j.neuroimage.2005.02.004

Fan, J., McCandliss, B. D., Sommer, T., Raz, A., & Posner, M. I. (2002). Testing the efficiency and independence of attentional networks. *Journal of Cognitive Neuroscience*, *14*(3), 340–347. https://doi.org/10.1162/089892902317361886

Faraone, S. V. (2018). The pharmacology of amphetamine and methylphenidate: Relevance to the neurobiology of attention-deficit/hyperactivity disorder and other psychiatric comorbidities. In

Neuroscience and Biobehavioral Reviews (Vol. 87, pp. 255–270). Pergamon. https://doi.org/10.1016/j.neubiorev.2018.02.001

Faul, F., Erdfelder, E., Lang, A. G., & Buchner, A. (2007). G*Power 3: a flexible statistical power analysis program for the social, behavioral, and biomedical sciences. *Behavior Research Methods*, *39*(2), 175–191. https://doi.org/10.3758/BF03193146

Feifel, D., Farber, R. H., Clementz, B. A., Perry, W., & Anllo-Vento, L. (2004). Inhibitory deficits in ocular motor behavior in adults with attention-deficit/hyperactivity disorder. *Biological Psychiatry*, *56*(5), 333–339. https://doi.org/10.1016/j.biopsych.2004.06.019

Feingold, J., Gibson, D. J., Depasquale, B., & Graybiel, A. M. (2015). Bursts of beta oscillation differentiate postperformance activity in the striatum and motor cortex of monkeys performing movement tasks. *Proceedings of the National Academy of Sciences of the United States of America*, *112*(44), 13687–13692. https://doi.org/10.1073/pnas.1517629112

Fernandez-Duque, D., & Posner, M. I. (1997). Relating the mechanisms of orienting and alerting. *Neuropsychologia*, *35*(4), 477–486. https://doi.org/10.1016/S0028-3932(96)00103-0

Fernandez-Ruiz, J., Hakvoort Schwerdtfeger, R. M., Alahyane, N., Brien, D. C., Coe, B. C., & Munoz, D. P. (2020). Dorsolateral prefrontal cortex hyperactivity during inhibitory control in children with ADHD in the

antisaccade task. *Brain Imaging and Behavior*, *14*(6), 2450–2463. https://doi.org/10.1007/s11682-019-00196-3

Fernandez-Ruiz, J., Peltsch, A., Alahyane, N., Brien, D. C., Coe, B. C., Garcia, A., & Munoz, D. P. (2018). Age related prefrontal compensatory mechanisms for inhibitory control in the antisaccade task. *NeuroImage*, *165*, 92–101. https://doi.org/10.1016/j.neuroimage.2017.10.001

Ferree, T. C., Eriksen, K. J., & Tucker, D. M. (2000). Regional head tissue conductivity estimation for improved EEG analysis. *IEEE Transactions on Biomedical Engineering*, *47*(12), 1584–1592. https://doi.org/10.1109/10.887939

Ferrier, D. (1874). On the localisation of the functions of the brain. *British Medical Journal*, *2*(729), 766–767. https://doi.org/10.1136/bmj.2.729.766

Ferrier, D. (1875). Experiments on the brain of monkeys.—No. I. *Proceedings of the Royal Society of London*, *23*(156–163), 409–430. https://doi.org/10.1098/rspl.1874.0058

Fiebelkorn, I. C., & Kastner, S. (2019). A Rhythmic Theory of Attention. *Trends in Cognitive Sciences*, *23*(2), 87–101. https://doi.org/10.1016/j.tics.2018.11.009

Field, A. (2013). *Discovering Statistics Using IBM SPSS Statistics* (4th ed.). SAGE Publications Inc.

Fischer, B., & Boch, R. (1983). Saccadic eye movements after extremely short reaction times in the monkey. *Brain Research*, *260*(1), 21–26. https://doi.org/10.1016/0006-8993(83)90760-6

Fischer, B., & Ramsperger, E. (1984). Human express saccades: extremely short reaction times of goal directed eye movements. *Experimental Brain Research 1984 57:1*, *57*(1), 191–195. https://doi.org/10.1007/BF00231145

Fischer, B., & Weber, H. (1993). Express saccades and visual attention. *Behavioral and Brain Sciences*, *16*(3), 553–567. https://doi.org/10.1017/S0140525X00031575

Fischl, B. (2012). FreeSurfer. *NeuroImage*, *62*(2), 774–781. https://doi.org/10.1016/j.neuroimage.2012.01.021

Fischl, B., Sereno, M. I., & Dale, A. M. (1999). Cortical surface-based analysis: II. Inflation, flattening, and a surface-based coordinate system. *NeuroImage*, *9*(2), 195–207. https://doi.org/10.1006/nimg.1998.0396

Fischl, B., Sereno, M. I., Tootell, R. B. H., & Dale, A. M. (1999). High-resolution intersubject averaging and a coordinate system for the cortical surface. *Human Brain Mapping*, *8*(4), 272–284. https://doi.org/10.1002/(SICI)1097-0193(1999)8:4<272::AID-HBM10>3.0.CO;2-4

Foote, S. L., & Berridge, C. W. (2019). New developments and future

directions in understanding locus coeruleus - Norepinephrine (LC-NE) function. *Brain Research*, *1709*, 81–84. https://doi.org/10.1016/J.BRAINRES.2018.09.033

Foote, S. L., Bloom, F. E., & Aston-Jones, G. (1983). Nucleus locus ceruleus: New evidence of anatomical and physiological specificity. In *Physiological Reviews* (Vol. 63, Issue 3, pp. 844–914). Physiol Rev. https://doi.org/10.1152/physrev.1983.63.3.844

Ford, K. A., Goltz, H. C., Brown, M. R. G., & Everling, S. (2005). Neural processes associated with antisaccade task performance investigated with event-related fMRI. *Journal of Neurophysiology*, *94*(1), 429–440. https://doi.org/10.1152/jn.00471.2004

Fox, M. D., Snyder, A. Z., Vincent, J. L., Corbetta, M., Van Essen, D. C., & Raichle, M. E. (2005). The human brain is intrinsically organized into dynamic, anticorrelated functional networks. *Proceedings of the National Academy of Sciences of the United States of America*, *102*(27), 9673–9678. https://doi.org/10.1073/pnas.0504136102

Franceschini, S., & Bertoni, S. (2019). Improving action video games abilities increases the phonological decoding speed and phonological short-term memory in children with developmental dyslexia. *Neuropsychologia*, *130*, 100–106. https://doi.org/10.1016/j.neuropsychologia.2018.10.023

Franceschini, S., Bertoni, S., Ronconi, L., Molteni, M., Gori, S., & Facoetti,

A. (2015). “Shall We Play a Game?”: Improving Reading Through Action Video Games in Developmental Dyslexia. *Current Developmental Disorders Reports*, *2*(4), 318–329. https://doi.org/10.1007/s40474-015-0064-4

Franceschini, S., Gori, S., Ruffino, M., Pedrolli, K., & Facoetti, A. (2012). A causal link between visual spatial attention and reading acquisition. *Current Biology*, *22*(9), 814–819. https://doi.org/10.1016/j.cub.2012.03.013

Franceschini, S., Gori, S., Ruffino, M., Viola, S., Molteni, M., & Facoetti, A. (2013). Action video games make dyslexic children read better. *Current Biology*, *23*(6), 462–466. https://doi.org/10.1016/j.cub.2013.01.044

Franceschini, S., Trevisan, P., Ronconi, L., Bertoni, S., Colmar, S., Double, K., Facoetti, A., & Gori, S. (2017). Action video games improve reading abilities and visual-to-auditory attentional shifting in English-speaking children with dyslexia. *Scientific Reports*, *7*(1), 1–12. https://doi.org/10.1038/s41598-017-05826-8

Fredrikson, M., Furmark, T., Olsson, M. T., Fischer, H., Andersson, J., & Langstrom, B. (1998). Functional neuroanatomical correlates of electrodermal activity: A positron emission tomographic study. *Psychophysiology*, *35*(2), 179–185. https://doi.org/10.1111/1469-8986.3520179

Freedman, E. G. (2008). Coordination of the eyes and head during visual

orienting. *Experimental Brain Research*, *190*(4), 369–387. https://doi.org/10.1007/S00221-008-1504-8

Friedman, M. C., Chhabildas, N., Budhiraja, N., Willcutt, E. G., & Pennington, B. F. (2003). Etiology of the comorbidity between RD and ADHD: Exploration of the non-random mating hypothesis. *American Journal of Medical Genetics - Neuropsychiatric Genetics*, *120 B*(1), 109–115. https://doi.org/10.1002/ajmg.b.20029

Fu, K. M. G., Foxe, J. J., Murray, M. M., Higgins, B. A., Javitt, D. C., & Schroeder, C. E. (2001). Attention-dependent suppression of distracter visual input can be cross-modally cued as indexed by anticipatory parieto-occipital alpha-band oscillations. *Cognitive Brain Research*, *12*(1), 145–152. https://doi.org/10.1016/S0926-6410(01)00034-9

Furlan, M., Smith, A. T., & Walker, R. (2016). An fMRI investigation of preparatory set in the human cerebral cortex and superior colliculus for pro- and anti-saccades. *PLoS ONE*, *11*(7), e0158337. https://doi.org/10.1371/journal.pone.0158337

Gamer, M., Bauermann, T., Stoeter, P., & Vossel, G. (2007). Covariations among fMRI, skin conductance, and behavioral data during processing of concealed information. *Human Brain Mapping*, *28*(12), 1287–1301. https://doi.org/10.1002/hbm.20343

Gandhi, N. J., & Katnani, H. A. (2011). Motor functions of the superior colliculus. *Annual Review of Neuroscience*, *34*, 205–231.

https://doi.org/10.1146/annurev-neuro-061010-113728

García-Baos, A., D'Amelio, T., Oliveira, I., Collins, P., Echevarria, C., Zapata, L. P., Liddle, E., & Supèr, H. (2019). Novel interactive eye-tracking game for training attention in children with attention-deficit/hyperactivity disorder. *The Primary Care Companion for CNS Disorders*, *21*(4), 19m02428. https://doi.org/10.4088/PCC.19m02428

Gawne, T. J. (2000). The simultaneous coding of orientation and contrast in the responses of V1 complex cells. *Experimental Brain Research*, *133*(3), 293–302. https://doi.org/10.1007/s002210000381

Gaymard, B., Ploner, C. J., Rivaud, S., Vermersch, A. I., & Pierrot-Deseilligny, C. (1998). Cortical control of saccades. *Experimental Brain Research*, *123*(1–2), 159–163. https://doi.org/10.1007/s002210050557

Geissler, J., Romanos, M., Hegerl, U., & Hensch, T. (2014). Hyperactivity and sensation seeking as autoregulatory attempts to stabilize brain arousal in ADHD and mania? *ADHD Attention Deficit and Hyperactivity Disorders*, *6*(3), 159–173. https://doi.org/10.1007/s12402-014-0144-z

Gelbard-Sagiv, H., Magidov, E., Sharon, H., Hendler, T., & Nir, Y. (2018). Noradrenaline Modulates Visual Perception and Late Visually Evoked Activity. *Current Biology*, *28*(14), 2239–2249. https://doi.org/10.1016/j.cub.2018.05.051

Germanò, E., Gagliano, A., & Curatolo, P. (2010). Comorbidity of ADHD and

dyslexia. *Developmental Neuropsychology*, *35*(5), 475–493. https://doi.org/10.1080/87565641.2010.494748

Geva, R., Zivan, M., Warsha, A., & Olchik, D. (2013). Alerting, orienting or executive attention networks: Differential patters of pupil dilations. *Frontiers in Behavioral Neuroscience*, *7*(145), 1–11. https://doi.org/10.3389/fnbeh.2013.00145

Gillary, G., & Niebur, E. (2016). The Edge of Stability: Response Times and Delta Oscillations in Balanced Networks. *PLoS Computational Biology*, *12*(9), e1005121. https://doi.org/10.1371/journal.pcbi.1005121

Gilzenrat, M. S., Nieuwenhuis, S., Jepma, M., & Cohen, J. D. (2010). Pupil diameter tracks changes in control state predicted by the adaptive gain theory of locus coeruleus function. *Cognitive, Affective and Behavioral Neuroscience*, *10*(2), 252–269. https://doi.org/10.3758/CABN.10.2.252

Gladwin, T. E., Hashemi, M. M., van Ast, V., & Roelofs, K. (2016). Ready and waiting: Freezing as active action preparation under threat. *Neuroscience Letters*, *619*, 182–188. https://doi.org/10.1016/j.neulet.2016.03.027

Glass, B. D., Maddox, W. T., & Love, B. C. (2013). Real-Time Strategy Game Training: Emergence of a Cognitive Flexibility Trait. *PLoS ONE*, *8*(8), e70350. https://doi.org/10.1371/journal.pone.0070350

Godijn, R., & Theeuwes, J. (2004). The relationship between inhibition of return and saccade trajectory deviations. *Journal of Experimental*

Psychology: Human Perception and Performance, *30*(3), 538–554. https://doi.org/10.1037/0096-1523.30.3.538

Goldberg, D., & Williams, P. (1988). *A user's guide to the General Health Questionnaire*. Windsor: NFER-Nelson.

Gonçalves, S., De Munck, J. C., Heethaar, R. M., Lopes Da Silva, F. H., & Van Dijk, B. W. (2000). The application of electrical impedance tomography to reduce systematic errors in the EEG inverse problem - A simulation study. *Physiological Measurement*, *21*(3), 379–393. https://doi.org/10.1088/0967-3334/21/3/304

Gong, G., He, Y., Concha, L., Lebel, C., Gross, D. W., Evans, A. C., & Beaulieu, C. (2009). Mapping anatomical connectivity patterns of human cerebral cortex using in vivo diffusion tensor imaging tractography. *Cerebral Cortex*, *19*(3), 524–536. https://doi.org/10.1093/cercor/bhn102

Goodwin, A., Salomone, S., Bolton, P., Charman, T., Jones, E. J. H., Pickles, A., Robinson, E., Smith, T., Sonuga-Barke, E. J. S., Wass, S., & Johnson, M. H. (2016). Attention training for infants at familial risk of ADHD (INTERSTAARS): Study protocol for a randomised controlled trial. *Trials*, *17*(608), 1–12. https://doi.org/10.1186/s13063-016-1727-0

Goto, Y., Hatakeyama, K., Kitama, T., Sato, Y., Kanemura, H., Aoyagi, K., Sugita, K., & Aihara, M. (2010). Saccade eye movements as a quantitative measure of frontostriatal network in children with ADHD.

Brain and Development, *32*(5), 347–355. https://doi.org/10.1016/j.braindev.2009.04.017

Gottlieb, J., & Goldberg, M. E. (1999). Activity of neurons in the lateral intraparietal area of the monkey during an antisaccade task. *Nature Neuroscience*, *2*(10), 906–912. https://doi.org/10.1038/13209

Graham, F. K., & Clifton, R. K. (1966). Heart-rate change as a component of the orienting response. *Psychological Bulletin*, *65*(5), 305–320. https://doi.org/10.1037/h0023258

Graham, F. K., & Jackson, J. C. (1970). Arousal Systems and Infant Heart Rate Responses. *Advances in Child Development and Behavior*, *5*(C), 59–117. https://doi.org/10.1016/S0065-2407(08)60465-6

Green, C. S., & Bavelier, D. (2003). Action video game modifies visual selective attention. *Nature*, *423*(6939), 534–537. https://doi.org/10.1038/nature01647

Green, C. S., & Bavelier, D. (2006). Enumeration versus multiple object tracking: the case of action video game players. *Cognition*, *101*(1), 217–245. https://doi.org/10.1016/j.cognition.2005.10.004

Green, C. S., Sugarman, M. A., Medford, K., Klobusicky, E., & Bavelier, D. (2012). The effect of action video game experience on task-switching. *Computers in Human Behavior*, *28*(3), 984–994. https://doi.org/10.1016/j.chb.2011.12.020

Greenwood, P. M., Lin, M. K., Sundararajan, R., Fryxell, K. J., & Parasuraman, R. (2009). Synergistic effects of genetic variation in nicotinic and muscarinic receptors on visual attention but not working memory. *Proceedings of the National Academy of Sciences of the United States of America*, *106*(9), 3633–3638. https://doi.org/10.1073/pnas.0807891106

Grefkes, C., & Fink, G. R. (2005). The functional organization of the intraparietal sulcus in humans and monkeys. *Journal of Anatomy*, *207*(1), 3–17. https://doi.org/10.1111/j.1469-7580.2005.00426.x

Groom, M. J., Cahill, J. D., Bates, A. T., Jackson, G. M., Calton, T. G., Liddle, P. F., & Hollis, C. (2010). Electrophysiological indices of abnormal error-processing in adolescents with attention deficit hyperactivity disorder (ADHD). *Journal of Child Psychology and Psychiatry*, *51*(1), 66–76. https://doi.org/10.1111/j.1469-7610.2009.02128.x

Groom, M. J., Liddle, E. B., Scerif, G., Liddle, P. F., Batty, M. J., Liotti, M., & Hollis, C. P. (2013). Motivational incentives and methylphenidate enhance electrophysiological correlates of error monitoring in children with attention deficit/hyperactivity disorder. *Journal of Child Psychology and Psychiatry and Allied Disciplines*, *54*(8), 836–845. https://doi.org/10.1111/jcpp.12069

Groom, M. J., Scerif, G., Liddle, P. F., Batty, M. J., Liddle, E. B., Roberts, K. L., Cahill, J. D., Liotti, M., & Hollis, C. (2010). Effects of Motivation

and Medication on Electrophysiological Markers of Response Inhibition in Children with Attention-Deficit/Hyperactivity Disorder. *Biological Psychiatry*, *67*(7), 624–631. https://doi.org/10.1016/j.biopsych.2009.09.029

Guitton, D., Buchtel, H. A., & Douglas, R. M. (1985). Frontal lobe lesions in man cause difficulties in suppressing reflexive glances and in generating goal-directed saccades. *Experimental Brain Research*, *58*(3), 455–472. https://doi.org/10.1007/BF00235863

Guo, C. C., Sturm, V. E., Zhou, J., Gennatas, E. D., Trujillo, A. J., Hua, A. Y., Crawford, R., Stables, L., Kramer, J. H., Rankin, K., Levenson, R. W., Rosen, H. J., Miller, B. L., & Seeley, W. W. (2016). Dominant hemisphere lateralization of cortical parasympathetic control as revealed by frontotemporal dementia. *Proceedings of the National Academy of Sciences of the United States of America*, *113*(17), E2430–E2439. https://doi.org/10.1073/pnas.1509184113

Haar, S., & Faisal, A. A. (2020). Brain Activity Reveals Multiple Motor-Learning Mechanisms in a Real-World Task. *Frontiers in Human Neuroscience*, *14*(354), 1–11. https://doi.org/10.3389/fnhum.2020.00354

Habgood, M. P. J., & Ainsworth, S. E. (2011). Motivating children to learn effectively: Exploring the value of intrinsic integration in educational games. *Journal of the Learning Sciences*, *20*(2), 169–206. https://doi.org/10.1080/10508406.2010.508029

Habibi, A., Damasio, A., Ilari, B., Sachs, M. E., & Damasio, H. (2018). Music training and child development: A review of recent findings from a longitudinal study. *Annals of the New York Academy of Sciences*, *1423*(1), 73–81. https://doi.org/10.1111/nyas.13606

Haegens, S., Nácher, V., Luna, R., Romo, R., & Jensen, O. (2011). α-Oscillations in the monkey sensorimotor network influence discrimination performance by rhythmical inhibition of neuronal spiking. *Proceedings of the National Academy of Sciences of the United States of America*, *108*(48), 19377–19382. https://doi.org/10.1073/pnas.1117190108

Hakvoort Schwerdtfeger, R. M., Alahyane, N., Brien, D. C., Coe, B. C., Stroman, P. W., & Munoz, D. P. (2013). Preparatory neural networks are impaired in adults with attention-deficit/hyperactivity disorder during the antisaccade task. *NeuroImage: Clinical*, *2*(1), 63–78. https://doi.org/10.1016/j.nicl.2012.10.006

Hall, K. M., Irwin, M. M., Bowman, K. A., Frankenberger, W., & Jewett, D. C. (2005). Illicit use of prescribed stimulant medication among college students. *Journal of American College Health*, *53*(4), 167–174. https://doi.org/10.3200/JACH.53.4.167-174

Hallett, P. E. (1978). Primary and secondary saccades to goals defined by instructions. *Vision Research*, *18*(10), 1279–1296. https://doi.org/10.1016/0042-6989(78)90218-3

Hämäläinen, M. S., Hari, R., Ilmoniemi, R. J., Knuutila, J., & Lounasmaa, O. V. (1993). Magnetoencephalography theory, instrumentation, and applications to noninvasive studies of the working human brain. *Reviews of Modern Physics*, *65*(2), 413–497. https://doi.org/10.1103/RevModPhys.65.413

Hämäläinen, M. S., Lin, F. H., & Mosher, J. C. (2010). Anatomically and Functionally Constrained Minimum-Norm Estimates. In P. C. Hansen, M. L. Kringelbach, & R. Salmelin (Eds.), *MEG: An Introduction to Methods* (pp. 186–215). Oxford University Press. https://doi.org/10.1093/acprof:oso/9780195307238.003.0008

Hamm, J. P., Dyckman, K. A., McDowell, J. E., & Clementz, B. A. (2012). Pre-cue fronto-occipital alpha phase and distributed cortical oscillations predict failures of cognitive control. *Journal of Neuroscience*, *32*(20), 7034–7041. https://doi.org/10.1523/JNEUROSCI.5198-11.2012

Händel, B. F., Haarmeier, T., & Jensen, O. (2011). Alpha oscillations correlate with the successful inhibition of unattended stimuli. *Journal of Cognitive Neuroscience*, *23*(9), 2494–2502. https://doi.org/10.1162/jocn.2010.21557

Hanes, D. P., Patterson, W. F., & Schall, J. D. (1998). Role of frontal eye fields in countermanding saccades: Visual, movement, and fixation activity. *Journal of Neurophysiology*, *79*(2), 817–834. https://doi.org/10.1152/jn.1998.79.2.817

Hanslmayr, S., Aslan, A., Staudigl, T., Klimesch, W., Herrmann, C. S., & Bäuml, K. H. (2007). Prestimulus oscillations predict visual perception performance between and within subjects. *NeuroImage*, *37*(4), 1465–1473. https://doi.org/10.1016/j.neuroimage.2007.07.011

Hardy, G. E., Shapiro, D. A., Haynes, C. E., & Rick, J. E. (1999). Validation of the General Health Questionnaire-12 using a sample of employees from England's health care services. *Psychological Assessment*, *11*(2), 159–165. https://doi.org/10.1037/1040-3590.11.2.159

Harmony, T. (2013). The functional significance of delta oscillations in cognitive processing. *Frontiers in Integrative Neuroscience*, *7*(83), 1–10. https://doi.org/10.3389/fnint.2013.00083

Hart, H., Radua, J., Nakao, T., Mataix-Cols, D., & Rubia, K. (2013). Meta-analysis of functional magnetic resonance imaging studies of inhibition and attention in attention-deficit/hyperactivity disorder: Exploring task-specific, stimulant medication, and age effects. *JAMA Psychiatry*, *70*(2), 185–198. https://doi.org/10.1001/jamapsychiatry.2013.277

Hartung, C. M., Canu, W. H., Cleveland, C. S., Lefler, E. K., Mignogna, M. J., Fedele, D. A., Correia, C. J., Leffingwell, T. R., & Clapp, J. D. (2013). Stimulant medication use in college students: Comparison of appropriate users, misusers, and nonusers. *Psychology of Addictive Behaviors*, *27*(3), 832–840. https://doi.org/10.1037/a0033822

Hasselmo, M. (2005). Expecting the unexpected: Modeling of

neuromodulation. *Neuron*, *46*(4), 526–528. https://doi.org/10.1016/j.neuron.2005.05.007

Hayes, T. R., & Petrov, A. A. (2016a). Pupil diameter tracks the exploration-exploitation trade-off during analogical reasoning and explains individual differences in fluid intelligence. *Journal of Cognitive Neuroscience*, *28*(2), 308–318. https://doi.org/10.1162/jocn_a_00895

Hayes, T. R., & Petrov, A. A. (2016b). Mapping and correcting the influence of gaze position on pupil size measurements. *Behavior Research Methods*, *48*(2), 510–527. https://doi.org/10.3758/s13428-015-0588-x

Heinz, A., & Schlagenhauf, F. (2010). Dopaminergic dysfunction in schizophrenia: Salience attribution revisited. *Schizophrenia Bulletin*, *36*(3), 472–485. https://doi.org/10.1093/schbul/sbq031

Hennessy, S. L., Sachs, M. E., Ilari, B., & Habibi, A. (2019). Effects of Music Training on Inhibitory Control and Associated Neural Networks in School-Aged Children: A Longitudinal Study. *Frontiers in Neuroscience*, *13*(1080), 1–16. https://doi.org/10.3389/fnins.2019.01080

Hermans, E. J., Henckens, M. J. A. G., Roelofs, K., & Fernández, G. (2013). Fear bradycardia and activation of the human periaqueductal grey. *NeuroImage*, *66*, 278–287. https://doi.org/10.1016/j.neuroimage.2012.10.063

Hertrich, I., Dietrich, S., Blum, C., & Ackermann, H. (2021). The Role of the Dorsolateral Prefrontal Cortex for Speech and Language Processing.

Frontiers in Human Neuroscience, *15*(645209), 1–16. https://doi.org/10.3389/fnhum.2021.645209

Hess, E. H., & Polt, J. M. (1960). Pupil size as related to interest value of visual stimuli. *Science*, *132*(3423), 349–350. https://doi.org/10.1126/science.132.3423.349

Hess, E. H., & Polt, J. M. (1964). Pupil size in relation to mental activity during simple problem-solving. *Science*, *143*(3611), 1190–1192. https://doi.org/10.1126/science.143.3611.1190

Hikosaka, O., Takikawa, Y., & Kawagoe, R. (2000). Role of the basal ganglia in the control of purposive saccadic eye movements. *Physiological Reviews*, *80*(3), 953–978. https://doi.org/10.1152/physrev.2000.80.3.953

Hinds, O. P., Polimeni, J. R., Rajendran, N., Balasubramanian, M., Amunts, K., Zilles, K., Schwartz, E. L., Fischl, B., & Triantafyllou, C. (2009). Locating the functional and anatomical boundaries of human primary visual cortex. *NeuroImage*, *46*(4), 915–922. https://doi.org/10.1016/j.neuroimage.2009.03.036

Hinds, O. P., Rajendran, N., Polimeni, J. R., Augustinack, J. C., Wiggins, G., Wald, L. L., Diana Rosas, H., Potthast, A., Schwartz, E. L., & Fischl, B. (2008). Accurate prediction of V1 location from cortical folds in a surface coordinate system. *NeuroImage*, *39*(4), 1585–1599. https://doi.org/10.1016/j.neuroimage.2007.10.033

Hjortkjær, J., Märcher-Rørsted, J., Fuglsang, S. A., & Dau, T. (2020).

Cortical oscillations and entrainment in speech processing during working memory load. *European Journal of Neuroscience*, *51*(5), 1279–1289. https://doi.org/10.1111/ejn.13855

Hodgson, T., Chamberlain, M., Parris, B., James, M., Gutowski, N., Husain, M., & Kennard, C. (2007). The role of the ventrolateral frontal cortex in inhibitory oculomotor control. *Brain*, *130*(6), 1525–1537. https://doi.org/10.1093/brain/awm064

Holmes, J., Gathercole, S. E., Place, M., Dunning, D. L., Hilton, K. A., & Elliott, J. G. (2010). Working memory deficits can be overcome: Impacts of training and medication on working memory in children with ADHD. *Applied Cognitive Psychology*, *24*(6), 827–836. https://doi.org/10.1002/acp.1589

Howells, F. M., Stein, D. J., & Russell, V. A. (2010). Perceived mental effort correlates with changes in tonic arousal during attentional tasks. *Behavioral and Brain Functions*, *6*(39), 1–15. https://doi.org/10.1186/1744-9081-6-39

Howes, O. D., & Kapur, S. (2009). The Dopamine Hypothesis of Schizophrenia: Version III—The Final Common Pathway. *Schizophrenia Bulletin*, *35*(3), 549–562. https://doi.org/10.1093/SCHBUL/SBP006

Huang, X., Xu, K., Chu, C., Jiang, T., & Yu, S. (2017). Weak higher-order interactions in macroscopic functional networks of the resting brain.

Journal of Neuroscience, *37*(43), 10481–10497. https://doi.org/10.1523/JNEUROSCI.0451-17.2017

Hubert-Wallander, B., Green, C. S., Sugarman, M., & Bavelier, D. (2011). Changes in search rate but not in the dynamics of exogenous attention in action videogame players. *Attention, Perception, and Psychophysics*, *73*(8), 2399–2412. https://doi.org/10.3758/s13414-011-0194-7

Huerta, M. F., Krubitzer, L. A., & Kaas, J. H. (1987). Frontal eye field as defined by intracortical microstimulation in squirrel monkeys, owl monkeys, and macaque monkeys II. cortical connections. *Journal of Comparative Neurology*, *265*(3), 332–361. https://doi.org/10.1002/cne.902650304

Hurtig, T., Ebeling, H., Taanila, A., Miettunen, J., Smalley, S. L., McGough, J. J., Loo, S. K., Järvelin, M. R., & Moilanen, I. K. (2007). ADHD symptoms and subtypes: Relationship between childhood and adolescent symptoms. *Journal of the American Academy of Child and Adolescent Psychiatry*, *46*(12), 1605–1613. https://doi.org/10.1097/chi.0b013e318157517a

Husain, M., Mannan, S., Hodgson, T., Wojciulik, E., Driver, J., & Kennard, C. (2001). Impaired spatial working memory across saccades contributes to abnormal search in parietal neglect. *Brain*, *124*(5), 941–952. https://doi.org/10.1093/brain/124.5.941

Husain, M., Parton, A., Hodgson, T. L., Mort, D., & Rees, G. (2003). Self-

control during response conflict by human supplementary eye field. *Nature Neuroscience*, *6*(2), 117–118. https://doi.org/10.1038/nn1005

Hwang, K., Ghuman, A. S., Manoach, D. S., Jones, S. R., & Luna, B. (2014). Cortical neurodynamics of inhibitory control. *Journal of Neuroscience*, *34*(29), 9551–9561. https://doi.org/10.1523/JNEUROSCI.4889-13.2014

Hwang, K., Ghuman, A. S., Manoach, D. S., Jones, S. R., & Luna, B. (2016). Frontal preparatory neural oscillations associated with cognitive control: A developmental study comparing young adults and adolescents. *NeuroImage*, *136*, 139–148. https://doi.org/10.1016/j.neuroimage.2016.05.017

Hwang, K., Shine, J. M., & D'esposito, M. (2019). Frontoparietal Activity Interacts With Task-Evoked Changes in Functional Connectivity. *Cerebral Cortex*, *29*(2), 802–813. https://doi.org/10.1093/cercor/bhy011

Hwang, K., Velanova, K., & Luna, B. (2010). Strengthening of top-down frontal cognitive control networks underlying the development of inhibitory control: A functional magnetic resonance imaging effective connectivity study. *Journal of Neuroscience*, *30*(46), 15535–15545. https://doi.org/10.1523/JNEUROSCI.2825-10.2010

Ingale, M., Cordeiro, R., Thentu, S., Park, Y., & Karimian, N. (2020). ECG Biometric Authentication: A Comparative Analysis. *IEEE Access*, *8*, 117853–117866. https://doi.org/10.1109/ACCESS.2020.3004464

Ioannides, A. A., Corsi-Cabrera, M., Fenwick, P. B. C., Del Rio Portilla, Y.,

Laskaris, N. A., Khurshudyan, A., Theofilou, D., Shibata, T., Uchida, S., Nakabayashi, T., & Kostopoulos, G. K. (2004). MEG Tomography of Human Cortex and Brainstem Activity in Waking and REM Sleep Saccades. *Cerebral Cortex*, *14*(1), 56–72. https://doi.org/10.1093/cercor/bhg091

Jack, A. I., Shulman, G. L., Snyder, A. Z., McAvoy, M., & Corbetta, M. (2006). Separate Modulations of Human V1 Associated with Spatial Attention and Task Structure. *Neuron*, *51*(1), 135–147. https://doi.org/10.1016/j.neuron.2006.06.003

Jackson, G. M., Mueller, S. C., Hambleton, K., & Hollis, C. P. (2007). Enhanced cognitive control in Tourette Syndrome during task uncertainty. *Experimental Brain Research*, *182*(3), 357–364. https://doi.org/10.1007/s00221-007-0999-8

Jackson, J. C., Kantowitz, S. R., & Graham, F. K. (1971). Can Newborns Show Cardiac Orienting? *Child Development*, *42*(1), 107. https://doi.org/10.2307/1127068

Jamadar, S. D., Johnson, B. P., Clough, M., Egan, G. F., & Fielding, J. (2015). Behavioral and Neural Plasticity of Ocular Motor Control: Changes in Performance and fMRI Activity Following Antisaccade Training. *Frontiers in Human Neuroscience*, *9*(653), 1–13. https://doi.org/10.3389/fnhum.2015.00653

James, W. (1890). *The Principles of Psychology, Volume 1*. Holt.

Jamshidifarsani, H., Garbaya, S., Lim, T., Blazevic, P., & Ritchie, J. M. (2019). Technology-based reading intervention programs for elementary grades: An analytical review. *Computers and Education*, *128*, 427–451. https://doi.org/10.1016/j.compedu.2018.10.003

Jennings, J. R. (1992). Is it Important That the Mind is in a Body? Inhibition and the Heart. *Psychophysiology*, *29*(4), 369–383. https://doi.org/10.1111/J.1469-8986.1992.TB01710.X

Jennings, J. R., & van der Molen, M. W. (2005). Preparation for speeded action as a psychophysiological concept. *Psychological Bulletin*, *131*(3), 434–459. https://doi.org/10.1037/0033-2909.131.3.434

Jennings, J. R., van der Molen, M. W., & Steinhauer, S. R. (1998). Preparing the heart, eye, and brain: Foreperiod length effects in a nonaging paradigm. *Psychophysiology*, *35*(1), 90–98. https://doi.org/10.1111/1469-8986.3510090

Jennings, J. R., van der Molen, M. W., & Tanase, C. (2009). Preparing hearts and minds: cardiac slowing and a cortical inhibitory network. *Psychophysiology*, *46*(6), 1170–1178. https://doi.org/10.1111/J.1469-8986.2009.00866.X

Jennings, J. R., & Wood, C. C. (1977). Cardiac Cycle Time Effects on Performance, Phasic Cardiac Responses, and Their Intercorrelation in Choice Reaction Time. *Psychophysiology*, *14*(3), 297–307. https://doi.org/10.1111/j.1469-8986.1977.tb01179.x

Jensen, C. M., Amdisen, B. L., Jørgensen, K. J., & Arnfred, S. M. H. (2016). Cognitive behavioural therapy for ADHD in adults: systematic review and meta-analyses. *ADHD Attention Deficit and Hyperactivity Disorders*, *8*(1), 3–11. https://doi.org/10.1007/s12402-016-0188-3

Jensen, O., Bonnefond, M., & VanRullen, R. (2012). An oscillatory mechanism for prioritizing salient unattended stimuli. *Trends in Cognitive Sciences*, *16*(4), 200–206. https://doi.org/10.1016/j.tics.2012.03.002

Jensen, O., & Mazaheri, A. (2010). Shaping functional architecture by oscillatory alpha activity: Gating by inhibition. *Frontiers in Human Neuroscience*, *4*(186), 1–8. https://doi.org/10.3389/fnhum.2010.00186

Jensen, O., Pan, Y., Frisson, S., & Wang, L. (2021). An oscillatory pipelining mechanism supporting previewing during visual exploration and reading. *Trends in Cognitive Sciences*, *25*(12), 1033–1044. https://doi.org/10.1016/j.tics.2021.08.008

Jensen, P. S. (1999). A 14-month randomized clinical trial of treatment strategies for attention-deficit/hyperactivity disorder. *Archives of General Psychiatry*, *56*(12), 1073–1086. https://doi.org/10.1001/archpsyc.56.12.1073

Jepma, M., & Nieuwenhuis, S. (2011). Pupil diameter predicts changes in the exploration-exploitation trade-off: Evidence for the adaptive gain theory. *Journal of Cognitive Neuroscience*, *23*(7), 1587–1596.

https://doi.org/10.1162/jocn.2010.21548

Jerbi, K., Ossandón, T., Hamamé, C. M., Senova, S., Dalal, S. S., Jung, J., Minotti, L., Bertrand, O., Berthoz, A., Kahane, P., & Lachaux, J. P. (2009). Task-related gamma-band dynamics from an intracerebral perspective: Review and implications for surface EEG and MEG. *Human Brain Mapping*, *30*(6), 1758–1771. https://doi.org/10.1002/hbm.20750

Jiang, J., Beck, J., Heller, K., & Egner, T. (2015). An insula-frontostriatal network mediates flexible cognitive control by adaptively predicting changing control demands. *Nature Communications*, *6*(8165), 1–11. https://doi.org/10.1038/ncomms9165

Jiang, K., Yi, Y., Li, L., Li, H., Shen, H., Zhao, F., Xu, Y., & Zheng, A. (2019). Functional network connectivity changes in children with attention-deficit hyperactivity disorder: A resting-state fMRI study. *International Journal of Developmental Neuroscience*, *78*, 1–6. https://doi.org/10.1016/j.ijdevneu.2019.07.003

Johnston, K., & Everling, S. (2006). Monkey dorsolateral prefrontal cortex sends task-selective signals directly to the superior colliculus. *Journal of Neuroscience*, *26*(48), 12471–12478. https://doi.org/10.1523/JNEUROSCI.4101-06.2006

Johnston, K., Levin, H. M., Koval, M. J., & Everling, S. (2007). Top-Down Control-Signal Dynamics in Anterior Cingulate and Prefrontal Cortex

Neurons following Task Switching. *Neuron*, *53*(3), 453–462. https://doi.org/10.1016/j.neuron.2006.12.023

Jones, S. R. (2016). When brain rhythms aren't 'rhythmic': implication for their mechanisms and meaning. *Current Opinion in Neurobiology*, *40*, 72–80. https://doi.org/10.1016/j.conb.2016.06.010

Joshi, S., & Gold, J. I. (2020). Pupil Size as a Window on Neural Substrates of Cognition. *Trends in Cognitive Sciences*, *24*(6), 466–480. https://doi.org/10.1016/J.TICS.2020.03.005

Joshi, S., Li, Y., Kalwani, R. M., & Gold, J. I. (2016). Relationships between Pupil Diameter and Neuronal Activity in the Locus Coeruleus, Colliculi, and Cingulate Cortex. *Neuron*, *89*(1), 221–234. https://doi.org/10.1016/j.neuron.2015.11.028

Jung, J. Y., Jackson, S. R., Nam, K., Hollis, C., & Jackson, G. M. (2015). Enhanced saccadic control in young people with Tourette syndrome despite slowed pro-saccades. *Journal of Neuropsychology*, *9*(2), 172–183. https://doi.org/10.1111/jnp.12044

Jurkiewicz, M. T., Gaetz, W. C., Bostan, A. C., & Cheyne, D. (2006). Post-movement beta rebound is generated in motor cortex: Evidence from neuromagnetic recordings. *NeuroImage*, *32*(3), 1281–1289. https://doi.org/10.1016/j.neuroimage.2006.06.005

Kahneman, D., & Beatty, J. (1966). Pupil diameter and load on memory. *Science*, *154*(3756), 1583–1585.

https://doi.org/10.1126/science.154.3756.1583

Kamp, S. M., & Donchin, E. (2015). ERP and pupil responses to deviance in an oddball paradigm. *Psychophysiology*, *52*(4), 460–471. https://doi.org/10.1111/psyp.12378

Kanai, R., Muggleton, N., & Walsh, V. (2012). Transcranial direct current stimulation of the frontal eye fields during pro- and antisaccade tasks. *Frontiers in Psychiatry*, *3*(45), 1–10. https://doi.org/10.3389/fpsyt.2012.00045

Kaplan, B. J., Dewey, D. M., Crawford, S. G., & Wilson, B. N. (2001). The term comorbidity is of questionable value in reference to developmental disorders: Data and theory. *Journal of Learning Disabilities*, *34*(6), 555–565. https://doi.org/10.1177/002221940103400608

Kapur, S. (2003). Psychosis as a state of aberrant salience: A framework linking biology, phenomenology, and pharmacology in schizophrenia. *American Journal of Psychiatry*, *160*(1), 13–23. https://doi.org/10.1176/appi.ajp.160.1.13

Kapur, S., Mizrahi, R., & Li, M. (2005). From dopamine to salience to psychosis-linking biology, pharmacology and phenomenology of psychosis. *Schizophrenia Research*, *79*(1), 59–68. https://doi.org/10.1016/j.schres.2005.01.003

Karatekin, C., Bingham, C., & White, T. (2010). Oculomotor and pupillometric indices of pro- and antisaccade performance in youth-

onset psychosis and attention deficit/hyperactivity disorder. *Schizophrenia Bulletin*, *36*(6), 1167–1186. https://doi.org/10.1093/schbul/sbp035

Kardamakis, A. A., & Moschovakis, A. K. (2009). Optimal control of gaze shifts. *Journal of Neuroscience*, *29*(24), 7723–7730. https://doi.org/10.1523/JNEUROSCI.5518-08.2009

Kawashima, R., Tanji, J., Okada, K., Sugiura, M., Sato, K., Kinomura, S., Inoue, K., Ogawa, A., & Fukuda, H. (1998). Oculomotor sequence learning: A positron emission tomography study. *Experimental Brain Research*, *122*(1), 1–8. https://doi.org/10.1007/s002210050485

Kershner, J. R. (2021). An Evolutionary Perspective of Dyslexia, Stress, and Brain Network Homeostasis. *Frontiers in Human Neuroscience*, *14*(575546), 1–16. https://doi.org/10.3389/FNHUM.2020.575546

Kher, R. (2019). Signal Processing Techniques for Removing Noise from ECG Signals. *J Biomed Eng Res*, *3*(1), 1–9. https://doi.org/10.17303

Kingstone, A., & Klein, R. M. (1993). What are human express saccades? *Perception & Psychophysics*, *54*(2), 260–273. https://doi.org/10.3758/BF03211762

Klein-Schwartz, W. (2002). Abuse and toxicity of methylphenidate. *Current Opinion in Pediatrics*, *14*(2), 219–223. https://doi.org/10.1097/00008480-200204000-00013

Klein, C. H., Raschke, A., & Brandenbusch, A. (2003). Development of pro- and antisaccades in children with attention-deficit hyperactivity disorder (ADHD) and healthy controls. *Psychophysiology*, *40*(1), 17–28. https://doi.org/10.1111/1469-8986.00003

Klein, R. G., Mannuzza, S., Ramos Olazagasti, M. A., Roizen, E., Hutchison, J. A., Lashua, E. C., & Castellanos, F. X. (2012). Clinical and Functional Outcome of Childhood Attention-Deficit/Hyperactivity Disorder 33 Years Later. *Archives of General Psychiatry*, *69*(12), 1295–1303. https://doi.org/10.1001/ARCHGENPSYCHIATRY.2012.271

Klimesch, W., Sauseng, P., & Hanslmayr, S. (2007). EEG alpha oscillations: The inhibition-timing hypothesis. *Brain Research Reviews*, *53*(1), 63–88. https://doi.org/10.1016/j.brainresrev.2006.06.003

Klingberg, T., Fernell, E., Olesen, P. J., Johnson, M., Gustafsson, P., Dahlström, K., Gillberg, C. G., Forssberg, H., & Westerberg, H. (2005). Computerized training of working memory in children with ADHD - A randomized, controlled trial. *Journal of the American Academy of Child and Adolescent Psychiatry*, *44*(2), 177–186. https://doi.org/10.1097/00004583-200502000-00010

Klingberg, T., Forssberg, H., & Westerberg, H. (2002). Training of working memory in children with ADHD. *Journal of Clinical and Experimental Neuropsychology*, *24*(6), 781–791. https://doi.org/10.1076/jcen.24.6.781.8395

Kluge, C., Bauer, M., Leff, A. P., Heinze, H. J., Dolan, R. J., & Driver, J. (2011). Plasticity of human auditory-evoked fields induced by shock conditioning and contingency reversal. *Proceedings of the National Academy of Sciences of the United States of America*, *108*(30), 12545–12550. https://doi.org/10.1073/pnas.1016124108

Kooij, J. J. S., Buitelaar, J. K., van den Oord, E. J., Furer, J. W., Rijnders, C. A. T., & Hodiamont, P. P. G. (2005). Internal and external validity of Attention-Deficit Hyperactivity Disorder in a population-based sample of adults. *Psychological Medicine*, *35*(6), 817–827. https://doi.org/10.1017/S003329170400337X

Kostandyan, M., Bombeke, K., Carsten, T., Krebs, R. M., Notebaert, W., & Boehler, C. N. (2019). Differential effects of sustained and transient effort triggered by reward – A combined EEG and pupillometry study. *Neuropsychologia*, *123*, 116–130. https://doi.org/10.1016/j.neuropsychologia.2018.04.032

Koyama, M., Hasegawa, I., Osada, T., Adachi, Y., Nakahara, K., & Miyashita, Y. (2004). Functional magnetic resonance imaging of macaque monkeys performing visually guided saccade tasks: Comparison of cortical eye fields with humans. *Neuron*, *41*(5), 795–807. https://doi.org/10.1016/S0896-6273(04)00047-9

Krasnow, B., Tamm, L., Greicius, M. D., Yang, T. T., Glover, G. H., Reiss, A. L., & Menon, V. (2003). Comparison of fMRI activation at 3 and 1.5 T during perceptual, cognitive, and affective processing. *NeuroImage*,

18(4), 813–826. https://doi.org/10.1016/S1053-8119(03)00002-8

Krinzinger, H., Hall, C. L., Groom, M. J., Ansari, M. T., Banaschewski, T., Buitelaar, J. K., Carucci, S., Coghill, D., Danckaerts, M., Dittmann, R. W., Falissard, B., Garas, P., Inglis, S. K., Kovshoff, H., Kochhar, P., McCarthy, S., Nagy, P., Neubert, A., Roberts, S., … Liddle, E. B. (2019). Neurological and psychiatric adverse effects of long-term methylphenidate treatment in ADHD: A map of the current evidence. *Neuroscience and Biobehavioral Reviews*, *107*, 945–968. https://doi.org/10.1016/j.neubiorev.2019.09.023

Kubota, Y., Sato, W., Toichi, M., Murai, T., Okada, T., Hayashi, A., & Sengoku, A. (2001). Frontal midline theta rhythm is correlated with cardiac autonomic activities during the performance of an attention demanding meditation procedure. *Cognitive Brain Research*, *11*(2), 281–287. https://doi.org/10.1016/S0926-6410(00)00086-0

Kucian, K., & von Aster, M. (2015). Developmental dyscalculia. *European Journal of Pediatrics*, *174*(1), 1–13. https://doi.org/10.1007/s00431-014-2455-7

Kurniawan, I. T., Grueschow, M., & Ruff, C. C. (2020). A pupil-linked arousal mechanism for deciding to engage in future physical effort. *BioRxiv*, 2020.02.25.964676. https://doi.org/10.1101/2020.02.25.964676

Kwon, S. J., Kim, Y., & Kwak, Y. (2018). Difficulties faced by university students with self-reported symptoms of attention-deficit hyperactivity

disorder: A qualitative study. *Child and Adolescent Psychiatry and Mental Health*, *12*(1), 1–8. https://doi.org/10.1186/s13034-018-0218-3

La Cour, P., & Petersen, M. (2015). Effects of Mindfulness Meditation on Chronic Pain: A Randomized Controlled Trial. *Pain Medicine (United States)*, *16*(4), 641–652. https://doi.org/10.1111/pme.12605

Lacadie, C. M., Fulbright, R. K., Rajeevan, N., Constable, R. T., & Papademetris, X. (2008). More accurate Talairach coordinates for neuroimaging using non-linear registration. *NeuroImage*, *42*(2), 717–725. https://doi.org/10.1016/j.neuroimage.2008.04.240

Lacey, B. C., & Lacey, J. I. (1974). Studies of heart rate and other bodily processes in sensorimotor behavior. In *Cardiovascular psychophysiology: Current issues in response mechanisms, biofeedback and methodollogy* (pp. 538–564). AldineTransaction. https://doi.org/10.4324/9781315081762-31

Lacey, B. C., & Lacey, J. I. (1978). Two-way communication between the heart and the brain: Significance of time within the cardiac cycle. *American Psychologist*, *33*(2), 99–113. https://doi.org/10.1037/0003-066X.33.2.99

Laeng, B., Sirois, S., & Gredebäck, G. (2012). Pupillometry: A window to the preconscious? *Perspectives on Psychological Science*, *7*(1), 18–27. https://doi.org/10.1177/1745691611427305

Landerl, K., & Moll, K. (2010). Comorbidity of learning disorders:

Prevalence and familial transmission. *Journal of Child Psychology and Psychiatry*, *51*(3), 287–294. https://doi.org/10.1111/j.1469-7610.2009.02164.x

Lane, R. D., McRae, K., Reiman, E. M., Chen, K., Ahern, G. L., & Thayer, J. F. (2009). Neural correlates of heart rate variability during emotion. *NeuroImage*, *44*(1), 213–222. https://doi.org/10.1016/j.neuroimage.2008.07.056

Laube, I., Matthews, N., Dean, A. J., O'Connell, R. G., Mattingley, J. B., & Bellgrove, M. A. (2017). Scopolamine reduces electrophysiological indices of distractor suppression: Evidence from a contingent capture task. *Frontiers in Neural Circuits*, *11*(99), 1–14. https://doi.org/10.3389/fncir.2017.00099

Lazzaro, G., Bertoni, S., Menghini, D., Costanzo, F., Franceschini, S., Varuzza, C., Ronconi, L., Battisti, A., Gori, S., Facoetti, A., & Vicari, S. (2021). Beyond Reading Modulation: Temporo-Parietal tDCS Alters Visuo-Spatial Attention and Motion Perception in Dyslexia. *Brain Sciences*, *11*(2), 1–17. https://doi.org/10.3390/brainsci11020263

Lee, A. K. C., Hämäläinen, M. S., Dyckman, K. A., Barton, J. J. S., & Manoach, D. S. (2011). Saccadic preparation in the frontal eye field is modulated by distinct trial history effects as revealed by magnetoencephalography. *Cerebral Cortex*, *21*(2), 245–253. https://doi.org/10.1093/cercor/bhq057

Lee, T. L., Yeung, M. K., Sze, S. L., & Chan, A. S. (2020). Computerized eye-tracking training improves the saccadic eye movements of children with attention-deficit/hyperactivity disorder. *Brain Sciences*, *10*(12), 1–9. https://doi.org/10.3390/brainsci10121016

Lee, T. L., Yeung, M. K., Sze, S. L., & Chan, A. S. (2021). Eye-tracking training improves inhibitory control in children with attention-deficit/hyperactivity disorder. *Brain Sciences*, *11*(3), 1–12. https://doi.org/10.3390/brainsci11030314

Lee, Y. J., Lee, S., Chang, M., & Kwak, H. W. (2015). Saccadic movement deficiencies in adults with ADHD tendencies. *ADHD Attention Deficit and Hyperactivity Disorders*, *7*(4), 271–280. https://doi.org/10.1007/s12402-015-0174-1

Leichnetz, G. R., Spencer, R. F., Hardy, S. G. P., & Astruc, J. (1981). The prefrontal corticotectal projection in the monkey; An anterograde and retrograde horseradish peroxidase study. *Neuroscience*, *6*(6), 1023–1041. https://doi.org/10.1016/0306-4522(81)90068-3

Libby, W. L., Lacey, B. C., & Lacey, J. I. (1973). Pupillary and Cardiac Activity During Visual Attention. *Psychophysiology*, *10*(3), 270–294. https://doi.org/10.1111/j.1469-8986.1973.tb00526.x

Liddle, E. B., Chou, Y. J., & Jackson, S. (2009). Perisaccadic mislocalization in dyslexia. *Neuropsychologia*, *47*(1), 77–82. https://doi.org/10.1016/j.neuropsychologia.2008.08.013

Liddle, E. B., Hollis, C., Batty, M. J., Groom, M. J., Totman, J. J., Liotti, M., Scerif, G., & Liddle, P. F. (2011). Task-related default mode network modulation and inhibitory control in ADHD: Effects of motivation and methylphenidate. *Journal of Child Psychology and Psychiatry and Allied Disciplines*, *52*(7), 761–771. https://doi.org/10.1111/j.1469-7610.2010.02333.x

Liddle, E. B., Price, D., Palaniyappan, L., Brookes, M. J., Robson, S. E., Hall, E. L., Morris, P. G., & Liddle, P. F. (2016). Abnormal salience signaling in schizophrenia: The role of integrative beta oscillations. *Human Brain Mapping*, *37*(4), 1361–1374. https://doi.org/10.1002/hbm.23107

Liston, C., Matalon, S., Hare, T. A., Davidson, M. C., & Casey, B. J. (2006). Anterior Cingulate and Posterior Parietal Cortices Are Sensitive to Dissociable Forms of Conflict in a Task-Switching Paradigm. *Neuron*, *50*(4), 643–653. https://doi.org/10.1016/j.neuron.2006.04.015

Little, S., Bonaiuto, J., Barnes, G., & Bestmann, S. (2019). Human motor cortical beta bursts relate to movement planning and response errors. *PLoS Biology*, *17*(10), e3000479. https://doi.org/10.1371/journal.pbio.3000479

Lockhofen, D. E. L., & Mulert, C. (2021). Neurochemistry of Visual Attention. *Frontiers in Neuroscience*, *15*(643597), 1–20. https://doi.org/10.3389/fnins.2021.643597

Lonergan, A., Doyle, C., Cassidy, C., MacSweeney Mahon, S., Roche, R. A.

P., Boran, L., & Bramham, J. (2019). A meta-analysis of executive functioning in dyslexia with consideration of the impact of comorbid ADHD. *Journal of Cognitive Psychology*, *31*(7), 725–749. https://doi.org/10.1080/20445911.2019.1669609

Lukasova, K., Silva, I. P., & Macedo, E. C. (2016). Impaired oculomotor behavior of children with developmental dyslexia in antisaccades and predictive saccades tasks. *Frontiers in Psychology*, *7*(987), 1–9. https://doi.org/10.3389/fpsyg.2016.00987

Luna, B., Thulborn, K. R., Strojwas, M. H., McCurtain, B. J., Berman, R. A., Genovese, C. R., & Sweeney, J. A. (1998). Dorsal cortical regions subserving visually guided saccades in humans: an fMRI study. *Cerebral Cortex*, *8*(1), 40–47. https://doi.org/10.1093/cercor/8.1.40

Lundqvist, M., Rose, J., Herman, P., Brincat, S. L. L., Buschman, T. J. J., & Miller, E. K. K. (2016). Gamma and Beta Bursts Underlie Working Memory. *Neuron*, *90*(1), 152–164. https://doi.org/10.1016/j.neuron.2016.02.028

Lynch, G. (2018). Using Pupillometry to Assess the Atypical Pupillary Light Reflex and LC-NE System in ASD. *Behavioral Sciences*, *8*(11), 108. https://doi.org/10.3390/bs8110108

Lyon, G. R., Shaywitz, S. E., & Shaywitz, B. A. (2003). A Definition of Dyslexia. *Annals of Dyslexia*, *53*(1), 1–14. https://doi.org/10.1007/s11881-003-0001-9

Machetanz, K., Berelidze, L., Guggenberger, R., & Gharabaghi, A. (2021). Brain–Heart Interaction During Transcutaneous Auricular Vagus Nerve Stimulation. *Frontiers in Neuroscience*, *15*(632697), 1–9. https://doi.org/10.3389/fnins.2021.632697

Macmillan, N. A., & Creelman, C. D. (2004). *Detection Theory: A User's Guide* (2nd ed.). Lawrence Erlbaum Associates, Inc., Publishers. https://doi.org/10.4324/9781410611147

Marino, R. A., Levy, R., & Munoz, D. P. (2015). Linking express saccade occurance to stimulus properties and sensorimotor integration in the superior colliculus. *Journal of Neurophysiology*, *114*(2), 879–892. https://doi.org/10.1152/jn.00047.2015

Marino, R. A., & Munoz, D. P. (2009). The effects of bottom-up target luminance and top-down spatial target predictability on saccadic reaction times. *Experimental Brain Research 2009 197:4*, *197*(4), 321–335. https://doi.org/10.1007/S00221-009-1919-X

Marshall, T. R., O'Shea, J., Jensen, O., & Bergmann, T. O. (2015). Frontal eye fields control attentional modulation of alpha and gamma oscillations in contralateral occipitoparietal cortex. *Journal of Neuroscience*, *35*(4), 1638–1647. https://doi.org/10.1523/JNEUROSCI.3116-14.2015

Martella, D., Aldunate, N., Fuentes, L. J., & Sánchez-Pérez, N. (2020). Arousal and Executive Alterations in Attention Deficit Hyperactivity

Disorder (ADHD). *Frontiers in Psychology*, *11*(1991), 1–7. https://doi.org/10.3389/fpsyg.2020.01991

Martin, A. B., Yang, X., Saalmann, Y. B., Wang, L., Shestyuk, A., Lin, J. J., Parvizi, J., Knight, R. T., & Kastner, S. (2019). Temporal dynamics and response modulation across the human visual system in a spatial attention task: An ECoG study. *Journal of Neuroscience*, *39*(2), 333–352. https://doi.org/10.1523/JNEUROSCI.1889-18.2018

Mathôt, S. (2018). Pupillometry: Psychology, physiology, and function. *Journal of Cognition*, *1*(1), 1–23, Art. 16. https://doi.org/10.5334/joc.18

Matsumoto, M., Inoue, K. I., & Takada, M. (2018). Causal Role of Neural Signals Transmitted From the Frontal Eye Field to the Superior Colliculus in Saccade Generation. *Frontiers in Neural Circuits*, *12*(69), 1–7. https://doi.org/10.3389/FNCIR.2018.00069

Mayes, S. D., Calhoun, S. L., & Crowell, E. W. (2000). Learning disabilities and ADHD: Overlapping spectrum disorders. *Journal of Learning Disabilities*, *33*(5), 417–424. https://doi.org/10.1177/002221940003300502

Mazziotta, J., Toga, A., Evans, A., Fox, P., Lancaster, J., Zilles, K., Woods, R., Paus, T., Simpson, G., Pike, B., Holmes, C., Collins, L., Thompson, P., MacDonald, D., Iacoboni, M., Schormann, T., Amunts, K., Palomero-Gallagher, N., Geyer, S., … Mazoyer, B. (2001). A four-dimensional probabilistic atlas of the human brain. *Journal of the American Medical*

Informatics Association, *8*(5), 401–430. https://doi.org/10.1136/jamia.2001.0080401

McAuliffe-Curtin, D., & Buckley, C. (1989). Review of alpha adrenoceptor function in the eye. *Eye*, *3*(4), 472–476. https://doi.org/10.1038/eye.1989.71

McCraty, R. (2011). Coherence: Bridging personal, social and global health. *Activitas Nervosa Superior Rediviva*, *53*(3), 85–102.

McDowell, J. E., Kissler, J. M., Berg, P., Dyckman, K. A., Gao, Y., Rockstroh, B., & Clementz, B. A. (2005). Electroencephalography/magnetoencephalography study of cortical activities preceding prosaccades and antisaccades. *NeuroReport*, *16*(7), 663–668. https://doi.org/10.1097/00001756-200505120-00002

McLaren, J. W., Erie, J. C., & Brubaker, R. F. (1992). Computerized analysis of pupillograms in studies of alertness. *Investigative Ophthalmology and Visual Science*, *33*(3), 671–676. https://europepmc.org/article/med/1544791

McMahon, C. M., Boisvert, I., de Lissa, P., Granger, L., Ibrahim, R., Lo, C. Y., Miles, K., & Graham, P. L. (2016). Monitoring alpha oscillations and pupil dilation across a performance-intensity function. *Frontiers in Psychology*, *7*(745), 1–12. https://doi.org/10.3389/fpsyg.2016.00745

McNorgan, C., Judson, C., Handzlik, D., & Holden, J. G. (2020). Linking ADHD and Behavioral Assessment Through Identification of Shared

Diagnostic Task-Based Functional Connections. *Frontiers in Physiology*, *11*(583005), 1–16. https://doi.org/10.3389/fphys.2020.583005

Menon, V., Adleman, N. E., White, C. D., Glover, G. H., & Reiss, A. L. (2001). Error-related brain activation during a Go/NoGo response inhibition task. *Human Brain Mapping*, *12*(3), 131–143. https://doi.org/10.1002/1097-0193(200103)12:3<131::AID-HBM1010>3.0.CO;2-C

Menon, V., & Uddin, L. Q. (2010). Saliency, switching, attention and control: a network model of insula function. *Brain Structure & Function*, *214*(5–6), 655–667. https://doi.org/10.1007/s00429-010-0262-0

Merriam, E. P., Colby, C. L., Thulborn, K. R., Luna, B., Olson, C. R., & Sweeney, J. A. (2001). Stimulus-response incompatibility activates cortex proximate to three eye fields. *NeuroImage*, *13*(5), 794–800. https://doi.org/10.1006/nimg.2000.0742

Meyer, K. N., Santillana, R., Miller, B., Clapp, W., Way, M., Bridgman-Goines, K., & Sheridan, M. A. (2020). Computer-based inhibitory control training in children with Attention-Deficit/Hyperactivity Disorder (ADHD): Evidence for behavioral and neural impact. *PLoS ONE*, *15*(11), e0241352. https://doi.org/10.1371/journal.pone.0241352

Mezzacappa, E., & Buckner, J. C. (2010). Working Memory Training for Children with Attention Problems or Hyperactivity: A School-Based

Pilot Study. *School Mental Health*, *2*(4), 202–208. https://doi.org/10.1007/s12310-010-9030-9

Miles, K., McMahon, C., Boisvert, I., Ibrahim, R., de Lissa, P., Graham, P., & Lyxell, B. (2017). Objective Assessment of Listening Effort: Coregistration of Pupillometry and EEG. *Trends in Hearing*, *21*, 1–13. https://doi.org/10.1177/2331216517706396

Mirpour, K., & Bisley, J. W. (2021). The roles of the lateral intraparietal area and frontal eye field in guiding eye movements in free viewing search behavior. *Journal of Neurophysiology*, *125*(6), 2144–2157. https://doi.org/10.1152/JN.00559.2020

Molina, B. S. G., Hinshaw, S. P., Swanson, J. M., Arnold, L. E., Vitiello, B., Jensen, P. S., Epstein, J. N., Hoza, B., Hechtman, L., Abikoff, H. B., Elliott, G. R., Greenhill, L. L., Newcorn, J. H., Wells, K. C., Wigal, T., Gibbons, R. D., Hur, K., & Houck, P. R. (2009). The MTA at 8 years: Prospective follow-up of children treated for combined-type ADHD in a multisite study. *Journal of the American Academy of Child and Adolescent Psychiatry*, *48*(5), 484–500. https://doi.org/10.1097/CHI.0b013e31819c23d0

Moll, K., Kunze, S., Neuhoff, N., Bruder, J., & Schulte-Körne, G. (2014). Specific learning disorder: Prevalence and gender differences. *PLoS ONE*, *9*(7), e103537. https://doi.org/10.1371/journal.pone.0103537

Moon, S. Y., Barton, J. J. S., Mikulski, S., Polli, F. E., Cain, M. S., Vangel,

M., Hämäläinen, M. S., & Manoach, D. S. (2007). Where left becomes right: A magnetoencephalographic study of sensorimotor transformation for antisaccades. *NeuroImage*, *36*(4), 1313–1323. https://doi.org/10.1016/j.neuroimage.2007.04.040

Morillas-Romero, A., Tortella-Feliu, M., Bornas, X., & Putman, P. (2015). Spontaneous EEG theta/beta ratio and delta–beta coupling in relation to attentional network functioning and self-reported attentional control. *Cognitive, Affective and Behavioral Neuroscience*, *15*(3), 598–606. https://doi.org/10.3758/s13415-015-0351-x

Morken, F., Jones, L. Ø., & Helland, W. A. (2021). Disorders of language and literacy in the prison population: A scoping review. *Education Sciences*, *11*(2), 1–25. https://doi.org/10.3390/educsci11020077

Mort, D. J., Perry, R. J., Mannan, S. K., Hodgson, T. L., Anderson, E., Quest, R., McRobbie, D., McBride, A., Husain, M., & Kennard, C. (2003). Differential cortical activation during voluntary and reflexive saccades in man. *NeuroImage*, *18*(2), 231–246. https://doi.org/10.1016/S1053-8119(02)00028-9

Mowlem, F., Agnew-Blais, J., Taylor, E., & Asherson, P. (2019). Do different factors influence whether girls versus boys meet ADHD diagnostic criteria? Sex differences among children with high ADHD symptoms. *Psychiatry Research*, *272*, 765–773. https://doi.org/10.1016/j.psychres.2018.12.128

Mueller, A., Krock, R. M., Shepard, S., & Moore, T. (2020). Dopamine Receptor Expression among Local and Visual Cortex-Projecting Frontal Eye Field Neurons. *Cerebral Cortex*, *30*(1), 148–164. https://doi.org/10.1093/cercor/bhz078

Mueller, S. C., Jackson, G. M., Dhalla, R., Datsopoulos, S., & Hollis, C. P. (2006). Enhanced cognitive control in young people with Tourette's syndrome. *Current Biology*, *16*(6), 570–573. https://doi.org/10.1016/j.cub.2006.01.064

Munoz, D. P., Armstrong, I. T., Hampton, K. A., & Moore, K. D. (2003). Altered control of visual fixation and saccadic eye movements in attention-deficit hyperactivity disorder. *Journal of Neurophysiology*, *90*(1), 503–514. https://doi.org/10.1152/jn.00192.2003

Munoz, D. P., Broughton, J. R., Goldring, J. E., & Armstrong, I. T. (1998). Age-related performance of human subjects on saccadic eye movement tasks. *Experimental Brain Research*, *121*(4), 391–400. https://doi.org/10.1007/s002210050473

Munoz, D. P., & Everling, S. (2004). Look away: The anti-saccade task and the voluntary control of eye movement. *Nature Reviews Neuroscience*, *5*(3), 218–228. https://doi.org/10.1038/nrn1345

Müri, R. M., Iba-Zizen, M. T., Derosier, C., Cabanis, E. A., & Pierrot-Deseilligny, C. (1996). Location of the human posterior eye field with functional magnetic resonance imaging. *Journal of Neurology*

Neurosurgery and Psychiatry, *60*(4), 445–448. https://doi.org/10.1136/jnnp.60.4.445

Murphy, P. R., Robertson, I. H., Balsters, J. H., & O'connell, R. G. (2011). Pupillometry and P3 index the locus coeruleus-noradrenergic arousal function in humans. *Psychophysiology*, *48*(11), 1532–1543. https://doi.org/10.1111/j.1469-8986.2011.01226.x

Mutschler, I., Wieckhorst, B., Kowalevski, S., Derix, J., Wentlandt, J., Schulze-Bonhage, A., & Ball, T. (2009). Functional organization of the human anterior insular cortex. *Neuroscience Letters*, *457*(2), 66–70. https://doi.org/10.1016/j.neulet.2009.03.101

Nácher, V., Ledberg, A., Deco, G., & Romo, R. (2013). Coherent delta-band oscillations between cortical areas correlate with decision making. *Proceedings of the National Academy of Sciences of the United States of America*, *110*(37), 15085–15090. https://doi.org/10.1073/pnas.1314681110

Nagai, Y., Critchley, H. D., Featherstone, E., Trimble, M. R., & Dolan, R. J. (2004). Activity in ventromedial prefrontal cortex covaries with sympathetic skin conductance level: A physiological account of a "default mode" of brain function. *NeuroImage*, *22*(1), 243–251. https://doi.org/10.1016/j.neuroimage.2004.01.019

Namkung, H., Kim, S. H., & Sawa, A. (2017). The Insula: An Underestimated Brain Area in Clinical Neuroscience, Psychiatry, and

Neurology. *Trends in Neurosciences*, *40*(4), 200–207. https://doi.org/10.1016/j.tins.2017.02.002

Nelson, S. M., Dosenbach, N. U. F., Cohen, A. L., Wheeler, M. E., Schlaggar, B. L., & Petersen, S. E. (2010). Role of the anterior insula in task-level control and focal attention. *Brain Structure & Function*, *214*(5–6), 669–680. https://doi.org/10.1007/s00429-010-0260-2

Neuper, C., & Pfurtscheller, G. (2001). Event-related dynamics of cortical rhythms: Frequency-specific features and functional correlates. *International Journal of Psychophysiology*, *43*(1), 41–58. https://doi.org/10.1016/S0167-8760(01)00178-7

Niendam, T. A., Laird, A. R., Ray, K. L., Dean, Y. M., Glahn, D. C., & Carter, C. S. (2012). Meta-analytic evidence for a superordinate cognitive control network subserving diverse executive functions. *Cognitive, Affective and Behavioral Neuroscience*, *12*(2), 241–268. https://doi.org/10.3758/s13415-011-0083-5

Nolte, G. (2003). The magnetic lead field theorem in the quasi-static approximation and its use for magnetoenchephalography forward calculation in realistic volume conductors. *Physics in Medicine and Biology*, *48*(22), 3637–3652. https://doi.org/10.1088/0031-9155/48/22/002

Nunan, D., Sandercock, G. R. H., & Brodie, D. A. (2010). A Quantitative Systematic Review of Normal Values for Short-Term Heart Rate

Variability in Healthy Adults. *Pacing and Clinical Electrophysiology*, *33*(11), 1407–1417. https://doi.org/10.1111/J.1540-8159.2010.02841.X

O'Neill, G. C., Tewarie, P. K., Colclough, G. L., Gascoyne, L. E., Hunt, B. A. E., Morris, P. G., Woolrich, M. W., & Brookes, M. J. (2017). Measurement of dynamic task related functional networks using MEG. *NeuroImage*, *146*, 667–678. https://doi.org/10.1016/j.neuroimage.2016.08.061

Okada, Y. C., Wu, J., & Kyuhou, S. (1997). Genesis of MEG signals in a mammalian CNS structure. *Electroencephalography and Clinical Neurophysiology*, *103*(4), 474–485. https://doi.org/10.1016/S0013-4694(97)00043-6

Oostenveld, R., Fries, P., Maris, E., & Schoffelen, J. M. (2011). FieldTrip: Open source software for advanced analysis of MEG, EEG, and invasive electrophysiological data. *Computational Intelligence and Neuroscience*, *2011*(Article ID: 156869), 1–9. https://doi.org/10.1155/2011/156869

Ossandón, T., Vidal, J. R., Ciumas, C., Jerbi, K., Hamamé, C. M., Dalal, S. S., Bertrand, O., Minotti, L., Kahane, P., & Lachaux, J. P. (2012). Efficient "pop-out" visual search elicits sustained broadband gamma activity in the dorsal attention network. *Journal of Neuroscience*, *32*(10), 3414–3421. https://doi.org/10.1523/JNEUROSCI.6048-11.2012

Ottosen, C., Larsen, J. T., Faraone, S. V., Chen, Q., Hartman, C., Larsson,

H., Petersen, L., & Dalsgaard, S. (2019). Sex Differences in Comorbidity Patterns of Attention-Deficit/Hyperactivity Disorder. *Journal of the American Academy of Child and Adolescent Psychiatry*, *58*(4), 412–422. https://doi.org/10.1016/j.jaac.2018.07.910

Palaniyappan, L., & Liddle, P. F. (2012). Does the salience network play a cardinal role in psychosis? An emerging hypothesis of insular dysfunction. *Journal of Psychiatry and Neuroscience*, *37*(1), 17–27. https://doi.org/10.1503/jpn.100176

Pardina-Torner, H., Carbonell, X., & Castejón, M. (2019). A comparative analysis of the processing speed between video game players and non-players. *Aloma*, *37*(1), 13–20. https://doi.org/10.51698/aloma.2019.37.1.13-20

Parker, C., Whear, R., Ukoumunne, O. C., Bethel, A., Thompson-Coon, J., Stein, K., & Ford, T. (2015). School exclusion in children with psychiatric disorder or impairing psychopathology: a systematic review. *Emotional and Behavioural Difficulties*, *20*(3), 229–251. https://doi.org/10.1080/13632752.2014.945741

Parton, A., Nachev, P., Hodgson, T. L., Mort, D., Thomas, D., Ordidge, R., Morgan, P. S., Jackson, S., Rees, G., & Husain, M. (2007). Role of the human supplementary eye field in the control of saccadic eye movements. *Neuropsychologia*, *45*(5), 997–1008. https://doi.org/10.1016/j.neuropsychologia.2006.09.007

Patron, E., Mennella, R., Messerotti Benvenuti, S., & Thayer, J. F. (2019). The frontal cortex is a heart-brake: Reduction in delta oscillations is associated with heart rate deceleration. *NeuroImage*, *188*, 403–410. https://doi.org/10.1016/j.neuroimage.2018.12.035

Paus, T. (1996). Location and function of the human frontal eye-field: A selective review. *Neuropsychologia*, *34*(6), 475–483. https://doi.org/10.1016/0028-3932(95)00134-4

Peel, T. R., Dash, S., Lomber, S. G., & Corneil, B. D. (2017). Frontal eye field inactivation diminishes superior colliculus activity, but delayed saccadic accumulation governs reaction time increases. *Journal of Neuroscience*, *37*(48), 11715–11730. https://doi.org/10.1523/JNEUROSCI.2664-17.2017

Peters, J. L., Crewther, S. G., Murphy, M. J., & Bavin, E. L. (2021). Action video game training improves text reading accuracy, rate and comprehension in children with dyslexia: a randomized controlled trial. *Scientific Reports*, *11*(18584). https://doi.org/10.1038/s41598-021-98146-x

Petersen, S. E., & Posner, M. I. (2012). The attention system of the human brain: 20 years after. *Annual Review of Neuroscience*, *35*, 73–89. https://doi.org/10.1146/annurev-neuro-062111-150525

Peterson, R. L., & Pennington, B. F. (2012). Developmental dyslexia. *The Lancet*, *379*(9830), 1997–2007. https://doi.org/10.1016/S0140-

6736(12)60198-6

Peterson, R. L., & Pennington, B. F. (2015). Developmental dyslexia. *Annual Review of Clinical Psychology*, *11*, 283–307. https://doi.org/10.1146/annurev-clinpsy-032814-112842

Petit, L., & Haxby, J. V. (1999). Functional anatomy of pursuit eye movements in humans as revealed by fMRI. *Journal of Neurophysiology*, *82*(1), 463–471. https://doi.org/10.1152/jn.1999.82.1.463

Phillips, J. M., Vinck, M., Everling, S., & Womelsdorf, T. (2014). A long-range fronto-parietal 5- to 10-Hz network predicts "top-down" controlled guidance in a task-switch paradigm. *Cerebral Cortex*, *24*(8), 1996–2008. https://doi.org/10.1093/cercor/bht050

Pierrot-Deseilligny, C., Müri, R. M., Ploner, C. J., Gaymard, B., Demeret, S., & Rivaud-Pechoux, S. (2003). Decisional role of the dorsolateral prefrontal cortex in ocular motor behaviour. *Brain*, *126*(6), 1460–1473. https://doi.org/10.1093/brain/awg148

Pierrot-Deseilligny, C., Ploner, C. J., Müri, R. M., Gaymard, B., & Rivaud-Péchoux, S. (2002). Effects of cortical lesions on saccadic eye movements in humans. *Annals of the New York Academy of Sciences*, *956*(1), 216–229. https://doi.org/10.1111/j.1749-6632.2002.tb02821.x

Pierrot-Deseilligny, C., Rivaud, S., Gaymard, B., & Agid, Y. (1991). Cortical control of reflexive visually-guided saccades. *Brain*, *114*(3), 1473–1485.

https://doi.org/10.1093/brain/114.3.1473

Pierrot-Deseilligny, C., Rivaud, S., Gaymard, B., Müri, R., & Vermersch, A. -I. (1995). Cortical control of saccades. *Annals of Neurology*, *37*(5), 557–567. https://doi.org/10.1002/ana.410370504

Pievsky, M. A., & McGrath, R. E. (2018). The Neurocognitive Profile of Attention-Deficit/Hyperactivity Disorder: A Review of Meta-Analyses. *Archives of Clinical Neuropsychology*, *33*(2), 143–157. https://doi.org/10.1093/arclin/acx055

Plichta, M. M., Vasic, N., Wolf, R. C., Lesch, K. P., Brummer, D., Jacob, C., Fallgatter, A. J., & Grön, G. (2009). Neural Hyporesponsiveness and Hyperresponsiveness During Immediate and Delayed Reward Processing in Adult Attention-Deficit/Hyperactivity Disorder. *Biological Psychiatry*, *65*(1), 7–14. https://doi.org/10.1016/j.biopsych.2008.07.008

Polanczyk, G. V., De Lima, M. S., Horta, B. L., Biederman, J., & Rohde, L. A. (2007). The worldwide prevalence of ADHD: A systematic review and metaregression analysis. *American Journal of Psychiatry*, *164*(6), 942–948. https://doi.org/10.1176/ajp.2007.164.6.942

Polanczyk, G. V., Willcutt, E. G., Salum, G. A., Kieling, C., & Rohde, L. A. (2014). ADHD prevalence estimates across three decades: An updated systematic review and meta-regression analysis. *International Journal of Epidemiology*, *43*(2), 434–442. https://doi.org/10.1093/ije/dyt261

Popov, T., Gips, B., Kastner, S., & Jensen, O. (2019). Spatial specificity of alpha oscillations in the human visual system. *Human Brain Mapping*, *40*(15), 4432–4440. https://doi.org/10.1002/hbm.24712

Porges, S. W. (2001). The polyvagal theory: Phylogenetic substrates of a social nervous system. *International Journal of Psychophysiology*, *42*(2), 123–146. https://doi.org/10.1016/S0167-8760(01)00162-3

Porges, S. W. (2007). The polyvagal perspective. *Biological Psychology*, *74*(2), 116–143. https://doi.org/10.1016/j.biopsycho.2006.06.009

Porges, S. W. (2011). *The Polyvagal Theory: Neurophysiological Foundations of Emotions Attachment, Communication, and Self-regulation*. W. W. Norton & Company.

Posner, M. I. (1980). Orienting of attention. *The Quarterly Journal of Experimental Psychology*, *32*(1), 3–25. https://doi.org/10.1080/00335558008248231

Posner, M. I., Nissen, M. J., & Klein, R. M. (1976). Visual dominance: An information-processing account of its origins and significance. *Psychological Review*, *83*(2), 157–171. https://doi.org/10.1037/0033-295X.83.2.157

Posner, M. I., & Petersen, S. E. (1990). The attention system of the human brain. *Annual Review of Neuroscience*, *13*, 25–42. https://doi.org/10.1146/annurev.ne.13.030190.000325

Rajkowski, J., Majczynski, H., Clayton, E., & Aston-Jones, G. (2004). Activation of monkey locus coeruleus neurons varies with difficulty and performance in a target detection task. *Journal of Neurophysiology*, *92*(1), 361–371. https://doi.org/10.1152/jn.00673.2003

Rapport, M. D., Orban, S. A., Kofler, M. J., & Friedman, L. M. (2013). Do programs designed to train working memory, other executive functions, and attention benefit children with ADHD? A meta-analytic review of cognitive, academic, and behavioral outcomes. *Clinical Psychology Review*, *33*(8), 1237–1252. https://doi.org/10.1016/J.CPR.2013.08.005

Rayner, K. (1998). Eye Movements in Reading and Information Processing: 20 Years of Research. *Psychological Bulletin*, *124*(3), 372–422. https://doi.org/10.1037/0033-2909.124.3.372

Rayner, K. (2009). Eye Movements in Reading: Models and Data. *Journal of Eye Movement Research*, *2*(5), 1. https://doi.org/10.16910/jemr.2.5.2

Rayner, K., Binder, K. S., Ashby, J., & Pollatsek, A. (2001). Eye movement control in reading: Word predictability has little influence on initial landing positions in words. *Vision Research*, *41*(7), 943–954. https://doi.org/10.1016/S0042-6989(00)00310-2

RECOGNeyesPromotion - YouTube. (2017, July 21). https://www.youtube.com/watch?v=HRjK8iJbkao

Ress, D., Backus, B. T., & Heeger, D. J. (2000). Activity in primary visual cortex predicts performance in a visual detection task. *Nature*

Neuroscience, *3*(9), 940–945. https://doi.org/10.1038/78856

Reyes del Paso, G. A., Montoro, C. I., & Duschek, S. (2015). Reaction time, cerebral blood flow, and heart rate responses in fibromyalgia: Evidence of alterations in attentional control. *Journal of Clinical and Experimental Neuropsychology*, *37*(4), 414–428. https://doi.org/10.1080/13803395.2015.1023265

Ribeiro, M. J., & Castelo-Branco, M. (2019). Neural correlates of anticipatory cardiac deceleration and its association with the speed of perceptual decision-making, in young and older adults. *NeuroImage*, *199*, 521–533. https://doi.org/10.1016/J.NEUROIMAGE.2019.06.004

Richer, F., & Beatty, J. (1987). Contrasting Effects of Response Uncertainty on the Task-Evoked Pupillary Response and Reaction Time. *Psychophysiology*, *24*(3), 258–262. https://doi.org/10.1111/j.1469-8986.1987.tb00291.x

Richlan, F., Kronbichler, M., & Wimmer, H. (2011). Meta-analyzing brain dysfunctions in dyslexic children and adults. *NeuroImage*, *56*(3), 1735–1742. https://doi.org/10.1016/j.neuroimage.2011.02.040

Riddle, J., Hwang, K., Cellier, D., Dhanani, S., & D'esposito, M. (2019). Causal evidence for the role of neuronal oscillations in top–down and bottom–up attention. *Journal of Cognitive Neuroscience*, *31*(5), 768–779. https://doi.org/10.1162/jocn_a_01376

Riddle, J., Vogelsang, D. A., Hwang, K., Cellier, D., & D'Esposito, M. (2020).

Distinct Oscillatory Dynamics Underlie Different Components of Hierarchical Cognitive Control. *Journal of Neuroscience*, *40*(25), 4945–4953. https://doi.org/10.1523/JNEUROSCI.0617-20.2020

Robinson, D. A. (1972). Eye movements evoked by collicular stimulation in the alert monkey. *Vision Research*, *12*(11), 1795–1808. https://doi.org/10.1016/0042-6989(72)90070-3

Robinson, S. E., & Vrba, J. (1999). Recent advances in biomagnetism. Functional neuroimaging by synthetic aperture magnetometry (SAM). *Tohoku University Press, Sendai*, 302–305.

Roelofs, K. (2017). Freeze for action: Neurobiological mechanisms in animal and human freezing. *Philosophical Transactions of the Royal Society B: Biological Sciences*, *372*(1718), 1–10. https://doi.org/10.1098/rstb.2016.0206

Rokem, A., Landau, A. N., Garg, D., Prinzmetal, W., & Silver, M. A. (2010). Cholinergic enhancement increases the effects of voluntary attention but does not affect involuntary attention. *Neuropsychopharmacology*, *35*(13), 2538–2544. https://doi.org/10.1038/npp.2010.118

Roth, Z. N., Ryoo, M., & Merriam, E. P. (2020). Task-related activity in human visual cortex. *PLoS Biology*, *18*(11), e3000921. https://doi.org/10.1371/journal.pbio.3000921

Rowe, J. B., Toni, I., Josephs, O., Frackowiak, R. S. J., & Passingham, R. E. (2000). The prefrontal cortex: Response selection or maintenance

within working memory? *Science*, *288*(5471), 1656–1660. https://doi.org/10.1126/science.288.5471.1656

Rubia, K. (2018). Cognitive neuroscience of attention deficit hyperactivity disorder (ADHD) and its clinical translation. *Frontiers in Human Neuroscience*, *12*(100), 1–23. https://doi.org/10.3389/fnhum.2018.00100

Ryan, S., Bonilha, L., & Jackson, S. R. (2006). Individual variation in the location of the parietal eye fields: A TMS study. *Experimental Brain Research*, *173*(3), 389–394. https://doi.org/10.1007/s00221-006-0379-9

Sachs, M., Kaplan, J., Der Sarkissian, A., & Habibi, A. (2017). Increased engagement of the cognitive control network associated with music training in children during an fMRI Stroop task. *PLoS ONE*, *12*(10), e0187254. https://doi.org/10.1371/journal.pone.0187254

Sales, P., Murphy, F., Murphy, S., & Lau, N. (2019). Burning the candle at both ends: motivations for non-medical prescription stimulant use in the American workplace. *Drugs: Education, Prevention and Policy*, *26*(4), 301–308. https://doi.org/10.1080/09687637.2019.1606895

Samuels, E., & Szabadi, E. (2008a). Functional Neuroanatomy of the Noradrenergic Locus Coeruleus: Its Roles in the Regulation of Arousal and Autonomic Function Part I: Principles of Functional Organisation. *Current Neuropharmacology*, *6*(3), 235–253. https://doi.org/10.2174/157015908785777229

Samuels, E., & Szabadi, E. (2008b). Functional Neuroanatomy of the

Noradrenergic Locus Coeruleus: Its Roles in the Regulation of Arousal and Autonomic Function Part II: Physiological and Pharmacological Manipulations and Pathological Alterations of Locus Coeruleus Activity in Humans. *Current Neuropharmacology*, *6*(3), 254–285. https://doi.org/10.2174/157015908785777193

Sapountzis, P., Paneri, S., & Gregoriou, G. G. (2018). Distinct roles of prefrontal and parietal areas in the encoding of attentional priority. *Proceedings of the National Academy of Sciences of the United States of America*, *115*(37), E8755–E8764. https://doi.org/10.1073/pnas.1804643115

Sara, S. J., & Bouret, S. (2012). Orienting and Reorienting: The Locus Coeruleus Mediates Cognition through Arousal. *Neuron*, *76*(1), 130–141. https://doi.org/10.1016/j.neuron.2012.09.011

Sauseng, P., Hoppe, J., Klimesch, W., Gerloff, C., & Hummel, F. C. (2007). Dissociation of sustained attention from central executive functions: Local activity and interregional connectivity in the theta range. *European Journal of Neuroscience*, *25*(2), 587–593. https://doi.org/10.1111/j.1460-9568.2006.05286.x

Schall, J. D., Zinke, W., Cosman, J. D., Schall, M. S., Paré, M., & Pouget, P. (2017). On the Evolution of the Frontal Eye Field: Comparisons of Monkeys, Apes, and Humans. In *Evolution of Nervous Systems* (2nd ed., Vol. 4, pp. 249–275). Elsevier. https://doi.org/10.1016/B978-0-12-804042-3.00130-5

Scharinger, C., Soutschek, A., Schubert, T., & Gerjets, P. (2015). When flanker meets the n-back: What EEG and pupil dilation data reveal about the interplay between the two central-executive working memory functions inhibition and updating. *Psychophysiology*, *52*(10), 1293–1304. https://doi.org/10.1111/psyp.12500

Scheres, A., Tontsch, C., Thoeny, A. L., & Kaczkurkin, A. (2010). Temporal Reward Discounting in Attention-Deficit/Hyperactivity Disorder: The Contribution of Symptom Domains, Reward Magnitude, and Session Length. *Biological Psychiatry*, *67*(7), 641–648. https://doi.org/10.1016/j.biopsych.2009.10.033

Schiller, P. H., Haushofer, J., & Kendall, G. (2004). An examination of the variables that affect express saccade generation. *Visual Neuroscience*, *21*(2), 119–127. https://doi.org/10.1017/S0952523804042038

Schlag-Rey, M., Amador, N., Sanchez, H., & Schlag, J. (1997). Antisaccade performance predicted by neuronal activity in the supplementary eye field. *Nature*, *390*(6658), 398–401. https://doi.org/10.1038/37114

Schlag, J., & Schlag-Rey, M. (1987). Evidence for a supplementary eye field. *Journal of Neurophysiology*, *57*(1), 179–200. https://doi.org/10.1152/jn.1987.57.1.179

Schultz, B. K., Evans, S. W., Langberg, J. M., & Schoemann, A. M. (2017). Outcomes for adolescents who comply with long-term psychosocial treatment for ADHD. *Journal of Consulting and Clinical Psychology*,

85(3), 250–261. https://doi.org/10.1037/ccp0000172

Sedgwick, J. A. (2018). University students with attention deficit hyperactivity disorder (ADHD): A literature review. *Irish Journal of Psychological Medicine*, *35*(3), 221–235. https://doi.org/10.1017/ipm.2017.20

Seeley, W. W. (2019). The salience network: A neural system for perceiving and responding to homeostatic demands. *Journal of Neuroscience*, *39*(50), 9878–9882. https://doi.org/10.1523/JNEUROSCI.1138-17.2019

Seeley, W. W., Menon, V., Schatzberg, A. F., Keller, J., Glover, G. H., Kenna, H., Reiss, A. L., & Greicius, M. D. (2007). Dissociable intrinsic connectivity networks for salience processing and executive control. *Journal of Neuroscience*, *27*(9), 2349–2356. https://doi.org/10.1523/JNEUROSCI.5587-06.2007

Sekihara, K., Nagarajan, S. S., Poeppel, D., & Marantz, A. (2004). Asymptotic SNR of scalar and vector minimum-variance beanformers for neuromagnetic source reconstruction. *IEEE Transactions on Biomedical Engineering*, *51*(10), 1726–1734. https://doi.org/10.1109/TBME.2004.827926

Seminowicz, D. A., & Moayedi, M. (2017). The Dorsolateral Prefrontal Cortex in Acute and Chronic Pain. *Journal of Pain*, *18*(9), 1027–1035. https://doi.org/10.1016/j.jpain.2017.03.008

Sergeant, J. A. (2005). Modeling attention-deficit/hyperactivity disorder: A

critical appraisal of the cognitive-energetic model. *Biological Psychiatry*, *57*(11), 1248–1255. https://doi.org/10.1016/j.biopsych.2004.09.010

Servan-Schreiber, D., Perlstein, W. M., Cohen, J. D., & Mintun, M. (1998). Selective pharmacological activation of limbic structures in human volunteers: A positron emission tomography study. *Journal of Neuropsychiatry and Clinical Neurosciences*, *10*(2), 148–159. https://doi.org/10.1176/jnp.10.2.148

Shaffer, F., McCraty, R., & Zerr, C. L. (2014). A healthy heart is not a metronome: an integrative review of the heart's anatomy and heart rate variability. *Frontiers in Psychology*, *5*(1040), 1–19. https://doi.org/10.3389/fpsyg.2014.01040

Shalev, R. S. (2004). Developmental dyscalculia. *Journal of Child Neurology*, *19*(10), 765–771. https://doi.org/10.1177/08830738040190100601

Sharma, R., Hicks, S., Berna, C. M., Kennard, C., Talbot, K., & Turner, M. R. (2011). Oculomotor dysfunction in amyotrophic lateral sclerosis: A comprehensive review. *Archives of Neurology*, *68*(7), 857–861. https://doi.org/10.1001/archneurol.2011.130

Shaw, M., Hodgkins, P., Caci, H., Young, S., Kahle, J., Woods, A. G., & Arnold, L. E. (2012). A systematic review and analysis of long-term outcomes in attention deficit hyperactivity disorder: Effects of

treatment and non-treatment. *BMC Medicine*, *10*(99), 1–15. https://doi.org/10.1186/1741-7015-10-99

Shaw, R., Grayson, A., & Lewis, V. (2005). Inhibition, ADHD, and computer games: The inhibitory performance of children with ADHD on computerized tasks and games. *Journal of Attention Disorders*, *8*(4), 160–168. https://doi.org/10.1177/1087054705278771

Shelley, B. P., & Trimble, M. R. (2004). The insular lobe of reil-its anatamico-functional, behavioural and neuropsychiatric attributes in humans - A review. *World Journal of Biological Psychiatry*, *5*(4), 176–200. https://doi.org/10.1080/15622970410029933

Sherman, M. A., Lee, S., Law, R., Haegens, S., Thorn, C. A., Hämäläinen, M. S., Moore, C. I., & Jones, S. R. (2016). Neural mechanisms of transient neocortical beta rhythms: Converging evidence from humans, computational modeling, monkeys, and mice. *Proceedings of the National Academy of Sciences of the United States of America*, *113*(33), E4885–E4894. https://doi.org/10.1073/pnas.1604135113

Shin, H., Law, R., Tsutsui, S., Moore, C. I., & Jones, S. R. (2017). The rate of transient beta frequency events predicts behavior across tasks and species. *ELife*, *6*(e29086), 1–31. https://doi.org/10.7554/eLife.29086

Siegle, G. J., Ichikawa, N., & Steinhauer, S. (2008). Blink before and after you think: Blinks occur prior to and following cognitive load indexed by pupillary responses. *Psychophysiology*, *45*(5), 679–687.

https://doi.org/10.1111/j.1469-8986.2008.00681.x

Silver, M. A., & Kastner, S. (2009). Topographic maps in human frontal and parietal cortex. *Trends in Cognitive Sciences*, *13*(11), 488–495. https://doi.org/10.1016/J.TICS.2009.08.005

Simonet, M., Meziane, H. B., Runswick, O. R., North, J. S., Williams, A. M., Barral, J., & Roca, A. (2019). The modulation of event-related alpha rhythm during the time course of anticipation. *Scientific Reports*, *9*(1), 1–11. https://doi.org/10.1038/s41598-019-54763-1

Sinnett, S., Spence, C., & Soto-Faraco, S. (2007). Visual dominance and attention: The Colavita effect revisited. *Perception and Psychophysics*, *69*(5), 673–686. https://doi.org/10.3758/BF03193770

Siqueiros Sanchez, M., Falck-Ytter, T., Kennedy, D. P., Bölte, S., Lichtenstein, P., D'Onofrio, B. M., & Pettersson, E. (2020). Volitional eye movement control and ADHD traits: a twin study. *Journal of Child Psychology and Psychiatry and Allied Disciplines*, *61*(12), 1309–1316. https://doi.org/10.1111/jcpp.13210

Sirois, S., & Brisson, J. (2014). Pupillometry. *Wiley Interdisciplinary Reviews: Cognitive Science*, *5*(6), 679–692. https://doi.org/10.1002/wcs.1323

Smith, A., Brice, C., Nash, J., Rich, N., & Nutt, D. J. (2003). Caffeine and central noradrenaline: Effects on mood, cognitive performance, eye movements and cardiovascular function. *Journal of*

Psychopharmacology, *17*(3), 283–292. https://doi.org/10.1177/02698811030173010

Smith, A., & Nutt, D. (1996). Noradrenaline and attention lapses. *Nature*, *380*(6572), 291. https://doi.org/10.1038/380291a0

Snowling, M. J. (2005). Specific learning difficulties. *Psychiatry*, *4*(9), 110–113. https://doi.org/10.1383/psyt.2005.4.9.110

Snowling, M. J., Hulme, C., & Nation, K. (2020). Defining and understanding dyslexia: past, present and future. *Oxford Review of Education*, *46*(4), 501–513. https://doi.org/10.1080/03054985.2020.1765756

Sokolov, E. N. (1963). Higher nervous functions; the orienting reflex. *Annual Review of Physiology*, *25*, 545–580. https://doi.org/10.1146/annurev.ph.25.030163.002553

Somsen, R., Jennings, J. R., & Van der Molen, M. (2002). Human vagal heart rate responses in warned reaction time tasks: A cross-validation with simulated vagus-sino-atrial node interactions. *Journal of Electrocardiology*, *35*(4), 231–237. https://doi.org/10.1054/jelc.2002.37190

Sonuga-Barke, E. J. S. (2002). Psychological heterogeneity in AD/HD - A dual pathway model of behaviour and cognition. *Behavioural Brain Research*, *130*(1–2), 29–36. https://doi.org/10.1016/S0166-4328(01)00432-6

Sonuga-Barke, E. J. S., Brandeis, D., Holtmann, M., & Cortese, S. (2014). Computer-based Cognitive Training for ADHD. A Review of Current Evidence. *Child and Adolescent Psychiatric Clinics of North America*, *23*(4), 807–824. https://doi.org/10.1016/j.chc.2014.05.009

Spagna, A., Kim, T. H., Wu, T., & Fan, J. (2020). Right hemisphere superiority for executive control of attention. *Cortex*, *122*, 263–276. https://doi.org/10.1016/j.cortex.2018.12.012

Spencer, T. J., Faraone, S. V., Tarko, L., McDermott, K., & Biederman, J. (2014). Attention-deficit/hyperactivity disorder and adverse health outcomes in adults. *Journal of Nervous and Mental Disease*, *202*(10), 725–731. https://doi.org/10.1097/NMD.0000000000000191

Spitzer, B., & Haegens, S. (2017). Beyond the status quo: A role for beta oscillations in endogenous content (RE)activation. *ENeuro*, *4*(4). https://doi.org/10.1523/ENEURO.0170-17.2017

Spreng, R. N., Stevens, W. D., Chamberlain, J. P., Gilmore, A. W., & Schacter, D. L. (2010). Default network activity, coupled with the frontoparietal control network, supports goal-directed cognition. *NeuroImage*, *53*(1), 303–317. https://doi.org/10.1016/j.neuroimage.2010.06.016

SR Research. (2017). *EyeLink® 1000 Plus User Manual, Version 1.0.12*. Mississauga, ON, Canada: SR Research Ltd.

Stanislaw, H., & Todorov, N. (1999). Calculation of signal detection theory

measures. *Behavior Research Methods, Instruments, and Computers*, *31*(1), 137–149. https://doi.org/10.3758/BF03207704

Stapleton-Kotloski, J. R., Kotloski, R. J., Popli, G., & Godwin, D. W. (2018). Magnetoencephalography: Clinical and Research Practices. *Brain Sciences*, *8*(8). https://doi.org/10.3390/BRAINSCI8080157

Stefanics, G., Hangya, B., Hernádi, I., Winkler, I., Lakatos, P., & Ulbert, I. (2010). Phase entrainment of human delta oscillations can mediate the effects of expectation on reaction speed. *Journal of Neuroscience*, *30*(41), 13578–13585. https://doi.org/10.1523/JNEUROSCI.0703-10.2010

Storebø, O. J., Pedersen, N., Ramstad, E., Kielsholm, M. L., Nielsen, S. S., Krogh, H. B., Moreira-Maia, C. R., Magnusson, F. L., Holmskov, M., Gerner, T., Skoog, M., Rosendal, S., Groth, C., Gillies, D., Buch Rasmussen, K., Gauci, D., Zwi, M., Kirubakaran, R., Håkonsen, S. J., … Gluud, C. (2018). Methylphenidate for attention deficit hyperactivity disorder (ADHD) in children and adolescents - assessment of adverse events in non-randomised studies. *Cochrane Database of Systematic Reviews*, *5*(5), CD012069. https://doi.org/10.1002/14651858.CD012069.pub2

Storebø, O. J., Ramstad, E., Krogh, H. B., Nilausen, T. D., Skoog, M., Holmskov, M., Rosendal, S., Groth, C., Magnusson, F. L., Moreira-Maia, C. R., Gillies, D., Buch Rasmussen, K., Gauci, D., Zwi, M., Kirubakaran, R., Forsbøl, B., Simonsen, E., & Gluud, C. (2015).

Methylphenidate for children and adolescents with attention deficit hyperactivity disorder (ADHD). *Cochrane Database of Systematic Reviews*, *11*(CD009885). https://doi.org/10.1002/14651858.CD009885.pub2

Strahler Rivero, T., Herrera Núñez, L. M., Uehara Pires, E., & Amodeo Bueno, O. F. (2015). ADHD rehabilitation through video gaming: A systematic review using PRISMA guidelines of the current findings and the associated risk of bias. *Frontiers in Psychiatry*, *6*(151), 1–16. https://doi.org/10.3389/fpsyt.2016.00173

Sturm, V. E., Brown, J. A., Hua, A. Y., Lwi, S. J., Zhou, J., Kurth, F., Eickhoff, S. B., Rosen, H. J., Kramer, J. H., Miller, B. L., Levenson, R. W., & Seeley, W. W. (2018). Network architecture underlying basal autonomic outflow: Evidence from frontotemporal dementia. *Journal of Neuroscience*, *38*(42), 8943–8955. https://doi.org/10.1523/JNEUROSCI.0347-18.2018

Swanson, J., Baler, R. D., & Volkow, N. D. (2011). Understanding the effects of stimulant medications on cognition in individuals with attention-deficit hyperactivity disorder: A decade of progress. *Neuropsychopharmacology*, *36*(1), 207–226. https://doi.org/10.1038/npp.2010.160

Tadel, F., Baillet, S., Mosher, J. C., Pantazis, D., & Leahy, R. M. (2011). Brainstorm: A user-friendly application for MEG/EEG analysis. *Computational Intelligence and Neuroscience*, *2011*.

https://doi.org/10.1155/2011/879716

Tadel, F., Bock, E., Niso, G., Mosher, J. C., Cousineau, M., Pantazis, D., Leahy, R. M., & Baillet, S. (2019). MEG/EEG group analysis with brainstorm. *Frontiers in Neuroscience*, *13*(FEB). https://doi.org/10.3389/fnins.2019.00076

Tajik-Parvinchi, D. J., & Sandor, P. (2013). Enhanced antisaccade abilities in children with Tourette syndrome: The Gap-effect Reversal. *Frontiers in Human Neuroscience*, *7*(768), 1–11. https://doi.org/10.3389/fnhum.2013.00768

Talairach, J., & Tournoux, P. (1988). Co-Planar Stereotaxis Atlas of the Human Brain. In *3-Dimensional Proportional System: An Approach to Cerebral Imaging*. Georg Thieme Verlag.

Tang, W., Jbabdi, S., Zhu, Z., Cottaar, M., Grisot, G., Lehman, J. F., Yendiki, A., & Haber, S. N. (2019). A connectional hub in the rostral anterior cingulate cortex links areas of emotion and cognitive control. *ELife*, *8*, e43761. https://doi.org/10.7554/eLife.43761.001

Tang, Y. Y., Yang, L., Leve, L. D., & Harold, G. T. (2012). Improving Executive Function and Its Neurobiological Mechanisms Through a Mindfulness-Based Intervention: Advances Within the Field of Developmental Neuroscience. *Child Development Perspectives*, *6*(4), 361–366. https://doi.org/10.1111/j.1750-8606.2012.00250.x

Tehovnik, E. J., Sommer, M. A., Chou, I. H., Slocum, W. M., & Schiller, P.

H. (2000). Eye fields in the frontal lobes of primates. *Brain Research Reviews*, *32*(2–3), 413–448. https://doi.org/10.1016/S0165-0173(99)00092-2

Thayer, J. F., Åhs, F., Fredrikson, M., Sollers, J. J., & Wager, T. D. (2012). A meta-analysis of heart rate variability and neuroimaging studies: Implications for heart rate variability as a marker of stress and health. *Neuroscience & Biobehavioral Reviews*, *36*(2), 747–756. https://doi.org/10.1016/J.NEUBIOREV.2011.11.009

Thayer, J. F., Hansen, A. L., Saus-Rose, E., & Johnsen, B. H. (2009). Heart rate variability, prefrontal neural function, and cognitive performance: The neurovisceral integration perspective on self-regulation, adaptation, and health. *Annals of Behavioral Medicine*, *37*(2), 141–153. https://doi.org/10.1007/s12160-009-9101-z

Thayer, J. F., & Lane, R. D. (2000). A model of neurovisceral integration in emotion regulation and dysregulation. *Journal of Affective Disorders*, *61*(3), 201–216. https://doi.org/10.1016/S0165-0327(00)00338-4

Theeuwes, J., & Godijn, R. (2004). Inhibition-of-return and oculomotor interference. *Vision Research*, *44*(12), 1485–1492. https://doi.org/10.1016/j.visres.2003.09.035

Thiele, A., & Bellgrove, M. A. (2018). Neuromodulation of Attention. *Neuron*, *97*(4), 769–785. https://doi.org/10.1016/J.NEURON.2018.01.008

Torgesen, J. K., Rashotte, C. A., & Wagner, R. K. (2012). *Test of Word Reading Efficiency - Second Edition (TOWRE-2)* (2nd ed). PRO-ED Inc.

Tremayne, P., & Barry, R. J. (2001). Elite pistol shooters: Physiological patterning of best vs. worst shots. *International Journal of Psychophysiology*, *41*(1), 19–29. https://doi.org/10.1016/S0167-8760(00)00175-6

Tripp, G., & Alsop, B. (2001). Sensitivity to Reward Delay in Children with Attention Deficit Hyperactivity Disorder (ADHD). *Journal of Child Psychology and Psychiatry*, *42*(5), 691–698. https://doi.org/10.1111/1469-7610.00764

Troksa, K., Kovacich, N., Moro, M., & Chavez, B. (2019). Impact of Central Nervous System Stimulant Medication Use on Growth in Pediatric Populations with Attention-Deficit/Hyperactivity Disorder: A Review. *Pharmacotherapy*, *39*(6), 665–676. https://doi.org/10.1002/phar.2192

Tzourio-Mazoyer, N., Landeau, B., Papathanassiou, D., Crivello, F., Etard, O., Delcroix, N., Mazoyer, B., & Joliot, M. (2002). Automated anatomical labeling of activations in SPM using a macroscopic anatomical parcellation of the MNI MRI single-subject brain. *NeuroImage*, *15*(1), 273–289. https://doi.org/10.1006/nimg.2001.0978

Uddin, L. Q. (2015). Salience processing and insular cortical function and dysfunction. *Nature Reviews Neuroscience*, *16*(1), 55–61. https://doi.org/10.1038/nrn3857

van der Molen, M. W., Boomsma, D. I., Jennings, J. R., & Nieuwboer, R. T. (1989). Does the Heart Know What the Eye Sees? A Cardiac/Pupillometric Analysis of Motor Preparation and Response Execution. *Psychophysiology*, *26*(1), 70–80. https://doi.org/10.1111/j.1469-8986.1989.tb03134.x

van der Wel, P., & van Steenbergen, H. (2018). Pupil dilation as an index of effort in cognitive control tasks: A review. *Psychonomic Bulletin and Review*, *25*(6), 2005–2015. https://doi.org/10.3758/s13423-018-1432-y

Van Der Werf, J., Jensen, O., Fries, P., & Medendorp, W. P. (2008). Gamma-band activity in human posterior parietal cortex encodes the motor goal during delayed prosaccades and antisaccades. *Journal of Neuroscience*, *28*(34), 8397–8405. https://doi.org/10.1523/JNEUROSCI.0630-08.2008

van Dijk, H., Schoffelen, J. M., Oostenveld, R., & Jensen, O. (2008). Prestimulus oscillatory activity in the alpha band predicts visual discrimination ability. *Journal of Neuroscience*, *28*(8), 1816–1823. https://doi.org/10.1523/JNEUROSCI.1853-07.2008

van Driel, J., Richard Ridderinkhof, K., & Cohen, M. X. (2012). Not all errors are alike: Theta and alpha EEG dynamics relate to differences in error-processing dynamics. *Journal of Neuroscience*, *32*(47), 16795–16806. https://doi.org/10.1523/JNEUROSCI.0802-12.2012

van Noordt, S. J. R., Desjardins, J. A., Gogo, C. E. T., Tekok-Kilic, A., & Segalowitz, S. J. (2017). Cognitive control in the eye of the beholder:

Electrocortical theta and alpha modulation during response preparation in a cued saccade task. *NeuroImage*, *145*(Part A), 82–95. https://doi.org/10.1016/j.neuroimage.2016.09.054

Van Veen, B. D., van Drongelen, W., Yuchtman, M., & Suzuki, A. (1997). Localization of brain electrical activity via linearly constrained minimum variance spatial filtering. *IEEE Transactions on Biomedical Engineering*, *44*(9), 867–880. https://doi.org/10.1109/10.623056

Varazzani, C., San-Galli, A., Gilardeau, S., & Bouret, S. (2015). Noradrenaline and dopamine neurons in the reward/effort trade-off: A direct electrophysiological comparison in behaving monkeys. *Journal of Neuroscience*, *35*(20), 7866–7877. https://doi.org/10.1523/JNEUROSCI.0454-15.2015

Veit, R., Flor, H., Erb, M., Hermann, C., Lotze, M., Grodd, W., & Birbaumer, N. (2002). Brain circuits involved in emotional learning in antisocial behavior and social phobia in humans. *Neuroscience Letters*, *328*(3), 233–236. https://doi.org/10.1016/S0304-3940(02)00519-0

Vernet, M., Quentin, R., Chanes, L., Mitsumasu, A., Valero-Cabré, A., & Valero-Cabre, A. (2014). Frontal eye field, where art thou? Anatomy, function, and non-invasive manipulation of frontal regions involved in eye movements and associated cognitive operations. *Frontiers in Integrative Neuroscience*, *8*(66), 1–24. https://doi.org/10.3389/fnint.2014.00066

Vrba, J., & Robinson, S. E. (2001). Signal processing in magnetoencephalography. *Methods*, *25*(2), 249–271. https://doi.org/10.1006/meth.2001.1238

Wagner, R. K., Zirps, F. A., Edwards, A. A., Wood, S. G., Joyner, R. E., Becker, B. J., Liu, G., & Beal, B. (2020). The Prevalence of Dyslexia: A New Approach to Its Estimation. *Journal of Learning Disabilities*, *53*(5), 354–365. https://doi.org/10.1177/0022219420920377

Wang, C.-A., Baird, T., Huang, J., Coutinho, J. D., Brien, D. C., & Munoz, D. P. (2018). Arousal Effects on Pupil Size, Heart Rate, and Skin Conductance in an Emotional Face Task. *Frontiers in Neurology*, *9*(1029), 1–13. https://doi.org/10.3389/fneur.2018.01029

Wang, C.-A., Brien, D. C., & Munoz, D. P. (2015). Pupil size reveals preparatory processes in the generation of pro-saccades and anti-saccades. *European Journal of Neuroscience*, *41*(8), 1102–1110. https://doi.org/10.1111/ejn.12883

Wang, C.-A., McInnis, H., Brien, D. C., Pari, G., & Munoz, D. P. (2016). Disruption of pupil size modulation correlates with voluntary motor preparation deficits in Parkinson's disease. *Neuropsychologia*, *80*, 176–184. https://doi.org/10.1016/j.neuropsychologia.2015.11.019

Wang, G. J., Volkow, N. D., Wigal, T., Kollins, S. H., Newcorn, J. H., Telang, F., Logan, J., Jayne, M., Wong, C. T., Han, H., Fowler, J. S., Zhu, W., & Swanson, J. M. (2013). Long-Term Stimulant Treatment Affects Brain

Dopamine Transporter Level in Patients with Attention Deficit Hyperactive Disorder. *PLOS ONE*, *8*(5), e63023. https://doi.org/10.1371/JOURNAL.PONE.0063023

Wang, X., Piñol, R. A., Byrne, P., & Mendelowitz, D. (2014). Optogenetic stimulation of locus ceruleus neurons augments inhibitory transmission to parasympathetic cardiac vagal neurons via activation of brainstem α1 and ß1 receptors. *Journal of Neuroscience*, *34*(18), 6182–6189. https://doi.org/10.1523/JNEUROSCI.5093-13.2014

Wang, Yan, Matsuzaka, Y., Shima, K., & Tanji, J. (2004). Cingulate cortical cells projecting to monkey frontal eye field and primary motor cortex. *NeuroReport*, *15*(10), 1559–1563. https://doi.org/10.1097/01.wnr.0000133300.62031.9b

Wang, Yanqiu, Cao, N., Lin, Y., Chen, R., & Zhang, J. (2020). Hemispheric Differences in Functional Interactions Between the Dorsal Lateral Prefrontal Cortex and Ipsilateral Motor Cortex. *Frontiers in Human Neuroscience*, *14*(202), 1–6. https://doi.org/10.3389/fnhum.2020.00202

Wass, S. V., de Barbaro, K., & Clackson, K. (2015). Tonic and phasic co-variation of peripheral arousal indices in infants. *Biological Psychology*, *111*, 26–39. https://doi.org/10.1016/j.biopsycho.2015.08.006

Wass, S. V., Porayska-Pomsta, K., & Johnson, M. H. (2011). Training attentional control in infancy. *Current Biology*, *21*(18), 1543–1547. https://doi.org/10.1016/j.cub.2011.08.004

Watanabe, T., Hirose, S., Wada, H., Imai, Y., Machida, T., Shirouzu, I., Konishi, S., Miyashita, Y., & Masuda, N. (2013). A pairwise maximum entropy model accurately describes resting-state human brain networks. *Nature Communications*, *4*(1370), 1–10. https://doi.org/10.1038/ncomms2388

Waterhouse, B. D., & Navarra, R. L. (2019). The locus coeruleus-norepinephrine system and sensory signal processing: A historical review and current perspectives. *Brain Research*, *1709*, 1–15. https://doi.org/10.1016/j.brainres.2018.08.032

Weber, H., & Fischer, B. (1994). Differential effects of non-target stimuli on the occurrence of express saccades in man. *Vision Research*, *34*(14), 1883–1891. https://doi.org/10.1016/0042-6989(94)90312-3

Wegener, S. P., Johnston, K., & Everling, S. (2008). Microstimulation of monkey dorsolateral prefrontal cortex impairs antisaccade performance. *Experimental Brain Research*, *190*(4), 463–473. https://doi.org/10.1007/s00221-008-1488-4

Weissman, D. H., Roberts, K. C., Visscher, K. M., & Woldorff, M. G. (2006). The neural bases of momentary lapses in attention. *Nature Neuroscience*, *9*(7), 971–978. https://doi.org/10.1038/nn1727

Wessel, J. R., Danielmeier, C., & Ullsperger, M. (2011). Error awareness revisited: Accumulation of multimodal evidence from central and autonomic nervous systems. *Journal of Cognitive Neuroscience*, *23*(10),

3021–3036. https://doi.org/10.1162/jocn.2011.21635

White, B. J., Kan, J. Y., Levy, R., Itti, L., & Munoz, D. P. (2017). Superior colliculus encodes visual saliency before the primary visual cortex. *Proceedings of the National Academy of Sciences of the United States of America*, *114*(35), 9451–9456. https://doi.org/10.1073/pnas.1701003114

White, T. P., Joseph, V., Francis, S. T., & Liddle, P. F. (2010). Aberrant salience network (bilateral insula and anterior cingulate cortex) connectivity during information processing in schizophrenia. *Schizophrenia Research*, *123*(2–3), 105–115. https://doi.org/10.1016/j.schres.2010.07.020

Willcutt, E. G. (2012). The Prevalence of DSM-IV Attention-Deficit/Hyperactivity Disorder: A Meta-Analytic Review. *Neurotherapeutics*, *9*(3), 490–499. https://doi.org/10.1007/s13311-012-0135-8

Willcutt, E. G., Pennington, B. F., Duncan, L., Smith, S. D., Keenan, J. M., Wadsworth, S., Defries, J. C., & Olson, R. K. (2010). Understanding the complex etiologies of developmental disorders: Behavioral and molecular genetic approaches. *Journal of Developmental and Behavioral Pediatrics*, *31*(7), 533–544. https://doi.org/10.1097/DBP.0b013e3181ef42a1

Woldemussie, E., Feldmann, B. J., & Chen, J. (1993). Characterization of muscarinic receptors in cultured human iris sphincter and ciliary

smooth muscle cells. *Experimental Eye Research*, *56*(4), 385–392. https://doi.org/10.1006/exer.1993.1052

Wu, X., Jiang, Y., Jiang, Y., Chen, G., Chen, Y., & Bai, X. (2021). The Influence of Action Video Games on Attentional Functions Across Visual and Auditory Modalities. *Frontiers in Psychology*, *12*, 2061. https://doi.org/10.3389/fpsyg.2021.611778

Xia, M., Wang, J., & He, Y. (2013). BrainNet Viewer: A Network Visualization Tool for Human Brain Connectomics. *PLoS ONE*, *8*(7), e68910. https://doi.org/10.1371/journal.pone.0068910

Yeo, B. T. T., Krienen, F. M., Sepulcre, J., Sabuncu, M. R., Lashkari, D., Hollinshead, M., Roffman, J. L., Smoller, J. W., Zöllei, L., Polimeni, J. R., Fisch, B., Liu, H., & Buckner, R. L. (2011). The organization of the human cerebral cortex estimated by intrinsic functional connectivity. *Journal of Neurophysiology*, *106*(3), 1125–1165. https://doi.org/10.1152/jn.00338.2011

Yep, R., Soncin, S., Brien, D. C., Coe, B. C., Marin, A., & Munoz, D. P. (2018). Using an emotional saccade task to characterize executive functioning and emotion processing in attention-deficit hyperactivity disorder and bipolar disorder. *Brain and Cognition*, *124*, 1–13. https://doi.org/10.1016/j.bandc.2018.04.002

Yerkes, R. M., & Dodson, J. D. (1908). The relation of strength of stimulus to rapidity of habit-formation. *Journal of Comparative Neurology and*

Psychology, *18*(5), 459–482. https://doi.org/10.1002/cne.920180503

Young, S., Moss, D., Sedgwick, O., Fridman, M., & Hodgkins, P. (2015). A meta-Analysis of the prevalence of attention deficit hyperactivity disorder in incarcerated populations. *Psychological Medicine*, *45*(2), 247–258. https://doi.org/10.1017/S0033291714000762

Yu, A. J., & Dayan, P. (2005). Uncertainty, neuromodulation, and attention. *Neuron*, *46*(4), 681–692. https://doi.org/10.1016/j.neuron.2005.04.026

Yuan, H., & Silberstein, S. D. (2016). Vagus Nerve and Vagus Nerve Stimulation, a Comprehensive Review: Part I. *Headache: The Journal of Head and Face Pain*, *56*(1), 71–78. https://doi.org/10.1111/HEAD.12647

Zekveld, A. A., Kramer, S. E., & Festen, J. M. (2010). Pupil response as an indication of effortful listening: The influence of sentence intelligibility. *Ear and Hearing*, *31*(4), 480–490. https://doi.org/10.1097/AUD.0b013e3181d4f251

Zhan, Y., Ma, J., Alexander-Bloch, A. F., Xu, K., Cui, Y., Feng, Q., Jiang, T., & Liu, Y. (2016). Longitudinal Study of Impaired Intra- and Inter-Network Brain Connectivity in Subjects at High Risk for Alzheimer's Disease. *Journal of Alzheimer's Disease*, *52*(3), 913–927. https://doi.org/10.3233/JAD-160008

Zhang, D., Lee, E. K. P., Mak, E. C. W., Ho, C. Y., & Wong, S. Y. S. (2021). Mindfulness-based interventions: An overall review. *British Medical*

Bulletin, *138*(1), 41–57. https://doi.org/10.1093/bmb/ldab005

Zhang, M., & Barash, S. (2000). Neuronal switching of sensorimotor transformations for antisaccades. *Nature*, *408*(6815), 971–975. https://doi.org/10.1038/35050097

Zhang, M., & Barash, S. (2004). Persistent LIP Activity in Memory Antisaccades: Working Memory for a Sensorimotor Transformation. *Journal of Neurophysiology*, *91*(3), 1424–1441. https://doi.org/10.1152/jn.00504.2003

Zhigalov, A., & Jensen, O. (2020). Alpha oscillations do not implement gain control in early visual cortex but rather gating in parieto-occipital regions. *Human Brain Mapping*, *41*(18), 5176–5186. https://doi.org/10.1002/hbm.25183

Zwi, M., Jones, H., Thorgaard, C., York, A., & Dennis, J. A. (2012). Parent Training Interventions for Attention Deficity Hyperactivity Disorder (ADHD) in Children Aged 5 to 18 years. *Campbell Systematic Reviews*, *8*(1), 1–100. https://doi.org/10.4073/csr.2012.2

Appendix A: MR Screening Questionnaire

The University of Nottingham

Sir Peter Mansfield Imaging Centre

MR Volunteer Safety Screening Questionnaire:

NAME	Date of Scan	Date of Birth
ADDRESS	Volunteer Number	
	Ethics Code	
Phone number	Weight	Height if applicable

R scanning uses strong magnetic fields. For your own safety and the safety of others it is **very important** ıat you do not go into the magnet halls with any metal in or on your body or clothing. Please answer the ollowing questions carefully and ask if anything is not clear. All information is held in the strictest confidence.

1. Do you have any implants in your body? e.g. replacement joints, drug pumps Y/N
2. Do you have aneurysm clips (clips put around blood vessels during surgery)? Y/N
3. Do you have a pacemaker or artificial heart valve? *(These stop working near MR Scanners)* Y/N
4. Have you ever had any surgery? Please give brief details over. Y/N
   (We do not need to know about uncomplicated caesarean delivery, vasectomy or termination of pregnancy)
5. Do you have any foreign bodies in your body (e.g. shrapnel)? Y/N
6. Have you ever worked in a machine tool shop without eye protection? Y/N
7. Do you wear a hearing aid or cochlear implant? Y/N
8. Could you be pregnant? (Pregnancy tests are available in the female toilets) Y/N
9. Have you ever suffered from tinnitus? Y/N
10. Do you wear dentures, a dental plate or a brace? Y/N
11. Are you susceptible to claustrophobia? Y/N
12. Do you suffer from blackouts, epilepsy or fits? Y/N
13. Do you have any tattoos? (If yes, you may be asked to read and sign another form) Y/N
14. Do you have any body piercing jewellery that cannot be removed? Y/N
15. Do you have any skin patches (trans-dermal patches)? Y/N
16. Do you have a coil in place (IUD) for contraception? Do you know what type? Y/N
17. Do you have any condition that may affect your ability to control your temperature ?
    (e.g. Do you have a fever, cardiovascular disease, hypertension, diabetes or cerebrovascular disease?) Y/N
18. Will you remove all metal including coins, body-piercing jewellery, false-teeth, hearing aids etc. before entering the magnet hall? *(lockers available by the changing rooms)* Y/N
19. Is there anything else you think we should know? Y/N

I have read and understood all the questions **Signature:**	**Date:**
Verified by: **Scanner Operator/MR Assistant Signature :**	**Date**

Appendix B: Volunteer Leaflet/Poster

Appendix C: Participant Information Sheet

Participant Information Sheet

Effect of RECOGNeyes training on brain networks

Names of Investigators: Dr. Elizabeth Liddle, Prof. Peter Liddle, Dr. Maddie Groom, Ms. Jyothika Kumar, Dr. Lauren Gascoyne, Ms. Alice Waitt

You are being invited to take part in a research study. Before you decide whether or not you wish to participate, it is important for you to understand why the research is being done and what it will involve. Please, take time to read the following information carefully. Talk to others about the study if you wish. Ask us if there is anything that is not clear or if you would like more information. Your participation is voluntary, and you may change your mind about being involved. You are free to withdraw at any point before or during the study. Withdrawal does not require a reason.

Thank you for reading this.

What is the purpose of the study?

We have developed a brain training game called RECOGNeyes with the aim of improving symptoms in people with specific learning difficulties such as attention deficit hyperactivity disorder (ADHD). This game involves using an inexpensive computer mounted eye tracker which tracks the participant's eye movements, allowing their own eyes to become the game controller. You can watch a video about the game here:

https://www.youtube.com/watch?v=HRjK8iJbkao

Developing better treatments depends on being able to measure the changes produced by treatment. Research studies have indicated that changes in the brain are good indicators of treatment effects. Therefore, in this study, our aim is to investigate how training on this game produces changes in the brain networks using magnetic resonance imaging (MRI) and magnetoencephalography (MEG).

Magnetoencephalography (MEG) is a non-invasive brain imaging technique for directly measuring brain activity. Brain cells communicate with one another by exchanging small electrical currents and these currents induce a magnetic field that is distributed around the head. Such fields are detectable using a MEG scanner and their measurement allows us to determine the location of any electrical activity in the brain, and how the patterns of that electrical activity change over time.

Why have I been chosen?

The study will involve healthy people aged 18 to 30, and we are particularly interested in people who have a specific learning difficulty such as ADHD, dyslexia, dyspraxia and dyscalculia. We would like to assess how training on the RECOGNeyes game can change the brain networks and also help with specific learning difficulties. Participants should not have a history of head injury or major medical illnesses and must not have conditions that are unsuitable for a MRI scan (e.g. pregnancy, hearing difficulties such as tinnitus, claustrophobia or metal in the body). Participants who have taken part in any other clinical research project in the last three months will also be excluded.

Do I have to take part?

It is up to you to decide whether or not to take part. If you do, you will be given this information sheet to keep and be asked to sign a consent form. You are still free to withdraw at any time and without giving a reason. A decision to withdraw at any time, or a decision not to take part, will not affect your legal rights.

What will happen to me if I take part?

Once you express an interest in participating in the study, a member of the research team will speak to you in order to explain the study to you in more detail and to make sure that there is nothing that excludes you from the study e.g. being unsuitable for an MRI scan.

The study itself consists of two visits to the Sir Peter Mansfield Imaging Centre (SPMIC), University Park (Nottingham), approximately two weeks apart, during which you will undergo training on the RECOGNeyes game at home. This is explained in more detail below.

First visit:

In the first visit, you will be asked to fill in a rating scale about the behaviours and problems sometimes experienced by adults with ADHD, a questionnaire about your health and also take two short reading tests. You will also be asked

for more details regarding your learning difficulties, if any, and also about regular medication intake or any other therapies you are receiving. Then, you will undergo a MEG scan so we can measure your brain activity. This involves you lying in a scanner that covers a part of your head (see the picture below). The researcher will ask you to perform a simple that involve seeing visual images on a screen and responding to them by moving your eyes. The MEG scan consists of short sessions with pauses in between, lasting for approximately 40 minutes in total. Before the scan we will provide light clothing to wear in the scanner.

Following this, you will undergo a MRI scan (see the picture of the scanner attached below). In the scanner room, you will be asked to lie on your back on a comfortable mat on a sliding bed. You will be given earplugs and pads that will reduce the sound of the scanner. You will also be given a call-bell that can be pushed at any time to stop the procedure and request assistance. Once you are comfortable, the bed will be slid into the scanner. When you lie in the MR scanner, it will cover most of your body, though the scanning will be done only on your head. Further instructions will be read to you through the headphones. We will be in communication with you throughout the scanning session. The MRI scan will last for 25 minutes.

After the scanning sessions, you will be introduced to the RECOGNeyes brain training game and will be provided with a portable eye tracker and a laptop in order to undertake the training at home. A demonstration on how to set up the eye tracker will be provided and then you will be shown how to navigate through the game. Time will be provided for practice on the game tasks and you will be allowed to ask the researcher any questions you may have. Following this, you will take away the eye tracker and laptop for two weeks in order to play the game and undertake a certain number of training sessions per week (maximum 4 per week). Each training session will last for 20 to 30 minutes. You will be given a sealed envelope which will contain information on how many training sessions you need to undertake each week. The first visit will last approximately 3 hours.

Two weeks of RECOGNeyes training:

For two weeks after the first visit, you will undergo RECOGNeyes training at your own convenience using the eye tracker and laptop provided. You will undergo the amount of training per week specified in the envelope provided to you. Details of how to space the training sessions will also be given in the envelope. The laptop will keep a record of your training progress and a log of the time you spend training. An investigator will be available by email or text to help you with your training schedule.

Second visit:

After you have completed training on RECOGNeyes, you will be asked to visit the Imaging Centre again. The second visit will involve another MEG scan, identical to the first one and a second MRI scan. You will also be asked to do the two reading tests and fill the questionnaire about your health again. The second visit will last approximately 2 hours. At the end of the second visit, you will be asked to fill a brief feedback form.

One of the MRI

A subject lying in an MEG

What do I have to do?

You must refrain from use of alcohol, cannabis or any other recreational drugs for 24 hours prior to each visit and also prior to undertaking each training session. Otherwise there is nothing that you will have to change about your daily routine. If you are taking regular medication, you should continue with your usual medication schedule.

During the scans, we will give you instructions regarding what we want you to do.

Expenses and payment

You will receive a £60 inconvenience allowance for participating in this study. If we need to exclude you from the experiment on the basis of information from the initial interview or for any other reason related to the study criteria after you arrive at the MR centre, you will still receive the full inconvenience allowance. If you withdraw from the study for medical reasons not associated with the study, you will receive an inconvenience allowance proportional to the length of the period of participation, but if you withdraw for any other reason, the inconvenience allowance to be received, if any, shall be at the discretion of the investigators.

What is the drug, device or procedure that is being tested?

This study is being undertaken in order to examine the effects of the eye-tracking game, RECOGNeyes on your brain networks. No drug is being tested in this study.

What are the side effects of any treatment or procedures received when taking part?

There are no known adverse effects of participating in a magnetic resonance imaging session, provided you do not have any contraindications to participate. Some people feel dizzy in the scanner, but this is rare. There are no known long-term effects of undergoing a MRI scan. Magnetoencephalography is an entirely passive scanning technique and involves no risks at all. If you have any concerns about your participation in this study, please contact Dr. Elizabeth Liddle at 0115 74 84012 or by email at elizabeth.liddle@nottingham.ac.uk. There are also no known adverse effects of using an eyetracker to play a computer game. However, if it makes your eyes feel tired, you can stop at any time.

What are the other possible disadvantages and risks of taking part?

Some people cannot be exposed to the strong magnetic fields in the MRI scanner due to medical/cosmetic procedures that have been performed on them, or accidents which may have resulted in metallic objects entering their bodies. We will therefore carry out a comprehensive safety questionnaire with you to ensure that there is no possibility that it would be unsafe to scan you. In order to obtain good quality images of your brain, you will need to keep as still as possible inside the scanner while you are performing the task. There is also the possibility that you might feel claustrophobic inside the narrow scanner tunnel. However, if you feel very uncomfortable you can stop the experiment at any time by pressing the call-bell.

We do ask that you do not take part if you think that you may be pregnant. There is no evidence that MRI scanning is a danger to a foetus, but the issue has yet to be well studied. If there is any likelihood you might be pregnant we will offer you a pregnancy test on each day of scanning.

What are the possible benefits of taking part?

We cannot promise the study will help you in any way. The purpose of the training game is to enhance attentional control in children and adults. We do anticipate some positive effects of the training on the brain but this work is at an early stage. We hope that you will find the computer games fun and that exposure to a research study to be an interesting experience. It is hoped that your participation will contribute to research into the development of the intervention aimed at helping people with specific learning difficulties such as ADHD. This might lead to better treatments for children and adults with specific learning difficulties in future.

What if unexpected information becomes available from the study?

The research scan is not the same as a routine clinical scan and therefore cannot be used to make a clinical diagnosis. However, if your scan reveals anything that suggests a possible clinical abnormality, we will inform your GP so that he or she might arrange any further investigations that might be required.

What if there is a problem?

If you have any questions or concerns about your participation in this study, please contact the Chief Investigator Dr. Elizabeth Liddle (details given below). The second point of contact is the FMHS Research Ethics Committee Administrator, c/o The University of Nottingham, Faculty PVC Office, B Floor, Medical School, Queen's Medical Centre Campus, Nottingham University

Hospitals, Nottingham, NG7 2UH or via E-mail: FMHS-ResearchEthics@nottingham.ac.uk

Will my taking part in the study be kept confidential?

We will follow ethical and legal practice and all information about you will be handled in confidence.

If you join the study, some parts of your data collected for the study will be looked at by authorised persons from the University of Nottingham who are organising the research. They may also be looked at by authorised people to check that the study is being carried out correctly. All will have a duty of confidentiality to you as a research participant and we will do our best to meet this duty.

All information which is collected about you during the course of the research will be kept **strictly confidential**, stored in a secure and locked office, and on a password protected database. Any information about you which leaves the university will have your name and address removed (anonymised) and a unique code will be used so that you cannot be recognised from it.

Your personal data (address, telephone number) will be kept for 12 months after the end of the study so that we are able to contact you about the findings of the study *and possible follow-up studies* (unless you advise us that you do not wish to be contacted).

All other data (research data) will be kept securely for at least 7 years. During this time all precautions will be taken by all those involved to maintain your confidentiality, only members of the research team will have access to your personal data. When it is finally disposed of this will be done securely.

What will happen if I don't want to carry on with the study?

Your participation is voluntary and you are free to withdraw at any time, without giving any reason, and without your legal rights being affected. If you withdraw then the information collected so far cannot be erased and this information may still be used in the project analysis.

Involvement of the General Practitioner/Family doctor (GP)

If your scan reveals anything that suggests a possible clinical abnormality, we will inform your GP so that he or she might arrange any further investigations that might be required.

What will happen to the results of the research study?

Results from this study will be published in academic journals. You may request copies of any published articles related to this study. You will not be identified in any report or publication.

Who is organising and funding the research?

This study is organised by the investigators listed above at the University of Nottingham. The source of funding for this project is the Medical Research Council.

Who has reviewed the study?

This study has been reviewed and given favourable opinion by the University of Nottingham, Medical School Ethics Committee

Contact Details:

If you are interested in participating in this study or have any questions, please contact Ms. Jyothika Kumar at jyothika.kumar1@nottingham.ac.uk. If you have any concerns, please contact the principal investigator Dr. Elizabeth Liddle at 0115 74 84012 or by email at elizabeth.liddle@nottingham.ac.uk.

You will be given a copy of the information sheet and a signed consent form to keep. Thank you very much for considering taking part in our study.

School of Medicine
Division of Psychiatry and Applied Psychology
Institute of Mental Health
Triumph Road, Nottingham NG7 2TU.

Appendix D: Visual attention network regions, peak activation coordinates literature search

I conducted an independent literature search collating peak activation coordinates reported in functional brain imaging literature on gaze control and visual attention to obtain coordinates to use in source localisation analysis. Where possible, I have endeavoured to report primary sources of coordinates for the chosen ROIs and the relevant sulci and gyri they are based upon. When necessary, I used the online application of the Nonlinear Yale MNI to Talairach Conversion Algorithm (Lacadie et al., 2008) to convert original Talairach coordinates to MNI space. Note for bilateral regions, not all studies report from both hemispheres so some studies will appear unpaired in the tables. Since I only used the mean peak activation coordinates reported in the literature to derive the final average coordinates for each ROI, standard deviations and ranges are not quoted within my summary tables. To minimise any bias from extreme values, the median *x*, *y*, and *z* coordinates for each ROI were extracted to pre-define seed regions for source localisation analysis (see Chapter 7, Section 7.2.3).

Frontal eye field

As described in Chapter 2, Section 2.2.2, the description of the location of the FEF in the human brain can vary, and some studies also choose to divide the FEF into superior and inferior precentral sulcus (sPCS and iPCS) portions. Table 7 and Table 8 contain coordinates for the right and left FEF, respectively. Where studies have chosen to use the sPCS and iPCS portions, these are listed as separate region labels in Table 7 and Table 8.

Hwang et al. (2010) includes fMRI coordinates for adults, teenagers, and children to study neurodevelopmental changes, but I have only reported the coordinates from the adult sample since their age range of 18-27 overlapped with the RECOGNeyes sample. Since more recent MEG studies by Hwang et al. (2014, 2016) adopt the Destrieux automated atlas approach to define ROIs (Destrieux et al., 2010), I have endeavoured to report coordinate information from citations in their study justification and description of each chosen ROI. Moon et al. (2007) (in Hwang et al., 2014, 2016) and Lee et al. (2011) (in Hwang et al., 2014) are cited for the FEF, but these studies also used automated atlases. However, Luna et al. (1998) did include coordinate information and was cited in the majority of this group of studies (Hwang et al., 2010, 2014; A. K. C. Lee et al., 2011; Moon et al., 2007). There are multiple entries for each ROI from Luna et al. (1998) for both the mean peak activation voxel location per ROI across subjects and the peak activation voxel location for each ROI from group averaged data

were reported. Hwang et al. (2019) included coordinates for the right iPCS, but this was not referred to as the FEF, which may explain why it is less similar to the other iPCS coordinates in Table 7 and Table 8. In another study by the same group, Riddle et al. (2019) selected the right sPCS to represent the human FEF region involved in contralateral eye movements to apply rhythmic TMS to.

Table 7 and Table 8 also incorporates the comparison table from Vernet et al. (2014) of FEF coordinates reported in different neuroimaging studies. Most of these studies had low subject numbers (N = 3-10), except for the meta-analysis by Paus (1996) who examined 8 PET lesion and cerebral blood flow studies that investigated the role and location of the FEF. This meta-analysis was inconclusive, and these coordinates may be outdated to use for converting into MNI space (as done in a tDCS study by Kanai et al. (2012)), compared to other more recent studies using fMRI which has greater spatial resolution. For this reason, I extended my literature search to other studies primarily using fMRI with saccade and visual attention tasks, as well as other MEG studies to match the technique adopted in RECOGNeyes.

This includes Jamadar et al. (2015), who used fMRI to observe changes after antisaccade training, where two sets of coordinates are reported: T1 = Study Table 1 peak regions for antisaccade > baseline; T2 = Study Table 2 peak regions for antisaccade session 2 > session 1. From an fMRI study conducted by Brown et al. (2006), there are separate coordinates

activated during prosaccade and antisaccade responses, respectively. Spreng et al. (2010) report coordinates for regions activated during visuospatial planning in the dorsal attentional network (DAN), which also included the DLPFC. A recent MEG study by Bells et al. (2020) focussed on saccadic reaction times and report peak activation coordinates.

I also included coordinates from the resting-state fMRI study by Androulakis et al. (2017), even though they investigated chronic migraine rather than saccades, because many of their regions overlapped with our oculomotor ROIs including for the FEF and intraparietal sulcus (IPS), as well as salience network locations for the DLPFC and insula. Brier et al. (2012) assembled a table of coordinates from previous studies for each ROI (refer to study for more details) and has since been cited by more recent papers (Huang et al., 2017; Zhan et al., 2016).

Table 7: Right FEF coordinates.

Region	**Source**	**Imaging method**	***N***	**Coordinates**		
				x	*y*	*z*
Right FEF (from table in Vernet	(Paus, 1996) meta-analysis	PET	62 (from 8 studies)	TAL: 31 MNI: 31	-2 -5	47 50
	(Petit & Haxby, 1999)	fMRI	5	TAL: 36 MNI: 36	-10 -13	47 50

et al. (2014))	(Luna et al., 1998)	fMRI	10	TAL: 34 MNI: 34	-3 -6	47 50
	Data from (Kawashima et al., 1998) used by (Tehovnik et al., 2000)	PET	9	TAL: 37 MNI: 38	26 25	29 29
	(Ioannides et al., 2004)	MEG	3	TAL: 32 MNI: 33	10 9	34 35
Right FEF	(Mort et al., 2003)	fMRI	12	TAL: 28 MNI: 27	-6 -10	50 54
	(M. R. G. Brown et al., 2006) prosaccade response	fMRI	10	TAL: 36 MNI: 36	-5 -9	50 54
	(M. R. G. Brown et al., 2006) antisaccade response	fMRI	10	TAL: 35 MNI: 35	-4 -8	50 54
	(Hwang et al., 2010)	fMRI	27 adults	TAL: 26 MNI: 25	-6 -11	59 65
	(Spreng et al., 2010)	fMRI	20	26	8	60
	(Brier et al., 2012)	Refer to paper for reviewed literature details		31	-5	54
	(Kanai et al., 2012)	tDCS	16	31.3	-4.5	50.9
	(Jamadar et al., 2015)	fMRI	23	T1: 27 T2: 30	-13 -4	52 49

	(Androulakis et al., 2017)	fMRI	29	24	-13	52
	(Yeo et al., 2011)	fMRI	Refer to paper for meta-analysis details	26	-6	48
	(Bells et al., 2020)	MEG	14	TAL: 26 MNI: 26	1 0	40 42
Right FEF: sPCS	(Luna et al., 1998) (mean across subjects)	fMRI	10	TAL: 34.2 MNI: 34	-3.4 -6	46.9 50
	(Luna et al., 1998) (peak in group average data)	fMRI	10	TAL: 38 MNI: 37	-9 -13	55 60
	(Riddle et al., 2019)	TMS / fMRI	16	27	0	57
Right FEF: iPCS	(Luna et al., 1998) (mean across subjects)	fMRI	10	TAL: 43.7 MNI: 45	7.5 7	38.3 39
	(Luna et al., 1998) (peak in group average data)	fMRI	10	TAL: 48 MNI: 49	5 3	44 46
	(Spreng et al., 2010)	fMRI	20	46	8	28
	(Hwang et al., 2019)	fMRI	25	20	-8	56
Median R FEF				**31.15**	**-5.5**	**50.45**

Table 8: Left FEF coordinates.

Region	Source	Imaging method	*N*	MNI coordinates		
				x	*y*	*z*
Left FEF (from table in Vernet et al. (2014))	(Paus, 1996)	PET	62 (from 8 studies)	TAL: -32 MNI: -32	-2 -5	46 50
	(Petit & Haxby, 1999)	fMRI	5	TAL: -35 MNI: -35	-18 -21	46 50
	(Luna et al., 1998)	fMRI	10	TAL: -30 MNI: -30	-7 -10	49 53
	Data from (Kawashima et al., 1998) used by (Tehovnik et al., 2000)	PET	9	TAL: -37 MNI: -38	26 26	29 30
	(Ioannides et al., 2004)	MEG	3	TAL: -41 MNI: -42	12 12	34 36
Left FEF	(Mort et al., 2003)	fMRI	12	TAL: -40 MNI: -41	0 -2	44 47
	(M. R. G. Brown et al., 2006) prosaccade response	fMRI	10	TAL: -38 MNI: -38	-6 -9	47 51
	(M. R. G. Brown et al., 2006) antisaccade response	fMRI	10	TAL: -34 MNI: -34	-5 -8	49 53

	(Hwang et al., 2010)	fMRI	27 adults	TAL: -28 MNI: -28	-9 -13	60 66
	(Spreng et al., 2010)	fMRI	20	-24	6	56
	(Brier et al., 2012)	Refer to paper for reviewed literature details		-29	-5	55
	(Kanai et al., 2012)	tDCS	16	-32.3	-4.4	49.8
	(Jamadar et al., 2015)	fMRI	23	T1: -27 T2: -27	-4 -1	58 67
	(Androulakis et al., 2017)	fMRI	29	-24	-13	52
	(Yeo et al., 2011)	fMRI	Refer to paper for meta-analysis details	-26	-6	48
	(Bells et al., 2020)	MEG	14	TAL: -25 MNI: -26	2 1	40 43
Left FEF: sPCS	(Luna et al., 1998) (mean across subjects)	fMRI	10	TAL: -30.2 MNI: -30	-4.1 -7	49.1 53
	(Luna et al., 1998) (peak in group average data)	fMRI	10	TAL: -25 MNI: -25	-12 -16	53 58
Left FEF: iPCS	(Luna et al., 1998) (mean across subjects)	fMRI	10	TAL: -42.6 MNI: -44	7.3 6	40.6 44

(Luna et al., 1998) (peak in group average data)	fMRI	10	TAL: -52 MNI: -54	0 -1	37 39
(Spreng et al., 2010)	fMRI	20	-40	4	28
Median left FEF			**-31**	**-4.7**	**50.5**

Dorsal lateral prefrontal cortex (DLPFC)

The DLPFC has historically been defined as Brodmann areas 9 and 46 (discussed in Rowe et al. (2000)). However, as discussed in the Chapter 2, Section 2.2.3, there are variations in the reporting of the DLPFC, where it has even been suggested the DLPFC can be further divided into another two regions (Cieslik et al., 2013). Therefore, it was important to collate peak coordinates from functionally relevant studies addressing saccadic control and visual attention, including studies using the DLPFC as a main node in the dorsal attention network (DAN). Sometimes the DLPFC is referred to within the salience network, executive network, and orbital frontoinsula (FI). Coordinates for the right and left DLPFC are included in Table 9 and Table 10, respectively.

Variations in the range of reported peaks are likely due to the aforementioned reasons. Some coordinates that were notably inconsistent with the range of coordinates in the table and outside BA 9 and 46 were

those from Jamadar et al. (2015), where they are actually situated in right and left BA 6 and left BA 32.

Briley et al. (2018) decided that the DLPFC coordinates from Yeo et al. (2011) did not correspond well with those from Fair et al. (2009), so they used the coordinates from the latter instead. Therefore, I included the original Talairach coordinates from Fair et al. (2009) and converted them into MNI coordinates.

Huang et al. (2017) quote coordinates for various functional network regions, so I verified the sources for these coordinate locations (Brier et al., 2012; Watanabe et al., 2013; Zhan et al., 2016). Brier et al. (2012) includes a series of coordinates obtained from different studies, which is then cited by Zhan et al. (2016). However the source for the DLPFC coordinates used by Huang were from Watanabe et al. (2013) who originally cited their DLPFC coordinates from a meta-analysis (Dosenbach et al., 2006). Dosenbach et al. (2006) only includes the right DLPFC, but it has been interpreted as bilateral coordinates in Talairach space (Dosenbach et al., 2007; Fair et al., 2009). I decided to use the original bilateral Talairach coordinates stated in these papers to be closer estimations to the original source, rather than the converted MNI coordinates quoted in later studies (Huang et al., 2017; Watanabe et al., 2013).

Seeley et al. (2007) reported MNI coordinates for functional connectivity with ROIs and a separate ICA analysis. The right DLPFC was one of the ROIs in the functional connectivity analysis, derived from

Krasnow et al. (2003). Curtis & D'Esposito (2003) incorrectly reports the DLPFC from Rowe et al. (2000) as being in MNI space but these are actually in Talairach space. Ossandón et al. (2012) was an unusual study using multilead EEG depth electrodes implanted into the brain of intractable epilepsy patients and reported DAN activation including the DLPFC. Breukelaar et al. (2017) did a longitudinal study involving cognitive control networks and used the DLPFC node as reported in a meta-analysis by Niendam et al. (2012). Breukelaar et al. (2017) uses MNI space but the original meta-analysis was done in Talairach space, so I have taken the original Talairach coordinates and converted to MNI coordinates.

Table 9: Right DLPFC coordinates.

Source	**Imaging method**	***N***	**MNI coordinates**		
			x	*y*	*z*
(Rowe et al., 2000)	fMRI	6	TAL: 42	38	28
			MNI: 43	37	28
(Menon et al., 2001)	fMRI	14	TAL: 26	46	30
			MNI: 27	46	32
(Fox et al., 2005)	fMRI	10	TAL: 38	41	22
			MNI: 39	41	22
(Liston et al., 2006)	fMRI	19	TAL: 36	34	36
			MNI: 36	32	38

(Cole & Schneider, 2007)	fMRI	9	TAL: 33	33	44
			MNI: 33	31	47
			TAL: 36	38	34
			MNI: 37	37	36
			TAL: 38	41	32
			MNI: 39	40	33
			TAL: 37	39	36
			MNI: 37	38	38
(Seeley et al., 2007) derived from Krasnow et al. (2003)	fMRI	14	44	36	20
(Seeley et al., 2007) functional connectivity analysis with FI	fMRI	14	40	44	18
(Seeley et al., 2007) functional connectivity analysis with right DLPFC	fMRI	14	46	36	18
(Seeley et al., 2007) ICA salience network	fMRI	21	30	48	22
(Seeley et al., 2007) ICA executive network	fMRI	21	46	46	14
(Dosenbach et al., 2007; Fair et al., 2009)	Meta-analysis source	183 cross-subjects analysis by Dosenbach et al., (2006)	TAL: 43	22	34
			MNI: 44	21	34

(Chang & Glover, 2010)	fMRI	12	45	48	26
(Spreng et al., 2010)	fMRI	20	46	42	22
(Ossandón et al., 2012)	Intracranial EEG	24	TAL: 43 MNI: 44	39 39	22 22
(Niendam et al., 2012) referred as middle frontal gyrus, BA 46	Meta-analysis mixed methods	Meta-analysis of 193 studies	TAL: 40 MNI: 41	30 29	28 27
(Jamadar et al., 2015)	fMRI	23	T1: 54	-1	24
(Androulakis et al., 2017)	fMRI	29	30	48	22
Median Right DLPFC			**40.5**	**38.5**	**25**

Table 10: Left DLPFC coordinates.

Source	**Imaging method**	***N***	**MNI coordinates**		
			x	y	z
(Menon et al., 2001)	fMRI	14	TAL: -34 MNI: -34	50 50	32 34
(Fox et al., 2005)	fMRI	10	TAL: -40 MNI: -41	39 39	26 27
(Liston et al., 2006)	fMRI	19	TAL: -33 MNI: -34	41 41	35 38

(Cole & Schneider, 2007)	fMRI	9	TAL: -37	33	37
			MNI: -38	32	40
			TAL: -41	32	35
			MNI: -42	31	37
			TAL: -38	44	21
			MNI: -39	45	22
(Seeley et al., 2007) functional connectivity analysis with FI	fMRI	14	-30	44	22
(Seeley et al., 2007) functional connectivity analysis with right DLPFC	fMRI	14	-42	34	20
(Seeley et al., 2007) ICA salience network	fMRI	21	-38	52	10
(Seeley et al., 2007) ICA executive network	fMRI	21	-34	46	6
(Dosenbach et al., 2007; Fair et al., 2009)	Meta-analysis source	183 cross-subjects analysis by Dosenbach et al., (2006)	TAL: -43	22	34
			MNI: -44	22	36
(Chang & Glover, 2010)	fMRI	12	-46	45	26
(Spreng et al., 2010)	fMRI	20	-40	36	24
(Ossandón et al., 2012)	Intracranial EEG	24	TAL: -39	28	25
			MNI: -40	29	26

(Niendam et al., 2012) referred as middle frontal gyrus, BA 46	Meta-analysis mixed methods	Meta-analysis of 193 studies	TAL: -40 MNI: -41	26 26	28 29
(Jamadar et al., 2015)	fMRI	23	T1: -12 T2: -48	23 -1	34 34
(Androulakis et al., 2017)	fMRI	29	-38	52	10
Median Left DLPFC			**-39.5**	**37.5**	**26.5**

Parietal eye field

As discussed in Chapter 2, Section 2.2.4, there are some discrepancies regarding the human PEF location that corresponds to the equivalent of the monkey LIP. Due to the multiple terms that describe this region, I have collated coordinates together under the synonymous region labels for 'PEF', 'LIP' and 'IPS' to include for the right and left hemispheres in Table 11 and Table 12, respectively. Similar saccadic and visual attention studies to those used for obtaining FEF and DLPFC coordinates were also used to obtain coordinates for the PEF, LIP or IPS equivalent. The PEF was determined the most appropriate label to refer to this ROI within the context of the RECOGNeyes study.

In regard to the PEF/LIP equivalent when quoted as the 'IPS', I believe this is not part of the lateral IPS since there are larger differences between the coordinates of the lateral IPS from Luna et al. (1998) compared

to other parts of the IPS. Also, I consulted the centroid coordinates from Briley et al. (2018) that includes some of our ROIs, and they use the IPS as an ROI with coordinates (± 43, -50, 46). However, these were not included as they are outside the general range of our ROIs. Table 3 in Yeo et al. (2011) quotes a region specifically labelled as LIP, so this is included in the tables for each hemisphere (identical coordinates whereby the *x*-coordinate is mirrored).

Koyama et al. (2004) conducted a BOLD fMRI study using an identical saccade task performed by monkeys and humans, including the anterior and posterior superior parietal lobule (SPL) regions along the IPS, and the IPS/transverse occipital sulcus (TOS) region near the borders for the parietal and occipital cortices. Koyama et al. (2004) concluded that activation in the monkey dorsal LIP correlated mostly with human posterior SPL, but I have included coordinates for all three bilateral regions in Table 11 and Table 12.

An issue I encountered is that some of the studies that state the locations in Talairach coordinates are outside the head when converted into MNI space, so I have highlighted these in red in the tables, e.g., Merriam et al. (2001). It is possible these conversions are not always compatible and may be an issue with discrepancies in older studies using Talairach space.

Table 11: Right PEF coordinates.

Region	Source	Imaging method	*N*	MNI coordinates		
				x	*y*	*z*
Right PEF/LIP	(Merriam et al., 2001) visually guided saccade	fMRI	11	17	-81	60
	(Merriam et al., 2001) compatible task	fMRI	11	17	-81	60
	(Merriam et al., 2001) mixed task	fMRI	11	19	-87	52
	(Yeo et al., 2011)	fMRI	Refer to paper for meta-analysis summary	28	-61	60
	(Bells et al., 2020)	MEG	14	20	-63	37
Right IPS	(Mort et al., 2003)	fMRI	12	35	-63	65
	(Koyama et al., 2004) IPS/TOS	fMRI	20	22	-78	28
	(Hwang et al., 2010)	fMRI	27 adults	25	-64	58
	(Brier et al., 2012) Posterior IPS	Refer to paper for reviewed literature details		28	-65	51

	(Jamadar et al., 2015)	fMRI	23	T1/T2: 27	-55	58
	(Riddle et al., 2019)	TMS / fMRI	16	29	-56	56
	(Hwang et al., 2019)	fMRI	25	26	-58	60
Right SPL (posterior)	(Koyama et al., 2004)	fMRI	20	22	-62	60
Right SPL (anterior)	(Koyama et al., 2004)	fMRI	20	34	-50	56
Right SPL (medial IPS)	(Luna et al., 1998) mean across subjects	fMRI	10	20	-66	61
	(Luna et al., 1998) peak in group average data	fMRI	10	23	-72	57
Right IPL (lateral IPS)	(Luna et al., 1998) mean across subjects	fMRI	10	43	-42	-56
	(Luna et al., 1998) peak in group average data	fMRI	10	49	-46	50
Median right PEF				**25.5**	**-63**	**57.5**

Table 12: Left PEF coordinates.

Region	Source	Imaging method	*N*	MNI coordinates		
				x	*y*	*z*
Left PEF/ LIP	(Merriam et al., 2001) visually guided saccade	fMRI	11	-21	-76	59
	(Merriam et al., 2001) compatible task	fMRI	11	-20	-80	60
	(Merriam et al., 2001) mixed task	fMRI	11	-26	-80	54
	(Yeo et al., 2011)	fMRI	Refer to paper for meta-analysis summary	-28	-61	60
	(Bells et al., 2020)	MEG	14	-26	-60	39
Left IPS	(Mort et al., 2003)	fMRI	12	-30	-58	57
	(Koyama et al., 2004) IPS/TOS	fMRI	20	-22	-84	26
	(Hwang et al., 2010)	fMRI	27 adults	-26	-67	55
	(Brier et al., 2012) Posterior IPS	Refer to paper for reviewed literature details		-26	-65	52

	(Jamadar et al., 2015)	fMRI	23	T1: -24 T2: -24	-55 -58	55 55
Left SPL (posterior)	(Koyama et al., 2004)	fMRI	20	-22	-62	60
Left SPL (anterior)	(Koyama et al., 2004)	fMRI	20	-28	-58	54
Left SPL (medial IPS)	(Luna et al., 1998) mean across subjects	fMRI	10	-19	60	64
	(Luna et al., 1998) peak in group average data	fMRI	10	-25	-61	58
Left IPL (lateral IPS)	(Luna et al., 1998) mean across subjects	fMRI	10	-40	-49	46
	(Luna et al., 1998) peak in group average data	fMRI	10	-31	-44	43
Median left PEF				**-26**	**-61**	**55**

Anterior insula

As described in Chapter 2, Section 2.2.5, both the anterior insula and anterior cingulate cortex (ACC) are involved in the salience network, and are supported to contribute to cognitive control, attention, and autonomic nervous system functioning. However, the ACC is reported to have low signal-to-noise ratio (SNR) in MEG studies (Hwang et al., 2014, 2016). Since

it is likely to be difficult to achieve good SNR from the ACC, we decided not to include it as an ROI.

Coordinates for the right anterior insula are in Table 13 and coordinates for the left anterior insula are in Table 14. As well as using coordinates reported in visual attention and saccadic studies, some papers concerned the salience network as well as autonomic processing. Where relevant, coordinates were from healthy controls (HC) rather than patient groups. Critchley et al. (2000) conducted a PET study measuring regional cerebral blood flow (rCBF). Peak activation coordinates only labelled as the insula in Table 13 and Table 14 are included from functionally relevant studies that we anticipated to have activated the anterior portion.

Table 13: Right anterior insula coordinates.

Source	**Imaging method**	***N***	**MNI coordinates**		
			x	*y*	*z*
Right anterior insula reported from Mutschler et al. (2009) table of activations related to autonomic processing					
(Fredrikson et al., 1998) reported as insula cortex	PET	6	TAL: 52 MNI: 55	17 21	-8 -15
(Servan-Schreiber et al., 1998)	PET	10	TAL: 32 MNI: 34	-2 1	-8 -14
(Critchley et al., 2000)	PET	6	*Greater rCBF and high heartrate:*		

			TAL: 28	14	6
			MNI: 29	17	3
			TAL: 62	6	-14
			MNI: 65	11	-21
			Greater rCBF and low heartrate:		
			TAL: 40	2	-16
			MNI: 42	7	-24
			TAL: 42	-14	4
			MNI: 44	-14	0
(Veit et al., 2002)	fMRI	7 (HC group only)	57	12	-6
			48	21	-12
(Nagai et al., 2004)	fMRI	8	36	24	-8
(Birbaumer et al., 2005)	fMRI	10 HC vs 10 psychopaths	36	12	-15
(Critchley et al., 2005) error processing and sympathetic arousal	fMRI	15	34	16	-11
(Critchley et al., 2005) error processing independent of autonomic response	fMRI	15	34	28	2
(Gamer et al., 2007)	fMRI	14	48	18	-5
Right Insula					
(M. R. G. Brown et al., 2006)	fMRI	10	TAL: 49	3	17

prosaccade response			MNI: 52	5	15
(M. R. G. Brown et al., 2006) antisaccade response	fMRI	10	TAL: 52 MNI: 55	5 7	17 15
(Cole & Schneider, 2007)	fMRI	9	TAL: 34 MNI: 36 TAL: 35 MNI: 36	18 20 13 14	11 9 19 18
(Chang & Glover, 2010)	fMRI	12	45	13	4
(Hwang et al., 2010)	fMRI	27 adults	TAL: 36 MNI: 38	17 19	10 8
(T. P. White et al., 2010)	fMRI	19 HC and 19 schizo-phrenic patients	TAL: 42 MNI: 45	0 3	0 -5
(Deen et al., 2011) ventral anterior insula	fMRI	30	32	10	-6
(Deen et al., 2011) dorsal anterior insula	fMRI	30	35	7	3
(Brier et al., 2012)	Refer to study for literature review details		43	7	2
(Jamadar et al., 2015)	fMRI	23	T1: 39	11	4
(Briley et al., 2018) quoting Yeo et al. (2011)	Yeo atlas = fMRI	Yeo atlas = 1000	31	11	8
(Hwang et al., 2019)	fMRI	25	42	24	0

Median right anterior insula	**40.5**	**12**	**0**

Table 14: Left anterior insula coordinates.

Source	Imaging methods	*N*	MNI coordinates		
			x	*y*	*z*
Left anterior insula reported from Mutschler et al. (2009) table of activations related to autonomic processing					
(Servan-Schreiber et al., 1998)	PET	10	TAL: -36 MNI: -37	4 8	-8 -14
(Veit et al., 2002)	fMRI	7 HC	-57	9	-3
(Birbaumer et al., 2005)	fMRI	10 HC vs 10 psychopaths	-36	3	-12
(Critchley et al., 2005) error processing and sympathetic arousal	fMRI	15	-34	18	-11
(Critchley et al., 2005) error processing independent of autonomic response	fMRI	15	-32	22	-2
(Lane et al., 2009)	PET	12	-30	10	-10
Left Insula					
(M. R. G. Brown et al., 2006)	fMRI	10	TAL: -36 MNI: -38	4 6	13 12

prosaccade response					
(M. R. G. Brown et al., 2006) antisaccade response	fMRI	10	TAL: -43 MNI: -45	7 9	14 13
(Cole & Schneider, 2007)	fMRI	9	TAL: -33 MNI: -35 TAL: -34 MNI: -36	-18 -17 -17 -16	9 7 11 8
(Chang & Glover, 2010)	fMRI	12	-39	8	5
(Hwang et al., 2010)	fMRI	27 adults	TAL: -34 MNI: -35	14 17	10 9
(T. P. White et al., 2010)	fMRI	19 HC and 19 schizo-phrenic patients	TAL: -41 MNI: -43	-11 -10	9 7
(Deen et al., 2011) ventral anterior insula	fMRI	30	-33	13	-7
(Deen et al., 2011) dorsal anterior insula	fMRI	30	-38	6	2
(Brier et al., 2012)	Refer to study for literature review details		-42	6	4
(Jamadar et al., 2015)	fMRI	23	T1: -36 T2: -33	10 14	3 4
(Briley et al., 2018) quoting Yeo et al. (2011)	Yeo atlas = fMRI	Yeo atlas = 1000	-31	11	8
Median left anterior insula			**-36**	**9**	**4**

Primary visual cortex (V1)

The primary visual cortex (V1), encapsulated in Brodmann's Area (BA) 17, is one of the most identifiable anatomical regions in the cerebral cortex, due to a distinct set of horizontally protruding myelinated axons known as the stria of Gennari (Hinds et al., 2008, 2009) at the calcarine sulcus that run parallel to the cortical surface. Since the primary visual cortex is a large region containing many subareas, peak activation coordinates for the "visual cortex", "calcarine" and "V1" had a large foci range. Therefore, instead of functionally defining this area, an anatomical approach was used by taking the median of the left and right BA 17 coordinates (see Table 15), to encompass a central area of V1 across both hemispheres. This is because both coordinates are close to the midline and MEG has relatively poor spatial resolution to justify two separate ROI coordinates close to the midline.

Table 15: V1 ROI coordinates derivation from BA 17.

	MNI coordinates		
Region label	***x***	***y***	***z***
BA 17 Right	9.722	-80.832	5.779
BA 17 Left	-11.367	-77.659	6.072
Median BA 17 for V1 ROI	**-0.82**	**-79.25**	**5.93**

Appendix E: Effects of different total amounts of time spent playing RECOGNeyes on baseline-adjusted change in outcome measures

Elizabeth Liddle, Peter Liddle, Abdulrhman Shalabi, Alice Waitt.

Summary

To investigate dose-related effects of RECOGNeyes training, we computed change scores (Day 2 minus Day 1) for a range of outcome measures, and regressed them on baseline score so as to control for effects of baseline. Outcome measures included gaze control measures, MEG measures of anticipatory oscillatory power during the antisaccade task; phasic autonomic responses during the antisaccade task, and resting state connectivity between ROIs, measured using fMRI.

We then tested the between-subjects correlations between total minutes spent playing RECOGNeyes (as recorded in game logs) and baseline-adjusted change scores.

Gaze control

We considered the following measures of gaze control as evidenced by antisaccade task performance and eye-movements during passage reading:

Antisaccade task:

- d´ score as a measure of accuracy
- Median antisaccade RT minus median prosaccade RT as a measure of antisaccade RT cost (subtracting prosaccade RT from antisaccade RT gives a measure of the "time cost" of having to inhibit the prepotent prosaccade before making the antisaccade, controlling for prosaccade speed).

Reading

- Standard deviation of first landing place in word
- Mean length of skipped words
- Mean fixation duration
- Proportion of saccades that were regressive

Adjusted change scores for these measures were entered as dependent variables into a multivariate GLM with Total Minutes Played (TMP) as a continuous predictor.

TMP was a significant multivariate predictor, $F(6, 18) = 3.822$, $p = .012$, indicating that variance shared between these measures of change was significantly associated with time spent playing RECOGNeyes.

The direction of change associated with greater TMP was in the direction expected for improved gaze control in all cases. Greater TMP was associated with smaller standard deviation of first landing place; shorter mean length of skipped words; shorter fixation duration; smaller proportion of regressive saccades; reduced antisaccade cost; higher d´ accuracy score. Two of these change measures reached statistical significance in the univariate analysis: antisaccade cost, $F(1, 23) = 5.419$, $p = .014$, and fixation duration, $F(1, 23) = 5.529$, $p = .028$.

MEG measures

Anticipatory alpha in the FEF and anticipatory beta in DLPFC were proposed a priori as measures of inhibitory control that might be impacted by gaze control training, following the finding by Hwang et al. (2014, 2016) of greater FEF alpha and DLPFC beta on antisaccade trials, and a positive correlation between FEF alpha and antisaccade accuracy, with adolescents showing less FEF alpha than young adults (Hwang et al., 2016). TMP was a significant predictor of change in both measures, but negatively. Greater TMP was associated with a greater reduction in both FEF alpha, $r(N=23) = -.417$, $p = .047$, and DLPFC beta, $r(N=23) = -.472$, $p = .023$. Neither were

significantly correlated with change in accuracy, but greater reduction in DLPFC beta was associated with reduced antisaccade RT cost, $r(N=23) = .461$, $p = .027$.

These findings suggest that improvement in gaze control in this sample was associated with reduced DLPFC beta, and that both improved gaze control and reduced DLPFC beta were associated with greater time spent playing RECOGNeyes.

Autonomic measures

TMP was not significantly correlated with changes in phasic pupil dilation rate nor with changes in cardiac deceleration rate.

Resting state connectivity within the visual attention network

On each assessment day, following MEG acquisition, resting state MRI (rsMRI) data was acquired for 10 minutes. Functional connectivity was computed between same ROIs of the visual attention network used for MEG analysis, with the difference that the greater spatial resolution of MR imaging allowed for bilateral V1 ROIs to be specified. Connectivity was

computed between ROIs within each hemisphere, and between left-right homotopic ROI pairs. These are shown in Figure 1. Connectivity change values for Day2-Day1 connectivity were adjusted for baseline values as for the other outcome measures, and then correlated with TMP.

Figure 1 shows the values for the correlation between TMP and adjusted change in connectivity. Greater TMP was associated with reduced homotopic connectivity, $F(1, 31) = 7.188$, $p = .012$, suggesting increased independence of visual attention networks in the two hemispheres. Children with ADHD have been found to have greater homotopic connectivity than typically developing controls (K. Jiang et al., 2019).

In contrast, greater TMP was associated with increased within-hemisphere connectivity in the left hemisphere. At baseline, connectivity was significantly lower in the left hemisphere than in the right; a greater reduction in this difference was associated with greater time spent playing RECOGNeyes, $F(1, 31) = 5.509$, $p = .025$. These rsMRI findings indicate that RECOGNeyes training may have effected plastic changes in brain connectivity that are apparent even during rest i.e. when not engaged in a gaze-control task. They also suggest that these changes may include greater integration of the left hemisphere attentional network and greater independence of it from the right hemisphere network.

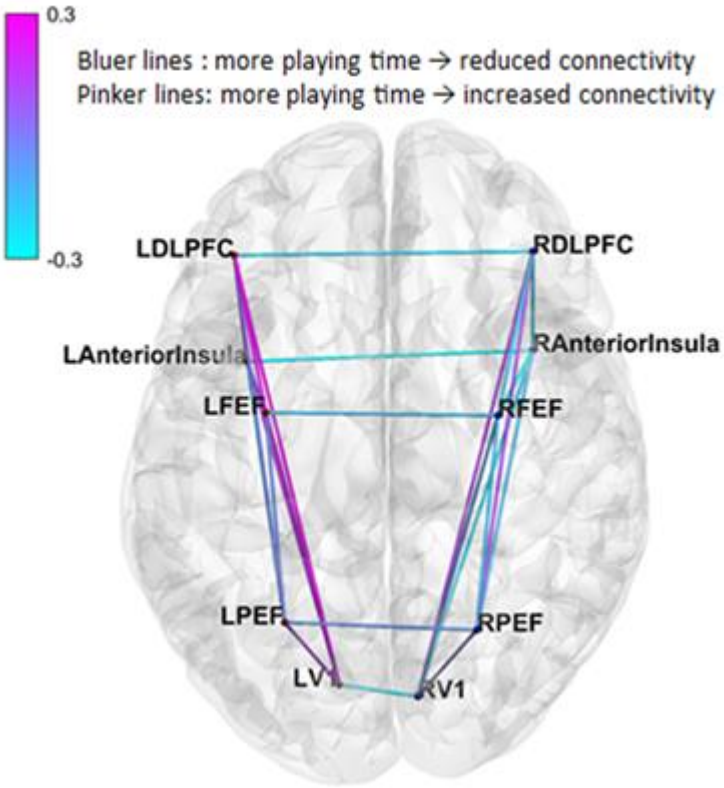
0.3
-0.3
Bluer lines : more playing time → reduced connectivity
Pinker lines: more playing time → increased connectivity
LDLPFC
RDLPFC
LAnteriorInsula
RAnteriorInsula
LFEF
RFEF
LPEF
RPEF
LV1
RV1

Figure 1